Fisheries and Oceans Canada | Pêches et Océans Canada
Ecosystems and Oceans Science | Sciences des écosystèmes et des océans

Canadian Science Advisory Secretariat (CSAS)

Research Document 2026/068

Pacific Region

Assessment of Petrale Sole in British Columbia in 2024

Mackenzie Mazur, Kendra Holt, Nick Fisch, and Philina English

Fisheries and Oceans Canada
Pacific Biological Station
3190 Hammond Bay Road
Nanaimo, BC V9T 6N7

October 2026

Canada

Foreword

This series documents the scientific basis for the evaluation of aquatic resources and ecosystems in Canada. As such, it addresses the issues of the day in the time frames required and the documents it contains are not intended as definitive statements on the subjects addressed but rather as progress reports on ongoing investigations.

Published by:

Fisheries and Oceans Canada
Canadian Science Advisory Secretariat
200 Kent Street
Ottawa ON K1A 0E6

http://www.dfo-mpo.gc.ca/csas-sccs/
DFO.CSAS-SCAS.MPO@dfo-mpo.gc.ca



© His Majesty the King in Right of Canada, as represented by the Minister of the Department of Fisheries and Oceans, 2026

This report is published under the Open Government Licence - Canada

ISSN 1919-5044
ISBN 978-1-100-00475-4 Cat. No. Fs70-5/2025-068E-PDF

Correct citation for this publication:

Mazur, M., Holt, K., Fisch, N., and English, P. 2026. Assessment of Petrale Sole in British Columbia in 2024. DFO Can. Sci. Advis. Sec. Res. Doc. 2026/068. vi + 180 p.

Aussi disponible en français :

Mazur, M., Holt, K., Fisch, N. et English, P. 2025. Évaluation de la plie de Californie en Colombie-Britannique en 2024. Secr. can. des avis sci. du MPO. Doc. de rech. 2026/068. vi + 198 p.

TABLE OF CONTENTS

ABSTRACT vi
1. INTRODUCTION 1
1.1. OBJECTIVES FOR 2024 STOCK ASSESSMENT 2
1.2. STOCK STRUCTURE 3
2. METHODS 5
2.1. DATA INPUTS 5
2.1.1. Fishery Catch 8
2.1.2. Indices of Abundance 8
2.1.3. Age and Length Composition 8
2.2. BIOLOGICAL PARAMETERS 9
2.3. STOCK ASSESSMENT MODELLING 10
2.3.1. Base Ensemble Model 12
2.3.2. Sensitivity Analyses 12
2.4. REFERENCE POINTS 14
2.5. PROJECTIONS FOR HARVEST ADVICE 16
2.6. ENVIRONMENTAL CONDITIONS AND SPECIES BIOLOGY 16
2.6.1. Bayesian time-series regressions 16
2.6.3. Environmental conditions potentially impacting demersal juvenile and adult body condition 17
3. RESULTS 17
3.1. MODEL DIAGNOSTICS 17
3.1.1. Index fits 17
3.1.2. Composition fits 20
3.1.3 Retrospective Analysis 34
3.2. BASE ENSEMBLE MODEL RESULTS 39
3.2.1. Estimated Parameters 39
3.2.2. Rationale for MSY-based Reference Points 44
3.2.3. Stock Status 45
3.2.4. Decision Tables 50
3.3. SENSITIVITY ANALYSES 54
3.4. ENVIRONMENTAL CONDITIONS AND SPECIES BIOLOGY 59
3.4.1. Environmental conditions potentially impacting recruitment 59
3.4.2. Body condition indices 61
3.4.3. Environmental conditions potentially impacting body condition 62
4. DISCUSSION 63
4.1. OVERALL 63
4.2. UPDATES FROM 2006 ASSESSMENT 63
4.3. COMPARISON TO PETRALE SOLE ON THE US WEST COAST 64

4.4. UNCERTAINTY IN AGE COMPOSITION DATA 64
4.5. UNCERTAINTY IN HISTORICAL CATCH 66
4.6. UNCERTAINTY IN STOCK DELINEATION 66
4.7. PRODUCTIVITY AND ENVIRONMENTAL IMPACTS 66
4.8. ASSESSMENT SCHEDULE 67
4.9. RECOMMENDATIONS 67
ACKNOWLEDGEMENTS 68
REFERENCES CITED 69
APPENDIX A. FISHERY AND CATCH HISTORY 74
A.1. FISHERY HISTORY 74
A.1.1. 1930's – 1960's 74
A.1.2. 1960's – 1995 74
A.1.3. 1996 – present 75
A.2. CATCH DATA 76
A.2.1. Retained Catch 77
A.2.2. Discarded Catch 78
LITERATURE CITED 81
APPENDIX B. BIOLOGICAL ANALYSES 82
B.1. VON BERTALANFFY GROWTH MODEL 82
B.2. WEIGHT-LENGTH MODEL 84
B.3. MATURITY 86
B.4. AGE AND LENGTH COMPOSITION 88
B.4.1. Age and Length Composition Expansion 88
B.5. AGEING ERROR 106
LITERATURE CITED 108
APPENDIX C. COMMERCIAL FISHERY CPUE STANDARDIZATION 109
C.1. FLEET DEFINTION 109
C.1.1. Historical Fleet: 1954 – 1995 109
C.1.2. Modern Fleet: 1996 - 2023 109
C.2. STANDARDIZATION PREDICTORS 110
C.3. RESULTS 111
C.3.1. Historical CPUE (1954-1995) 111
C.3.2. Modern CPUE (1996 – 2023) 119
LITERATURE CITED 125
APPENDIX D. SURVEY INDICES 127
D.1. DFO SYNOPTIC TRAWL SURVEYS: GEOSTATISTICAL MODELLING 127
D.1.1. Methods 127
D.1.2. Results 130
D.2. NOAA TRIENNIAL TRAWL SURVEY 135
LITERATURE CITED 136

APPENDIX E. STOCK SYNTHESIS MODEL STRUCTURE 137
LITERATURE CITED 141
APPENDIX F. MCMC DIAGNOSTICS 143
APPENDIX G. SENSITIVITY ANALYSIS WITH MLE OUTPUTS 152
APPENDIX H. FITS TO LENGTH COMPOSITIONS FROM THE LENGTH AND CONDITIONAL-AGE-AT-LENGTH MODEL 157
APPENDIX I. TIME-SERIES REGRESSIONS BETWEEN ENVIRONMENTAL CONDITIONS AND SPECIES BIOLOGY 159
I.1. ENVIRONMENTAL DATA SOURCES AND SPATIOTEMPORAL AGGREGATION 159
I.2. BIOLOGICAL RESPONSE VARIABLES WITH UNCERTAINTY 162
I.3. TIME-SERIES REGRESSION 162
LITERATURE CITED 168
APPENDIX J. SEX AND MATURITY SPECIFIC INDICES OF BODY CONDITION 169
J.1. SPLITTING SPECIMENS AND TOTAL CATCH BY SEX AND MATURITY 169
J.2. SPATIOTEMPORAL ESTIMATES OF BIOMASS DENSITY 170
J.3. POPULATION INDICES OF LE CREN'S BODY CONDITION 175
LITERATURE CITED 179

ABSTRACT

This paper presents a new stock assessment framework and reports the status for Petrale Sole (*Eopsetta jordani*) off the British Columbia (BC) coast using data through 2023 in offshore waters (all areas except for 4B). The BC Petrale Sole stock was last assessed with data up to 2006. This stock assessment evaluated a single BC coastwide population (5ABCDE3CD). There is currently no evidence suggesting distinct biological stocks of Petrale Sole off the BC coast. A two-sex statistical catch-at-age model developed with Stock Synthesis was used to assess Petrale Sole stock status. The model was fit to catch data (from 1938 to 2023), three survey indices (from 2003 to 2023), and age composition data from the fishery and surveys (from 2004 to 2019). Spatial heterogeneity of a coast-wide population was addressed by estimating separate selectivities for the three surveys. Natural mortality (*M*) had to be fixed at an assumed value to get a reasonable fit to data, but the stock recruitment steepness parameter was estimated using an informative prior distribution. A Bayesian framework was used in model fitting with the Markov Chain Monte Carlo 'No U-Turn Sampling' procedure. The assumed value of *M* was identified as a key uncertainty in this stock assessment, leading to the development of an ensemble model based on three separate models that differed in *M*. This approach allowed uncertainty arising from the choice of *M* to be incorporated into estimated stock status and harvest advice. Maximum sustainable yield (MSY)-based reference points are recommended for characterizing stock status and informing harvest decisions. The stock status in 2024 was estimated to be healthy, with female spawning stock biomass in 2024 (B_{2024}) well above B_{MSY} in the ensemble model as well as in each of the three individual *M* models. In all cases, there was a 100% probability that B_{2024} was above the LRP. Fishing pressure was also estimated to be relatively low at present compared to F_{MSY}, with *F* in 2023 estimated to be at 24% (95% credible interval = 10 – 46%) of F_{MSY}. Projections predict the stock to be healthy under varying levels of catch, with the probability of *F* being below F_{MSY} decreasing at catch levels above MSY. Sensitivity analyses show that most uncertainties resulted in a relatively small impact on the output, but different *M* assumptions resulted in large differences, supporting the choice for a base ensemble model. Environmental conditions were not incorporated into the stock assessment, but relationships between environmental conditions and Petrale Sole dynamics were explored, which could potentially inform the use of environmental variables in future assessments.

1. INTRODUCTION

Petrale Sole (*Eopsetta jordani*) is a right-eyed flatfish of the family Pleuronectidae that inhabits the Northeast Pacific Ocean, with a range extending from Baja California to the Aleutian Islands in Alaska (Love 2011). Petrale Sole is typically found on soft-bottom substrata at depths ranging from 0 to 500 m, depending on the time of year. Petrale Sole have a strong seasonality in their distribution. In winter months, they tend to aggregate in well-defined deepwater spawning locations, while in summer the species is more evenly dispersed at shallower depths along the continental shelf (Pedersen 1975, Powell et al. 2022). Petrale Sole feed predominantly on fish and pelagic or semi-pelagic invertebrates with euphausiids being the dominant prey source, followed by herring (*Clupea pallasii*), sand lance (*Ammodytes hexapterus*), and shrimp (pandalids) in order of declining frequency (Ketchen and Forrester 1966). Petrale Sole also feed on crab, octopi, squid, anchovies, hake, and other smaller rockfish and flatfish (Kravitz et al. 1977; Birtwell et al. 1984; Reilly et al. 1994; Love 1996; Pearsall and Fargo 2007). Petrale Sole are more piscivorous at larger sizes (Allen et al. 2006).

Within British Columbia (BC), Petrale Sole is primarily harvested by the multi-species groundfish trawl fishery. The Petrale Sole fishery in BC developed rapidly between the 1930s and 1950s due to high demand for Petrale Sole as a food fish. Much of the catch in early years was taken by US vessels fishing in Canadian waters (Ketchen and Forrester 1966). The fishery peaked in 1948 with 6,193 tonnes of catch recorded in BC waters. The discovery of deepwater spawning aggregations of Petrale Sole off Vancouver Island in 1953 helped maintain relatively stable annual catch levels despite declining catches from inshore, summertime fishing localities. By the late 1950s and 1960s, Petrale Sole abundance in BC was considered depressed due to overexploitation. Management restrictions were put in place to protect spawning aggregations and limit directed fisheries. During this time, Petrale Sole fell to a species of secondary importance for the trawl fishery. Seasonal trip limits and restrictions on directed fishing remained in place until the move to Individual Transferable Quota (ITQ) management for the Integrated Groundfish Fishery starting in 1996-1997, at which time a coastwide Total Allowable Catch (TAC) was implemented. At present, Petrale Sole TAC is set at a coastwide level of 900 t under the Pacific Groundfish Integrated Fishery Management Plan (DFO 2024a). Catch levels, including discards, over 2019-2023 have averaged 630 t per year, with a range of 485 – 769 t (Figure 1). Petrale Sole discards are relatively low. More details on the fishery are available in Appendix A.

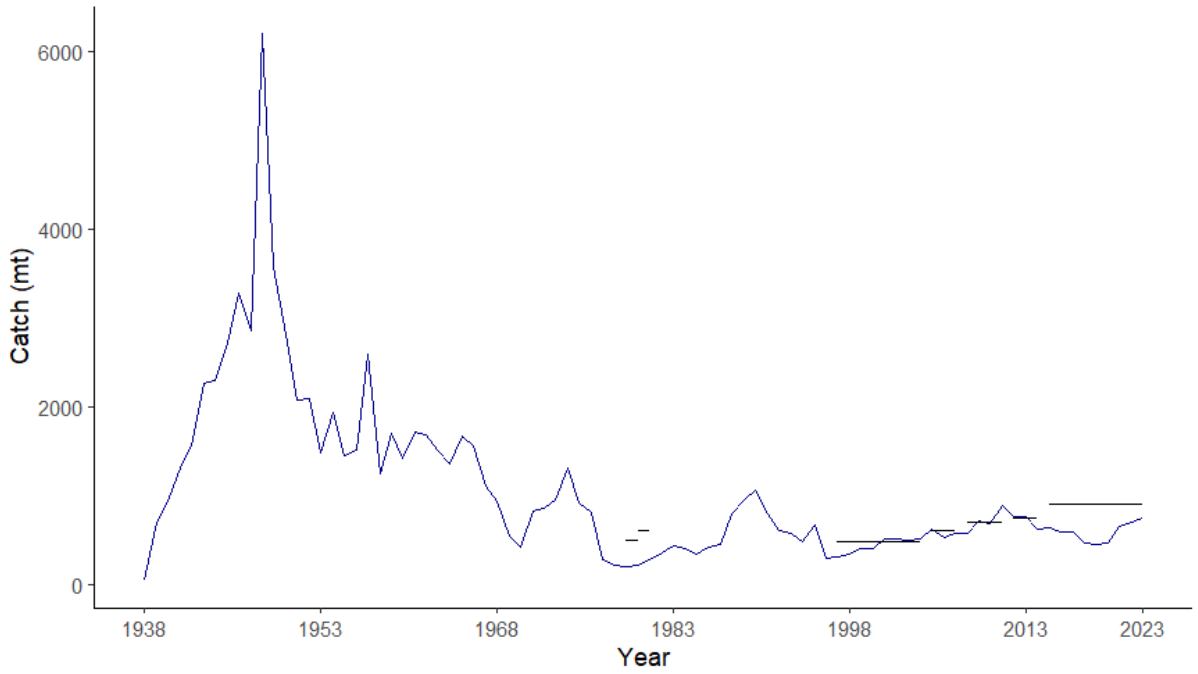


Figure 1. Petrale Sole catch (dark blue lines) and total allowable catches (horizontal black lines).

1.1. OBJECTIVES FOR 2024 STOCK ASSESSMENT

Fisheries and Oceans Canada (DFO) Groundfish Management Unit (GMU) has requested an assessment of Petrale Sole (*Eopsetta jordani*) in British Columbia (BC) relative to reference points that are consistent with the DFO Precautionary Approach (DFO 2009). The last stock assessment was done in 2006 using a delay-difference model (Starr 2009). The resulting advice had high uncertainty, as evidenced by high sensitivity to assumed natural mortality (M) and data selection rules used when creating fishery-dependent catch-per-unit-effort (CPUE) abundance indices. Prior to the stock assessment in 2006, there were BC Petrale Sole stock assessments in 2003 (Starr and Fargo 2004) and 1998 (Fargo 1999). Previous stock assessment models for Petrale Sole did not incorporate age and/or length composition data, due to limited data availability at the time. The current assessment uses a more data-intensive statistical catch-at-age model given an additional 17 years of data since 2006, as well as the development of the Groundfish Multispecies Synoptic Bottom Trawl Surveys in the early 2000s.

The objectives of the current 2024 stock assessment are to:

1. Assess the suitability of a new assessment model framework for Petrale Sole in BC implemented via the Stock Synthesis program (Methot et al. 2020). Various model structures, including age- and size-structured assessment models, and data sets will be considered and reviewed.
2. Discuss and recommend a limit reference point (LRP), including the biological considerations and rationale used to make such a determination, as well as candidate upper stock reference (USR), candidate removal reference (RR) and candidate target reference points (TRPs) for Petrale Sole in BC. Provide a rationale if the LRP, candidate USR, and candidate RR differ from the Precautionary Approach (PA) Policy default reference points (0.4 B_{MSY}, 0.8 B_{MSY}, and F_{MSY}, respectively).

3. Describe the sources of uncertainty related to input data and model assumptions and explore how these uncertainties affect model predictions of productivity, reference points, and trends in biomass and recruitment.
4. Identify the preferred approach using a base model, or reference set of models to be combined using an ensemble approach, that can be used to characterize stock status for Petrale Sole in BC. Assess the current status of Petrale Sole in BC waters relative to the recommended reference points.
5. Using probabilistic decision tables, evaluate the consequences of a range of harvest policies on projected biomass (and exploitation rate) relative to the reference points out to 10 years.
6. If the stock status is estimated to be below the LRP, provide guidance consistent with the development of rebuilding plans under the PA framework for Petrale Sole, to satisfy recent legislation (*Fisheries Act*).
7. Examine how environmental conditions and aspects of the species biology may affect the stock as required in the "Guidelines for Implementing the Fish Stocks Provisions in the *Fisheries Act*."
8. Recommend an appropriate interval between formal stock assessments presented at a regional peer review meeting, indicators used to characterize stock status in the intervening years, and/or triggers of an earlier than scheduled assessment (DFO 2016). Provide a rationale if indicators and triggers cannot be identified.

1.2. STOCK STRUCTURE

For the purpose of this stock assessment, we assume a single BC stock covering all offshore management areas (Pacific Marine Fisheries Commission major areas 3CD, 5A-E; Figure 2). Petrale Sole also occur in inshore waters in the Strait of Georgia (Area 4B); however, catches have always been low (Appendix A) and Petrale Sole is rarely encountered on research surveys in this area. As a result, we follow the approach taken in previous BC stock assessments of excluding this region from the modelled offshore stock.

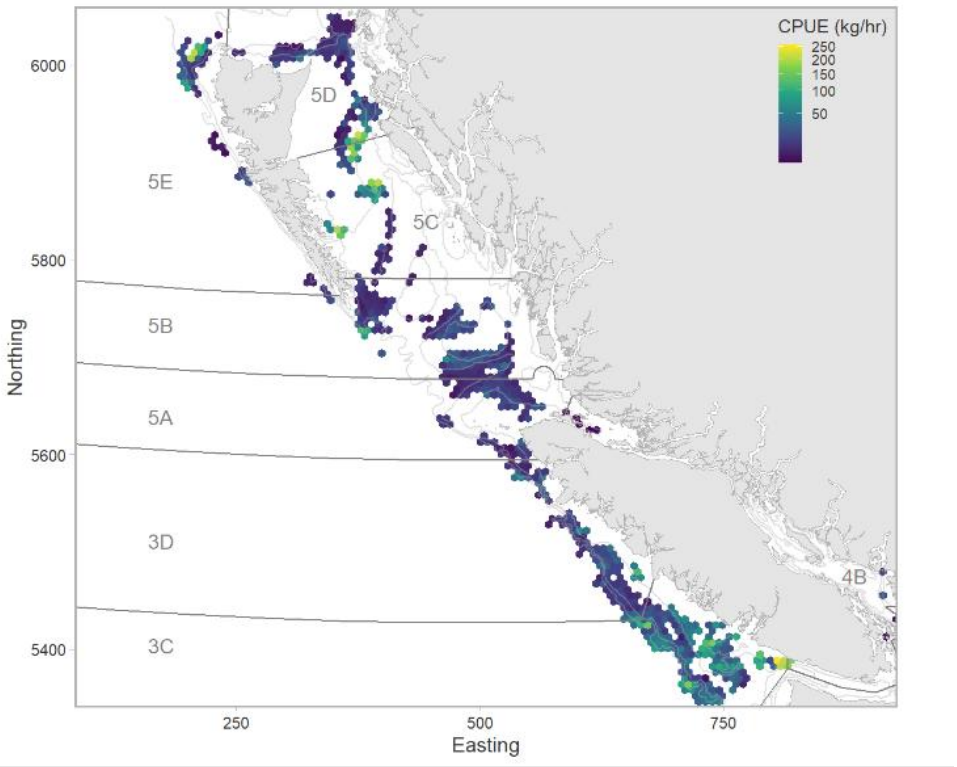


Figure 2. Average fishery catch-per-unit-effort (CPUE) for Petrale Sole off the coast of British Columbia from 1996 to 2023 shown with Pacific Marine Fisheries Commission (PFMC) major areas, which are similar, but not identical, to DFO's Groundfish Management Areas. This assessment covers one coastwide stock: PFMC areas 3C-D and 5A-E. The Strait of Georgia (PFMC Area 4B) is not included in the coastwide stock. PMFC areas 3A-B are in the USA.

Stock structure for Petrale Sole in BC is not well-understood. Numerous tagging studies were undertaken in US and Canadian waters between the 1930s and early 1970s to increase understanding of Petrale Sole movement (Alverson and Chatwin 1957, Ketchen and Forrester 1966, Pederson 1975). Petrale Sole was shown to spawn in discrete deep-water sites in the winter and migrate inshore in a northerly direction to summer feeding grounds each year (Alverson and Chatwin 1957, Ketchen and Forrester 1966, Pedersen 1975). Adults displayed strong homing behaviour to the same deep-water spawning aggregations each year (Pedersen 1975).

The northward pattern of post-spawning migration leads to substantial transboundary movement of adults from winter spawning grounds in Washington State to summer feeding grounds on the West Coast of Vancouver Island. Fish tagged on Washington state spawning grounds were recovered from summer feeding habitats extending from Hecate Strait to Central Oregon, although the primary range of recovered tags extended from Washington state to mid-Vancouver Island (Ketchen and Forrester 1966, Pederson 1975). Northward post-spawning migration patterns also lead to movement among management areas within BC. Most of the summer recoveries of fish tagged at winter spawning aggregations off Estavan in Area 3D were from Areas 3D, 5A, and 5B, but some as far north as Areas 5C and 5D (Alverson and Chatwin 1957).

Transboundary movement of pelagic life stages between Washington and BC has also been proposed with a biophysical individual-based model (IBM) recently used to show mechanisms for transboundary connectivity between Washington State spawning grounds and inner shelf

settlement areas in BC (Santa Cruz et al. 2023). The IBM predicted that the strong influence of northward alongshore transport resulted in 33-70% of annual successful juveniles from US spawning grounds settling in Canadian waters extending from Vancouver Island up to the southern tip of Moresby Island (Areas 5C, 5E).

For the purpose of this stock assessment, a single BC stock covering all offshore management areas (3CD, 5A-E) was assumed for several reasons. First, there is no single, clearly defined breakpoint between northern and southern areas along the BC coast given the overlap on summer feeding grounds of fish tagged at different spawning aggregations further south. While there is a strong link between US spawning aggregations and summer feeding habitats in Area 3C, some US spawners also migrate further north into Area 3D where they mix with fish that spawn in Area 3D. Second, observations that a small subset of Petrale Sole individuals made long-distance migrations along the coast (e.g., northern California to La Perouse Bank; Ketchen and Forrester 1966) combined with substantial possible northward movement of pelagic life stages along the BC coast (Santa Cruz et al. 2023), suggest that genetic mixing could be occurring between spawning aggregations. Finally, there are no apparent differences in estimated growth parameters between management areas (3CD, 5AB, and 5CD; Appendix B).

The assumption of a single coastwide BC stock is consistent with the last two stock assessments for Petrale Sole in BC, which assumed a single coastwide stock covering groundfish areas 3CD5ABCD (Starr and Fargo 2004; Starr 2009). Data from the west coast of Haida Gwaii (Area 5E) were not included in the modelled stock in either of these assessments due to low catch levels and data. Prior to 2004, stock assessments for Petrale Sole in BC assumed two discrete stocks based on historical tagging data, with one stock thought to occur off the southwest coast of Vancouver Island (Area 3C) and the other extending from northwest Vancouver Island through Queen Charlotte Sound and into Hecate Strait (Areas 3D, 5ABCD; Fargo 1999). Recent US assessments of Petrale Sole have also moved away from assessing separate southern and northern stocks and now assume a single stock from California to Washington for reasons that are similar to those identified here for BC (Wetzel 2019, Taylor et al. 2023).

2. METHODS

2.1. DATA INPUTS

Petrale Sole stock abundance and population composition are monitored via trawl survey indices and age and length composition data, as well as fishery-dependent age and length composition data (Table 1). All data sources considered have CPUE, age composition, and length composition data associated with them, with the exception of the National Oceanic and Atmospheric Administration (NOAA) Triennial Survey which does not have age composition data. Also, the historical fishery data from 1938 to 1953 also only includes catch data. Petrale Sole is also encountered in Groundfish Hard Bottom Longline surveys and in International Pacific Halibut Commission Fishery- Independent Setline Survey; however, we did not consider these surveys here because catches for Petrale Sole are generally low and variable in these surveys.

All data, except for the NOAA Triennial Survey data and historical fishery catch data, were extracted using the gfdata R package, which was developed as a reproducible tool to support the Groundfish Data Synopsis Report (Anderson et al. 2019), but note that only users with access to DFO's Pacific Biological Station network and permissions to access the groundfish databases can extract data. The NOAA Triennial Survey index was provided by P. Starr, because the data available for this survey on the groundfish databases did not include area

swept, which is necessary to calculate CPUE. The same index was used in the previous Petrale Sole assessment (Starr 2009). Historical catch data were from Ketchen and Forrester (1966).

Table 1. Data available for Petrale Sole in British Columbia.

Source	Years	CPUE	Age Comps	Length Comps
Historical Fishery	1938-1953	-	-	-
Fishery	1954-2022	X	X	X
West Coast Vancouver Island Multispecies Small-Mesh Bottom Trawl Survey	1975-2023	X	X	X
Hecate Strait Multispecies Assemblage Bottom Trawl Survey	1984-2003	X	X	X
Queen Charlotte Sound Synoptic Bottom Trawl Survey	2003-2021	X	X	X
Hecate Strait Synoptic Bottom Trawl Survey	2005-2021	X	X	X
West Coast Vancouver Island Synoptic Bottom Trawl Survey	2004-2022	X	X	X
West Coast Haida Gwaii Synoptic Bottom Trawl Survey	2006-2022	X	X	X
Triennial Survey (Canadian waters only)	1980-2001	X	-	X

An overview of data time series selected to parameterize the three assessment models used to provide stock status and harvest advice (which combined are called the base ensemble model) are shown in Figure 3. In the base ensemble model, age composition data from the fishery and the Queen Charlotte Sound (QCS), Hecate Strait (HS), and West Coast Vancouver Island (WCVI) Synoptic Surveys were used. Standardized CPUE from the Synoptic Surveys and fishery catch from 1938 to 2023 were also used.

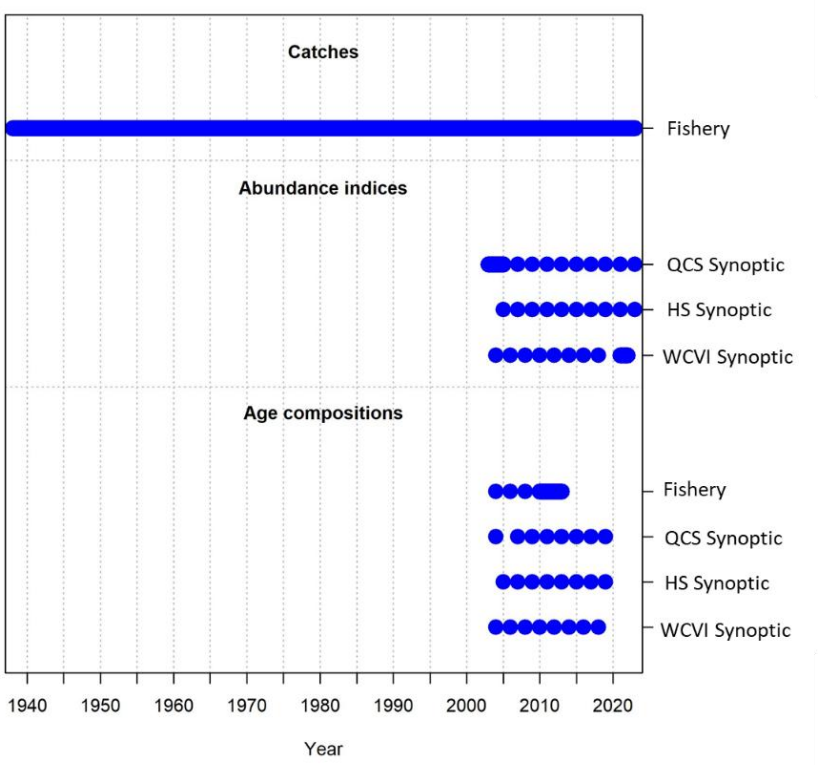


Figure 3. Data used in the base ensemble model from 1938 to 2023. QCS: Queen Charlotte Sound, HS: Hecate Strait, WCVI: West Coast Vancouver Island. Figure created with r4ss package.

Fishery CPUE was not used as an index of abundance in the base model due to concerns about reliability. The relationship between fishery CPUE and abundance is often non-stationary due to changes in fleet efficiency, fishery targeting behaviour, the spatial distribution of the population (including density-dependent habitat selection) and seasonal shifts in fishing effort (Hillborn and Walters 1992, Maunder et al. 2006). CPUE standardization analyses were undertaken to help account for some of these changes (Appendix C). However, the fleet behaviour of targeting of spawning aggregations in some years still created concerns about potential hyperstability in the series, which occurs when CPUE remains high despite declining abundance. Fishery-independent abundance indices from surveys were considered more reliable.

Data from the WCVI Multispecies Small-Mesh Bottom Trawl and HS Multispecies Assemblage Bottom Trawl Surveys were not used in the base model since the standardized indices were uncertain, with CVs around 1.25 and 0.29, respectively. Data from the West Coast Haida Gwaii Synoptic Bottom Trawl were not used, since catches and composition data for Petrale Sole are variable in this survey. Data from the Triennial Survey were not used, since the Triennial survey did not collect age data, and a major assumption would have to be made regarding the selectivity of the Triennial survey. Additionally, length composition data from the fishery and three Synoptic Surveys included in the base model were not used given a poor fit to length compositions when attempted using a model fit to length and conditional age-at-length data. However, the use of the data that were excluded from the base model were explored in sensitivity analyses. Brief summaries of each data type used for the current assessment are provided in sections 2.1.1 – 2.1.4 below, while more detailed descriptions are provided in Appendices A – D. Code used to extract and aggregate data is available upon request.

2.1.1. Fishery Catch

Catches in Canadian waters prior to 1954 are available only by year from Ketchen and Forrester (1966). US vessels fished in Canadian waters prior to the establishment of the Economic Exclusion Zone (EEZ) in 1977. US trawl vessels started targeting Petrale Sole off the WCVI and into Georgia Strait in the 1930s, with some vessels moving up into Queen Charlotte Sound by the late 1940s (Ketchen and Forrester 1966). From 1953 to 1957, U.S. vessels heavily targeted deep-water spawning aggregations of Petrale Sole off the WCVI. This ended with an international moratorium on deep-water fishing for Petrale Sole in 1957 (Ketchen and Forrester 1966).

The Canadian catch data from 1954 to 2023 were extracted using the gfdata R package. Fishery catches and age compositions from Area 4B were removed, as Area 4B was not included in this assessment. Landed catch data were available from 1954 to 2023, and discard data were available from 1996 to 2023. Discards were at relatively low levels. From 1996 to 2023, discards were added to the landed catch data to produce the total catch. Prior to 1996, an average ratio of discards to landings from 1996 to 2023 was multiplied with landings to calculate the discards, which were then added to the landings to produce total catch. More details on fishery catch are provided in Appendix A.

2.1.2. Indices of Abundance

QCS, HS, and WCVI Synoptic Bottom Trawl Survey indices were used in the stock assessment model. These surveys are part of DFO's ongoing Groundfish Synoptic Bottom Trawl Surveys, which have operated off Canada's west coast since 2003-2005. They are random-stratified trawl surveys targeting a wide range of finfish species. These surveys operate as three distinct surveys in different portions of the coast (WCVI, QCS, and HS) and typically occur biennially, with different survey areas fished in alternating years. The QCS Synoptic survey provides data from 2003 to 2023; the HS Synoptic survey provides data from 2005 to 2023; and the WCVI Synoptic survey provides data from 2004 to 2022.

Survey datasets for each of the three synoptic trawl surveys were extracted from DFO databases using the gfdata R package. The expected spatial trawl survey biomass densities were modelled using geostatistical spatiotemporal GLMMs (generalized linear mixed effect models; Anderson et al. 2024) applied to data from each of the three synoptic trawl surveys independently. For each synoptic trawl survey, spatiotemporal models were fit with and without a depth covariate and with Tweedie, delta-lognormal, and delta-gamma families. The best model for each synoptic trawl survey was chosen with the Akaike information criterion (AIC) and used to model the survey index. All three standardized survey indices show increasing trends. More details on survey index standardization are available in Appendix D.

2.1.3. Age and Length Composition

Age composition data were available from the commercial bottom trawl fishery as well as from the three research surveys from 2004 to 2019. Age composition data were available from the Synoptic Surveys up to 2018 or 2019 depending on the survey, where the final year of commercial age data was 2013. Age composition data were expanded (from raw aged samples to stock-wide survey and commercial catch proportions caught at age) using the same method as the Redstripe Rockfish assessment (Starr and Haigh 2021; Appendix B).

Sample sources used to collect age and length composition data from fisheries have changed over time in BC. Between the 1990s and 2000s, most samples were 'sorted', meaning that they were divided into landed or discarded catch prior to sample selection. The majority of fishery samples were taken from landed catch (called 'keepers'), although a small portion of samples

came from ‘discards’. Starting in the late 2000s and continuing until the end of our fishery samples time series, there was a shift to samples being ‘unsorted’, which means that they included both ‘keepers’ and ‘discards’. Unsorted data were collected through the observer program. In some early years (1950s to 1960s), there were unsorted data that were most likely not unsorted, but there were no keeper codes in the original data. These data were converted to keepers. Only unsorted fishery age composition data were used in the assessment model so that the age compositions are representative of the catch time series used for this assessment, which includes both landed and discarded catch. Sorted age composition data were not considered since older fish exist in the sorted data than in the unsorted data in a given year, and the range of ages should be wider in the unsorted data than in the sorted data. One commercial age sample with a length less than 10 cm was removed since the age associated with this small fish was unrealistic. Additionally, if there were less than three fishing trips with ages that were sexed in a given year, the fishery age compositions for that year were not used in the stock assessment model. Annual sexed fishery age compositions from less than three fishing trips were likely not representative of the age composition of the fishery catch. Unsorted fishery age data was much less abundant than age data from the surveys.

Length composition data, which were used in a sensitivity analysis, were available for more years than were age composition data (Figure B - 11), although the final year available for commercial length compositions remained 2013. More recent years of length composition data relative to the age composition data were available from the surveys (2022 and 2023 compared to 2019 from the age compositions, Figure B - 12-Figure B - 14). These data were binned to the resolution of 4cm. The length composition data were expanded using the same methods as the age compositions (Appendix B).The age compositions within length bins were used as conditional age-at-lengths in a sensitivity analysis, and were not expanded (treated as random samples within each length bin).

A bootstrapping procedure, similar to that developed in Stewart and Hamel (2014), was used to determine input sample sizes as a measure of sampling variance for the age composition, length composition, and conditional age-at-length compositions fit in the assessment models. This bootstrapping procedure is described in further detail in Appendix B.

2.2. BIOLOGICAL PARAMETERS

Data used to determine the length-age and length-weight relationships included paired age-length and length-weight data from all surveys. Commercial data were not used in the growth relationships due to the potential bias towards larger fish at a given age or length. A von Bertalanffy growth function was used for the length-age relationship and a linear regression was used to model the log(weight)~log(length) relationship. A logistic function was used to develop a maturity at age relationship, combining commercial and survey data. Commercial data were included in this relationship because the commercial data covers more of the spawning period (winter) for Petrale Sole than the survey data, which occurs in the spring/summer. All growth and maturity relationships were assumed to be constant over time. More details on the growth and maturity parameters are available in Appendix B.

Natural mortality is often an uncertain and difficult parameter to estimate in stock assessments; however it can be highly influential as it is related to productivity and reference points and hence management advice (Maunder et al. 2023). For example, bias of M in stock assessment modelling can lead to biased estimated exploitation rates (Clark 1999) as it may result in biased estimated biomass (Punt et al. 2021). Estimating M is difficult because it is confounded with other model parameter estimates (i.e. steepness, catchability, selectivity, etc.; Magnusson and Hilborn 2007). Attempts at estimating M within the Petrale Sole assessment resulted in a model that would not converge; thus estimating M was not pursued further nor estimated using a

Bayesian routine. Because of this, M for both sexes of Petrale Sole was fixed at 0.154, based on the Hamel and Cope (2022) method for determining M based on maximum age. Hamel (2015) refined and published a method for combining meta-analytic approaches relating M to other life-history parameters. Hamel and Cope (2022) updated the relationship between maximum age and M from Hamel (2015) with a corrected application of an updated database from Then et al. (2015). The 0.154 value is based on a maximum age of 35 for Petrale Sole for each sex (after age outliers with ≤1 observation were removed):

$$M = \frac{5.4}{A_{MAX}} = \frac{5.4}{35} = 0.154$$

Eq. 1

Several large ages (>26) were observed for both females and males, suggesting that M may not be that different between sexes. The U.S. Petrale Sole assessment estimated a M of 0.142 for females and a M of 0.155 for males (Taylor et al. 2023), similar to the estimate of 0.154 from Hamel and Cope (2022) [with a maximum age of 35].

Sensitivity analyses (see below) did show a large impact on model output regarding the fixed value assumed for M. In order to incorporate uncertainty in M into the model and management advice, although the fixed estimate of 0.154 was considered the most plausible value for M, model output from assessments assuming fixed M at 0.124 and 0.184 were combined within an ensemble (see 2.3.1). To reflect what we deem the most plausible M hypothesis given the data, that being M=0.154 for each sex, we weighted the ensemble as 50% comprising of output from the assessment model with M=0.154, and 50% comprising of output the assessment models with M=0.124 and M=0.184 (25% each). We refer to the individual assessment model with a fixed M of 0.154 as the baseM model (and that with M=0.124 and M=0.184 as the lowM and highM models, respectively). A larger range of Ms was not used in the base ensemble model, because models with a fixed M below 0.124 resulted in a model that did not converge, and models with a fixed M above 0.184 were not considered so that there was a symmetric difference in M for the low and high M models.

2.3. STOCK ASSESSMENT MODELLING

A two-sex statistical catch-at-age model implemented using the Stock Synthesis (SS) modelling framework (Methot and Wetzel 2013, Methot et al. 2020) was used to model Petrale Sole population dynamics in the combined PMFC areas 3CD+5ABCDE. SS has been used for many other stock assessments in the region (Edwards et al. 2022, Starr and Haigh 2023, DFO 2024b, to name a few). An ensemble modelling approach that combined three different stock assessment model fits was used as the primary basis for characterizing stock status and harvest advice, with results from additional model fits presented as sensitivity analyses.

The model for Petrale Sole was two-sex, assumed one aggregated fishing fleet, and used survey indices and age composition data. Given the availability and magnitude of historical catch data, the first year of the assessment was in 1938, which was the first year of recorded catches for Petrale Sole (See Appendix A for more details on catch). As a result, the stock was assumed to be at an unfished state at the beginning of 1938.

A von Bertalanffy growth model was assumed for length-at-age (Appendix B.1), a linear regression for log(weight):log(length) relationship (Appendix B.2), and maturity-at-age was modelled as logistic (Appendix B.3). Fecundity-at-age was assumed proportional to mean weight-at-age and spawning stock biomass (*B*) was assumed to be made up of only females. Growth and maturity-at-age parameters were fixed, constant over time, and determined via the methods described in Appendix B. Annual recruitment was treated as stochastic and estimated

as annual multiplicative lognormal deviations about mean recruitment, where mean recruitment was determined from a Beverton-Holt stock recruitment curve (with steepness and unfished recruitment estimated). The standard deviation (SD) of the log of recruitment deviations was fixed at 0.636, obtained from the recruitment SD estimated for flatfish in the meta-analysis of Thorson et al. (2014).

Selectivity-at-age was estimated as an asymptotic function (forced from a double normal parameterization) and was time invariant for the fishery and surveys. Male selectivity parameters were offset from female selectivity parameters given differences in growth, behaviour and habitat. Spatial heterogeneity of a coast-wide population was addressed by estimating separate selectivities for the three surveys. Dome-shaped selectivity was not assumed in the base model, because there was no evidence that the habitat surveyed by each of the surveys would not support older fish. Less older fish are caught in the WCVI Synoptic Survey (Appendix B), but this could be a result of the limited sampling of ages in the Synoptic Surveys or a result of higher exploitation of Petrale Sole in the United States impacting the age structure at the southern range of the BC Petrale Sole stock given the potential for a transboundary stock. It is unlikely that the habitat in the WCVI is a nursery ground that would not support older fish. Estimating dome-shaped selectivity was attempted, but the model did not converge. The age compositions were fit with a multinomial likelihood with the input sample size determined from bootstrapping (Appendix B.4.2). An analytical solution was used for catchability of each survey. Each of the survey indices was fit using a lognormal likelihood, with a parameter estimated for each as an additional standard deviation that was added to the annual input standard deviation values (obtained from standardization, Appendix D).

An informative prior was applied to steepness and broad uninformative priors were applied to the log of the unfished recruitment (Ln(R0)) and selectivity parameters to aid in model stability. The steepness prior was based on a literature review of flatfish steepness estimates from the literature, which was initially developed for the BC Rock Sole (*Lepidopsetta* spp.) stock (Holt et al. 2016), and assumed a beta distribution with a mean of 0.85 and a CV of 10%. The total number of parameters estimated was 99. Parameters for R0, steepness, extra standard deviations for the survey indices, selectivity, and recruitment deviations were estimated in the each of the models comprising the ensemble.

More details on model structure are available in Appendix E. Code used to prepare Stock Synthesis files will be made available upon request.

All three models which made up the ensemble were fitted using a Bayesian estimation routine that used MCMC 'No U-turn Sampling' (NUTS), implemented with the R package `adnuts` (Monnahan and Kristensen 2018, Monnahan 2018 for R package). We also used MCMC analyses for a subset of sensitivity analyses that had good model fit diagnostics from maximum likelihood estimation (explored using the R package `r4SS`, Taylor et al. 2021). Each MCMC sampling procedure was run for 16,000 iterations divided among 8 chains (2000 samples / chain), with the first 250 samples from each chain discarded for warm-up. The remaining samples from all 8 chains were then merged, creating a total sample of 14,000 iterations for each model. We used MCMC diagnostics to look for signs of non-convergence in MCMC samples, with poor convergence being defined as parameters with a potential scale reduction factor $\hat{R}$ >1.01 or effective sample size < 400 (Vehtari et al. 2021, Monnahan 2024).

We used a variety of methods to assess model fit to data. For survey indices, we visually examined model fits to data, in addition to using standard deviations of the normalized residuals (SDNRs) to asses fit and runs tests to assess whether the sign of the residuals was random with respect to time (Wald and Wolfowitz 1940; Carvalho et al. 2017). For composition data, we examined One-step-ahead (OSA) residuals. OSA residuals are residuals that have been de-

correlated (or corrected for correlations) and converted to conform to a standard normal distribution under a correctly specified model (Trijoulet et al. 2023). They are designed for observations that are not normally distributed or independent. The de-correlation is necessary for compositional observations in stock assessments due to the fact that compositions must sum to 1, thus each observation is correlated. Consequently, Pearson residuals for multivariate distributions such as compositions are improper. For more information on the derivation of OSA residuals, please see Trijoulet et al. (2023). For results from assessments herein, the compResidual package in R was used to calculate OSA residuals. Finally, we conducted retrospective analyses on each model by successively removing five years of data and refitting the assessment. We evaluated retrospective patterns visually and by using Mohn's rho (Mohn 1999).

We present estimated biomass trends in units of female spawning stock biomass, which we denote simply as '*B*'. Associated biomass-based reference points are also presented as female spawning stock biomass, including female spawning stock biomass at maximum sustainable yield (B_{MSY}) and female spawning stock biomass at unfished equilibrium (B_0). Stock status is characterized as the ratio of female spawning stock biomass in a given year of interest (e.g., B_{2024}, or future years for harvest projections) relative to reference points.

2.3.1. Base Ensemble Model

Given the uncertainty in M as well as the sensitivity of model results to the specification of M (see Results section), the base model was an ensemble model with low (0.124), medium (0.154), and high (0.184) fixed M values. The medium M (baseM) value of 0.154 was based on maximum age from the meta-analytic relationship developed in Hamel and Cope (2022) [using the maximum age for each sex of Petrale Sole in the database]. The low and high M assumptions were an arbitrary difference of ±0.03 from the assumption based on maximum age. To create the ensemble model, the posteriors of the individual models with different M values were combined with 50%/25%/25% weighting for the medium, low, and high M choices, respectively. This was achieved by combining the entire posterior of the medium M model with a random sample of the low M model and a random sample of the high M model (where the size of the samples were 50% the size of the full posterior). We chose 50/25/25 weighting, because we viewed the medium M hypothesis as the most plausible given its basis in the Hamel and Cope (2022) meta-analysis, while the other M values were lower and higher than the medium value by an arbitrary value of 0.03 . Results for stock status estimates and decision tables are presented for the full ensemble. Results for sensitivity analyses are presented for each M level separately. MCMC diagnostics are presented in Appendix F.

2.3.2. Sensitivity Analyses

A variety of sensitivity analyses were conducted to explore uncertainties in the stock assessment model. Sensitivities that used MCMC sampling are listed in Table 2. Natural mortality assumptions were a focus in the sensitivity analysis due to the uncertainty in M. Although the lowM, baseM, and highM scenarios were combined in an ensemble approach to determine stock status, we also present them as separate sensitivity analyses to show the effect of M.

Additionally, a major uncertainty in this assessment was the age data, because of their limited spatial coverage and lack of availability past 2019 (See Appendix B). However, the Synoptic Surveys have length data through to the end of the time series (2023). In a given year, length data were much more abundant than age data. Another sensitivity (hereafter referred to as "Length+CAAL") explored using length data which filled in gaps in age composition data, especially in recent years. This model incorporates length data by including length compositions

and conditional-age-at-length (CAAL) compositions in the stock assessment model. The difference between this sensitivity and the base model was that length data were included, age compositions were conditional on length, and von Bertalanffy parameters were estimated within the assessment model. Length bins were 12-60 cm by 4 cm.

Conditional age-at-length data are paired age-length observations treated as a measure of the age distribution for a specific length bin. This provides more information than age or length observations alone (Piner et al. 2016) and avoids double use of the data as ages are conditional on lengths. CAAL data can provide information on growth and other modeled processes controlling age-structure. CAAL data are commonly used in stock assessment models, and SS is an assessment framework that allows for the use of CAAL data. Many US West Coast groundfish assessments take advantage of this feature, including the most recent US Petrale Sole stock assessment (Taylor et al. 2023). When CAAL data are used in SS, the observed age distribution for a given length bin is compared to the model's expectation of that distribution, which requires an estimate of the stock age structure. Stock Synthesis assumes age-length data are random at size (Methot et al. 2020). The incorporation of CAAL data within an assessment also allows the improved ability to estimate growth within the stock assessment model, which can reduce bias in growth parameter estimation caused by selectivity (Francis 2016).

The base ensemble model fit composition data using a multinomial likelihood with input samples sizes determined via bootstrapping. A Dirichlet-multinomial likelihood was originally considered, however resulted in negligible downweighing of age compositions and thus model stability was improved using the multinomial with fixed input sample sizes. However, we present a model with compositions fit with Dirichlet-multinomial likelihoods as a sensitivity model (hereafter referred to as "Dirichlet").

We also considered a model with the Triennial survey index (hereafter referred to as "Triennial"). The base model does not include this index since there were no age data from this survey and thus selectivity would need to be assumed. This model assumed the Triennial survey selectivity mirrors that of the WCVI Synoptic Survey, since the Triennial survey operated off the WCVI. The Triennial survey index was used in the last Petrale Sole assessment (Starr 2009), which did not incorporate age data, so we consider it here as a sensitivity.

A model without discards was also included as a sensitivity (hereafter referred to as "NoDiscards"). Petrale Sole is unlikely to be discarded at high rates, and it is possible that some discards of Flathead sole were misidentified as Petrale Sole by observers (Brian Mose, Canadian Groundfish Research and Conservation Society; personal communication). Flathead Sole are much more likely to be discarded than Petrale Sole, since there is no market for Flathead Sole.

A model with decreased catch by 25% from 1938 to 1953 was also considered (hereafter referred to as "ReduceCatch"). Historical catch is high and uncertain compared to recent catch. Catch data prior to 1954 were not available in groundfish databases and were from reports (Ketchen and Forrester 1966).

Some sensitivity analyses did not result in acceptable MLE or MCMC diagnostics (i.e. estimated M, with fishery CPUE indices, without extra standard deviations for survey indices, with a lower and higher variation in recruitment, and with Francis weighting), so they are presented in Appendix G with MLE outputs.

Table 2. Sensitivity analyses of which MCMC posteriors were compared.

Scenario label	Description
baseM	Assumed M = 0.154
lowM	Assumed M = 0.124
highM	Assumed M = 0.184
Length+CAAL	With length and conditional age-at-length data
Dirichlet	With Dirichlet multinomial likelihood for age compositions
Triennial	With Triennial survey index
NoDiscards	Without discards
ReduceCatch	With catch from 1938-1953 reduced by 25%

2.4. REFERENCE POINTS

We characterized stock status and harvest advice using four different reference points based on DFO's Fishery Decision-making Framework Incorporating the Precautionary Approach (DFO 2009). The first three are based on biomass, while the fourth is based on a removal rate, typically fishing mortality or harvest rate:

1. **Limit reference point (LRP)**: represents the stock status below which serious harm is occurring to the stock,
2. **Upper stock reference point (USR)**: the stock level threshold below which removals must be progressively reduced in order to avoid reaching the LRP, and
3. **Target biomass level (B_{TARGET})**: determined by productivity objectives for the stock, broader biological considerations (e.g., prey species requirements), and social and economic objectives for the fishery,
4. **Maximum removal reference rate (maximum RR)**: set at the maximum acceptable removal rate for the stock.

The LRP is the only reference point that is set by DFO's Science Sector (Science). All other reference points are set by fisheries management using information provided by Science as well as other management considerations (DFO 2009; Marentette et al. 2022).

Under DFO's PA policy, provisional reference point values are suggested based on quantities associated with maximum sustainable yield (MSY). Provisional LRP and USRs are $0.4B_{MSY}$ (B_{MSY} = female spawning stock biomass at MSY) and $0.8B_{MSY}$, respectively, while the maximum RR is required to be at or below fishing mortality at maximum sustainable yield (F_{MSY}) with F_{MSY} identified as a provisional value. Alternatives to these provisional quantities can be used when deemed more appropriate due to stock-specific considerations such as data availability or species / ecosystem considerations (DFO 2009).

A range of indicators have been used to define fisheries reference points for Canadian fish stocks. Barrett et al. (2024) provide an overview of methods used to define LRPs in Canada and other jurisdictions, as well as considerations for selecting among methods. Alternatives to MSY-based indicators can include setting reference points based on proportions of unfished female spawning stock biomass (B_0), biomass-based reference points that represent the delineation of stock status into different zones (e.g., setting the LRP at the lowest level observed

for a given biomass indicator) and historical proxies for B_{MSY} based on the mean or median value of an indicator over a historical time period when the indicator is high and catches are high.

The 2009 Petrale Sole assessment pre-dated the development of the DFO PA Policy. Instead, it used historical reference points based on estimated biomass trajectories from 1966 – 2006 due to concerns about the reliability of estimated B_{MSY} and B_0 quantities (Starr 2009). These included a lower biomass reference (Lower B_{REF}) set at the minimum biomass over the 1966-2006 period, a target biomass reference (Target B_{REF}), and a target exploitation rate (U_{REF}) set at the average exploitation rate from 1966 to 2006.

For the current assessment, we set reference points at the provisional MSY-based values identified in the PA policy (Table 3). We do not present the LRP or TRP used for Petrale Sole in 2006 (Limit B_{REF}, Target B_{REF}) because these points no longer appear relevant based on the updated biomass time series. F_{MSY} was estimated by searching across a range of fishing mortality levels, calculating equilibrium *B* and catch at that level, calculating an optimal level using the Newton-Raphson method, and iterating to achieve convergence on the that level. B_{MSY} was the *B* associated with F_{MSY}. See Section 3.1.2 for more discussion of our rationale for presenting stock status and harvest advice relative to MSY-based reference points.

Table 3. Reference points identified in the Precautionary Approach policy and recommended for Petrale Sole in this assessment.

Reference Point	**Value**	**Rationale**
Limit Reference Point (LRP)	$0.4B_{MSY}$	– The indicator used to characterize biomass and associated B_{MSY} is female spawning stock biomass, which represents the reproductive capacity of the stock – Identified as a provisional LRP by the DFO PA Policy (DFO 2009) – B_{MSY} appears to be reliably estimated, with uncertainty to assumed M values accounted for through an ensemble model approach over three different values of M
Upper Stock Reference (USR)	$0.8\ B_{MSY}$	– Identified as a provisional USR by the DFO PA Policy (DFO 2009) – BMSY appears to be reliably estimated, with uncertainty to assumed M values accounted for through an ensemble model approach over three different values of M
Target Biomass	B_{MSY}	– Target is required to be at or above the USR – BMSY is the implied target from a maximum removal reference rate of FMSY
Maximum Removal Reference Rate (Maximum RR)	F_{MSY}	– Identified as a provisional maximum removal reference rate by the DFO PA Policy (DFO 2009) – FMSY appears to be reliably estimated, with uncertainty to assumed M values accounted for through an ensemble model approach over three different values of M

2.5. PROJECTIONS FOR HARVEST ADVICE

Decision tables give the projected stock status and fishing mortality rate relative to reference points under different constant catch harvest policies for the base ensemble model. Uncertainty in M was explicitly addressed by projecting with the base ensemble model, which combined posteriors from models with three different M assumptions. The population was projected for ten years under varying catch levels. Catch in 2024 was assumed to be equivalent to the catch level in 2023 (769.31 t). Catch levels from 2025 – 2034 ranged from 0 to 2000 t in increments of 250 t and were held constant among years throughout the projections. Selectivity, length-at-age, weight-length, and maturity-at-age assumptions used in the forecast period were the same as in the base ensemble stock assessment model. Recruitment was predicted from the spawner-recruit curve based on average mean recruitment (R_0), which is consistent with the approach used for recent British Columbia rockfish projections (Starr and Haigh 2022, 2023). A mean of recent recruitment estimates was not used as recruitment in the projections due to the uncertainty of recent recruitment estimates due to a lack of recent age data.

2.6. ENVIRONMENTAL CONDITIONS AND SPECIES BIOLOGY

2.6.1. Bayesian time-series regressions

To assess possible impacts of environmental conditions on Petrale Sole, we considered both recruitment and body condition as biological responses. For recruitment, we used 100 MCMC samples of the recruitment deviations from the model with a M assumption of 0.154 from the ensemble base model. We restricted this analysis to the period from 1995 to 2018 for which age data with the potential to inform recruitment estimates were available. Body condition was characterized using Le Cren's deviations from sex-specific estimated length-whole body weight relationships (Le Cren 1951). We first separated individuals and overall survey catches into immature, mature male, and mature female categories using an estimated length at 50% reproductive maturity. For each portion of the population (immature, mature males, mature females), we then estimated independent spatiotemporal biomass distributions, calculated Le Cren's relative deviations from the observed length-weight relationship, modelled spatiotemporal change in these deviations, and generated a density-weighted annual index of average condition for each category. To propagate uncertainty through subsequent analyses, w\e then took 100 samples of this overall condition index by constructing it with 100 samples from the joint parameter precision matrix.

For each recruitment and body condition time series sample (100 pairs per year), we tested the correlation between these biological responses and a range of environmental or ecosystem indices that were hypothesized to be important for Petrale Sole based on life history knowledge and existing literature (see Appendix I) and between mature body condition and a paired time series for recruitment in the following year. Correlations were tested using a Bayesian implementation of a time-series regression. Tests were first conducted on the median estimates for each variable combination to confirm convergence and then repeated for each sample (or pair of samples) from the input models. We then combined the posteriors from all the regressions across samples to derive posterior distributions that accounted for uncertainty in both the initial models and the regression model. Splitting of survey catches into sex and maturity classes and generation of annual body condition indices are described in Appendix J. Full description of Bayesian time-series regression and the details of all the following data sources are provided in Appendix I. The code that underlies both Appendices I and J is available upon request.

2.6.3. Environmental conditions potentially impacting demersal juvenile and adult body condition

We hypothesized that a more limited set of climate and biotic indices were likely to influence body condition of demersal juveniles and adults. Here, we focused on mean sea floor oxygen concentration and mean sea floor temperature for the period immediately prior to or overlapping most of the synoptic surveys (Apr–Jun) and at the depths where 95% of this species' biomass is captured on these surveys (50–200m). We again tested for relationships with total inshore euphausiid biomass, biomass of the dominant species, *Euphausia pacifica*, and of depth-integrated primary production. PDO and North Pacific Gyre Oscillation (NPGO) during this spring period were also included as potential indicators of correlated oceanographic conditions that could suggest the importance of variables not included in our analysis.

3. RESULTS

3.1. MODEL DIAGNOSTICS

3.1.1. Index fits

Fits to the survey indices for each model were acceptable (Figure 4 – Figure 6). SDNRs were all close to 1, suggesting the models were fitting the survey indices as well as expected given the assumed (and estimated) variance. The tests also suggested that the signs of the residuals were generally random with respect to time, the one exception being for the highM model fit to the QCS survey index (whose p-value was <0.05).

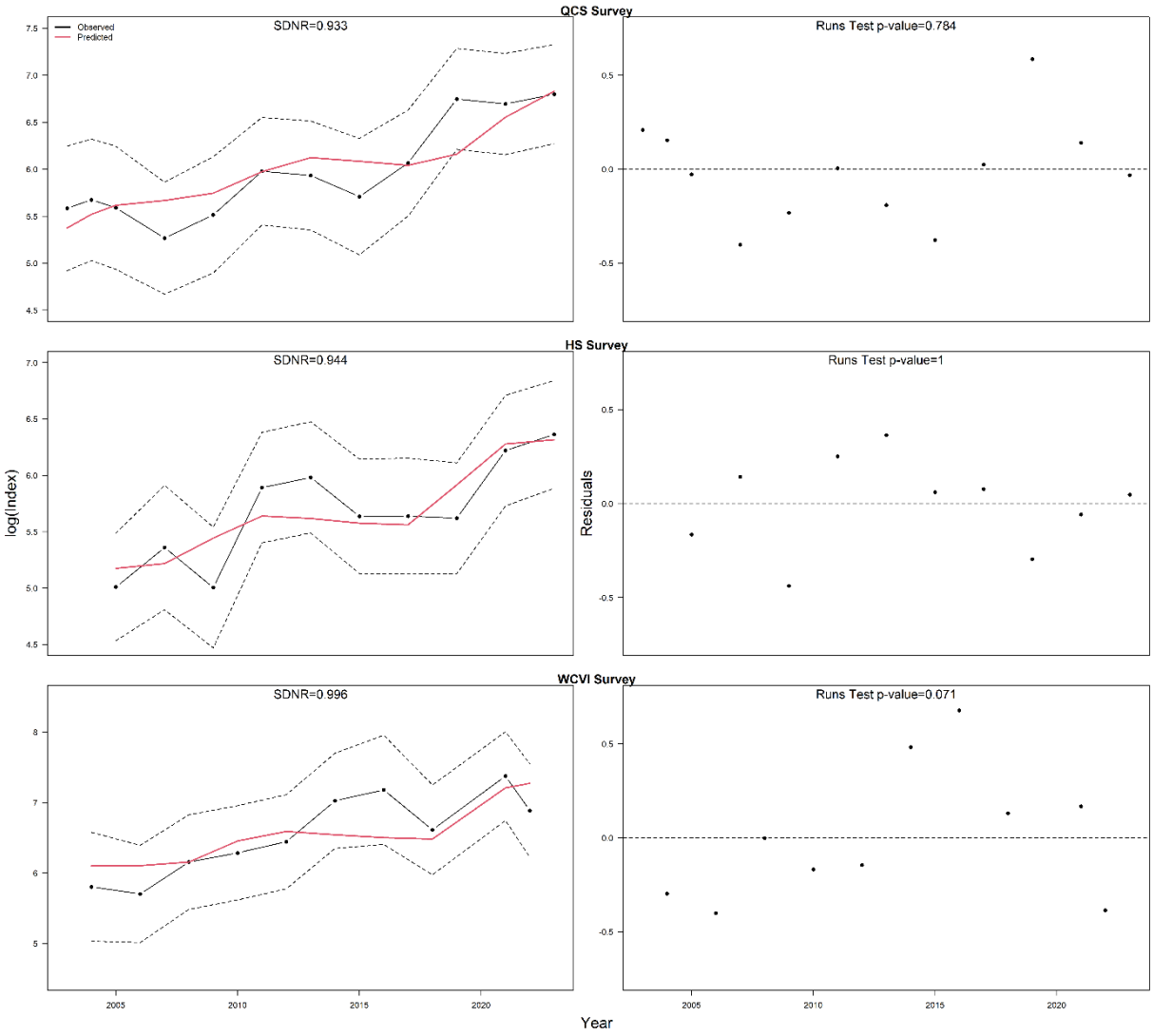


Figure 4. Fits to the survey indices for the baseM assessment model with M=0.154. The red line depicts the median predicted index from the baseM assessment model with M=0.154. The solid black line depicts the standardized survey index and the dotted line depicts the 95% confidence interval of the data calculated using the SEs from the standardization and an additive parameter estimated within the assessment. The label SDNR references the standard deviation of the normalized residuals, and the runs test p-value references a p-value from a runs test to assess whether the sign of the residuals is random with respect to time.

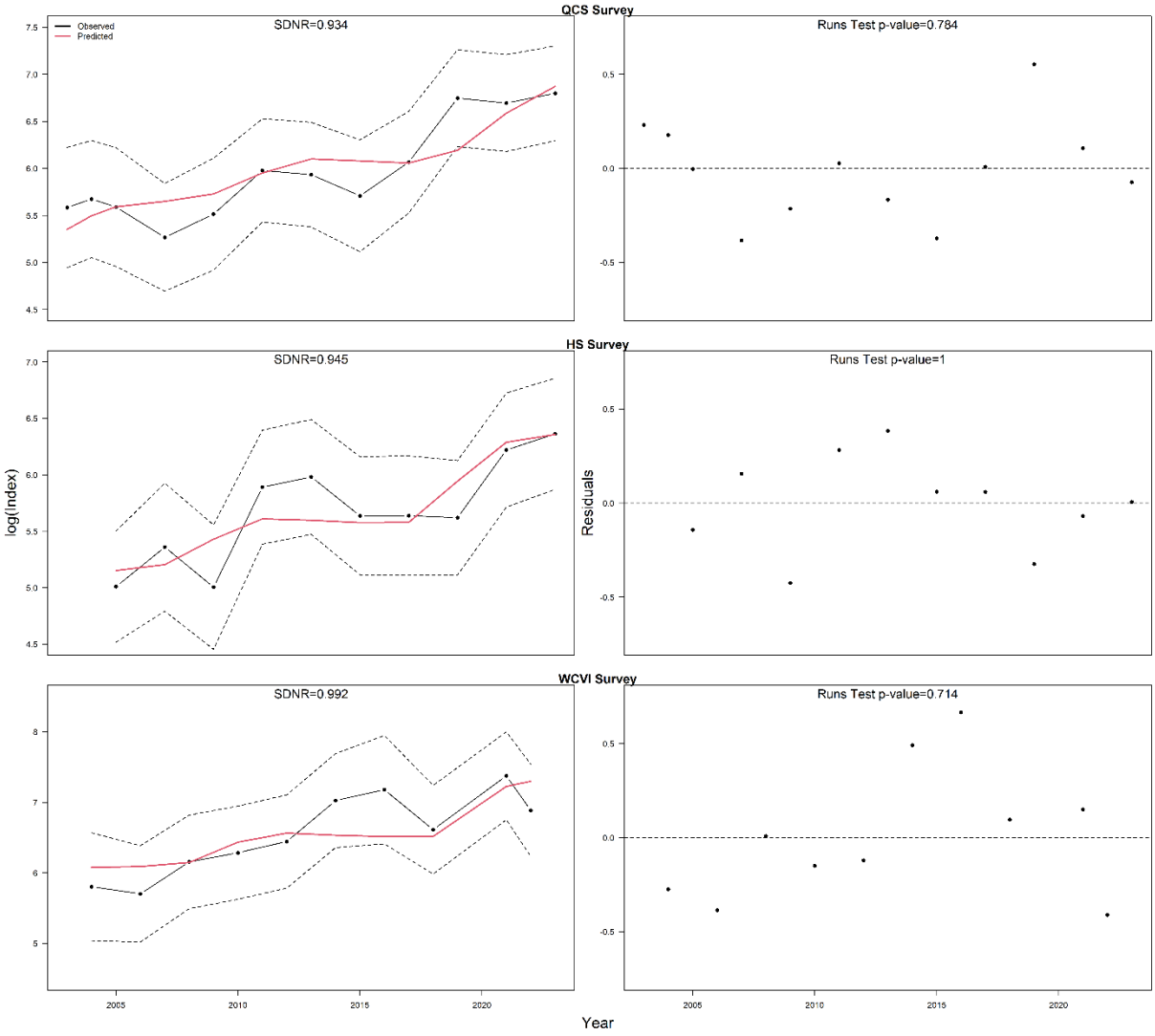


Figure 5. Fits to the survey indices for the lowM assessment model with M=0.124. The red line depicts the median predicted index from the lowM assessment model with M=0.124. The solid black line depicts the standardized survey index and the dotted line depicts the 95% confidence interval of the data calculated using the SEs from the standardization and an additive parameter estimated within the assessment. The label SDNR references the standard deviation of the normalized residuals, and the runs test p-value references a p-value from a runs test to assess whether the sign of the residuals is random with respect to time.

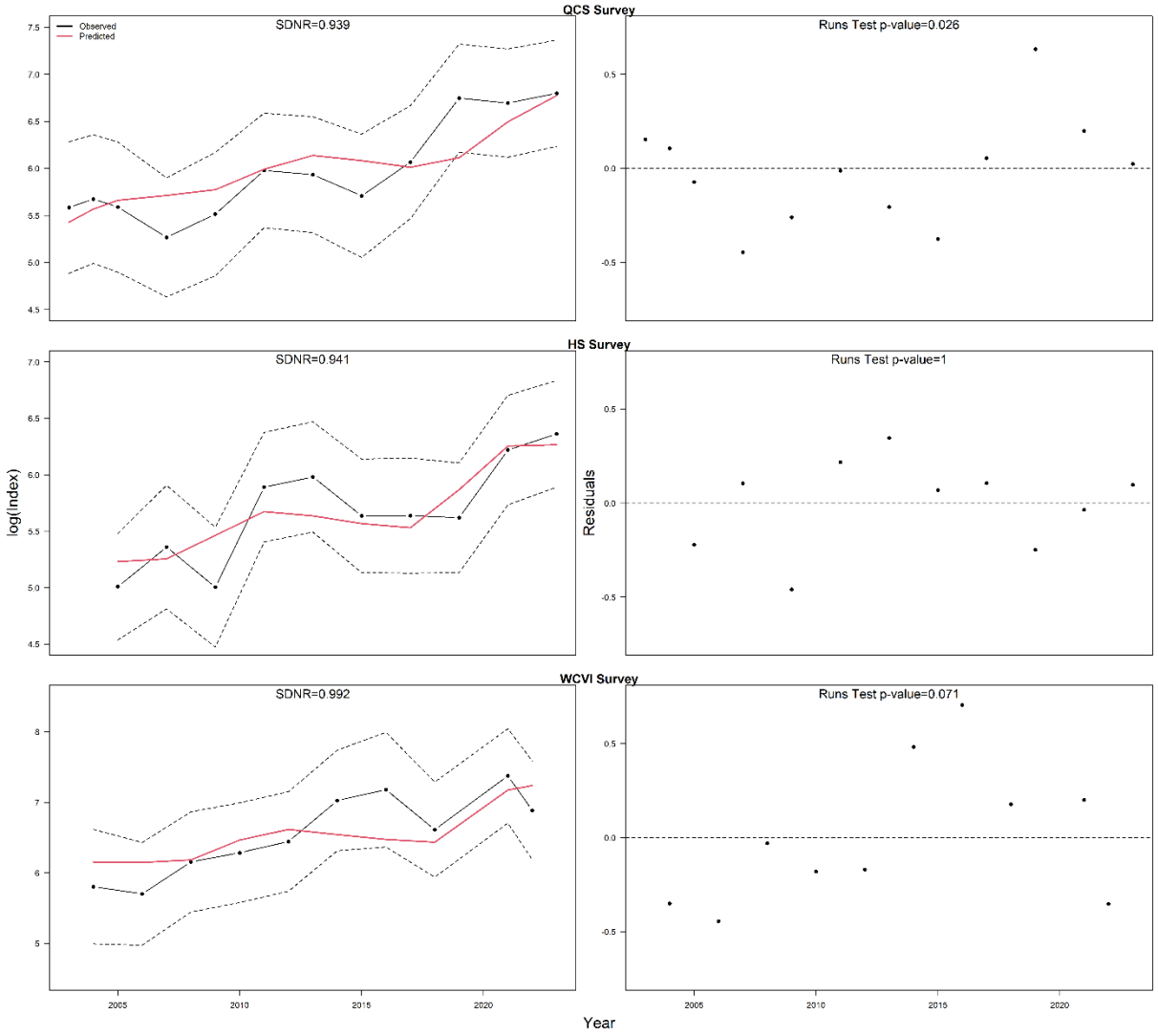


Figure 6. Fits to the survey indices for the highM assessment model with M=0.184. The red line depicts the median predicted index from the highM assessment model with M=0.184. The solid black line depicts the standardized survey index and the dotted line depicts the 95% confidence interval of the data calculated using the SEs from the standardization and an additive parameter estimated within the assessment. The label SDNR references the standard deviation of the normalized residuals, and the runs test p-value references a p-value from a runs test to assess whether the sign of the residuals is random with respect to time.

3.1.2. Composition fits

Composition fits for each model were deemed acceptable for the most part, with the exception of the fits to the QCS survey age compositions (Figure - Figure). Although the fits for QCS look visually acceptable (Figure , Figure , Figure 25), the OSA residuals and the resulting quantile-quantile plots for these residuals suggest misfit to the survey in each of the three individual models comprising the ensemble (Figure 10, Figure, Figure 26). This was likely a function of a consistent negative bias in the expected mean age of the composition for the QCS survey relative to that observed, largely driven by underestimating the composition of the plus group

Composition fits for each model were deemed acceptable for the most part, with the exception of the fits to the QCS survey age compositions (Figure 7 – Figure 30). Although the fits for QCS

look visually acceptable (Figure 9, Figure 17, Figure 25), the OSA residuals and the resulting quantile-quantile plots for these residuals suggest misfit to the survey in each of the three individual models comprising the ensemble (Figure 10, Figure 18, Figure 26). This was likely a function of a consistent negative bias in the expected mean age of the composition for the QCS survey relative to that observed, largely driven by underestimating the composition of the plus group.

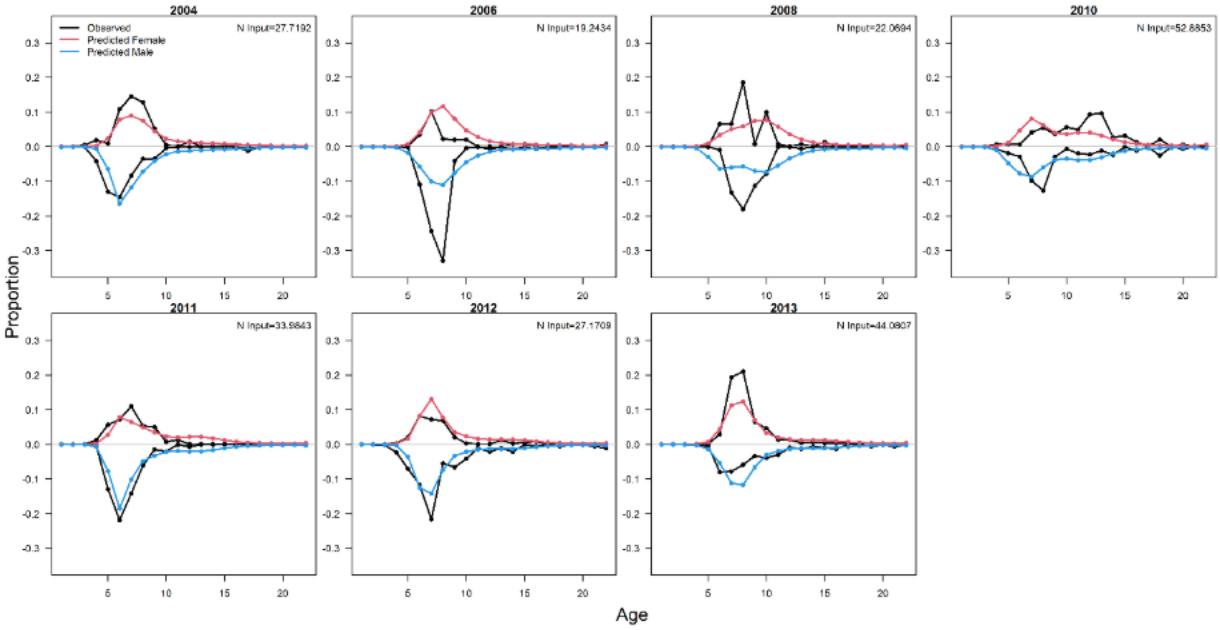


Figure 7. Fits to the fishery age composition data for the baseM assessment model with M=0.154. Shown are the medians of the posterior distribution for the predicted age composition in each year of available fishery age composition data. Depicted in red are the predicted female compositions and in blue the predicted male compositions. The label "N Input" denotes the input sample size determined based on the bootstrap procedure (Appendix B.4.2).

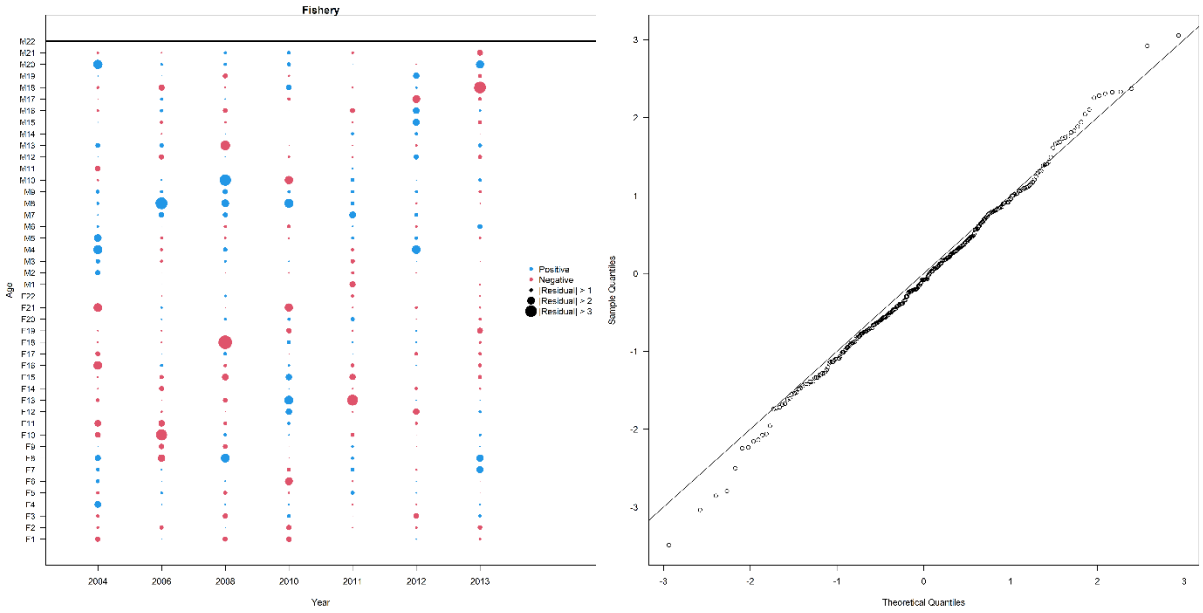


Figure 8. One-Step-Ahead (OSA) residuals for fits to the fishery age composition data for the baseM assessment model with M=0.154. Depicted are the residuals at the medians of the posterior distribution. The ages are labeled F1-F22 for females and M1-M22 for males. OSA residuals are calculated for the number of bins – 1, thus the final bin "M22" does not contain OSA residuals in this case. OSA residuals will be distributed iid standard normal, within and among years, under a correctly specified model and assuming that the last bin fits perfectly. When the absolute residuals are larger than 3 or there are clear correlations or other patterns across ages/years, then the assumption is likely violated and interpreted as model misfit.

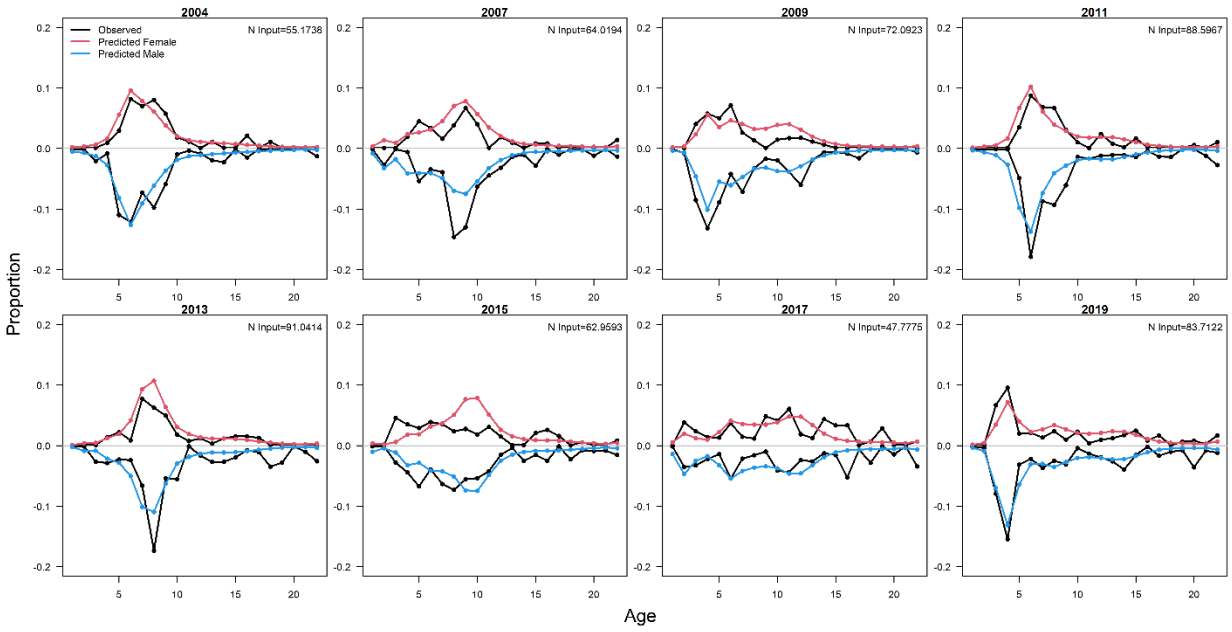


Figure 9. Fit to age composition data for the Queen Charlotte Sound survey data for the baseM assessment model with M=0.154. Shown are the medians of the posterior distribution for the predicted age composition in each year of available Queen Charlotte Sound survey age composition data. Depicted in red are the predicted female compositions and in blue the predicted male compositions. The label "N Input" denotes the input sample size determined based on the bootstrap procedure (Appendix B.4.2).

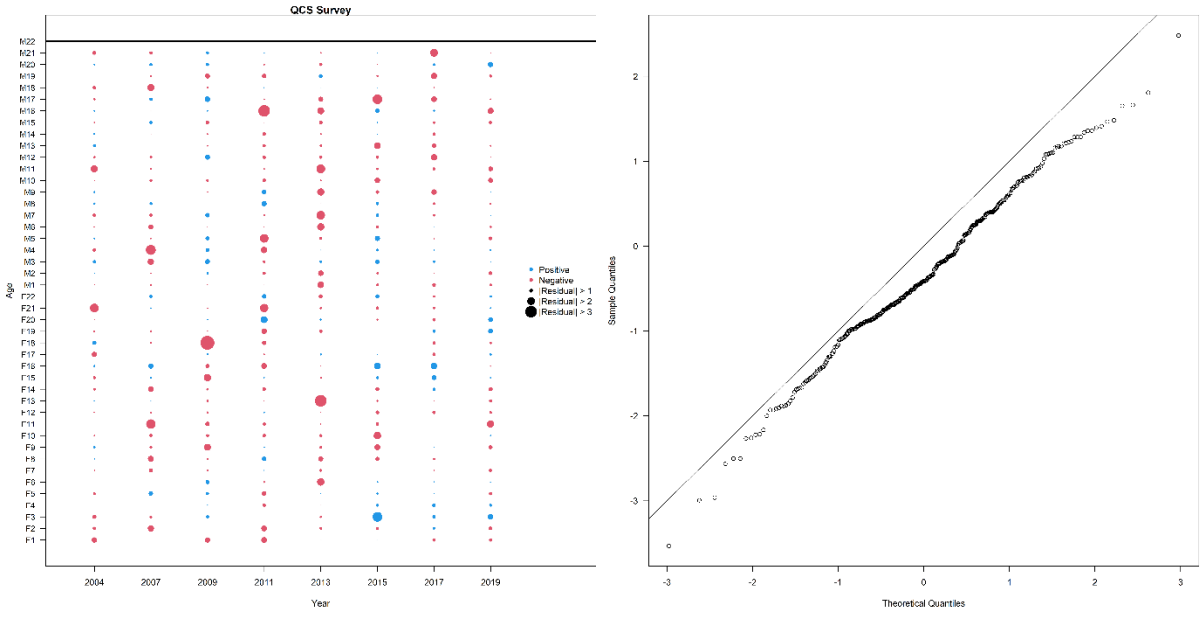


Figure 10. OSA residuals for fits to the Queen Charlotte Sound survey age composition data for the baseM assessment model with M=0.154. Depicted are the residuals at the medians of the posterior distribution. The ages are labeled F1-F22 for females and M1-M22 for males.

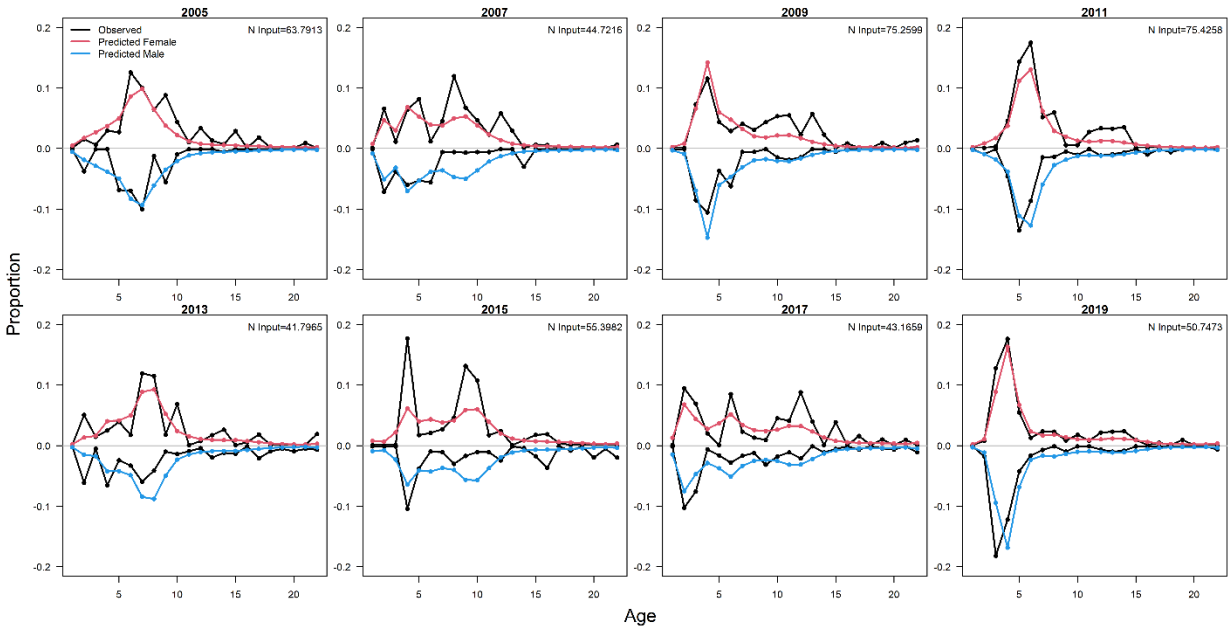


Figure 11. Fit to age composition data for Hecate Strait survey data for the baseM assessment model with M=0.154. Shown are the medians of the posterior distribution for the predicted age composition in each year of available Hecate Strait survey age composition data. Depicted in red are the predicted female compositions and in blue the predicted male compositions. The label "N Input" denotes the input sample size determined based on the bootstrap procedure (Appendix B.4.2).

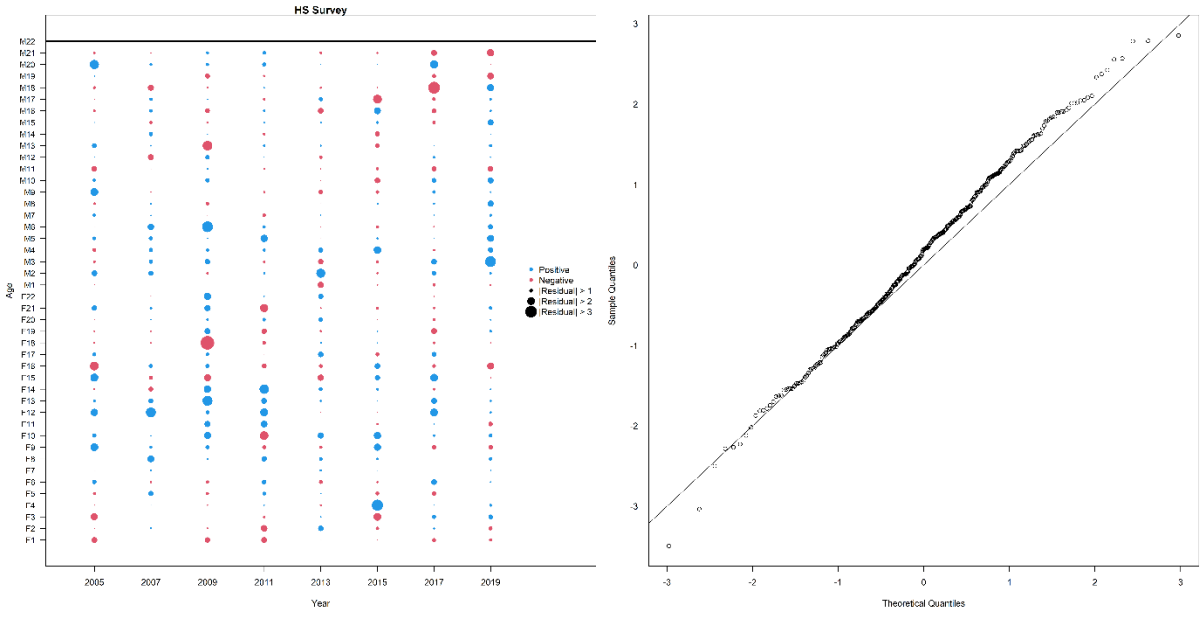


Figure 12. OSA residuals for fits to the Hecate Strait survey age composition data for the baseM assessment model with M=0.154. Depicted are the residuals at the medians of the posterior distribution. The ages are labeled F1-F22 for females and M1-M22 for males. OSA residuals are calculated for the number of bins – 1, thus the final bin "M22" does not contain OSA residuals in this case.

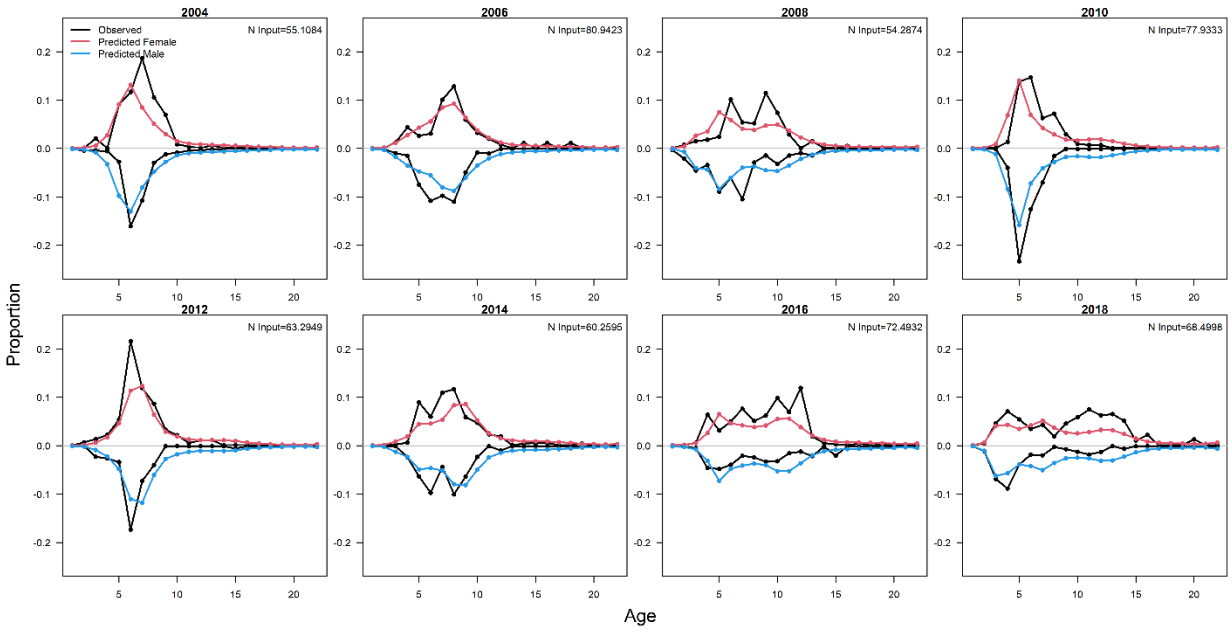


Figure 13. Fit to age composition data for West Coast Vancouver Island survey for the baseM assessment model with M=0.154. Shown are the medians of the posterior distribution for the predicted age composition in each year of available West Coast Vancouver Island survey age composition data. Depicted in red are the predicted female compositions and in blue the predicted male compositions. The label "N Input" denotes the input sample size determined based on the bootstrap procedure (Appendix B.4.2).

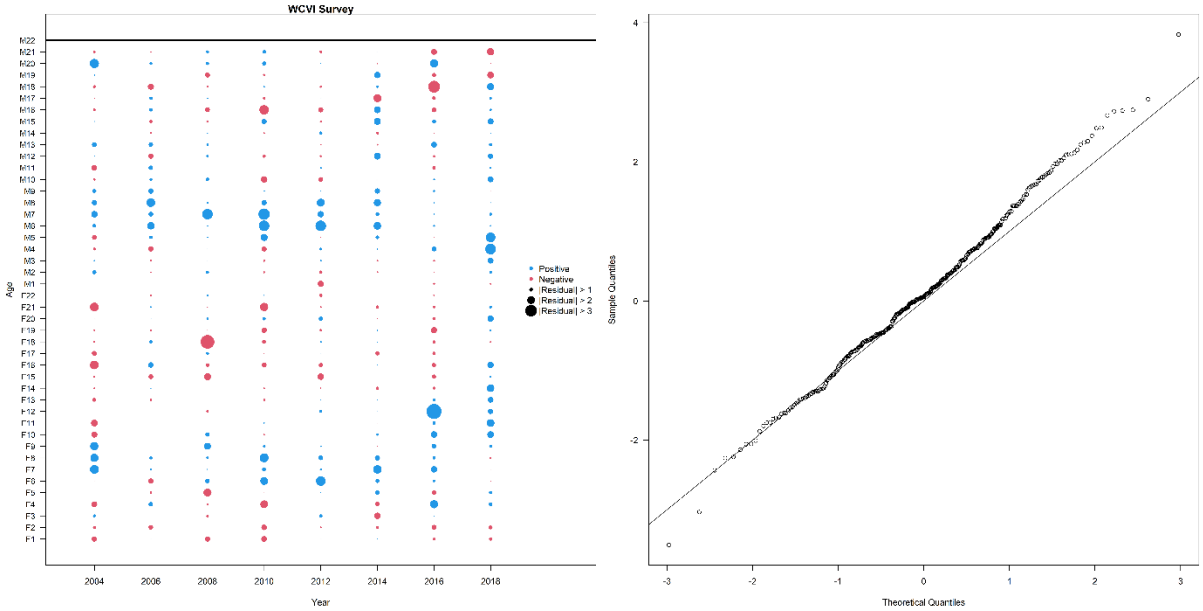


Figure 14. OSA residuals for fits to the West Coast of Vancouver Island survey age composition data. Depicted are the residuals at the medians of the posterior distribution. The ages are labeled F1-F22 for females and M1-M22 for males. OSA residuals are calculated for the number of bins – 1, thus the final bin "M22" does not contain residuals in this case.

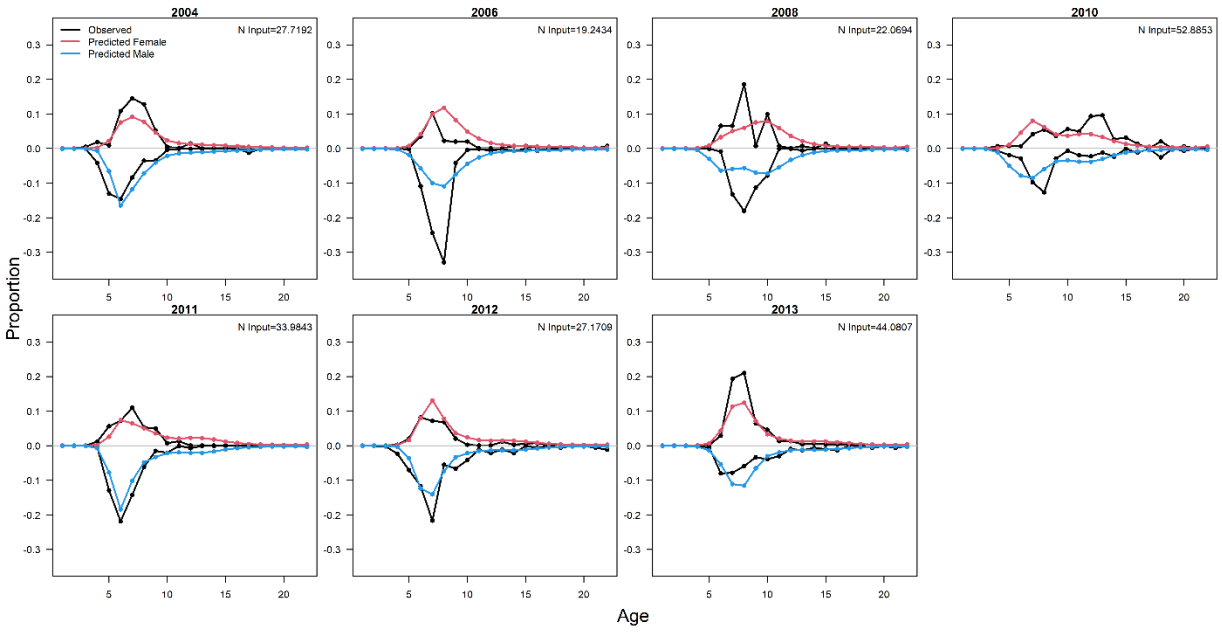


Figure 15. Fits to the fishery age composition data for the lowM assessment model with M=0.124. Shown are the medians of the posterior distribution for the predicted age composition in each year of available fishery age composition data. Depicted in red are the predicted female compositions and in blue the predicted male compositions. The label "N Input" denotes the input sample size determined based on the bootstrap procedure (Appendix B.4.2).

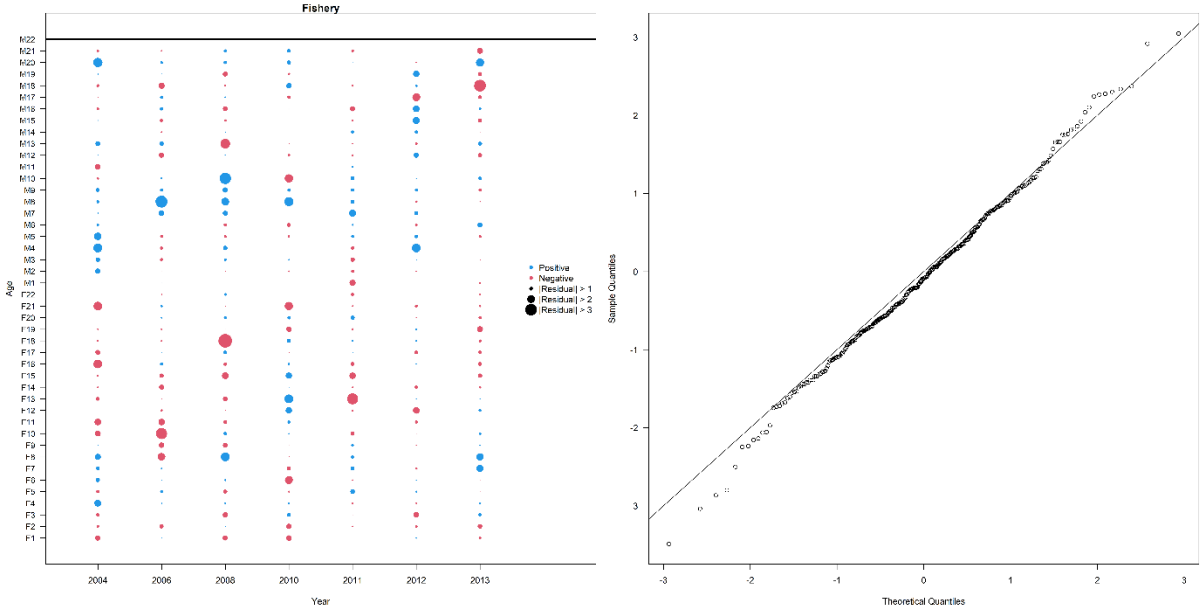


Figure 16. One-Step-Ahead (OSA) residuals for fits to the fishery age composition data for the lowM assessment model with M=0.124. Depicted are the residuals at the medians of the posterior distribution. The ages are labeled F1-F22 for females and M1-M22 for males. OSA residuals are calculated for the number of bins – 1, thus the final bin "M22" does not contain OSA residuals in this case.

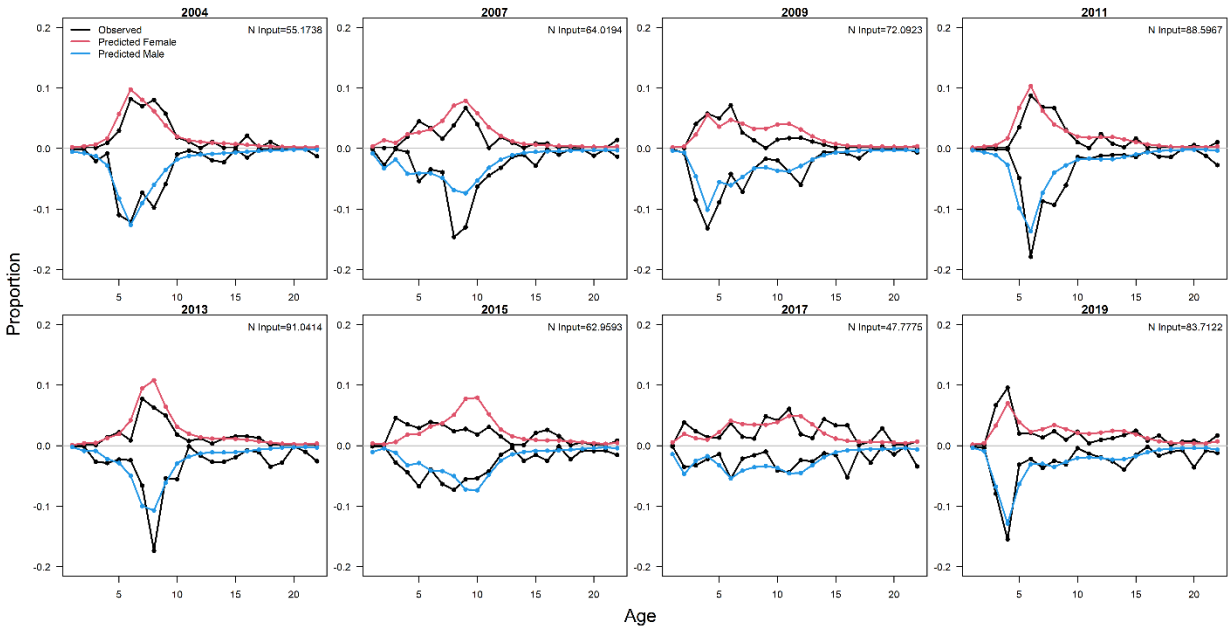


Figure 17. Fits to the QCS survey age composition data for the lowM assessment model with M=0.124. Shown are the medians of the posterior distribution for the predicted age composition in each year of available fishery age composition data. Depicted in red are the predicted female compositions and in blue the predicted male compositions. The label "N Input" denotes the input sample size determined based on the bootstrap procedure (Appendix B.4.2).

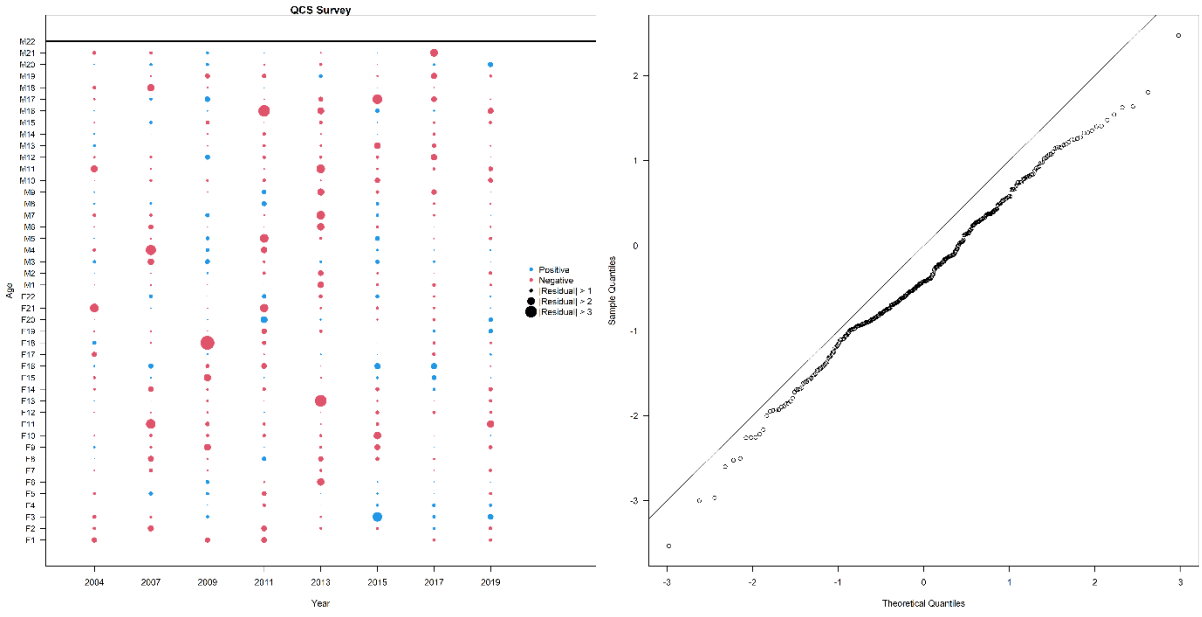


Figure 18. One-Step-Ahead (OSA) residuals for fits to the QCS survey age composition data for the lowM assessment model with M=0.124. Depicted are the residuals at the medians of the posterior distribution. The ages are labeled F1-F22 for females and M1-M22 for males. OSA residuals are calculated for the number of bins – 1, thus the final bin "M22" does not contain OSA residuals in this case.

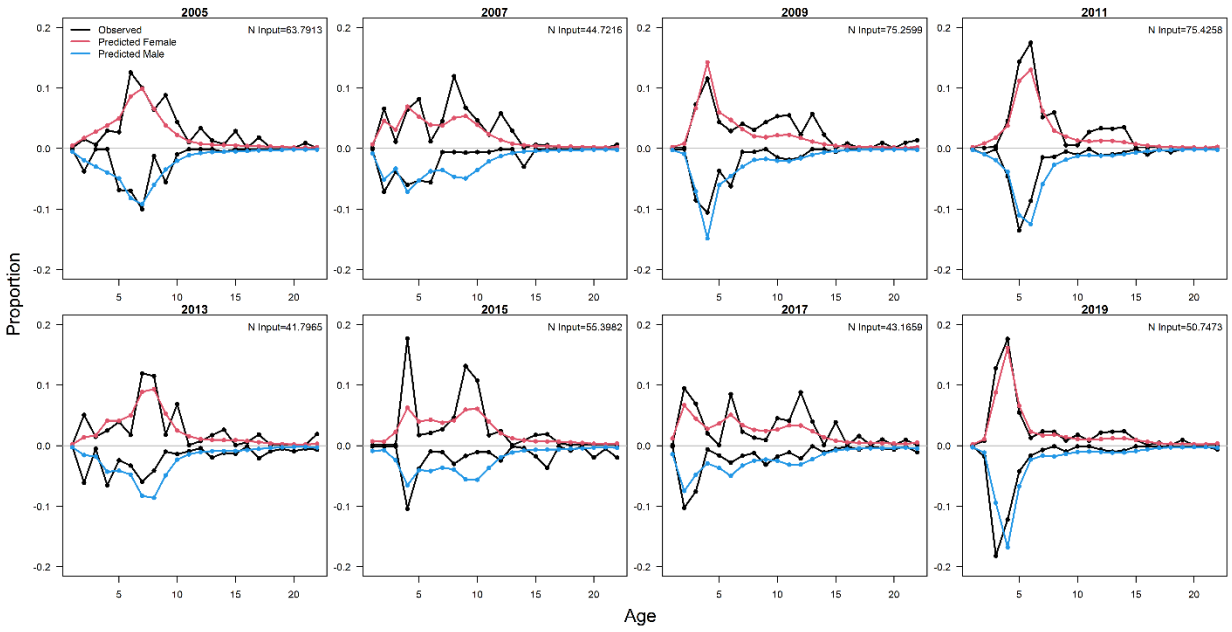


Figure 19. Fits to the HS survey age composition data for the lowM assessment model with M=0.124. Shown are the medians of the posterior distribution for the predicted age composition in each year of available fishery age composition data. Depicted in red are the predicted female compositions and in blue the predicted male compositions. The label "N Input" denotes the input sample size determined based on the bootstrap procedure (Appendix B.4.2).

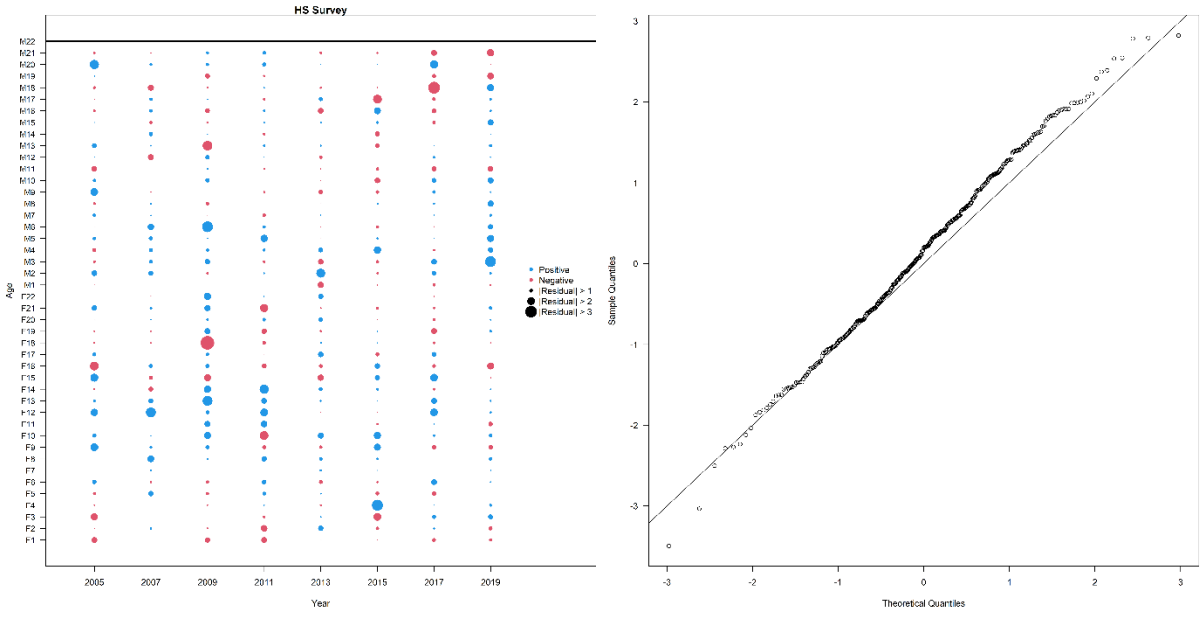


Figure 20. One-Step-Ahead (OSA) residuals for fits to the HS survey age composition data for the lowM assessment model with M=0.124. Depicted are the residuals at the medians of the posterior distribution. The ages are labeled F1-F22 for females and M1-M22 for males. OSA residuals are calculated for the number of bins – 1, thus the final bin "M22" does not contain OSA residuals in this case.

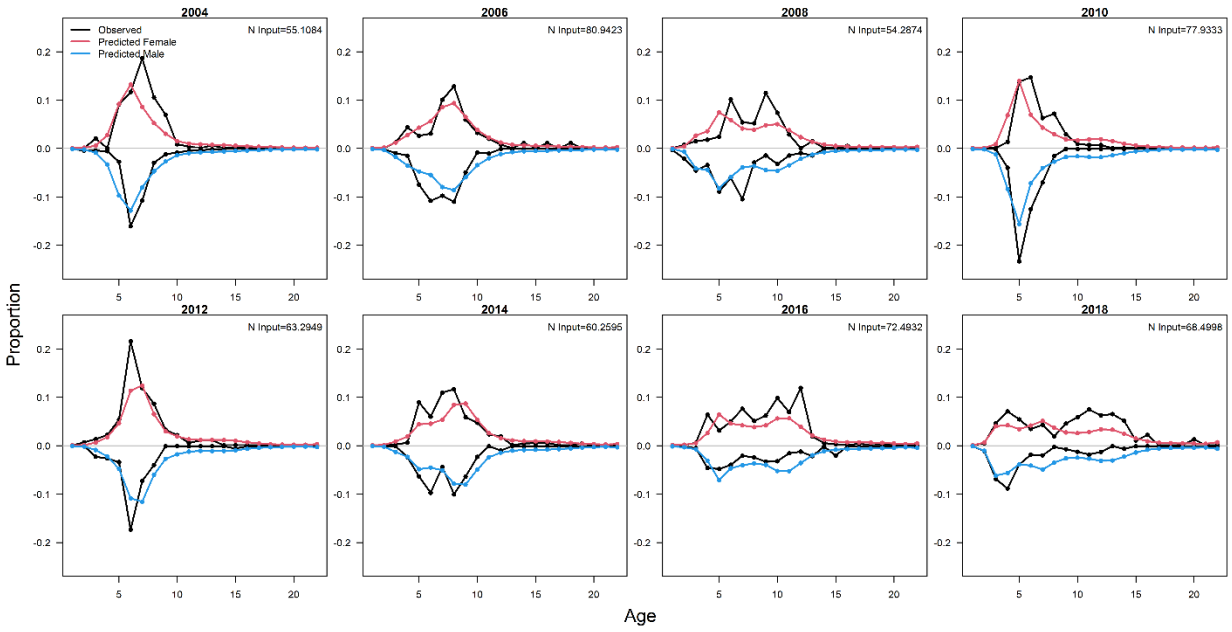


Figure 21. Fits to the WCVI survey age composition data for the lowM assessment model with M=0.124. Shown are the medians of the posterior distribution for the predicted age composition in each year of available fishery age composition data. Depicted in red are the predicted female compositions and in blue the predicted male compositions. The label "N Input" denotes the input sample size determined based on the bootstrap procedure (Appendix B.4.2).

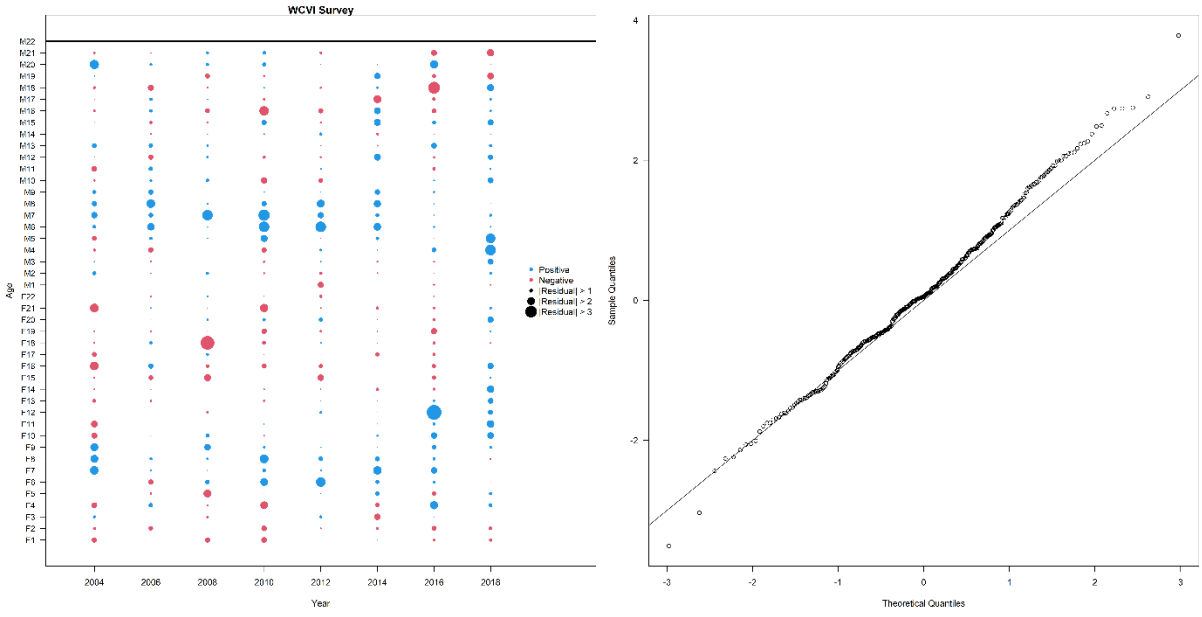


Figure 22. One-Step-Ahead (OSA) residuals for fits to the WCVI age composition data for the lowM assessment model with M=0.124. Depicted are the residuals at the medians of the posterior distribution. The ages are labeled F1-F22 for females and M1-M22 for males. OSA residuals are calculated for the number of bins – 1, thus the final bin "M22" does not contain OSA residuals in this case.

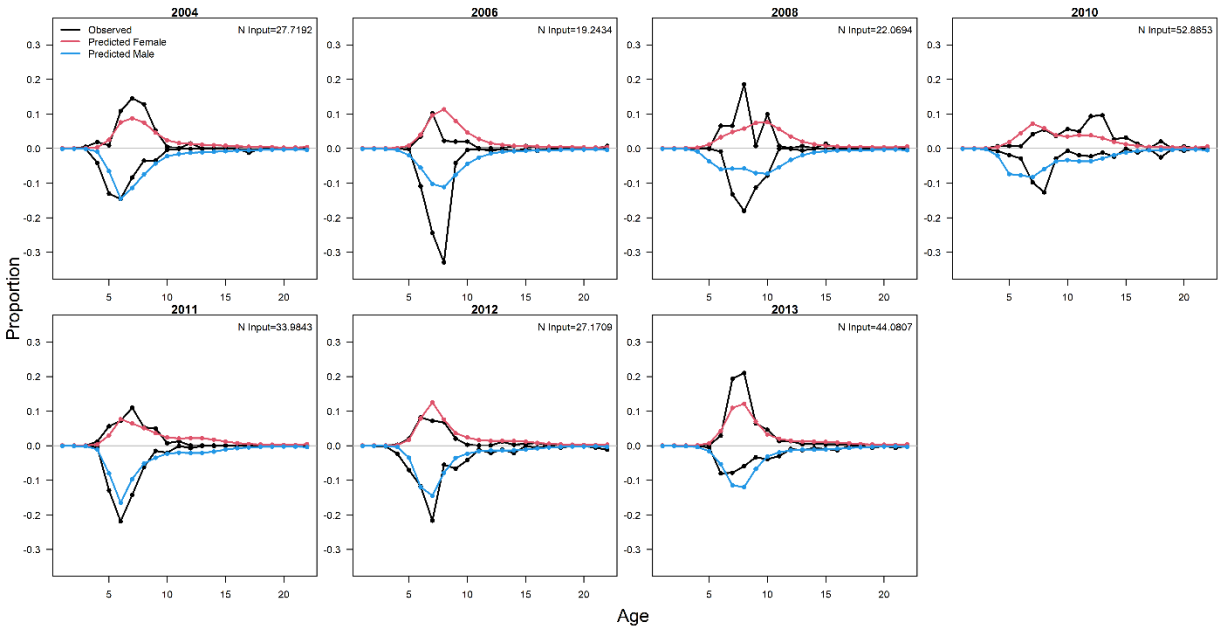


Figure 23. Fits to the fishery age composition data for the highM assessment model with M=0.184. Shown are the medians of the posterior distribution for the predicted age composition in each year of available fishery age composition data. Depicted in red are the predicted female compositions and in blue the predicted male compositions. The label "N Input" denotes the input sample size determined based on the bootstrap procedure (Appendix B.4.2).

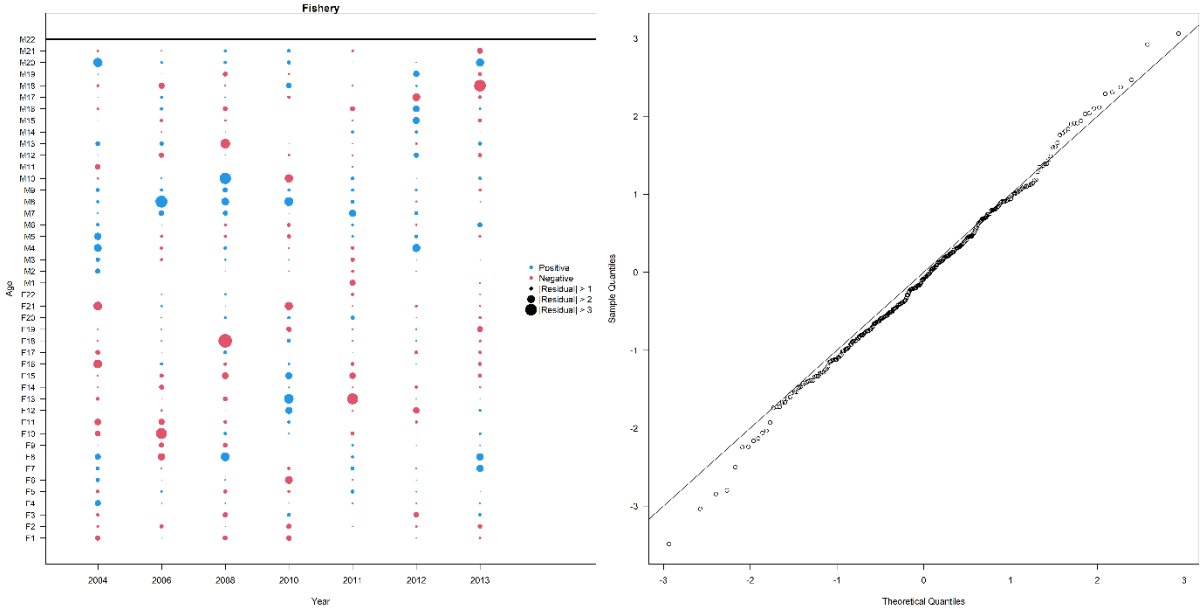


Figure 24. One-Step-Ahead (OSA) residuals for fits to the fishery age composition data for the highM assessment model with M=0.184. Depicted are the residuals at the medians of the posterior distribution. The ages are labeled F1-F22 for females and M1-M22 for males. OSA residuals are calculated for the number of bins – 1, thus the final bin "M22" does not contain OSA residuals in this case.

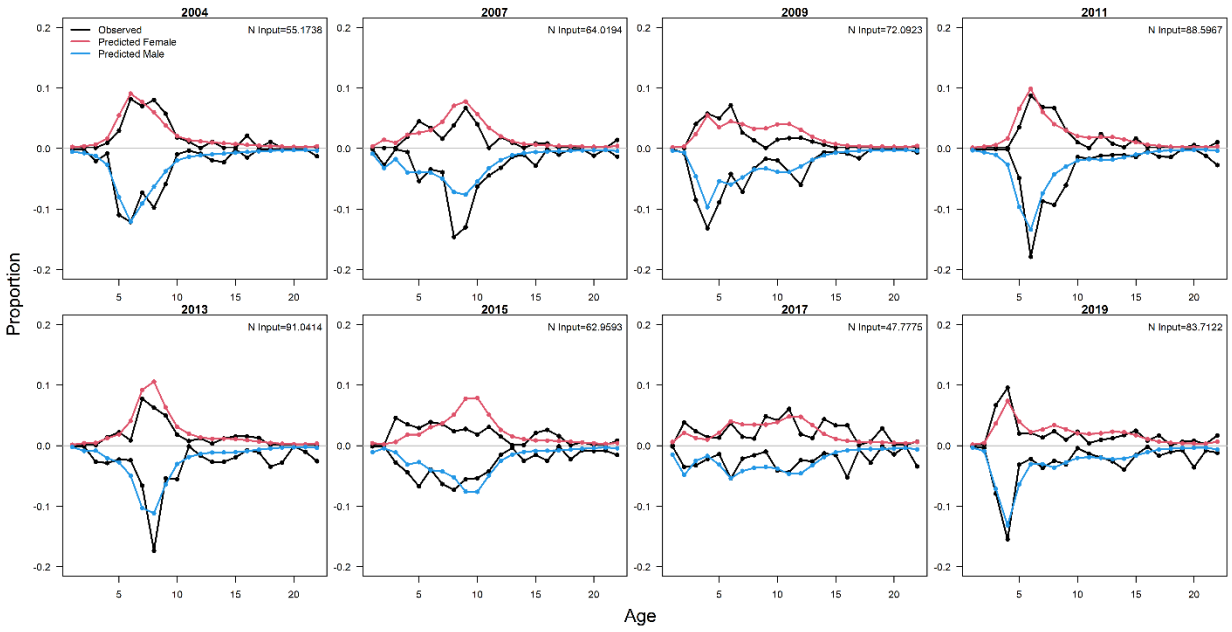


Figure 25. Fits to the QCS survey age composition data for the highM assessment model with M=0.184. Shown are the medians of the posterior distribution for the predicted age composition in each year of available fishery age composition data. Depicted in red are the predicted female compositions and in blue the predicted male compositions. The label "N Input" denotes the input sample size determined based on the bootstrap procedure (Appendix B.4.2).

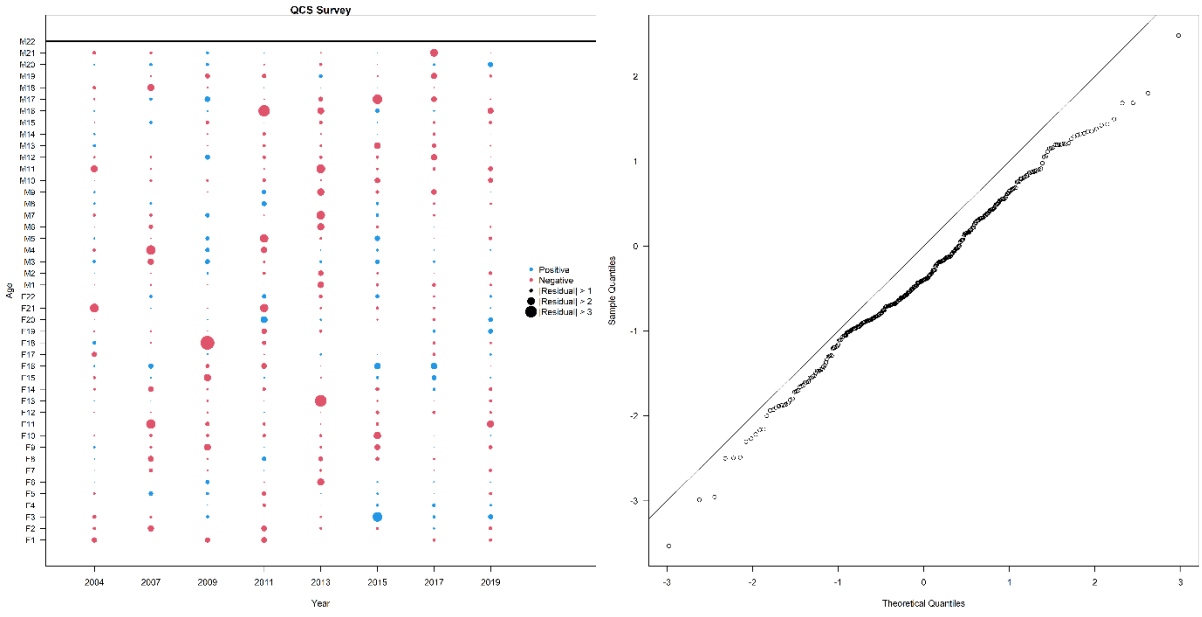


Figure 26. One-Step-Ahead (OSA) residuals for fits to the QCS survey age composition data for the highM assessment model with M=0.184. Depicted are the residuals at the medians of the posterior distribution. The ages are labeled F1-F22 for females and M1-M22 for males. OSA residuals are calculated for the number of bins – 1, thus the final bin "M22" does not contain OSA residuals in this case.

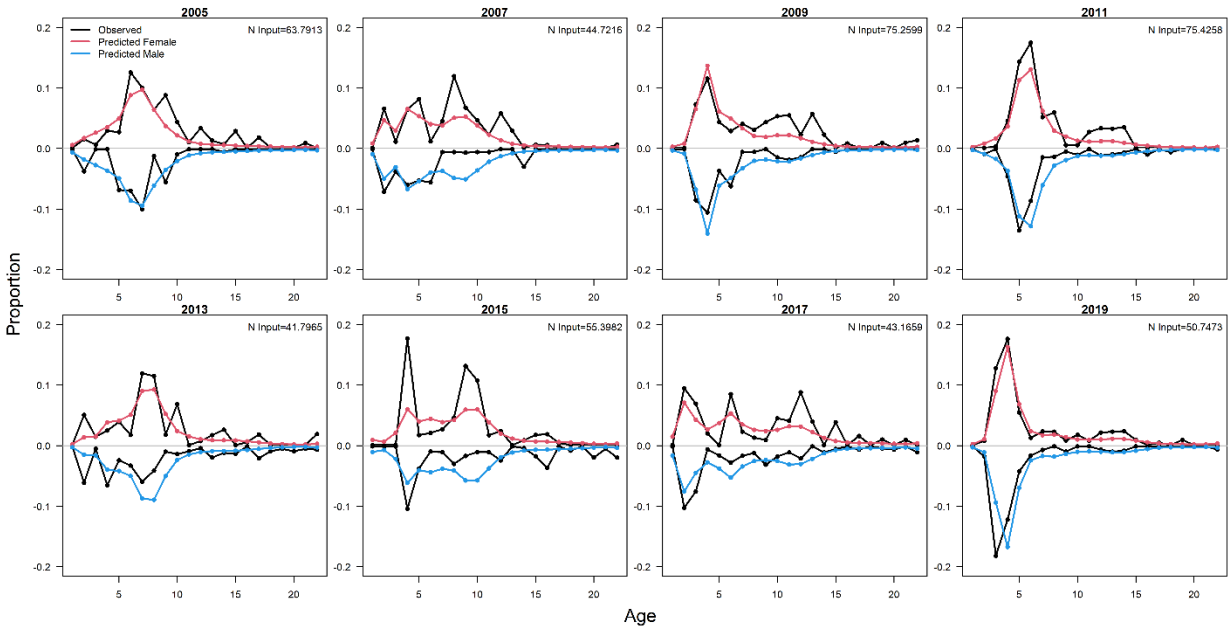


Figure 27. Fits to the HS survey age composition data for the highM assessment model with M=0.184. Shown are the medians of the posterior distribution for the predicted age composition in each year of available fishery age composition data. Depicted in red are the predicted female compositions and in blue the predicted male compositions. The label "N Input" denotes the input sample size determined based on the bootstrap procedure (Appendix B.4.2).

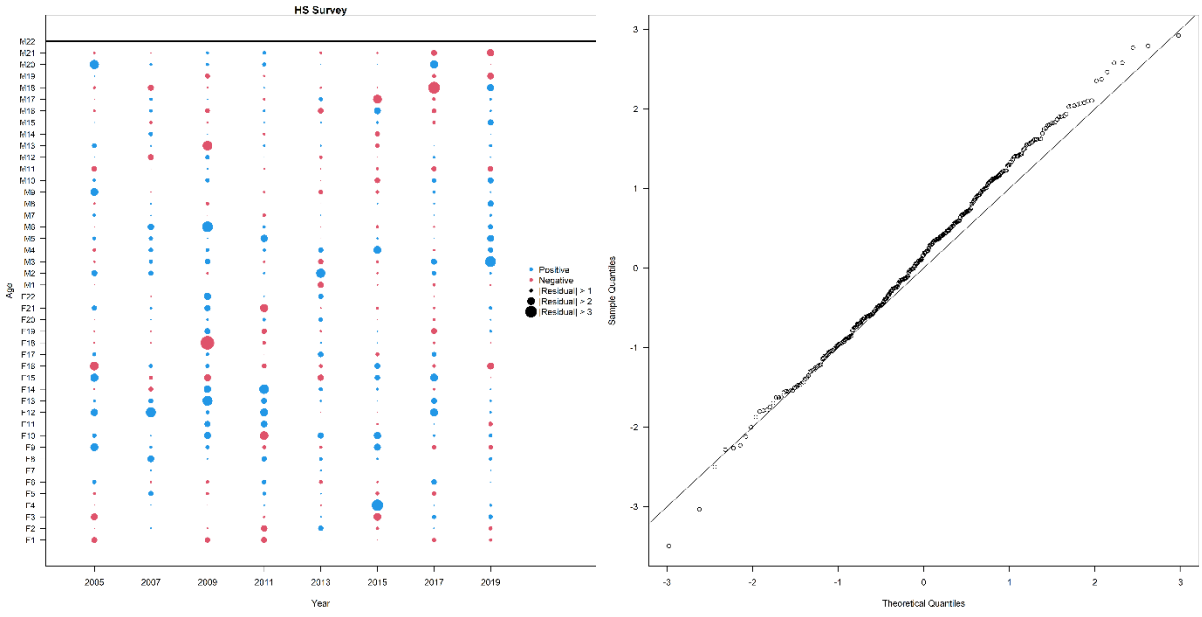


Figure 28. One-Step-Ahead (OSA) residuals for fits to the HS survey age composition data for the highM assessment model with M=0.184. Depicted are the residuals at the medians of the posterior distribution. The ages are labeled F1-F22 for females and M1-M22 for males. OSA residuals are calculated for the number of bins – 1, thus the final bin "M22" does not contain OSA residuals in this case.

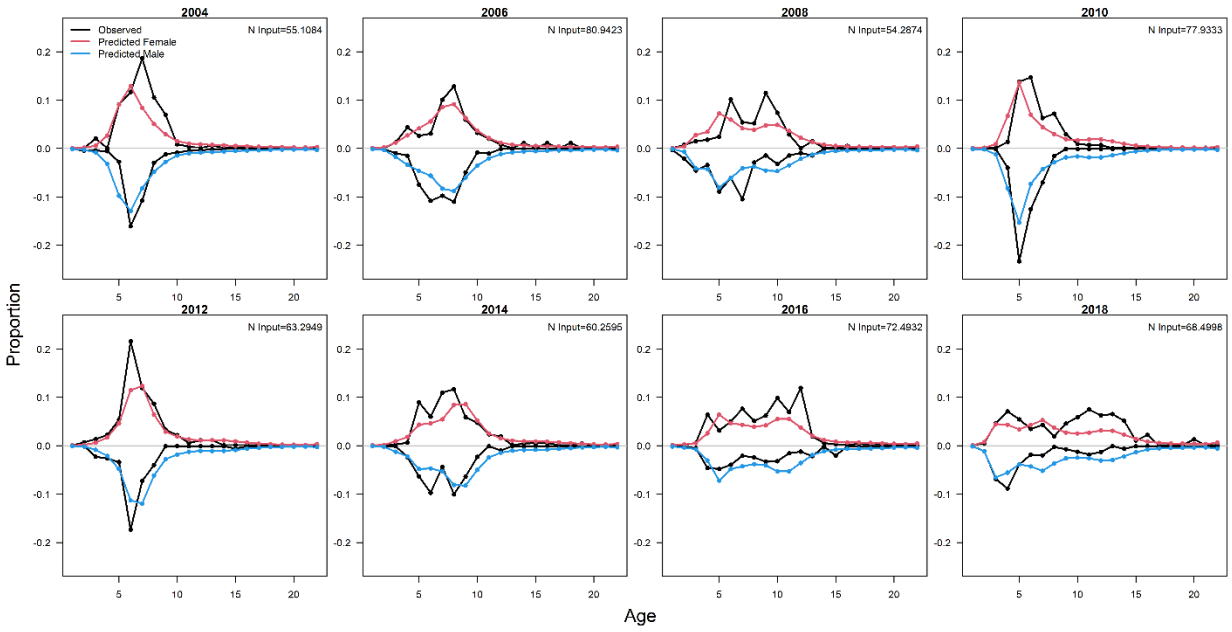


Figure 29. Fits to the WCVI survey age composition data for the highM assessment model with M=0.184. Shown are the medians of the posterior distribution for the predicted age composition in each year of available fishery age composition data. Depicted in red are the predicted female compositions and in blue the predicted male compositions. The label "N Input" denotes the input sample size determined based on the bootstrap procedure (Appendix B.4.2).

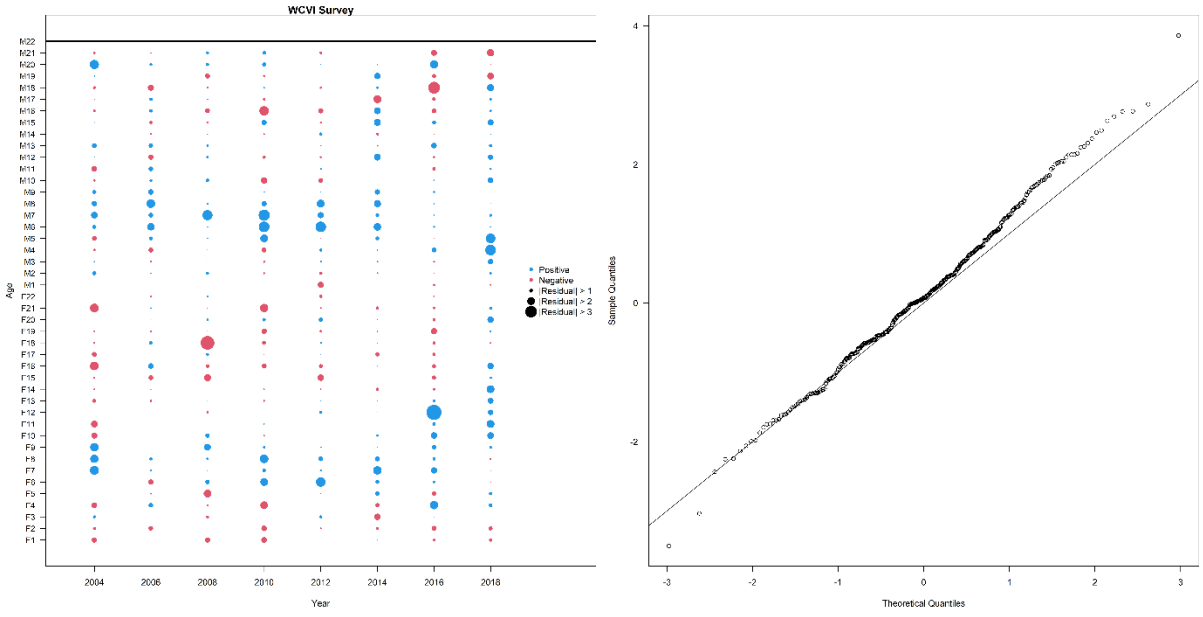


Figure 30. One-Step-Ahead (OSA) residuals for fits to the WCVI age composition data for the highM assessment model with M=0.184. Depicted are the residuals at the medians of the posterior distribution. The ages are labeled F1-F22 for females and M1-M22 for males. OSA residuals are calculated for the number of bins – 1, thus the final bin "M22" does not contain OSA residuals in this case.

3.1.3 Retrospective Analysis

Retrospective patterns for each model were minimal (Figures 31-36). Mohn's rho was low for each derived quantity, well within bounds deemed a possible cause for concern in retrospective analyses (Hurtado-ferro et al. 2015).

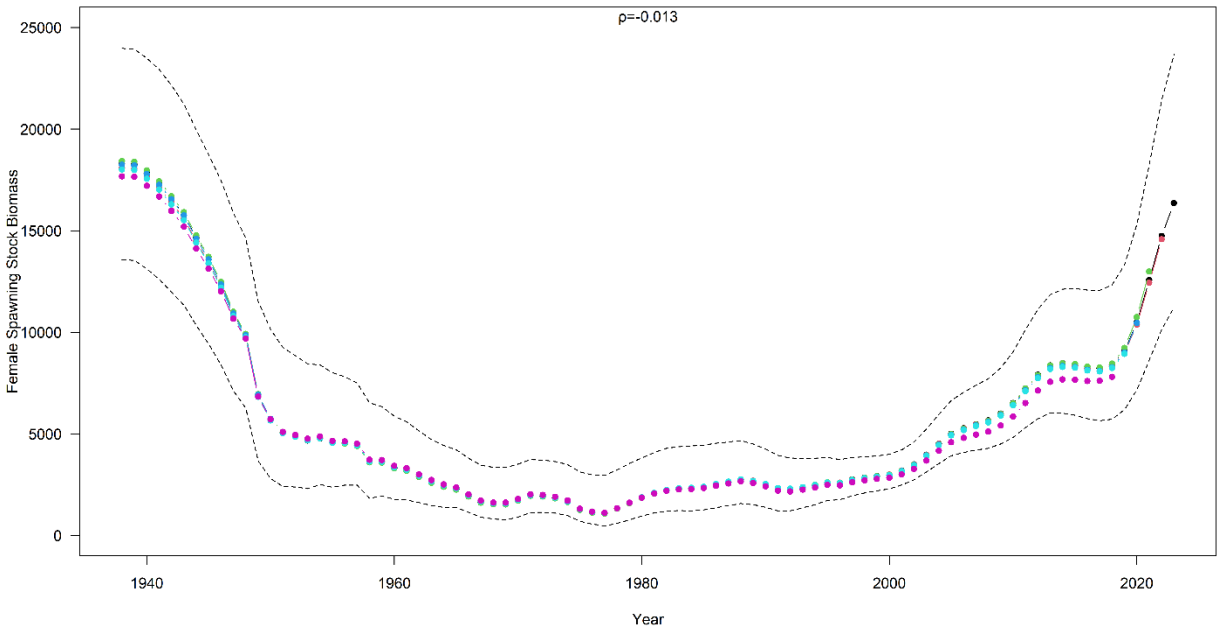


Figure 31. Retrospective analysis depicting female spawning stock biomass from the full baseM model (M=0.154, black line) and 5 peels (colored lines). The symbol ρ depicts Mohns rho (Mohn 1999). Depicted in points and solid lines are the medians of the posterior distribution for each model. The dotted line depicts the 95% equal-tailed credible intervals for the full baseM model.

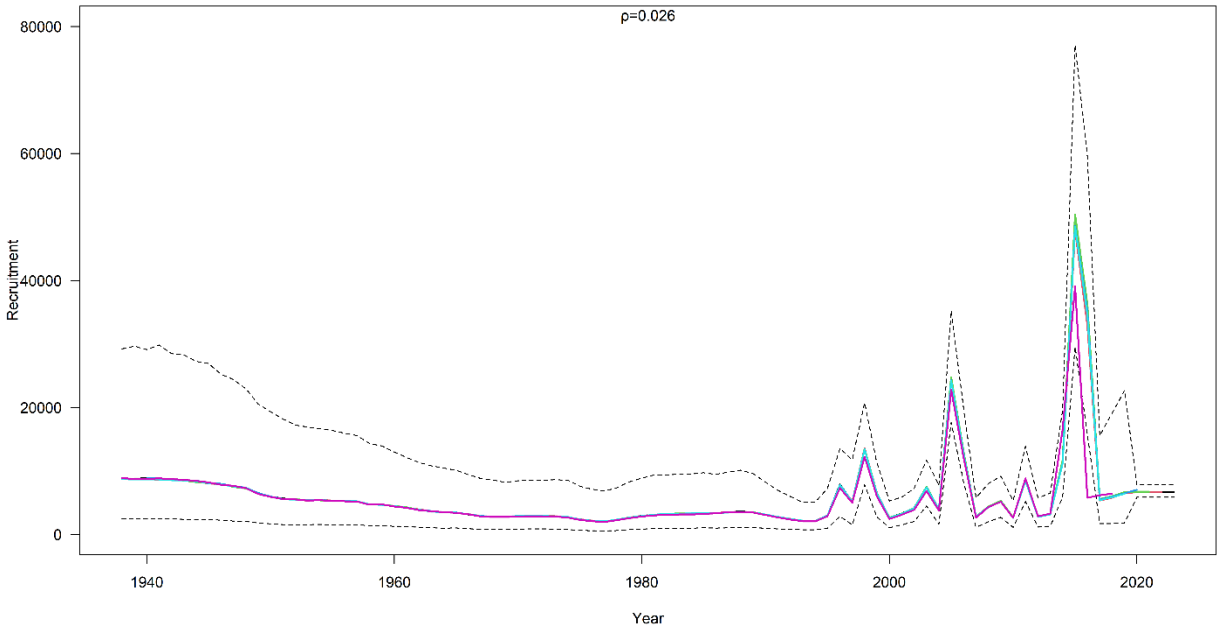


Figure 32. Retrospective analysis depicting recruitment (thousands) from the full baseM model (M=0.154) and 5 peels. The symbol ρ depicts Mohns rho (Mohn 1999). Depicted in solid lines are the medians of the posterior distribution for each model. The dotted line depicts the 95% equal-tailed credible intervals for the full baseM model.

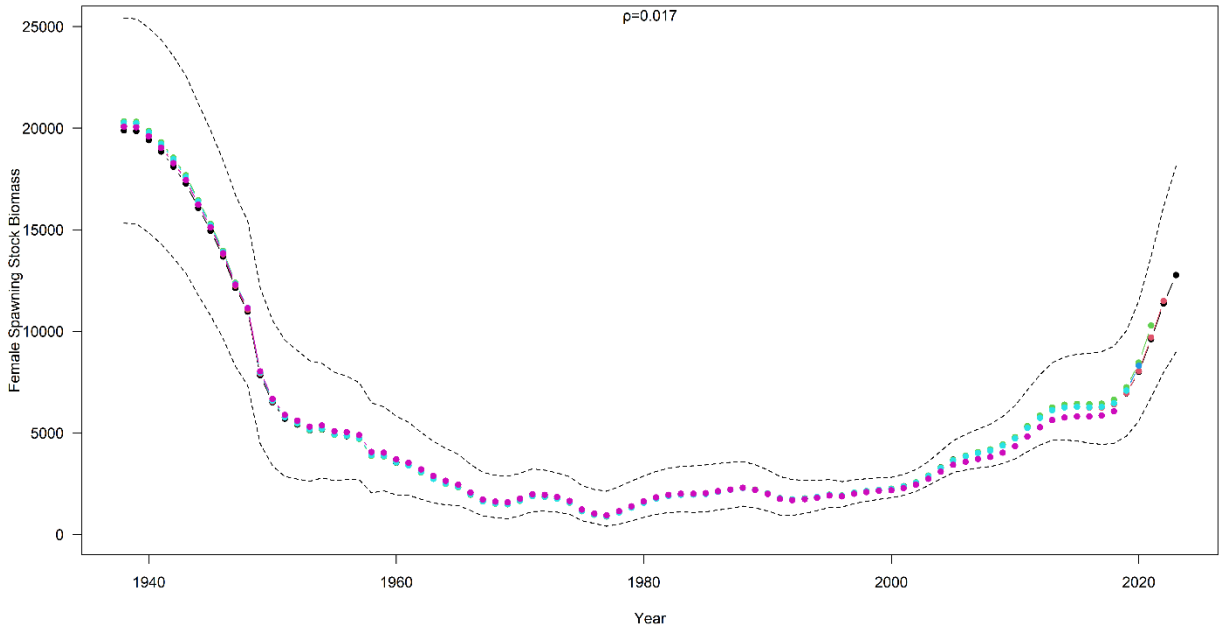


Figure 33. Retrospective analysis depicting female spawning stock biomass from the full lowM model (M=0.124, black line) and 5 peels (colored lines). The symbol ρ depicts Mohns rho (Mohn 1999). Depicted in points and solid lines are the medians of the posterior distribution for each model. The dotted line depicts the 95% equal-tailed credible intervals for the full lowM model.

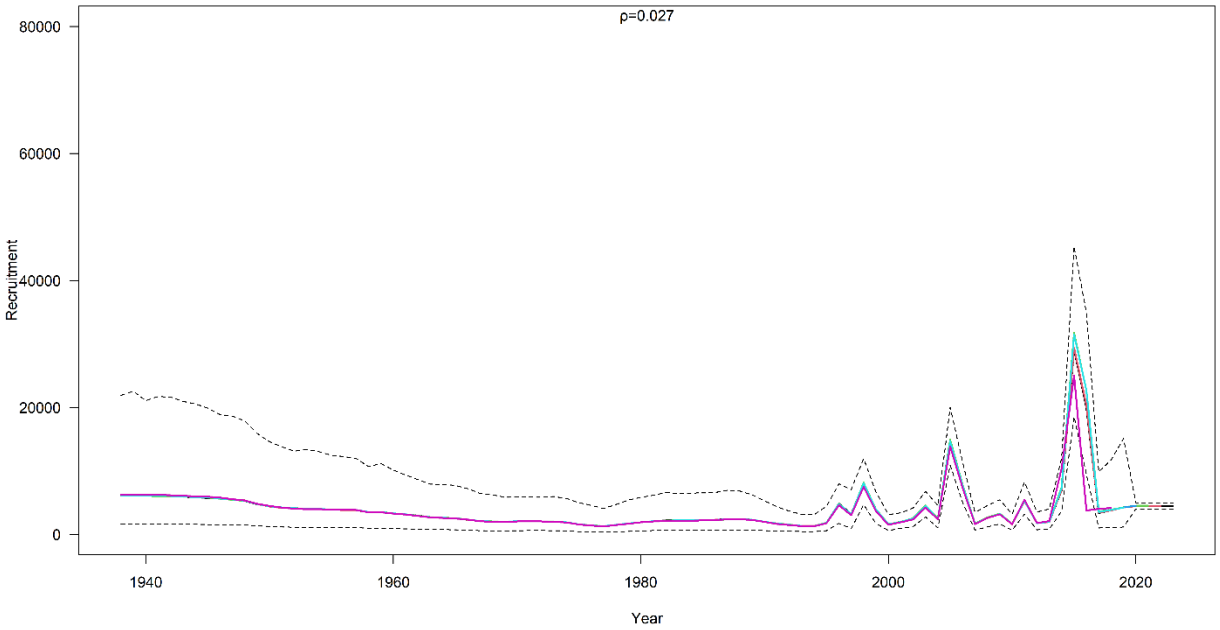


Figure 34. Retrospective analysis depicting recruitment (thousands) from the full lowM model (M=0.124) and 5 peels. The symbol ρ depicts Mohns rho (Mohn 1999). Depicted in solid lines are the medians of the posterior distribution for each model. The dotted line depicts the 95% equal-tailed credible intervals for the full lowM model.

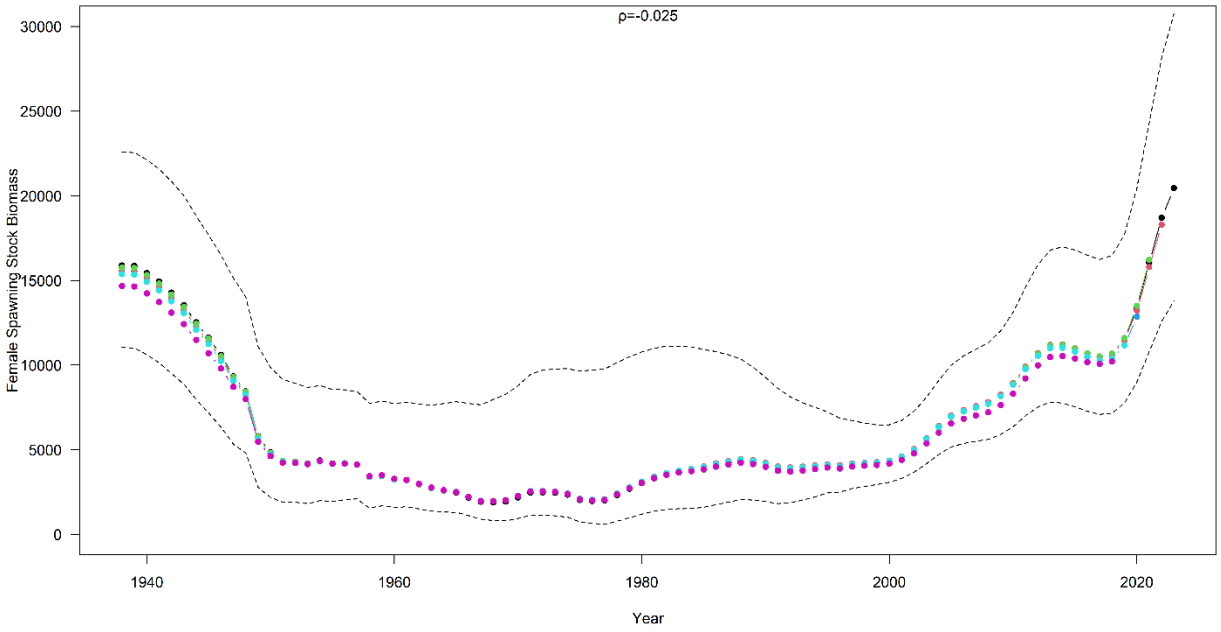


Figure 35. Retrospective analysis depicting female spawning stock biomass from the full highM model (M=0.184, black line) and 5 peels (colored lines). The symbol ρ depicts Mohns rho (Mohn 1999). Depicted in points and solid lines are the medians of the posterior distribution for each model. The dotted line depicts the 95% equal-tailed credible intervals for the full highM model.

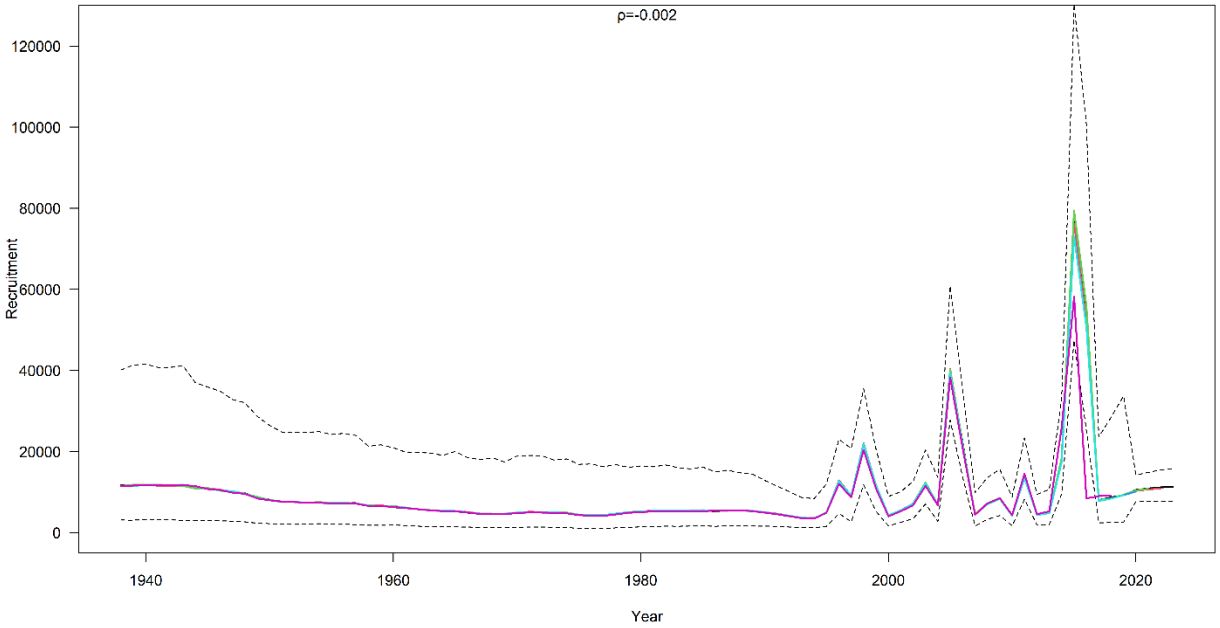


Figure 36. Retrospective analysis depicting recruitment (thousands) from the full highM model (M=0.184) and 5 peels. The symbol ρ depicts Mohns rho (Mohn 1999). Depicted in solid lines are the medians of the posterior distribution for each model. The dotted line depicts the 95% equal-tailed credible intervals for the full highM model.

3.2. BASE ENSEMBLE MODEL RESULTS

3.2.1. Estimated Parameters

In the base ensemble model, median steepness was estimated to be 0.6, and median ln(R0) was estimated to be 9.24 (Table 4; Figures 37 and 38). Extra standard deviations for survey indices medians ranged from 0.11 to 0.22, with the WCVI survey having the largest extra standard deviation. The QCS had the highest selectivity peak, followed by the fishery, then the WCVI survey, and then the HS survey (Table 4 and Figure 39).

Parameter estimates from the ensemble model were often similar to those from the individual baseM model, which is not surprising since the lowM and highM scenarios assumed symmetric deviations in base M in each direction and the baseM model was assigned a higher weight in the ensemble model (Table 4, Table 5). The ensemble model characterized increased uncertainty compared to the baseM model, with larger 95% credible intervals around parameter estimates (where, the 95% credible interval is characterized by the 2.5th and 97.5th percentiles of posterior distributions).

Ln(R0) was the lowest under the lowM scenario (Table 5; Figure 40). Median steepness was lowest under the baseM scenario, although steepness values were quite similar to each other among M scenarios (Figure 41). The highM scenario had the largest uncertainty in estimated Ln(R0) and steepness. The extra standard deviation for the QCS and WCVI indices increased with M, while the extra standard deviation for the HS index was similar across all three levels of M. Selectivity parameters varied somewhat based on the assumed level of M, but were relatively similar, with the exception being the fishery ascending width. For this parameter, the highM scenario had a positive ascending width estimate while the lowM and baseM scenarios both had negative estimates.

Management quantities varied among M scenarios (Table 5). Both B_0 and B_{MSY} decreased with increasing M, while estimated biomass in 2024, B_{2024}, increased with increasing M. Both MSY and F_{MSY} increased with increasing M, showing that the high M scenario characterized a more productive population that could sustain higher fishery impacts. Estimated stock status relative to reference points also varied among the three M scenarios (Table 5).The lowM scenario estimated the lowest B_{2024}/B_{MSY} ratio, while the highM scenario estimated the highest B_{2024}/B_{MSY} ratio (Table 5). The opposite trend occurred for F_{2023}/F_{MSY} ratios, with the ratio of F_{2023}/F_{MSY} increasing with decreasing *M.*

Table 4. Estimated parameters and management quantities for the base ensemble model (combined posteriors), shown as the 2.5th, 50th, and 97.5th percentiles from the ensemble posterior distribution

	Ensemble Base Model		
Parameter	**2.5%**	**50%**	**97.5%**
Ln(R0)	8.71	**9.24**	9.74
Steepness	0.47	**0.60**	0.85
Extra SD for QCS Index	0.08	**0.18**	0.34
Extra SD for HS Index	0.02	**0.11**	0.29
Extra SD for WCVI Index	0.10	**0.22**	0.38
Fishery selectivity peak (beginning age for the plateau)	6.15	**6.79**	8.02
fishery ascending width	-3.52	**-0.53**	1.08
fishery male offset	-1.09	**-0.65**	-0.22
QCS peak	7.63	**8.75**	10.02
QCS ascending width	2.00	**2.41**	2.79
QCS male offset	-1.24	**-0.78**	-0.34
HS peak	4.56	**5.47**	6.48
HS ascending width	1.03	**1.60**	2.10
HS male offset	-0.48	**-0.06**	0.35
WCVI peak	5.25	**5.93**	6.55
WCVI ascending width	0.47	**1.04**	1.49
WCVI male offset	-0.57	**-0.22**	0.13

	Ensemble Base Model		
Management Quantities	**2.5%**	**50%**	**97.5%**
B_{2024}	10,830	**17,330**	27,977
B_{MSY}	2,793	**5,704**	8,323
B_{2024}/B_{MSY}	1.62	**3.01**	5.60
$0.4B_{MSY}$	1,117	**2,282**	3,329
$B_{2024}/0.4B_{MSY}$	4.05	**7.53**	14.01
$0.8B_{MSY}$	2,234	**4,563**	6,658
$B_{2024}/0.8B_{MSY}$	2.03	**3.76**	7.00
B_0	12,215	**18,102**	24,349
B_{2024}/B_0	0.55	**0.96**	1.63
F_{2023}	0.013	**0.022**	0.036
F_{MSY}	0.067	**0.092**	0.171
F_{2023}/F_{MSY}	0.1	**0.24**	0.47
MSY	1,052	**1,352**	1,866

Table 5. Estimated parameters and management quantities for the three models that make up the base ensemble model: baseM (M=0.154), lowM (M=0.124), and highM (M=0.184). Parameter estimates are characterized as the 2.5th, 50th, and 97.5th percentiles from the individual model posterior distributions.

	baseM			lowM			highM		
Parameter	**2.5%**	**50%**	**97.5%**	**2.5%**	**50%**	**97.5%**	**2.5%**	**50%**	**97.5%**
Ln(R0)	8.95	**9.25**	9.52	8.62	**8.88**	9.13	9.14	**9.51**	9.86
Steepness	0.47	**0.59**	0.72	0.53	**0.62**	0.74	0.45	**0.601**	0.94
Extra SD for QCS Index	0.080	**0.17**	0.34	0.072	**0.16**	0.33	0.09	**0.19**	0.35
Extra SD for HS Index	0.022	**0.11**	0.30	0.028	**0.12**	0.30	0.02	**0.11**	0.29
Extra SD for WCVI Index	0.10	**0.22**	0.38	0.093	**0.21**	0.38	0.11	**0.24**	0.38
Fishery selectivity peak (beginning age for the plateau)	6.12	**6.64**	7.76	6.17	**6.69**	7.82	6.56	**7.33**	8.25
fishery ascending width	-3.94	**-0.90**	0.81	-3.42	**-0.84**	0.86	-0.84	**0.40**	1.31
fishery male offset	-1.06	**-0.63**	-0.21	-1.12	**-0.68**	-0.25	-1.14	**-0.66**	-0.22
QCS peak	7.62	**8.70**	9.93	7.52	**8.64**	10.04	7.85	**8.93**	10.15
QCS ascending width	1.99	**2.39**	2.77	1.97	**2.41**	2.82	2.05	**2.44**	2.80
QCS male offset	-1.23	**-0.78**	-0.34	-1.30	**-0.81**	-0.36	-1.17	**-0.74**	-0.32
HS peak	4.61	**5.44**	6.36	4.35	**5.24**	6.17	4.97	**5.74**	6.71
HS ascending width	1.04	**1.58**	2.06	0.90	**1.52**	2.03	1.23	**1.71**	2.18
HS male offset	-0.47	**-0.07**	0.35	-0.51	**-0.08**	0.35	-0.44	**-0.04**	0.36
WCVI peak	5.24	**5.89**	6.50	5.17	**5.84**	6.45	5.51	**6.09**	6.67
WCVI ascending width	0.44	**1.01**	1.46	0.42	**1.01**	1.47	0.68	**1.14**	1.53
WCVI male offset	-0.57	**-0.22**	0.13	-0.60	**-0.23**	0.12	-0.54	**-0.21**	0.12

	baseM			lowM			highM		
Management Quantities	**2.5%**	**50%**	**97.5%**	**2.5%**	**50%**	**97.5%**	**2.5%**	**50%**	**97.5%**
B_{2024}	11,788	**17,193**	24,891	9,543	**13,596**	19,344	14,228	**21,096**	31,714
B_{MSY}	3,790	**5,830**	8,370	4,225	**6,103**	8,418	2,355	**4,916**	8,007
B_{2024}/B_{MSY}	1.74	**2.99**	4.98	1.39	**2.33**	3.98	2.11	**3.64**	6.55
$0.4B_{MSY}$	1,516	**2,332**	3,348	1,690	**2,441**	3,367	942	**1,966**	3,203
$B_{2024}/0.4B_{MSY}$	4.34	**7.48**	12.45	3.48	**5.83**	9.96	5.27	**9.11**	16.37
$0.8B_{MSY}$	3,032	**4,664**	6,696	3,380	**4,882**	6,735	1,884	**3,932**	6,406
$B_{2024}/0.8B_{MSY}$	2.17	**3.74**	6.22	1.74	**2.91**	4.98	2.63	**4.56**	8.18
B_0	13,565	**18,282**	23,967	15,264	**19,904**	25,455	11,039	**15,878**	22,585
B_{2024}/B_0	0.61	**0.95**	1.40	0.47	**0.74**	1.16	0.71	**1.16**	1.91
F_{2023}	0.016	**0.022**	0.031	0.021	**0.029**	0.04	0.012	**0.017**	0.025
F_{MSY}	0.066	**0.091**	0.122	0.069	**0.089**	0.114	0.067	**0.102**	0.185
F_{2023}/F_{MSY}	0.15	**0.24**	0.42	0.2	**0.32**	0.53	0.08	**0.17**	0.31
MSY	1,057	**1,349**	1,697	1,015	**1,258**	1,544	1,134	**1,505**	2,151

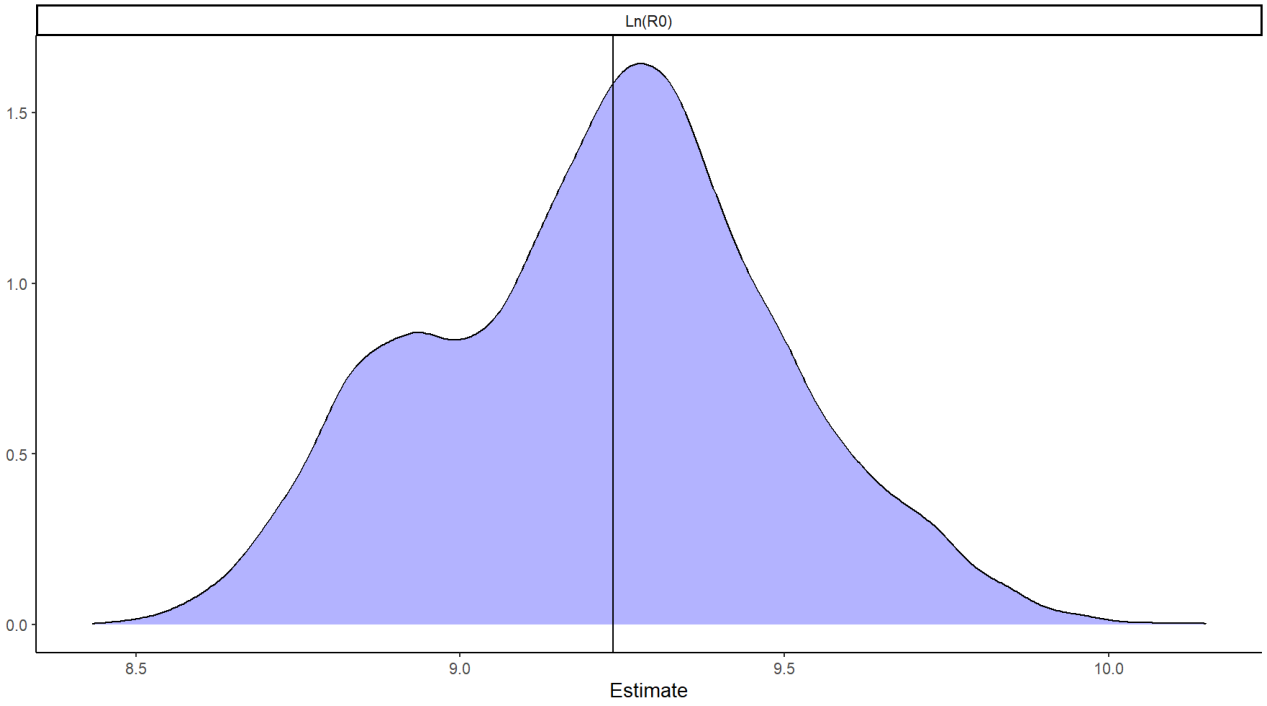


Figure 37. Posterior distribution of Ln(R0) from the base ensemble model. The black vertical represents the median.

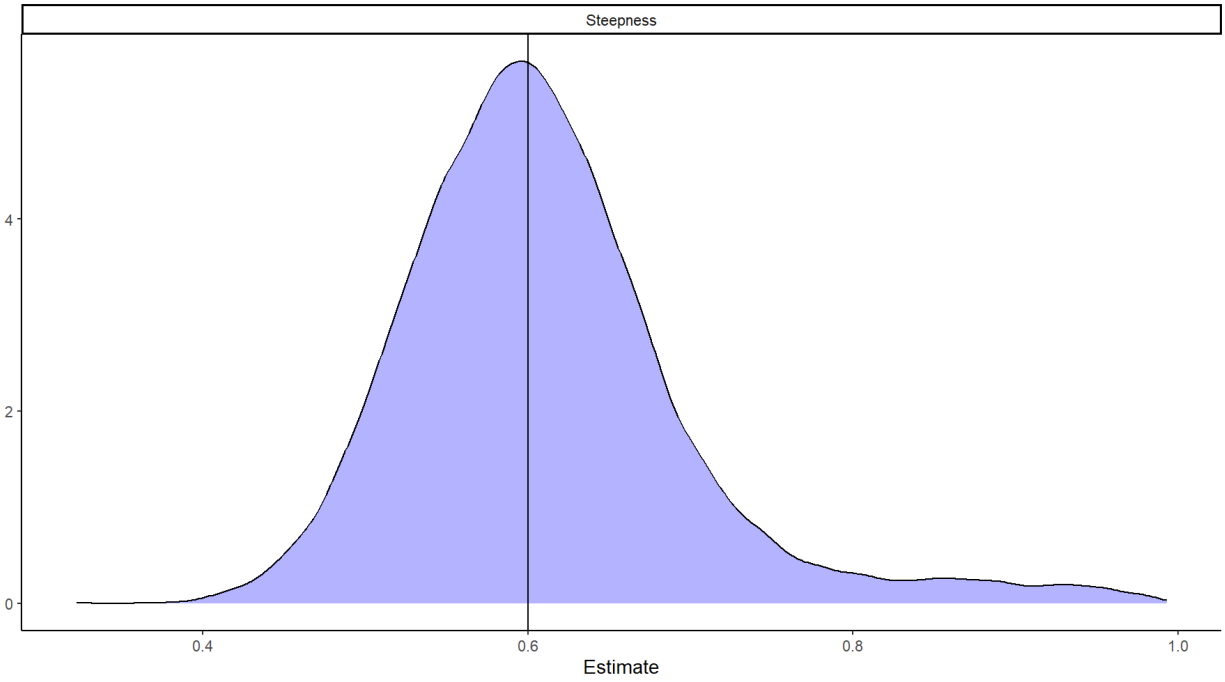


Figure 38. Posterior distribution of steepness from the base ensemble model. The black vertical represents the median.

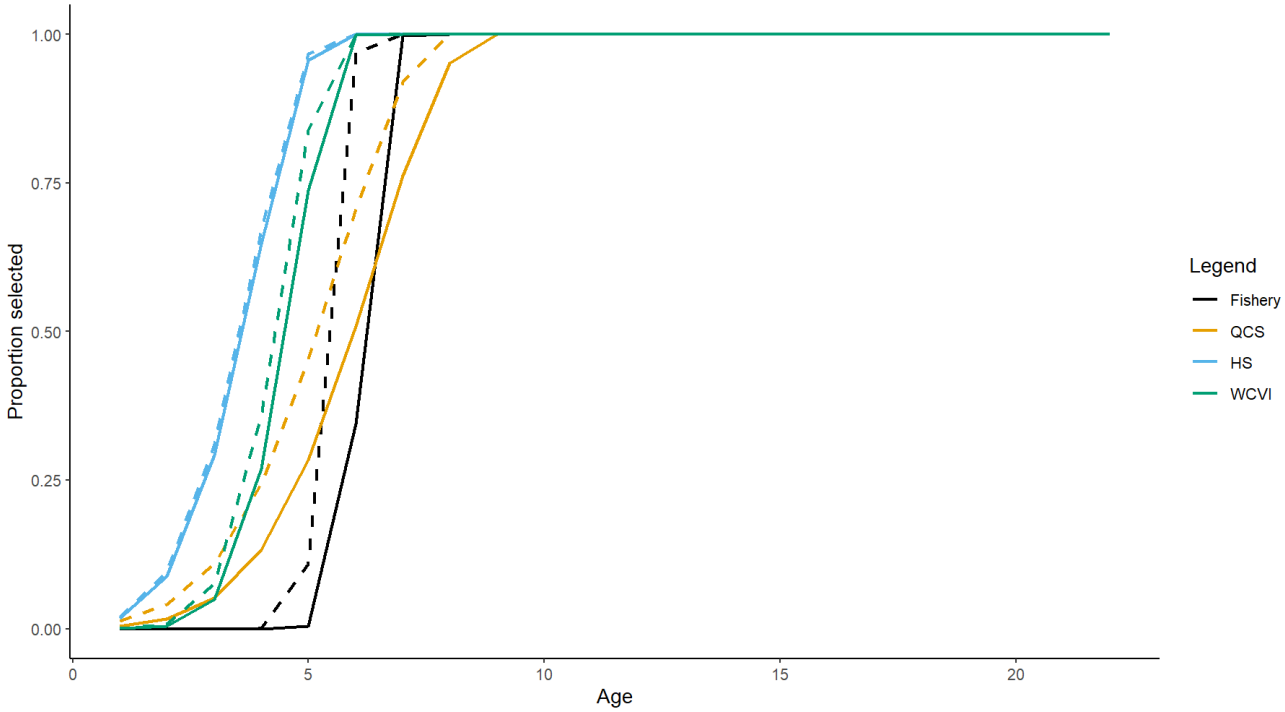


Figure 39. Median estimated selectivity curves from the combined posteriors from the base ensemble model for the fishery and surveys. The solid lines represent female selectivity curves, and the dashed lines represent male selectivity curves.

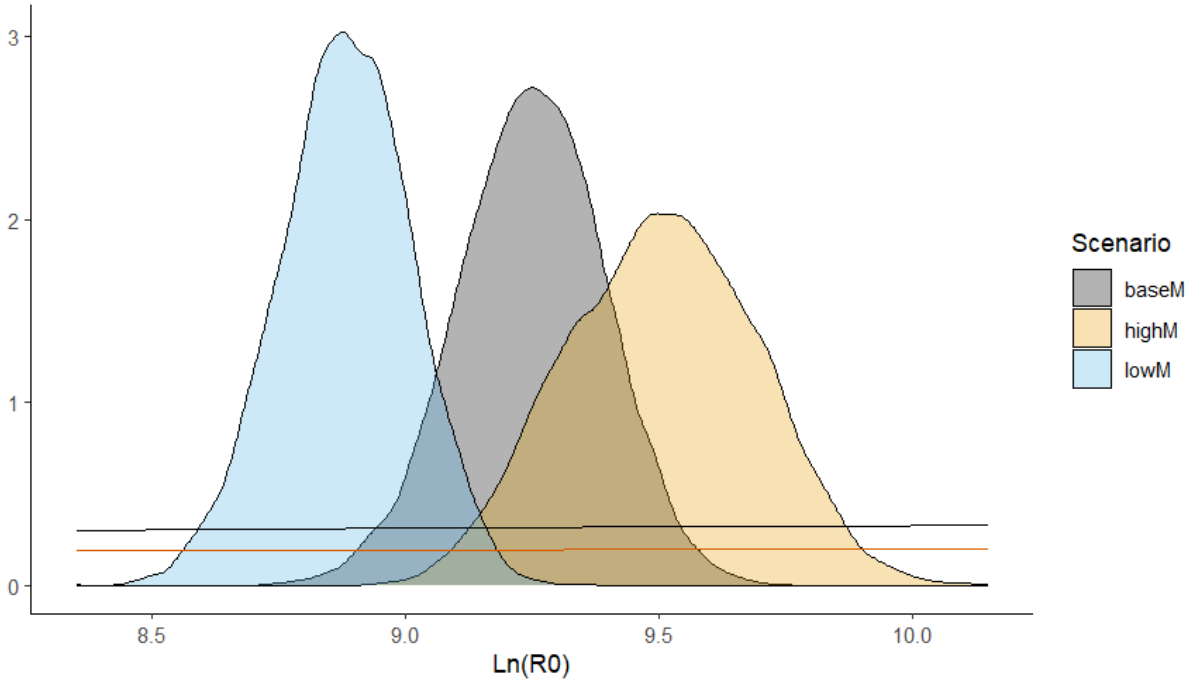


Figure 40. Prior and posterior distributions for Ln(R0) for the baseM (M=0.154), highM (M=0.184), and lowM (M=0.124) models. The black line represents the priors for the baseM and lowM models, and the orange line represents the prior for the highM model.

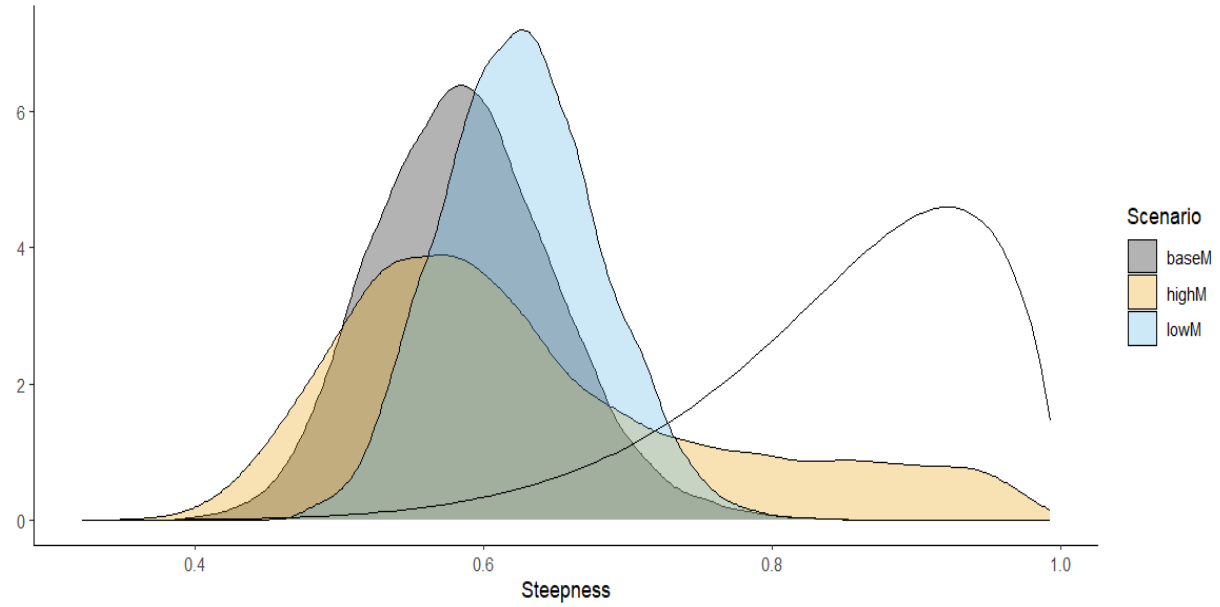


Figure 41. Prior and posterior distributions for steepness for the baseM (M=0.154), highM (M=0.184), and lowM (M=0.124) models. The black line represents the steepness prior.

3.2.2. Rationale for MSY-based Reference Points

The stock assessment model results led us to use MSY-based reference points for two reasons. First, the historical reference points used for Petrale Sole in 2006 (Starr 2009) were not appropriate for the updated biomass time series that extends from 1938 – 2023. As described in the 'Reference Points' section above, the 2006 assessment used a lower biomass reference (Lower B_{REF}) set at the minimum biomass over the 1966 - 2006 period, a target biomass reference (Target B_{REF}), and a target exploitation rate (U_{REF}) set at the average exploitation rate from 1966 to 2006. The minimum biomass over the period of 1938 – 2023 was estimated as $0.06B_0$ in 1977 based on the posterior median from the baseM model. This level is below the estimated posterior ratio of $0.4B_{MSY}$ / B_0 for the baseM model of $0.13B_0$ as well as the alternative LRP of $0.2B_0$ used for several Pacific Groundfish assessments (e.g., Grandin et al. 2026 for Arrowtooth Flounder). Setting the LRP at such a low ratio of B_0 may not be appropriate given concerns about non-stationarity in response to climatic change. It is unclear whether the stock would once again be able to recover from $0.06B_0$ if productivity conditions were more unfavorable than they were in the late 1970s and 1980s. Furthermore, the 2006 target biomass was set at the average biomass from 1977 – 1984, which was identified at the time as a period of relative stability from which the stock had since declined and then recovered. Looking at the longer 1938 – 2023 biomass time series estimated from this assessment, which used a much longer time period and a different model structure, this previous characterization of the 1977 – 1984 time period is no longer relevant. The stock is now estimated to be at the start of recovering from the historical low point in 1977 during this period.

Second, estimates B_{MSY} and F_{MSY}, as well as the estimated ratio of B_{MSY} / B_0, were relatively robust to the range of parameter and structural uncertainties we considered through sensitivity analyses (Figure 42). While unreliable estimates of B_{MSY} can be a justification for selecting proxies to MSY based on B_0 or historical indicators (Barrett et al. 2024, Grandin et al. 2026), there was no reason to reject MSY-based quantities in this case. While B_{MSY} and F_{MSY} were somewhat sensitive to assumed values of M, the ensemble model approach we used attempted

to capture this uncertainty when characterizing stock status and harvest advice using three different levels of *M*.

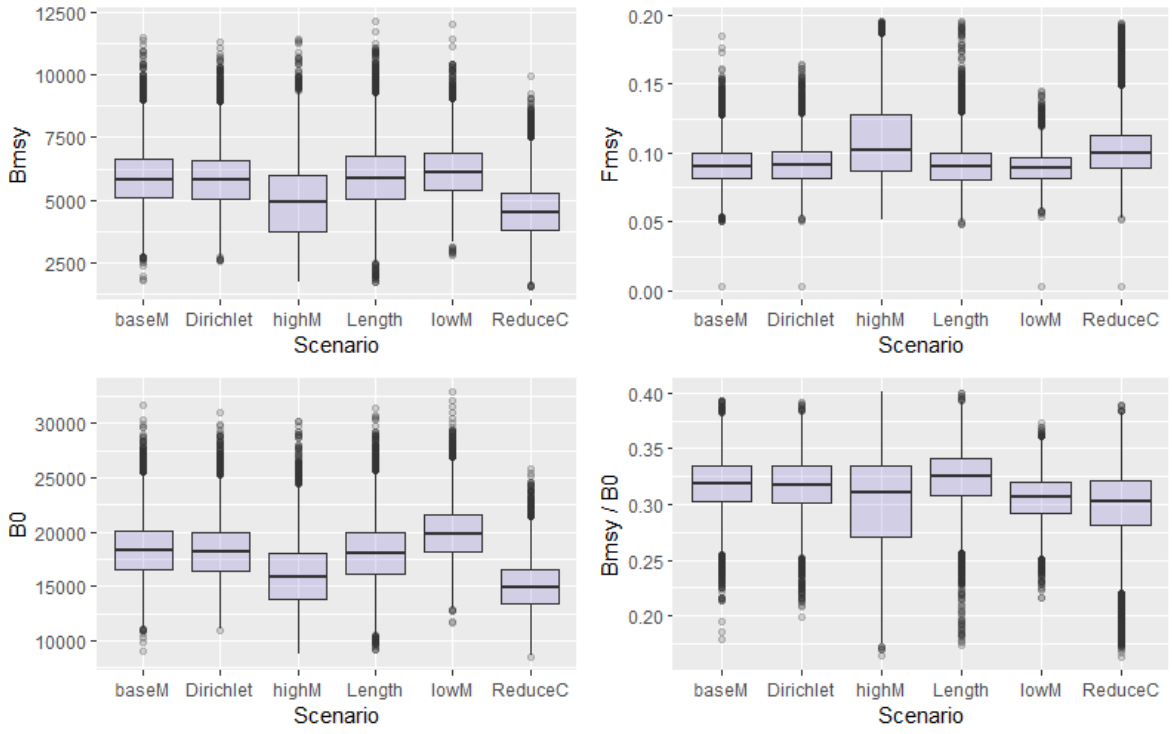


Figure 42. Posterior distributions of estimated reference points over a range of sensitivity analysis scenarios, where horizontal lines show the posterior median, the box shows the 25th and 75th intervals, and the whiskers show the approximated 95% confidence intervals around the median.

3.2.3. Stock Status

Based on results from the base ensemble model, the Petrale Sole stock was assessed to be above the LRP and candidate USR at the beginning of 2024, and fishing mortality in 2023 was below the candidate RR (Figure 45 and Figure 47). Much of the uncertainty in estimated biomass comes from the highM model in the base ensemble model (Figure 44). Given the stock assessment model began at an unfished state, the B_t in earlier years was close to unfished *B* (Figure 46). Median estimated B_t rapidly declined in early years and dropped below the candidate USR for the first time in 1955 (Figure 43). The stock continued to decline and dropped below the LRP for the first time in 1966. Median estimated B_t reached its lowest level in 1977 at 0.20 B_{MSY}. The stock then increased above the LRP in 1983. Since the 1970's estimated B_t has been increasing with a stable period from 2013 to 2018 and a rapid increase from 2019 to 2023. At the end of the time series, B_t was near unfished levels. Median estimated B_t has been over 0.8 B_{MSY} since 2005. Median estimated B_{2024} was at 3.00 B_{MSY}. However, the uncertainty was large, with a 95% posterior credible interval from 1.55 B_{MSY} to 7.95 B_{MSY}. Large recruitment events in 2015 and 2016 contributed to the rapid increase in B_t (Figures 48, 49, and 51). High recruitment events were also estimated in 1998, 2005, and 2006, although these events were not as high as in 2015 and 2016. Prior to 1996, there was not enough or no age data available to inform high recruitment events.

The median estimated fishing mortality rapidly increased in early years and then increased above F_{MSY} for the first time in 1945, and remained below F_{MSY} since 1996 (Figure 50). Fishing mortality peaked in 1948 and reached similar levels in 1974. Current fishing mortality levels

were estimated to be around the level in the late 1930s. Fishing mortality was estimated to be highly variable until 1996.

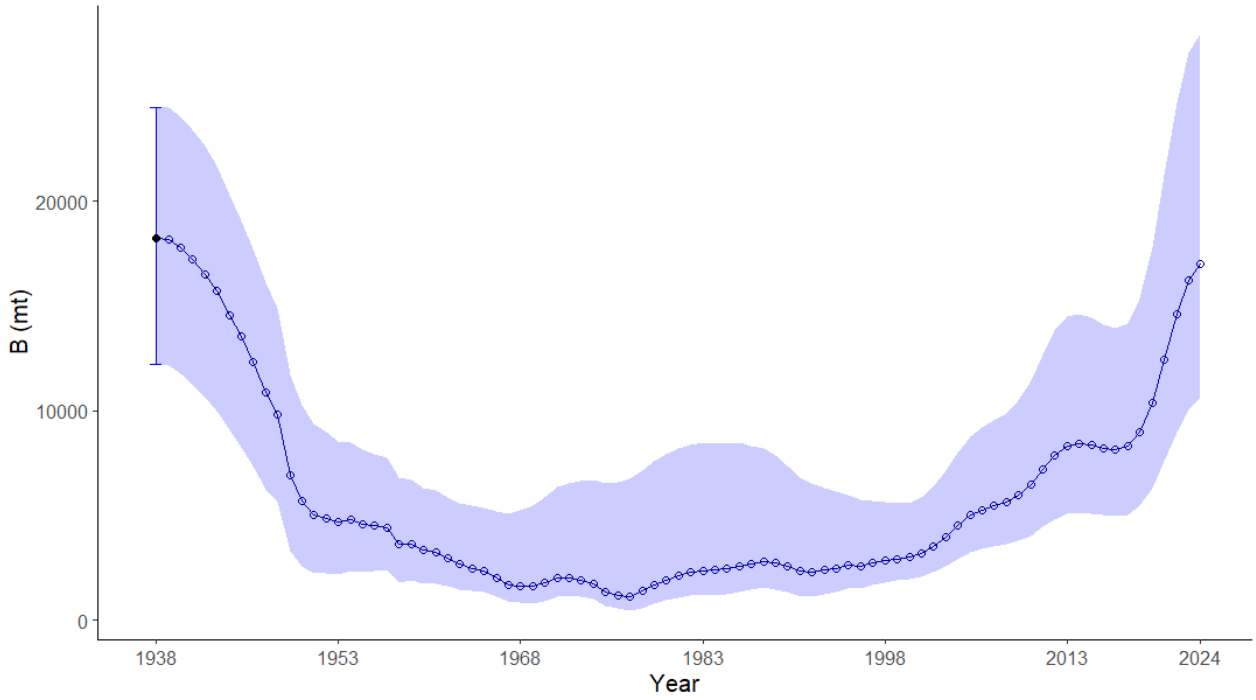


Figure 43. Median female spawning stock biomass (tonnes, points and lines) estimated from the base ensemble model from 1938 to 2024 with 95% credible intervals (shaded area). The error bar represents the initial unfished female spawning stock biomass estimated from the base ensemble model with a median (the center point) and 95% credible intervals.

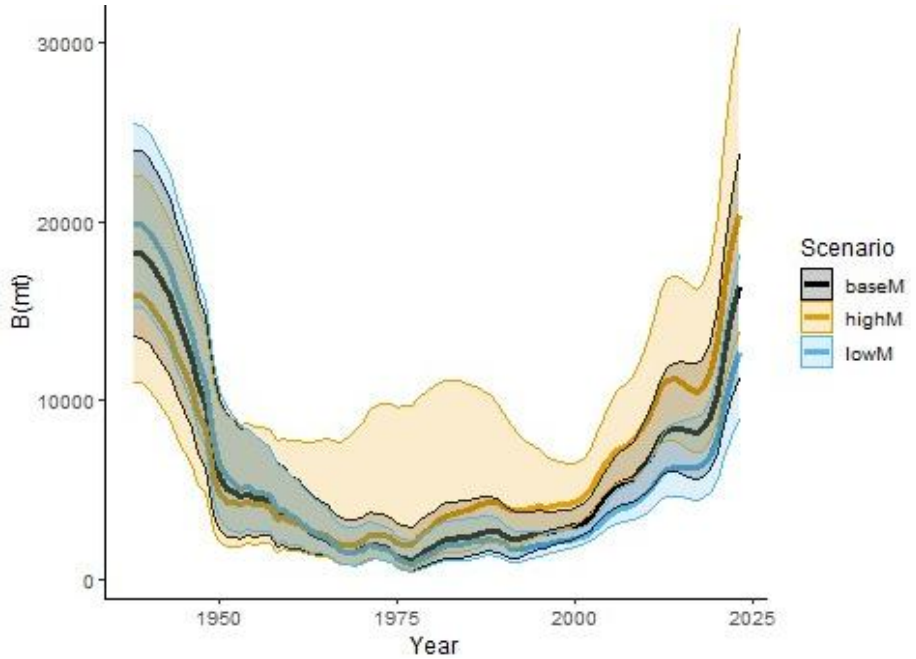


Figure 44. Median female spawning stock biomass (tonnes, points and lines) estimated from the baseM (M=0.154), highM (M=0.184) and lowM (M=0.124) models from 1938 to 2023 with 95% credible intervals (shaded area).

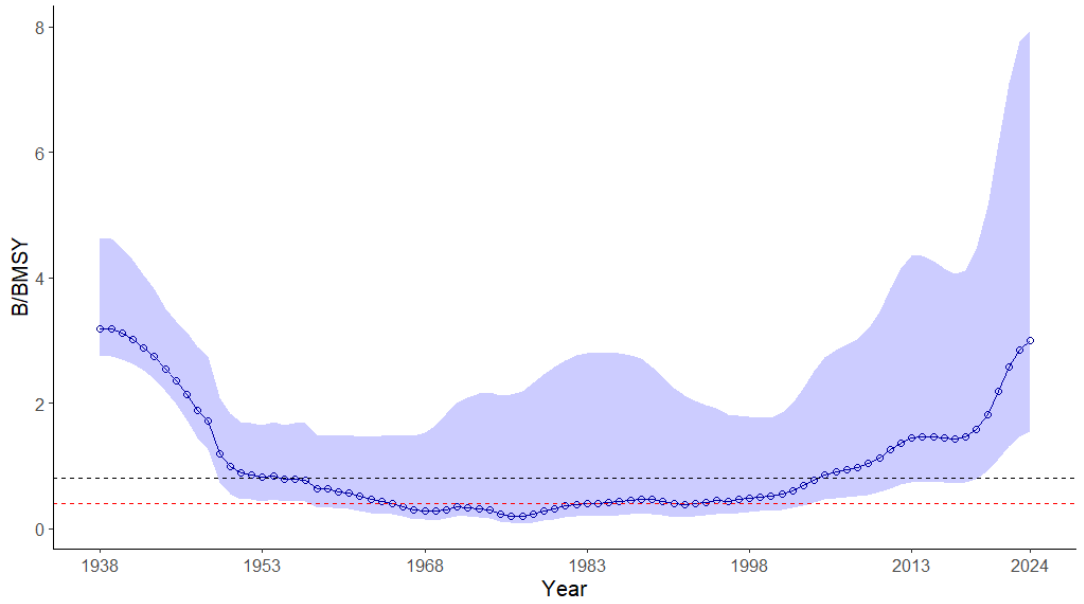


Figure 45. Median estimated female spawning stock biomass (B) to estimated female spawning stock biomass at maximum sustainable yield (BMSY) estimated from the base ensemble model from 1938 to 2024 with 95% credible intervals (shaded area). The horizontal red dashed line represents the recommended limit reference point at 0.4B_{MSY}, and the horizontal black dashed line represents the recommended upper stock reference at 0.8B_{MSY}.

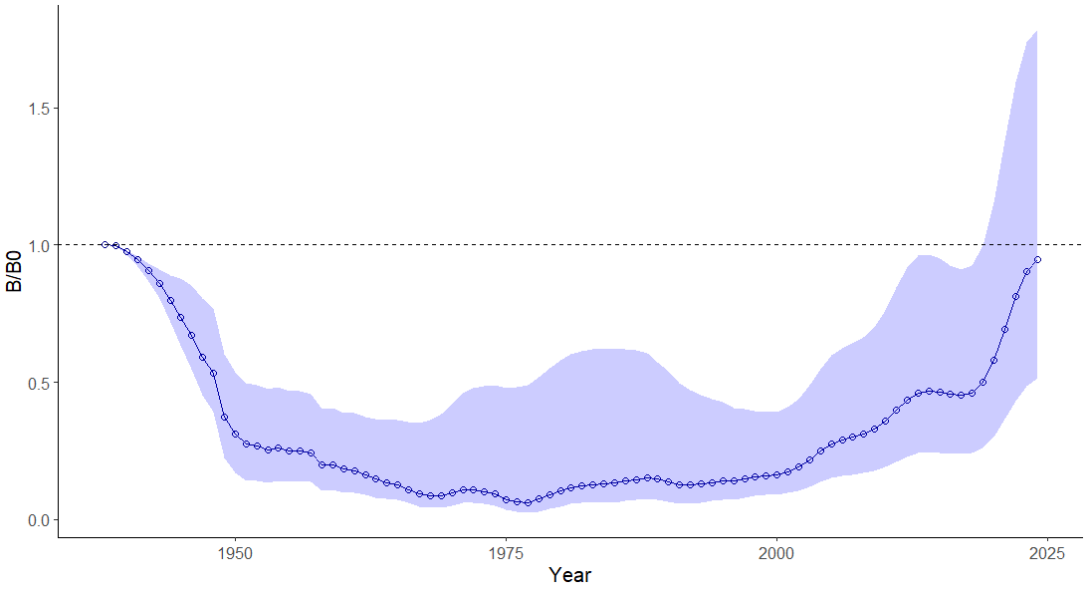


Figure 46. Median ratio of female spawning stock biomass (B) to unfished B (B0) estimated from the base ensemble model from 1938 to 2024 with 95% credible intervals (shaded area). The horizontal dashed line represents B_0.

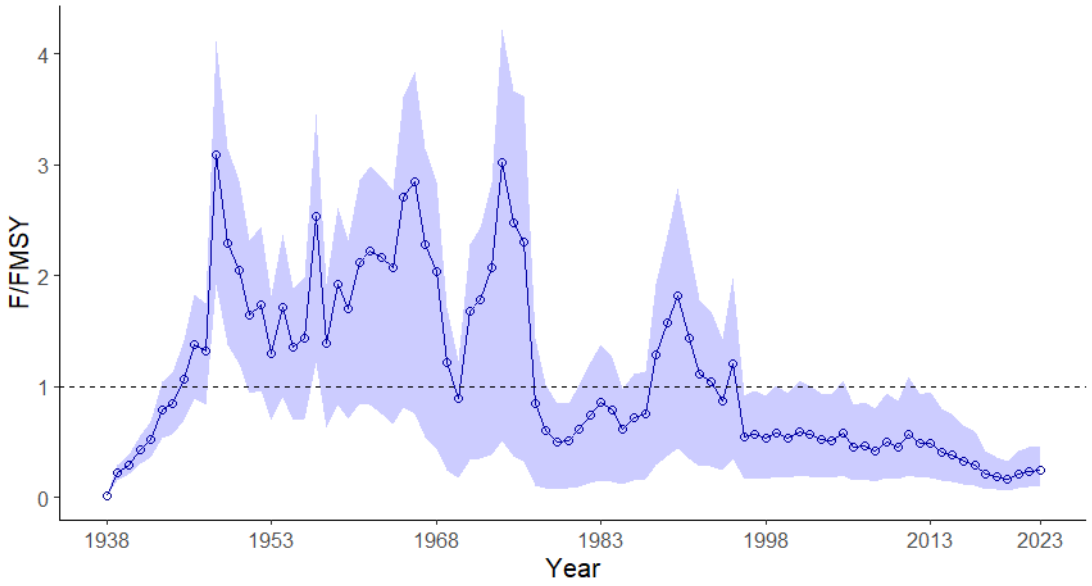


Figure 47. Median estimated fishing mortality (F) relative to estimated fishing mortality at maximum sustainable yield (F_{MSY}) estimated from the base ensemble model from 1938 to 2023 with 95% credible intervals (shaded area). The horizontal black dashed line represents the candidate Removal Reference (F_{MSY}).

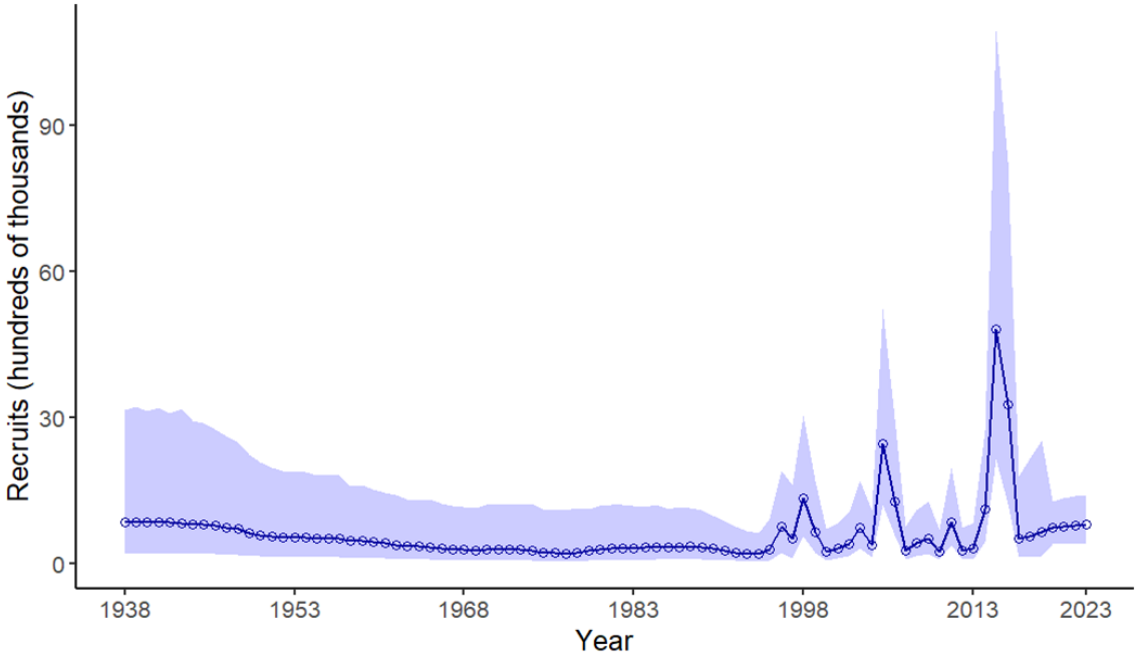


Figure 48. Median estimated age-0 recruits (number of males and females combined, points and solid lines) estimated from the base ensemble model from 1938 to 2023 with 95% credible intervals (shaded areas).

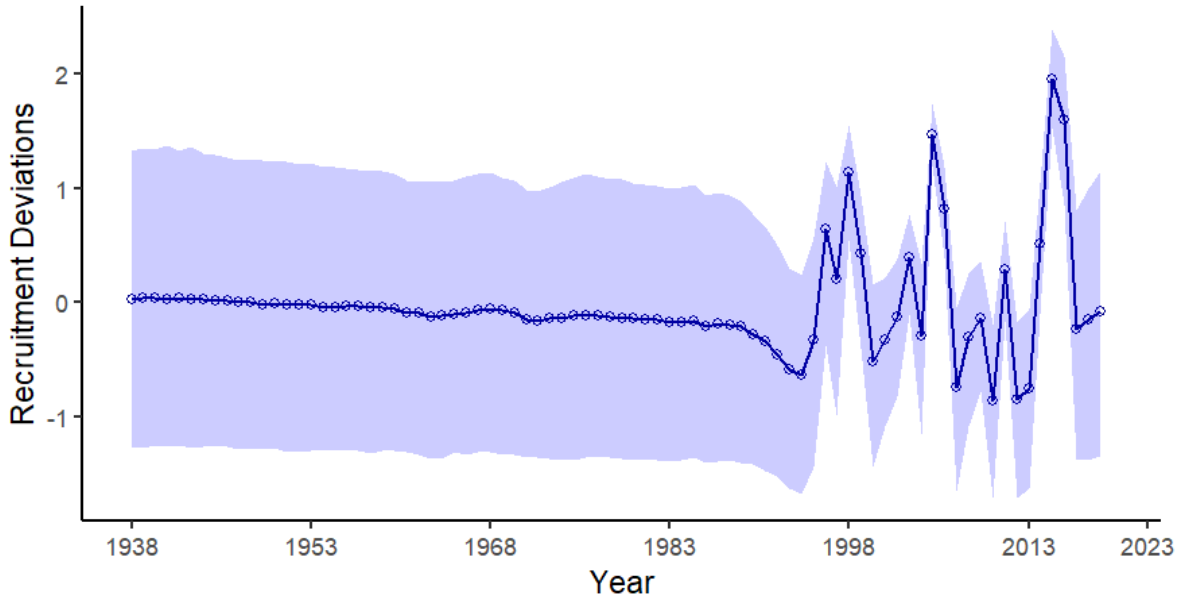


Figure 49. Median log recruitment deviations (points and solid lines) estimated from the base ensemble model from 1938 to 2019 with 95% credible intervals (shaded areas).

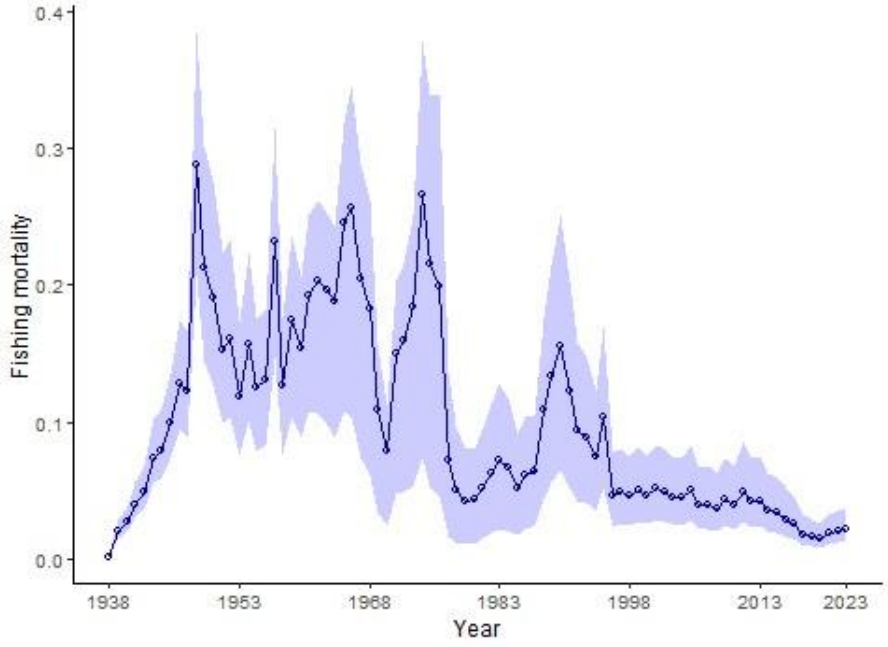


Figure 50. Median fishing mortality estimated from the base ensemble model from 1938 to 2023 with 95% credible intervals (shaded area).

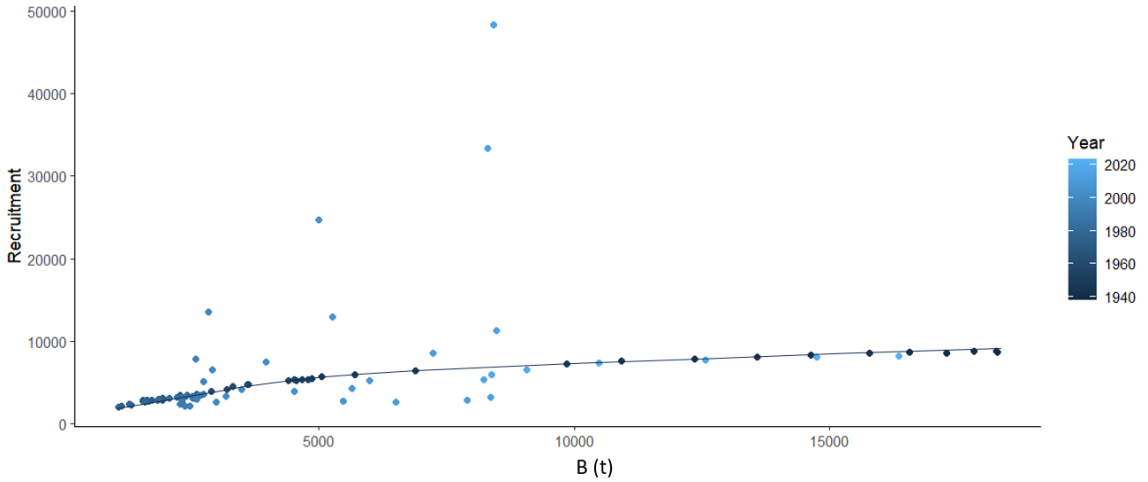


Figure 51. Median recruitment (thousands) vs. median spawning stock biomass (B) estimated from the base ensemble model from 1938 to 2023. The solid line represents the predicted Beverton-Holt stock-recruit curve.

3.2.4. Decision Tables

Projections for ten years from 2025 to 2034 under varying catch levels showed that stock status had a high probability of remaining above both the LRP and candidate USR over all constant catch policies considered (Tables 6-8 and Figure 52). The probability that B_t exceeded $0.4B_{MSY}$ was >99% for annual catches from 0- to 2,000 t for the ten years of the projection period (Table 6). The probability that B_t exceeded $0.8B_{MSY}$ was >99% for 0-1,500 t of catch over the ten year period (Table 7). Catch levels of 1,750-2,000 t resulted in probabilities just under 99% near the end of the ten years with the lowest being 95% in 2034 for 2000 t. As the constant catch level increased, *B* decreased more rapidly (Figures 52 and 54). In the projection period, the highM model begins above B_0, so projected *B* from the highM model declines with no catch, which is why projected *B* from the ensemble model declines. The probability that F_t in the projection period was below F_{MSY} was >99% for 0-1,000 t of catch over ten years (Table 8 and Figure 53). Probabilities of F_t being below F_{MSY} were still high for 1,250-1,500 t of catch (between 85% and >99%). Probabilities became lower with 1,750-2,000 t of catch, with the lowest being 30% for 2,000 t/y of catch at the end of the projection period in 2034.

Table 6. Probability that female spawning stock biomass in the projection exceeds the limit reference point ($0.4B_{MSY}$) under varying catch levels in tonnes for the ensemble model.

Catch (t/y)	2025	2026	2027	2028	2029	2030	2031	2032	2033	2034
0	>0.99	>0.99	>0.99	>0.99	>0.99	>0.99	>0.99	>0.99	>0.99	>0.99
250	>0.99	>0.99	>0.99	>0.99	>0.99	>0.99	>0.99	>0.99	>0.99	>0.99
500	>0.99	>0.99	>0.99	>0.99	>0.99	>0.99	>0.99	>0.99	>0.99	>0.99
750	>0.99	>0.99	>0.99	>0.99	>0.99	>0.99	>0.99	>0.99	>0.99	>0.99
1000	>0.99	>0.99	>0.99	>0.99	>0.99	>0.99	>0.99	>0.99	>0.99	>0.99
1250	>0.99	>0.99	>0.99	>0.99	>0.99	>0.99	>0.99	>0.99	>0.99	>0.99
1500	>0.99	>0.99	>0.99	>0.99	>0.99	>0.99	>0.99	>0.99	>0.99	>0.99
1750	>0.99	>0.99	>0.99	>0.99	>0.99	>0.99	>0.99	>0.99	>0.99	>0.99
2000	>0.99	>0.99	>0.99	>0.99	>0.99	>0.99	>0.99	>0.99	>0.99	>0.99

Table 7. Probability that female spawning stock biomass in the projection exceeds the upper stock reference (0.8B_{MSY}) under varying catch levels in tonnes for the ensemble model.

Catch (t/y)	2025	2026	2027	2028	2029	2030	2031	2032	2033	2034
0	>0.99	>0.99	>0.99	>0.99	>0.99	>0.99	>0.99	>0.99	>0.99	>0.99
250	>0.99	>0.99	>0.99	>0.99	>0.99	>0.99	>0.99	>0.99	>0.99	>0.99
500	>0.99	>0.99	>0.99	>0.99	>0.99	>0.99	>0.99	>0.99	>0.99	>0.99
750	>0.99	>0.99	>0.99	>0.99	>0.99	>0.99	>0.99	>0.99	>0.99	>0.99
1000	>0.99	>0.99	>0.99	>0.99	>0.99	>0.99	>0.99	>0.99	>0.99	>0.99
1250	>0.99	>0.99	>0.99	>0.99	>0.99	>0.99	>0.99	>0.99	>0.99	>0.99
1500	>0.99	>0.99	>0.99	>0.99	>0.99	>0.99	>0.99	>0.99	>0.99	>0.99
1750	>0.99	>0.99	>0.99	>0.99	>0.99	>0.99	>0.99	>0.99	>0.99	0.98
2000	>0.99	>0.99	>0.99	>0.99	>0.99	>0.99	>0.99	>0.99	0.97	0.95

Table 8. Probability that fishing mortality in the projection is below the maximum removal reference (F_{MSY}) under varying catch levels in tonnes for the ensemble model.

Catch (t/y)	2025	2026	2027	2028	2029	2030	2031	2032	2033	2034
0	>0.99	>0.99	>0.99	>0.99	>0.99	>0.99	>0.99	>0.99	>0.99	>0.99
250	>0.99	>0.99	>0.99	>0.99	>0.99	>0.99	>0.99	>0.99	>0.99	>0.99
500	>0.99	>0.99	>0.99	>0.99	>0.99	>0.99	>0.99	>0.99	>0.99	>0.99
750	>0.99	>0.99	>0.99	>0.99	>0.99	>0.99	>0.99	>0.99	>0.99	>0.99
1000	>0.99	>0.99	>0.99	>0.99	>0.99	>0.99	>0.99	>0.99	>0.99	>0.99
1250	>0.99	>0.99	>0.99	>0.99	>0.99	>0.99	>0.99	>0.99	0.98	0.98
1500	>0.99	>0.99	>0.99	0.98	0.97	0.95	0.93	0.91	0.89	0.85
1750	0.97	0.96	0.94	0.91	0.88	0.84	0.78	0.72	0.66	0.58
2000	0.92	0.89	0.85	0.79	0.72	0.64	0.55	0.47	0.38	0.3

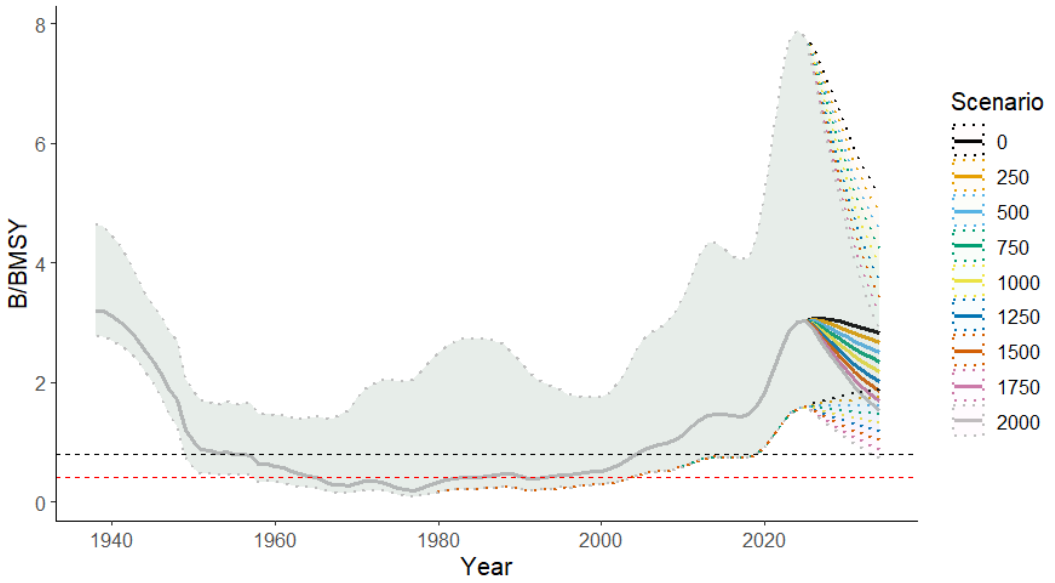


Figure 52. Median ratio (solid lines) of female spawning biomass to female spawning biomass at maximum sustainable yield (B/BMSY) with 95% credible intervals (dotted lines) predicted under each of the catch levels (coloured scenarios). The horizontal red dashed line represents the limit reference point at $0.4B_{MSY}$, and the horizontal black dashed line represents the candidate upper stock reference at $0.8B_{MSY}$.

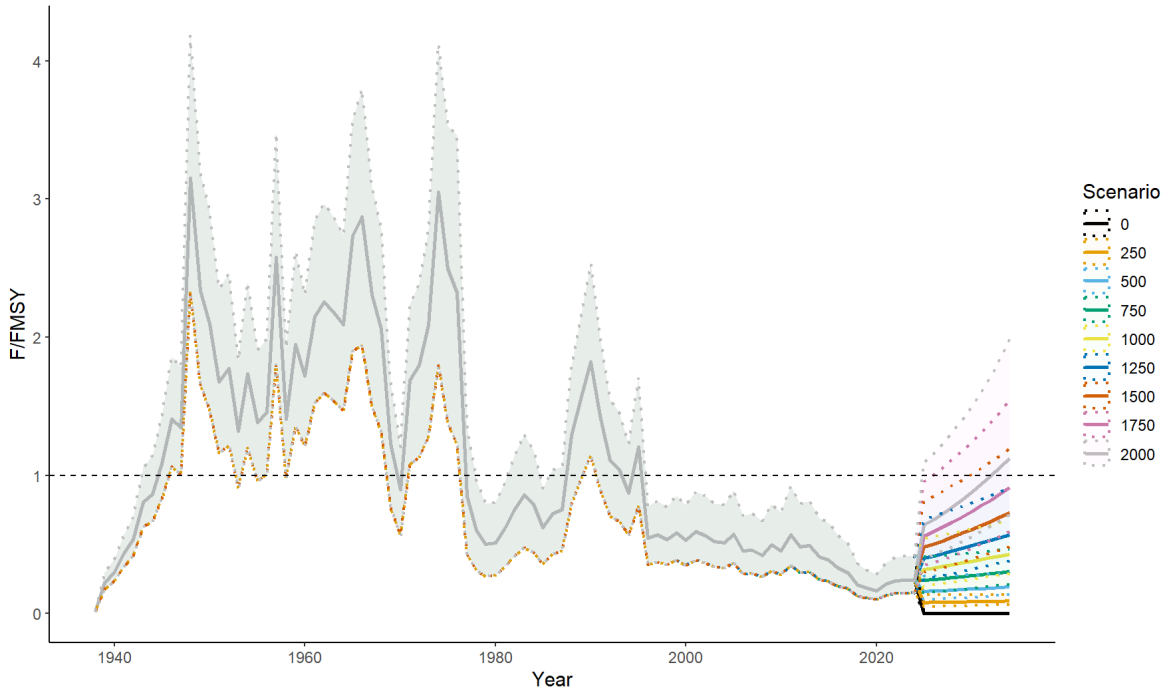


Figure 53. Median ratio of fishing mortality (F) to fishing mortality at maximum sustainable yield (FMSY) predicted under each of the catch levels. The dotted horizontal line represents the candidate removal reference.

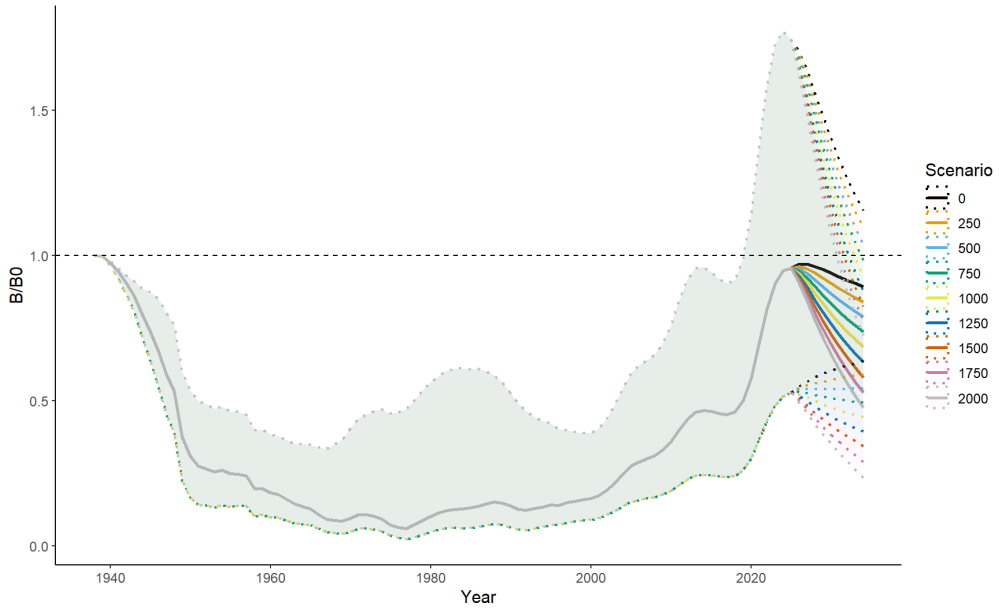


Figure 54. Median ratio (solid lines) of female spawning biomass to unfished female spawning biomass (B/B0) with 95% credible intervals (dotted lines) predicted under each of the catch levels (coloured scenarios). The horizontal black dashed line represents B_0.

3.3. SENSITIVITY ANALYSES

Among the set of sensitivity analyses for which MCMC analyses were run based on acceptable MLE diagnostics, the M assumption had the strongest impact on estimated stock trends, while including the Triennial index and using Dirichlet-multinomial likelihood had the smallest impact (Figures 55- 59). The lowM and highM scenarios had some of the most extreme biomass levels, with the lowM scenario having the highest estimate of B_0 in 1938 and one of the lowest estimates of B_{2024} among scenarios, while the high M scenario has a relatively low estimate of B_0 and the highest estimate of B_{2024} among the scenarios. These differences among the highM and lowM scenarios appear to arise from the highM scenario characterizing a more productive stock that has a higher R_0.

Reducing historical catch and using length and conditional-age-at-length data in the assessment model also had an impact on estimated parameters, although not as strong as the M assumption. Models with Dirichlet multinomial likelihood (Dirichlet) and the Triennial index (Triennial) resulted in nearly identical output as the model from the base model with M=0.154 (baseM). Models without discards (NoDiscards) and reduced catch from 1938 to 1953 (ReduceCatch) were also similar to the output from the baseM model except resulted in a slightly lower *B*. The ReduceCatch model also resulted in a higher B/B_{MSY} ratio than the baseM model. The model with length and conditional age at length data (Length+CAAL) resulted in a higher recruitment event in later years that the other models with age data only did not estimate (Figure 56). The Length+CAAL model also estimated smaller high recruitment events in earlier years than the baseM model, which resulted in a lower *B* and higher fishing mortality near the end of the time series (Figure 57). All sensitivities resulted in estimated *B* that was well above B_{MSY} at the end of the time series, with the highM scenario having the highest B/B_{MSY} ratio and the lowM scenario having the lowest B/B_{MSY} ratio. All sensitivities resulted in estimated fishing mortality that was well below F_{MSY} at the end of the time series, with the lowM scenario having the highest F/F_{MSY} ratio and the highM scenario having the lowest F/F_{MSY} ratio. Median steepness ranged between 0.58 and 0.63 among the sensitivities, with the Length+CAAL and

Triennial models having the lowest median steepness and the ReduceCatch model having the highest steepness (Table 9). The ReduceCatch model resulted in the lowest B_{MSY} (4,534 t), and the lowM model resulted in the highest B_{MSY} (6,103 t; Table 10). Growth parameters estimated from the Length+CAAL model were similar to the fixed growth parameters in the other models (Table 12).

Several additional sensitivity scenarios that were initially selected for consideration did not converge using MLE, including scenarios that included fishery CPUE as an abundance index, assumed higher or lower variation in recruitment, used different weighting scenarios (e.g., Francis), and did not include the extra standard deviations for survey indices (Appendix G).

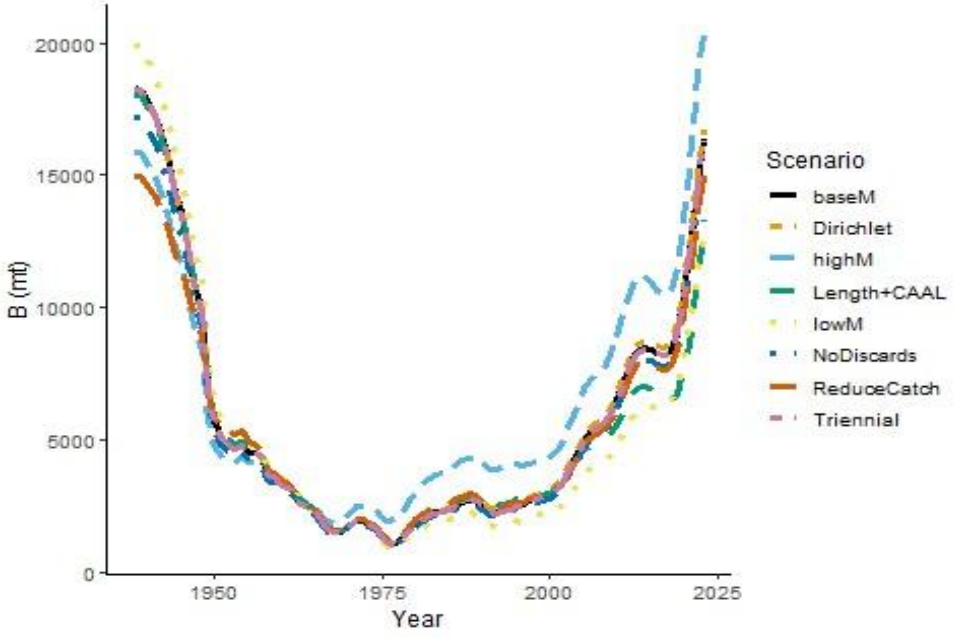


Figure 55. Median estimated female spawning stock biomass (B) from the model with M=0.154 from the base ensemble model and selected sensitivities, which also assume M=0.154 aside from the highM (0.184) and lowM (0.124) scenarios.

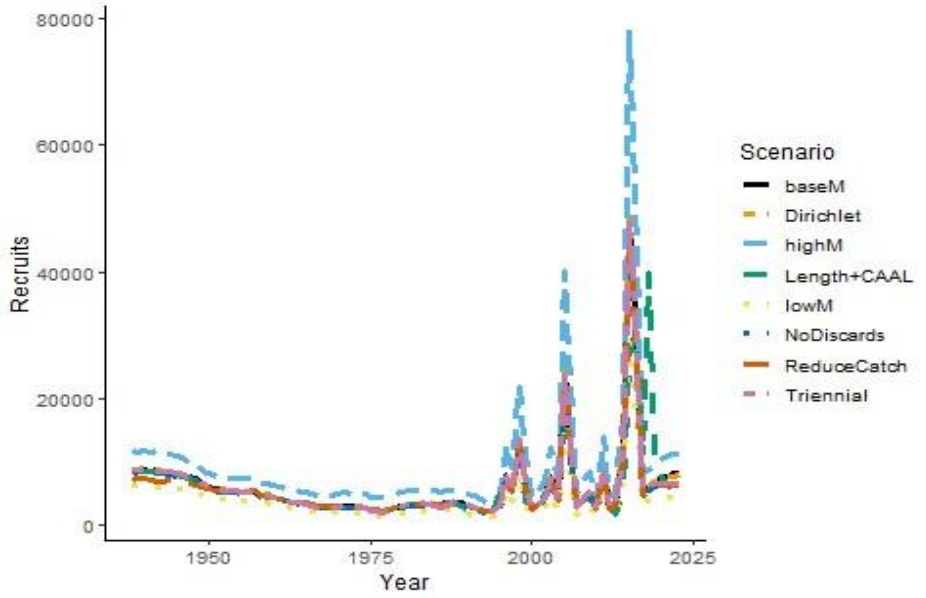


Figure 56. Median estimated recruitment (thousands) from the model with M=0.154 from the base ensemble model and selected sensitivities, which also assume M=0.154 aside from the highM (0.184) and lowM (0.124) scenarios.

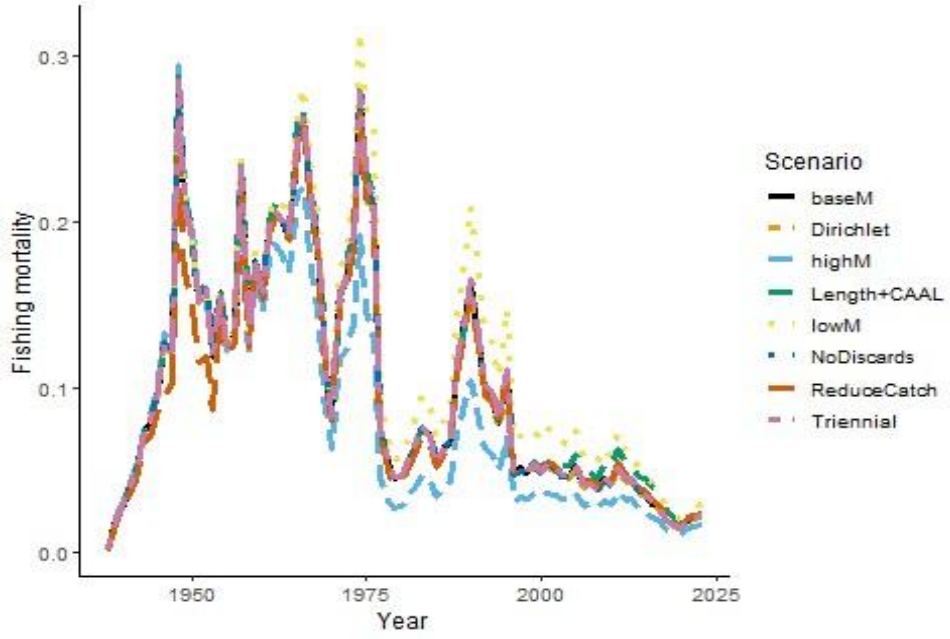


Figure 57. Median estimated fishing mortality from the model with M=0.154 from the base ensemble model and selected sensitivities, which also assume M=0.154 aside from the highM (0.184) and lowM (0.124) scenarios.

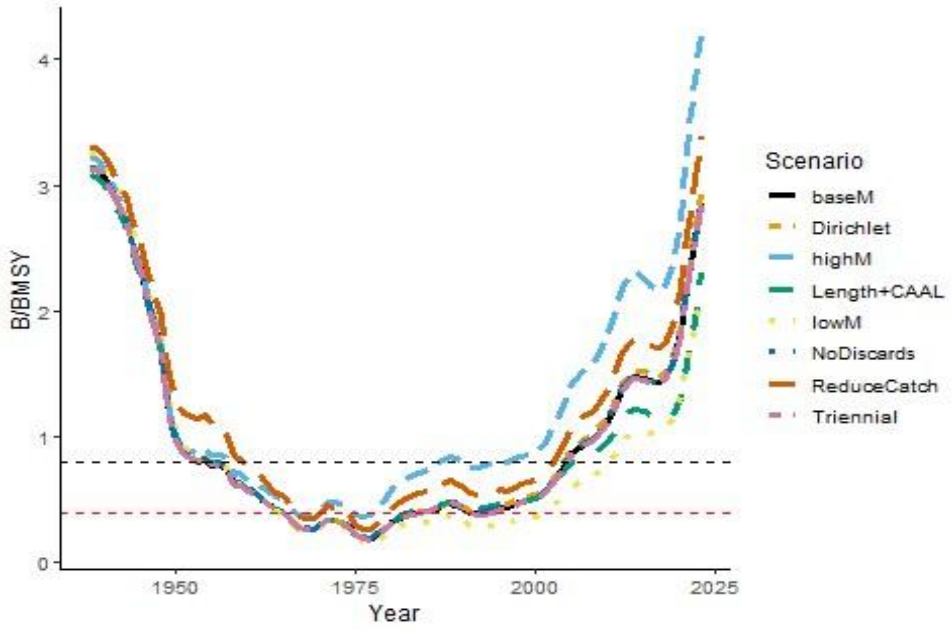


Figure 58. Median estimated female spawning stock biomass (B) to female spawning stock biomass at maximum sustainable yield (BMSY) ratio from the model with M=0.154 from the base ensemble model and selected sensitivities, which also assume M=0.154 aside from the highM (0.184) and lowM (0.124) scenarios. The dashed red line represents 0.4B_{MSY}, and the dashed black line represents 0.8B_{MSY}.

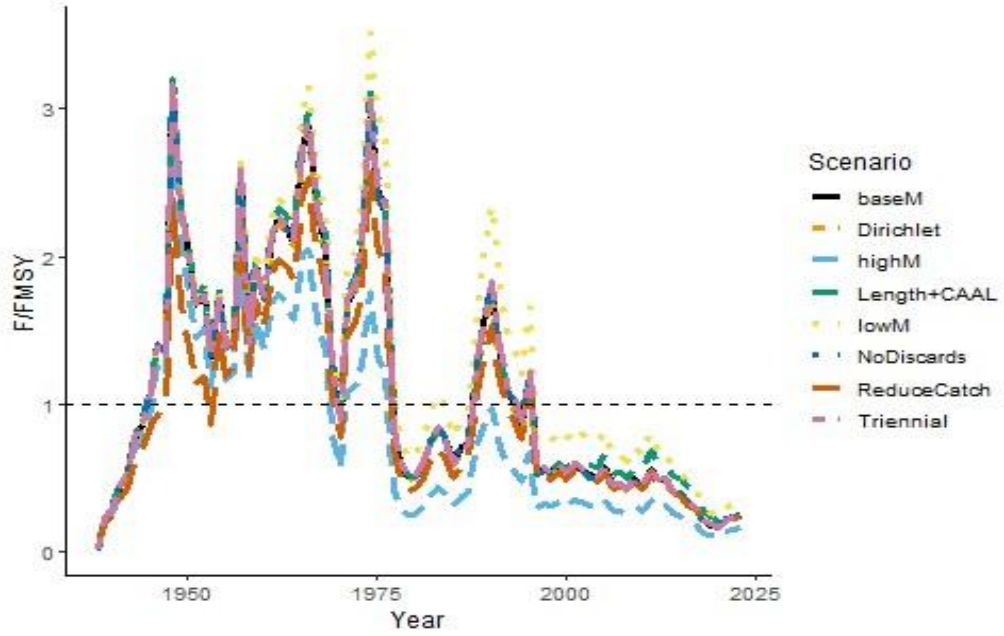


Figure 59. Median estimated fishing mortality (F) to fishing mortality at maximum sustainable yield (FMSY) ratio from the model with M=0.154 from the base ensemble model and selected sensitivities, which also assume M=0.154 aside from the highM (0.184) and lowM (0.124) scenarios. The black dashed line represents F_{MSY}.

Table 9. Median estimated log of virgin recruitment (Ln(R0)) and steepness parameters from the model with M=0.154 from the base ensemble model and selected sensitivities, which also assume M=0.154 aside from the highM (0.184) and lowM (0.124) scenarios.

Parameter	baseM	Dirichlet	highM	Length +CAAL	lowM	NoDiscards	Reduce Catch	Triennial
Ln(R0)	9.25	9.25	9.51	9.20	8.88	9.19	9.05	9.25
Steepness	0.59	0.59	0.60	0.58	0.62	0.59	0.63	0.58

Table 10. Median estimated B_{MSY} and F_{MSY} from the model with M=0.154 from the base ensemble model and selected sensitivities, which also assume M=0.154 aside from the highM (0.184) and lowM (0.124) scenarios.

Parameter	baseM	Dirichlet	highM	Length +CAAL	lowM	NoDiscards	Reduce Catch	Triennial
B_{MSY}	5830	5780	4916	5852	6103	5465	4534	5825
F_{MSY}	0.09	0.09	0.10	0.09	0.09	0.09	0.10	0.09

Table 11. Median negative log likelihoods under the model from the model with M=0.154 from the base ensemble model and selected sensitivities, which also assume M=0.154 aside from the highM (0.184) and lowM (0.124) scenarios.

Likelihood	baseM	Dirichlet	highM	Length+ CAAL	lowM	No Discards	Reduce Catch	Triennial
Total	432.95	1373.83	445.56	435.67	433.84	435.93	436.44	431.17
Catch	1.17E-05	7.79E-06	2.51E-05	1.17E-05	8.33E-06	1.05E-05	4.59E-06	1.46E-05
QCS Survey	-9.05	-9.06	-8.30	-9.05	-9.50	-9.00	-8.87	-9.03
HS Survey	-9.05	-9.11	-9.15	-9.05	-8.77	-9.08	-8.9428	-9.07
WCVI Survey	-5.64	-5.64	-5.16	-5.64	-5.77	-5.64	-5.44	-5.65
Fishery age compositions	65.03	205.43	66.88	65.03	65.25	65.03	65.01	65.11
QCS age compositions	134.74	434.04	134.42	134.74	136.16	134.51	134.94	134.97
HS age compositions	123.13	370.17	124.64	123.13	121.75	123.11	123.02	123.21
WCVI age compositions	119.52	358.84	119.23	119.52	118.80	119.62	119.00	119.11
Recruitment	7.85	12.90	10.34	10.57	10.41	10.99	11.85	10.56

Table 12. Median estimated growth parameters from the Length+CAAL model compared to the fixed growth parameters from the other models.

Parameter	Length+CAAL Median estimate	Fixed value from other models
Female length at minimum age	16.13	16.43
Female asymptotic length in the von-Bertalanffy growth equation (cm)	55.76	55.16
Female growth coefficient (K) in the von-Bertalanffy growth equation	0.15	0.16
Female variability in size at age 1	0.16	0.19
Female variability in size at ages 22+	0.05	0.08
Male length at minimum age	17.03	16.45
Male asymptotic length in the von-Bertalanffy growth equation (cm)	44.96	43.47
Male growth coefficient (K) in the von-Bertalanffy growth equation	0.20	0.23
Male variability in size at age 1	0.13	0.14
Male variability in size at ages 22+	0.04	0.05

3.4. ENVIRONMENTAL CONDITIONS AND SPECIES BIOLOGY

3.4.1. Environmental conditions potentially impacting recruitment

Recruitment deviations in Petrale Sole were found to be strongly positively correlated with spawning season PDO and sea surface temperature (SST), closely followed by spring SST and the total euphausiid biomass index for QCS (Figure 60). All of these relationships were at least slightly quadratic with stronger effects at higher values (Figure 61A,C–E). Summer SST, in contrast, showed weak evidence of a concave down relationship with mean summer surface temperatures over 14 ^{o}C beginning to predict a decline in recruitment (Figure 61F). The only strong negative relationship was with NPGO, which appeared essentially linear (Figure 61B).

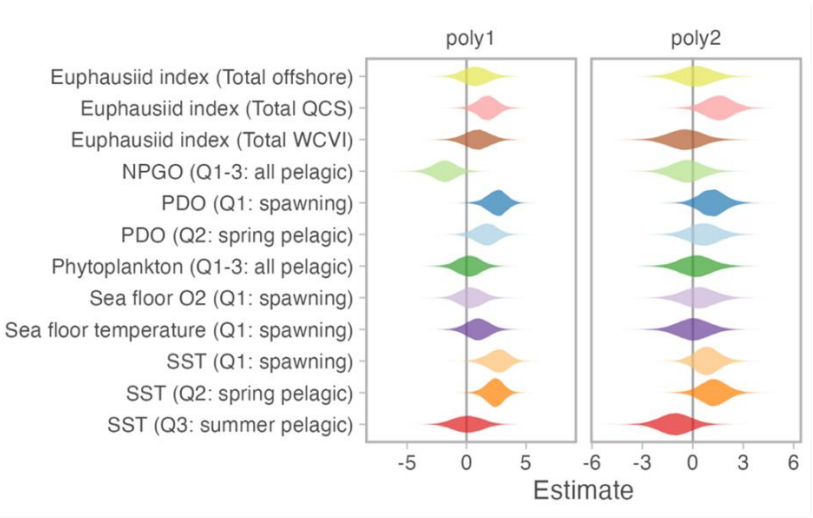


Figure 60. Density violin plots for first- (poly1: linear component) and second- (poly2: curvature component) order orthogonal polynomial coefficient posteriors from time-series regressions on 100 MCMC samples of recruitment deviations between 1995 and 2018 from the base model. Each violin contains 25000 MCMC samples.

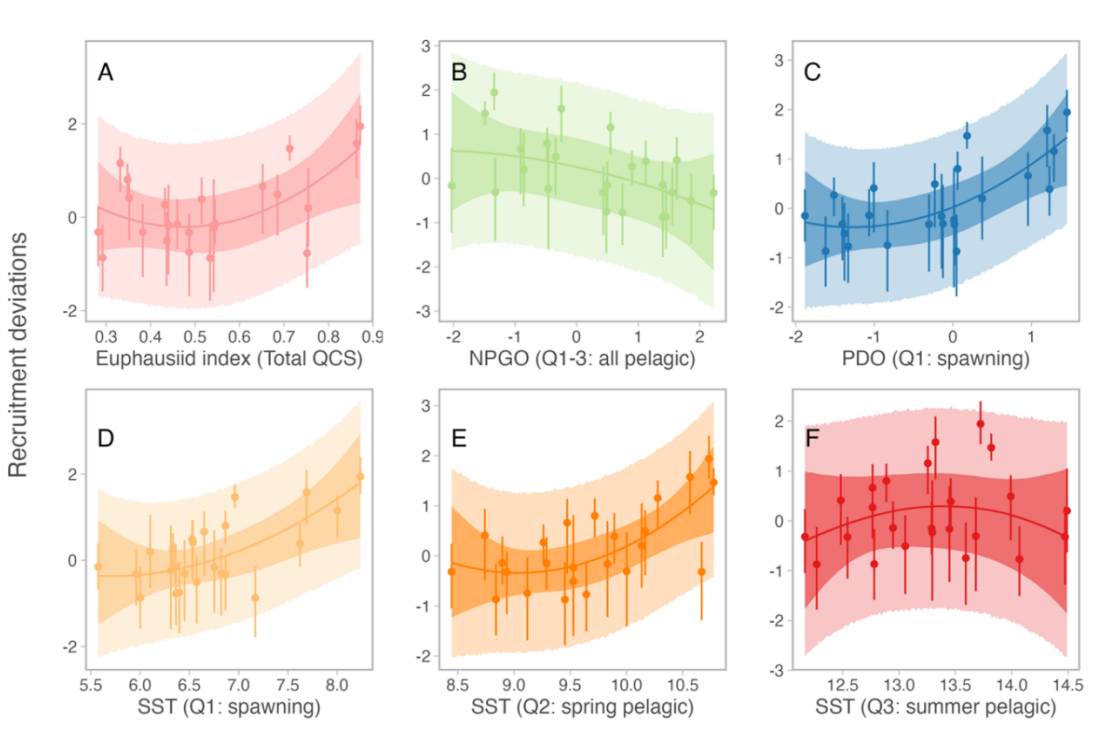


Figure 61. The five strongest predicted polynomial relationships between environmental conditions and recruitment deviations from the base model for 1995 through 2018 for the linear components (A–E) and the curvature components (A,C–F) of the polynomials. The darker shading represents the 95% CI in the predicted second order orthogonal polynomial relationship based on the combined posteriors from 100 time-series regressions, one for each MCMC sample. Lighter shading indicates a 95% credible interval from the full posterior prediction (i.e., including uncertainty on new "observations" of recruitment deviations). Vertical dot-lines represent the median recruitment deviation and 95% quantiles of observed values in the 100 MCMC samples.

3.4.2. Body condition indices

Indices of average body condition for immatures, mature males, and mature females all followed a similar general trajectory over the majority of the past 25 years (Figure 62). The only period when estimated average body condition dipped well below the observed average length-weight relationship was from 2007 to 2009. Following this period, immature condition rose steadily to its highest peak in 2012. All groups dipped again in 2013 but recovered in 2014. Since 2019, mature females tended to score higher than the other groups.

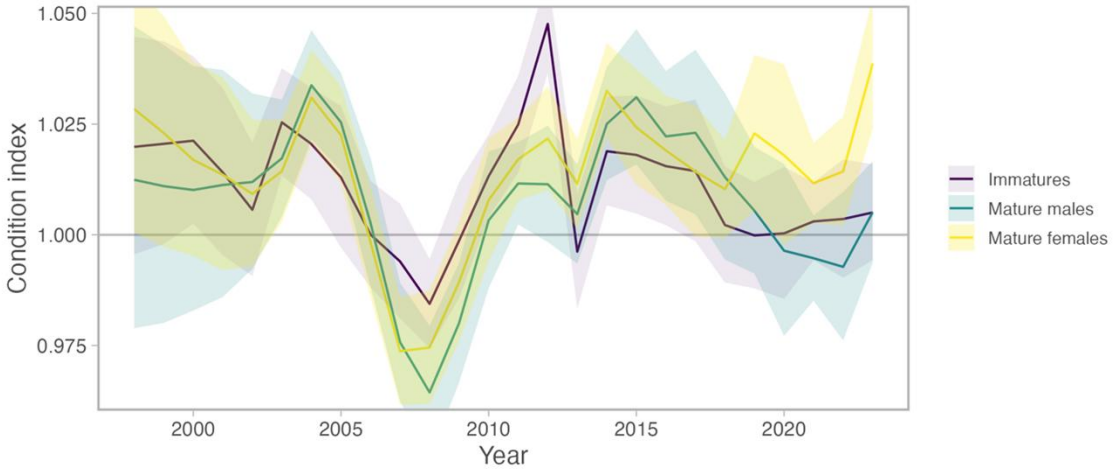


Figure 62. Annual average body condition deviations for immatures (purple), mature males (turquois), and mature females (yellow) estimated for the summer solstice in all areas sampled by synoptic trawl surveys using a spatiotemporal model. Samples and catches from small-mesh and multispecies assemblage trawl surveys were also included in these models to improve the spatiotemporal representativeness of the input data.

If mature condition deviations are fitted to recruitment in the following year, the relationship is weakly positive for both males and females (Figure 63). As expected, females show a slightly weaker relationship, potentially because their weight is more likely to be influenced by differences in reproductive state at the time of sampling.

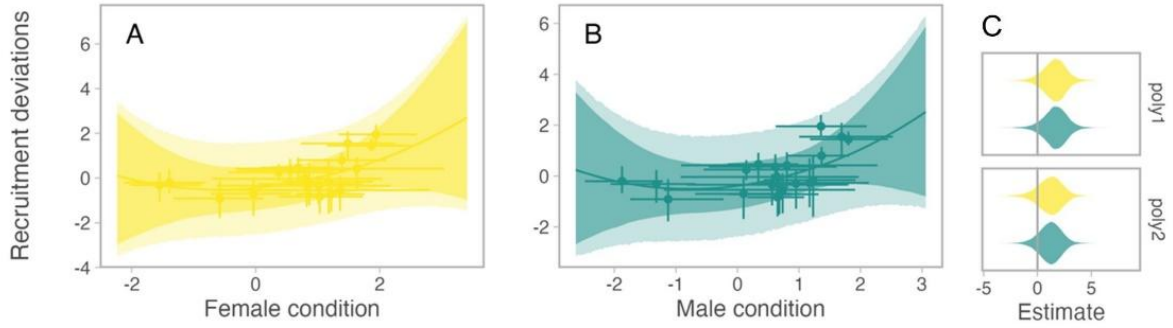


Figure 63. Predicted relationships between body condition in SDs from the mean of each time series for mature females (A, yellow) and mature males (B, turquois) and recruitment deviations from the model with an M of 0.154 from the ensemble base model for 1998 through 2018. The darker shading represents the uncertainty in the predicted relationship based on the combined posteriors from 100 time-series regressions, one for each pair of recruitment and body condition samples. Lighter shading indicates a 95% credible interval from the full posterior prediction (i.e., including uncertainty on new "observations" of recruitment deviations). Vertical dot-lines represent the median recruitment deviation and the 95% quantiles of observed values in the 100 MCMC samples. Horizontal dot-lines represent the median body condition deviations and the full range of values observed in the 100 samples. Density violin plots for slope estimate posteriors (C) are based on 25000 samples.

3.4.3. Environmental conditions potentially impacting body condition

The only consistent effect across all sex and maturity groups was a strong positive correlation between average body condition and average sea floor temperature (Figure 64). Immature body condition was also strongly positively correlated with sea floor oxygen concentration and NPGO. PDO was positively related to all groups, but only strongly so for mature males. Primary production was negatively associated with body condition for all groups, but only strongly so for immatures.

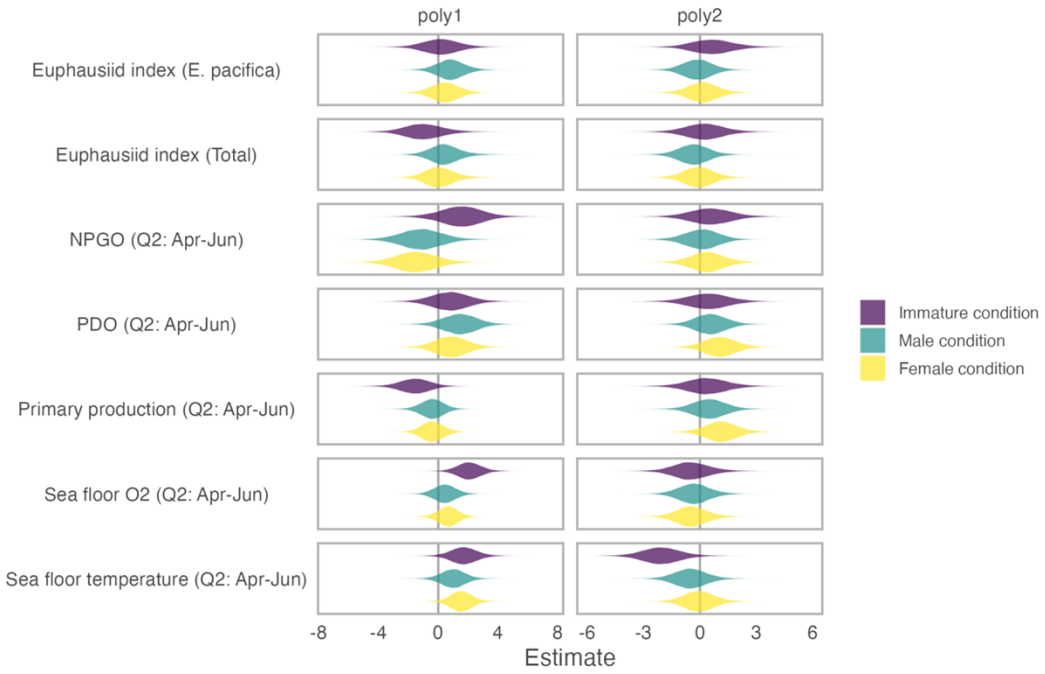


Figure 64. Density violin plots for first- (poly1: linear component) and second- (poly2: curvature component) order orthogonal polynomial coefficient posteriors from time-series regressions on 100 samples from the sex- and maturity-specific annual body condition indices for all available years (1998–2023). PDO and NPGO use this whole timeseries, while all other environmental covariates were only available through 2019. Each violin contains 25000 sample of the parameter distribution.

4. DISCUSSION

4.1. OVERALL

Stock Synthesis was used to fit a stock assessment model for Petrale Sole with catch data, three survey indices, and fishery and survey age composition data. Similar to many other stock assessments, M is an uncertainty for Petrale Sole and was not estimated within the stock assessment. Sensitivity analyses also show that M has the largest impact on model results. As a result, a base ensemble model with three different M levels (0.154, 0.124, and 0.184) was used to estimate stock status. MSY-based reference points were recommended since the historical based reference points from the last Petrale Sole assessment were no longer appropriate, and MSY-based reference points were robust across sensitivities. We discuss updates from the 2006 assessment, a comparison to the U.S. Petrale Sole assessment, uncertainties, future research, and an assessment schedule below.

4.2. UPDATES FROM 2006 ASSESSMENT

Both the modelling approach and available data series were substantially changed for this assessment compared to the last, limiting our ability to make a direct comparison on results. The last assessment of Petrale Sole in BC used a delay-difference model to estimate population dynamics between 1966 and 2006 (Starr 2009). Key data sources for the 2006 assessment included catch, trawl fishery CPUE from 1966 – 2005, and data from three fishery independent surveys. The survey series available at the time were relatively short (ranging from 3 to 11 years of data each) and age composition data were considered insufficient to inform a statistical catch-at-age model. As a result, the assessment required several assumptions including knife-

edge fishery selectivity at a fixed-age and a fixed value for steepness. The model fit also relied heavily on fishery-dependent CPUE from the trawl fishery. Given significant changes in fishery behaviour over time in response to management regulations, several options were considered for developing standardized CPUE indices, including two different data selection rules that attempted to correct for seasonal changes in directed fishing of Petrale Sole and the splitting of the CPUE series into two indices that covered different management regimes (i.e., before and after the introduction of ITQs). Model results in 2006 were highly sensitive the many of these assumptions, resulting in considerable uncertainty in both the scale of population biomass and trends in biomass between 1996 and 2006.

4.3. COMPARISON TO PETRALE SOLE ON THE US WEST COAST

Given the apparent movement of Petrale Sole between BC and Washington State waters, as well as the shared fishery history prior to 1977 with US vessels fishing in Canadian waters, some similarities in reconstructed biomass trends are not surprising. The most recent stock assessment for Petrale Sole along the US West Coast (Washington to California; Taylor et al. 2023) showed somewhat similar biomass trends as our assessment prior to the 1980s. In both cases, *B* was estimated to have declined consistently between the 1940s and 1970s. While both stocks are estimated to have increased *B* in subsequent years, the timing and magnitude of growth differs. In the US, biomass is estimated to have stayed at relatively low levels until the 2000s before increasing to around 50% of B_0 in 2017, while in Canada, biomass started increasing in the 1980s with ongoing and continued growth up to 93% B_0 at present. These differences are likely a result of differences in catch and fishing mortality trends throughout this period. The Canadian fishery had large catch reductions in the 1960s – 1970s, with catches remaining relatively low since then, while US fishery catches have been more stable. The Canadian stock is also estimated to have experienced large recruitment events in 2015-2016 that were larger than those previously predicted for Petrale Sole in BC. These events were not apparent for the US stock. Large recruitment events around 2015-2016 have been estimated for other groundfish species in BC, including Bocaccio Rockfish in 2016 (Starr and Haigh 2022) and Sablefish in 2015-2017 (Johnson et al. 2025). Around the same time from 2014-2016, the Northeast Pacific Ocean experienced a marine heatwave known as “the Blob”, which had significant impacts on the ecosystem (Boldt et al. 2023).

4.4. UNCERTAINTY IN AGE COMPOSITION DATA

Age composition data for Petrale Sole cover only a small portion of the reconstructed time period, with data ranging from 2004 – 2019. A lack of unsorted commercial fishery samples in the early part of the time period limited our ability to represent changes in fishery selectivity that are expected to have occurred due to large changes in management regulations and fleet behaviour over time (Appendix B). As a result, the assessment assumed a single-fishery selectivity curve over time and coastwide, which is an uncertain assumption given large changes in management regulations and fleet behaviour. The lack of recent (later than 2019) age composition data also led to uncertainty in recent recruitment estimates. We limited our fishery age and length composition data to sorted samples to ensure that data were representative of the total catch series used in this assessment, which combined landed catch and discards. However, given that only a small portion of Petrale Sole catch is discarded (5.5%), the sorting process may have a small effect on composition data. Future stock assessments of Petrale Sole should re-visit this decision. The inclusion of sorted samples would have allowed for an additional nine years of commercial fishery samples covering the years 1990 – 2001.

While age data limitations for historical fisheries are a common stock assessment challenge, the increasing paucity of age composition data from the fishery in recent years is less common and will lead to stock assessment challenges in the future. The last year with ageing estimates for Petrale Sole from BC fisheries was 2013. While otoliths were collected in reduced numbers (<100 / year) up until 2018, sample collection has since ceased due to the move to electronic monitoring in 2020. Without updated composition data from the fishery, the modelling approaches that have been developed here will not be able to improve the estimation of fishery selectivity in the future, or identify changing selectivity over time. A trawl catch sampling program for BC groundfish is currently being developed; however, work has yet to begin on developing methods for flatfish species. Increased sample sizes for fishery age composition data going forward would allow future stock assessments to represent multiple fishing areas or seasons, which would better align with the observed spatial and seasonal differences in fishery CPUE and provide a mechanism for modeling spatial catch-at-age in an assessment model. Using an 'areas-as-fleets' model formulation in future stock assessments may also allow better accounting of the spatial differences in the abundance and age structure of Petrale Sole in BC (Waterhouse et al. 2014). Ongoing age composition sampling is available from DFO's synoptic trawl surveys; however, limited resources for groundfish ageing in BC mean that only a portion of collected otoliths are read each year. Our look at the spatial distribution of aged samples for Petrale Sole showed that sampling was typically limited to only a few locations each year. Although not described in this paper, we attempted to deal with this issue by standardizing age and length compositions with a spatiotemporal model, but there was not enough data for reliable results. Perhaps a result of limited age data, residual patterns were apparent in the stock assessment model age composition fits, and attempts at estimating dome-shaped selectivity did not resolve the residual patterns.

A lack of data in fisheries stock assessment can lead to biased estimates of stock status and increased uncertainty (Chen et al. 2002). Yin and Sampson (2004) found that accuracy of stock assessment estimates was more influenced by increased age composition sampling than improvements in survey indices. The issue of limited age composition data is not specific to Petrale Sole in BC, as it is one of many species that would greatly benefit from more ageing effort. Trade-offs in allocating ageing efforts among species and a broader multi-species review of prioritization of age sampling and reading should be considered.

Sparse age composition data may have contributed to poor MLE convergence for several of the sensitivity scenarios considered (Appendix G). Other assessments have found poor convergence can be linked to the presence of age composition bins with zero observations (Cox et al. 2023). While a small constant was added to all age bins in the SS model formulation to prevent zero observations, future research should explore model sensitivity to the assumed additive constant to age bins when the proportion at age is zero.

The Length+CAAL sensitivity is a model that attempts to address the lack of age data by using length data, which are much more abundant than age data for Petrale Sole. The Length+CAAL model estimated a high recruitment event in later years, which the age composition data did not pick up, and estimated slightly lower high recruitment events in 2015 and 2016 than the baseM model. Due to the poor length composition fits, we chose to not present the Length+CAAL model as a base model (Appendix H). However, if age composition data are not available in recent years for future assessments, we recommend a length and conditional-age-at-length model be considered. Variation in growth patterns among fish in the same cohort (i.e., fast and slow growing fish), in addition to modeling dynamic numbers by length-within-age (to account for size based mortality) can be implemented in Stock Synthesis using the platoon feature (McGarvey et al. 2024), and this should be explored in future assessments as well.

4.5. UNCERTAINTY IN HISTORICAL CATCH

Historical catch from Ketchen and Forrester (1966) is quite high compared to recent catch, which resulted in a high fishing mortality in early years and also was the motivation for the ReduceCatch sensitivity, which had a larger impact than some of the other sensitivities. The model attempted to recreate historical catch by depleting the stock. It is not surprising that the assumed magnitude of historical catch has a large effect on the estimated scale and productivity of the stock since catch is the only data used in the model prior to 2003 when DFOs synoptic trawl survey began. As a result, all reconstructed dynamics in the early period were based on historical catch. Previous stock assessments for Petrale Sole in BC have opted to not use historical catch records from before 1954 due to concerns about reliability; however, initial attempts to start our current assessment at a fished state in 1954 showed high sensitivity to starting assumptions. As a result, we decided that utilizing the historical data (well-documented in Ketchen and Forrester 1966) was preferable given the value of information from this early, high catch period. Sensitivities with fishery CPUE were also considered but are only presented as MLE outputs because the models did not converge. Poor diagnostics with fishery CPUE are understandable, given the uncertainty in utilizing fishery CPUE as a measure of abundance even after standardization.

4.6. UNCERTAINTY IN STOCK DELINEATION

Another assumption that was uncertain was the stock delineation. We assumed a closed population, but Petrale Sole is known to migrate between the U.S. and Canada as both adults and pelagic larvae (Pedersen 1975, Santa Cruz et al. 2023). The U.S. Petrale Sole stock assessment also acknowledges this issue (Taylor et al. 2023). The similar estimated stock trends (especially in earlier years) by the U.S. assessment and this assessment provide further support that Petrale Sole may be a transboundary stock. Future assessments may want to consider testing the effect of assuming a single, closed BC stock in light of documented movement of Petrale Sole between BC and Washington state. Further studies on Petrale Sole movement would be beneficial to such an effort.

4.7. PRODUCTIVITY AND ENVIRONMENTAL IMPACTS

There are many research projects that could improve future Petrale Sole stock assessments, including a better understanding of productivity, climate impacts, and prey availability. Steepness was estimated to be around 0.6, which is on the low end of what may be expected for a flatfish (Myers et al. 1999) and at the tail of our prior distribution. We considered fixing steepness, but fixing steepness and M would result in fixing reference points (Mangel et al. 2013). However, Petrale Sole in BC occurs at the northern end of the range of their distribution, so a steepness of 0.6 may be realistic. Steepness is impacted by life history traits, such as maturity and mass at age, and these life history parameters can change over time (Miller and Brooks 2021). Thus, steepness may have changed between 1938 and 2024 with changing environmental conditions, but it is not clear as to when and how. In this assessment, we have not considered nonstationarity, but future research can guide future nonstationary assumptions for Petrale Sole assessments.

The environmental analyses in this assessment test various hypotheses as to how productivity may have changed, which could be explored in future assessments and research. Specifically, positive correlations between recruitment deviations and warmer SST in winter and spring were found, as well as between sea floor temperature and body condition indices of all sex and maturity groups. Furthermore, there was a weak positive relationship between the index of body condition for mature individuals and recruitment in the following year. Taken together this may suggest that steepness could increase under warmer conditions. The relationship between

recruitment and temperature was consistent with published findings in the literature, but this relationship could be related to wind direction facilitating inshore advection of eggs and larvae rather than temperature directly (Ketchen and Forrester 1966, Castillo et al. 1994).

It is also important to note that this has been true for the range of conditions present between 1995 and 2018, and further warming could become detrimental. Consistent with this possibility, the relationship between recruitment and summer SST become slightly dome-shaped, suggesting that impacts on recruitment might start becoming negative at SST over 14 ^{o}C.

Euphausiid abundance was also found to be positively correlated with both recruitment and mature male body condition (specifically biomass of *E. pacifica*). Immature body condition showed negative relationships with both primary production and total euphausiids, and positive relationships with both sea floor oxygen concentration and NPGO possibly suggesting some negative impact from upwelling conditions, potentially through impacts on oxygen concentrations.

We did not have indices of herring and sandlance at the appropriate spatial and temporal scales to include in this analysis, but those could be included in the future investigations. It would also be useful to know if diet composition has changed over time and whether these species remain the dominate prey for Petrale Sole.

In general, our results support the conclusions of Haltuch et al. (2020) that Petrale Sole recruitment strength is a product of multiple mechanisms acting at different early life history stages. Haltuch et al. (2020) focused specifically on the US stock in the California current ecosystem, where they showed that temperature and cross-shelf transport in various seasons could be combined to account for 73% of the variability in recruitment deviations. Interestingly, they also found a link between the spawning pre-conditioning period (May – October) and subsequent recruitment success that aligns with our finding that body condition in a given year was weakly correlated with spawning success in subsequent years.

4.8. ASSESSMENT SCHEDULE

Advice was also requested concerning the appropriate time interval between formal stock assessments presented at a regional peer review meeting, indicators used to characterize stock status in the intervening years, and/or triggers of an earlier than scheduled assessment (DFO 2016). The Petrale Sole stock is currently well above DFO's default USR of $0.8B_{MSY}$ and exploitation is below F_{MSY}; however, a lack of recent age data resulted in uncertainty in recent large recruitment estimates for 2015-2016. It is recommended that formal stock assessments occur every five years, but could be delayed up to ten years given the high values of estimated stock status in 2024. During intervening years, abundance trends could be tracked using indices from the synoptic surveys using the groundfish synopsis report (Anderson et al. 2019; Anderson et al. 2020; Anderson et al. 2024), which is updated regularly. The stock was estimated to be under the candidate USR in 2003, so a model-based coast-wide index, estimated using a geostatistical model, that falls below the mean 2003 index value may signify that the stock should be reassessed. Individual survey indices from the synoptic surveys could be used as secondary sources of information for prioritizing reassessment.

4.9. RECOMMENDATIONS

We recommend the following priorities for future data collection and research to support Petrale Sole stock assessment in BC:

1. Prioritize the collection of age and length composition data from trawl fisheries. The last year of available Petrale Sole otoliths from the commercial trawl fishery is 2017, although

sampling rates were <100 fish / year from 2013 onwards. Without updated composition data from the fishery, the modelling approaches that have been developed here will not be able to improve the estimation of fishery selectivity in the future, or identify changing selectivity over time.

2. Increase ageing effort and review the methods used to select otoliths for age reading from the DFO synoptic trawl surveys. For each survey series, the spatial coverage of aged otoliths in a given year was concentrated in a few locations, making it unclear how representative sampled age compositions were of the larger stock. This issue is not specific to Petrale Sole, as it is one of many species that would greatly benefit from a higher level of biological sampling from the fishery and ageing of otoliths from the surveys. Tradeoffs in allocating ageing resources among species and a broader multi-species review of prioritization of age sampling and reading should be considered.
3. Future work to develop length- and conditional-age-at-length models for Petrale Sole (or other groundfish species) in an attempt to compensate for limited age data should explore methods to represent variation in growth patterns among fish in the same cohort. In addition, research could include simulation analyses examining the effect of sparse age data, including the impact of an additive constant to age bins, on the performance of age-structured and conditional age-at-length models, or equivalently a literature review of current simulation studies on the topic.
4. Future assessments should consider testing the effect of assuming a single, closed BC stock in light of documented movement of Petrale Sole between BC and Washington state. Further studies on Petrale Sole movement and genetic stock delineation would also be beneficial to such an effort.
5. Continue work on the effects of environmental factors on Petrale Sole productivity and consider whether stock assessment modelling of recruitment dynamics and/or steepness could be improved through the incorporation on environmental variables into the stock assessment model. These efforts would be best supported by having information on contemporary diets and prey availability.

ACKNOWLEDGEMENTS

We would like to thank members of the Petrale Sole Stock Assessment Technical Working Group (Sean Anderson, Dana Haggarty, Rowan Haigh, Brian Mose, Lindsay Richardson-Deranger, Rachel Rickaby, Paul Starr, Bruce Turris, and Penny White) for their helpful feedback throughout and outside of the working group meetings. Thank you to the members of the Petrale Sole Stock Assessment Steering Committee (Erika Anderson, Dana Haggarty, Lindsay Richardson-Deranger, Rachel Rickaby, and Penny White) for supporting this process. We would also like to thank Rick Methot, Vlladena Gertseva, and Tom Carruthers for answering our Stock Synthesis questions. We would like to thank Chris Grandin for helping us run MCMCs on a faster machine. We also benefited from work done by Rob Kronlund during his time at DFO to compile the management history for Petrale Sole in BC (Appendix A, Table A-1). Finally, we would like to thank our reviewers: Ian Taylor and Paul Regular.

REFERENCES CITED

Allen, L.G., Pondella, D.J., and Horn, M.H. 2006. The ecology of marine fishes: California and adjacent waters. University of California Press, Los Angeles.

Alverson, D.L. and Chatwin, B.M. 1957. Results from tagging experiments on a spawning stock of petrale sole, *Eopsetta jordani* (Lockington). J. Fish. Board Can. 14(6), 953-974.

Anderson, S.C., Dunic, J.C., Keppel, E.A., and Edwards, A.M. 2024. A data synopsis for British Columbia groundfish: 2022 data update. Can. Tech. Rep. Fish. Aquat. Sci. 3624: viii + 267 p.

Anderson, S.C., Keppel, E.A., and Edwards, A.M. 2019. A reproducible data synopsis for over 100 species of British Columbia groundfsh. DFO Can. Sci. Advis. Sec. Res. Doc. 2019/041. vii + 321 p.

Anderson, S. C., Keppel, E. A., and Edwards, A. M. 2020. Reproducible visualization of raw fisheries data for 113 species improves transparency, assessment efficiency, and monitoring. Fisheries. 45(10), 535-543.

Barrett, T.J., Marentette, J.R., Forrest, R.E., Anderson, S.C., Holt, C.A., Ings, D.W., and Thiess, M.E. 2024. Technical Considerations for Stock Status and Limit Reference Points under the Fish Stocks Provisions. DFO Can. Sci. Advis. Sec. Res. Doc. 2024/029. v + 57 p.

Birtwell, I.K., Wood, M., and Gordon, D.K. 1984. Fish diets and benthic invertebrates in the estuary of the Somass River, Port Alberni, British Columbia. Can. Manuscript Rep. Fish. Aquat. Sci. 1799.

Boldt, J.L., Joyce, E., Tucker, S., and Gauthier, S. (Eds.). 2023. State of the physical, biological and selected fishery resources of Pacific Canadian marine ecosystems in 2022. Can. Tech. Rep. Fish. Aquat. Sci. 3542: viii + 312 p.

Carvalho, F., Punt, A.E., Chang, Y.J., Maunder, M.N., and Piner, K.R., 2017. Can diagnostic tests help identify model misspecification in integrated stock assessments?. Fisheries Research, 192, 28-40.

Castillo, G.C., Li, H.W., and Golden, J. T. 1994. Environmentally induced recruitment variation in petrale sole, *Eopsetta jordani*. Fishery Bulletin, 92(3), 481-493.

Chen, Y., Chen, L., and Stergiou, K.I. 2002. Impacts of data quantity on fisheries stock assessment. Aquatic Sciences, 65, 92-98.

Clark, W. G. 1999. Effects of an erroneous natural mortality rate on a simple age-structured stock assessment. Canadian Journal of Fisheries and Aquatic Sciences, 56(10), 1721-1731.

Cox, S.P., Kronlund, A.R., Lacko, L., and Jones, M. 2023. A Revised Operating Model for Sablefish in British Columbia, Canada in 2016. DFO Can. Sci. Advis. Sec. Res. Doc. 2023/023. vii + 127 p.

DFO. 2009. A fishery decision-making framework incorporating the Precautionary Approach. Online – last date modified: 2009-03-23.

DFO. 2016. Guidelines for providing interim-year updates and science advice for multi-year assessments. DFO Can. Sci. Advis. Sec. Sci. Advis. Rep. 2016/020.

DFO. 2024a. Groundfish Integrated Fisheries Management Plan 2024/25. 23-2317. 349 p.

DFO. 2024b. Pacific Ocean Perch (*Sebastes alutus*) Stock Assessment for British Columbia in 2023. DFO Can. Sci. Advis. Sec. Sci. Advis. Rep. 2024/012.

Edwards, A.M., Berger, A.M., Grandin, C.J. and Johnson, K.F. 2022. Status of the Pacifc Hake (whiting) stock in U.S. and Canadian waters in 2022. Prepared by the Joint Technical Committee of the U.S. and Canada Pacifc Hake/Whiting Agreement, National Marine Fisheries Service and Fisheries and Oceans Canada. 238 p.

Fargo, J. 1999. Flatfish Stock Assessments for the west coast of Canada for 1998 and Recommended Yield Options for 1999. DFO. Can. Stock. Assess. Sec. Res. Doc. 1999/17.

Francis, R.C. 2016. Growth in age-structured stock assessment models. Fisheries Research, 180, 77-86.

Haltuch, M.A., Tolimieri, N., Lee, Q., and Jacox, M.G. 2020. Oceanographic drivers of petrale sole recruitment in the California Current Ecosystem. Fisheries Oceanography, 29, 122–136.

Hamel, O.S. 2015. A method for calculating a meta-analytical prior for the natural mortality rate using multiple life history correlates. ICES Journal of Marine Science, 72(1), 62-69.

Hamel, O.S., and Cope, J.M. 2022. Development and considerations for application of a longevity-based prior for the natural mortality rate. Fisheries Research, 256, 106477.

Hilborn, R., and Walters, C. J. 1992. Quantitative Fisheries Stock Assessment: Choice, Dynamics and Uncertainty. Chapman and Hall, New York. 570 pp

Holt, K.R., Starr, P.J., Haigh, R., and Krishka, B. 2016. Stock Assessment and Harvest Advice for Rock Sole (*Lepidopsetta* spp.) in British Columbia. DFO Can. Sci. Advis. Sec. Res. Doc. 2016/009. ix + 256 p.

Hurtado-Ferro, F., Szuwalski, C.S., Valero, J.L., Anderson, S.C., Cunningham, C.J., Johnson, K.F., Licandeo, R., McGilliard, C.R., Monnahan, C.C., Muradian, M.L., and Ono, K. 2015. Looking in the rear-view mirror: bias and retrospective patterns in integrated, age-structured stock assessment models. ICES Journal of Marine Science, 72(1), 99-110.

Johnson, S.D.N., Cox, S.P., Holt, K.R., Lacko, L.C., Kronlund, A.R. and Rooper, C.N. 2025. Stock Status and Management Procedure Performance for the BC Sablefish (Anoplopoma fimbria) Fishery for 2022/23. DFO Can. Sci. Advis. Sec. Res. Doc. 2024/072. iv + 132 p.

Kravitz, M.J., Pearcy, W.G., and Guin, M.P. 1977. Food of five species of co-occurring flatfishes on Oregon's continental shelf. Fishery Bulletin, 74(4), 984–990.

Ketchen, K. S., and Forrester, C. R. 1966. Population dynamics of the Petrale Sole, *Eopsetta jordani*, in waters off western Canada (No. 153). Fisheries Research Board of Canada.

Love, M. 1996. Probably more than you want to know about the fishes of the Pacific Coast. Really Big Press, Santa Barbara, California.

Love, M.S., 2011. Certainly more than you want to know about the fishes of the Pacific Coast: a postmodern experience. Really Big Press, Santa Barbara, California.

Magnusson, A., and Hilborn, R. 2007. What makes fisheries data informative. Fish and Fisheries, 8(4), 337-358.

Marentette, J.M., Barrett, T.J., Ings, D.W., Thiess, M.E., and Olmstead M. 2022. Proceedings of the Limit Reference Points and the Fish Stocks Provisions: Joint Technical Expertise in Stock Assessment (TESA) / National Operational Guidelines (NOG) Task Force Virtual Workshop, November 29-December 3, 2021. Can. Tech. Rep. Fish. Aquat. Sci. 3515: vii + 66 p.

Maunder, M. N., Sibert, J. R. Fonteneau, A., Hampton, J., Kleiber, P., and Harley, S. J. 2006. Interpreting catch per unit effort data to assess the status of individual stocks and communities. ICES Journal of Marine Science, 63, 1373e1385.

Maunder, M. N., Hamel, O. S., Lee, H. H., Piner, K. R., Cope, J. M., Punt, A. E., Ianelli, J.N., Castillo-Jordán, C., Kapur, M.S., and Methot, R. D. 2023. A review of estimation methods for natural mortality and their performance in the context of fishery stock assessment. Fisheries Research, 257, 106489.

McGarvey, R., Methot, R.D., Punt, A.E., Matthews, J.M., Taylor, I.G., Feenstra, J.E., and Doering, K. 2024. Performance gains from incorporating dynamic numbers by length-within-age in fishery assessment models. Fisheries Research, 276, 107039.

Methot Jr, R. D., and Wetzel, C. R. 2013. Stock synthesis: a biological and statistical framework for fish stock assessment and fishery management. Fisheries Research, 142, 86-99.

Methot, R. D., Wetzel, C. R., Taylor, I. G., and Doering, K. 2020. Stock synthesis user manual: version 3.30. 15.

Miller, T. J., and Brooks, E. N. 2021. Steepness is a slippery slope. Fish and Fisheries, 22(3), 634-645.

Mohn, R., 1999. The retrospective problem in sequential population analysis: an investigation using cod fishery and simulated data. ICES Journal of Marine Science, 56(4), 473-488.

Monnahan, C.C. 2018. adnuts: No-U-Turn MCMC Sampling for 'ADMB' and ‘TMB’ Models. R package version 1.1.2.

Monnahan, C.C. 2024. Toward good practices for Bayesian data-rich fisheries stock assessments using a modern statistical workflow. Fisheries Research, 275.

Monnahan, C.C and Kristensen, K.. 2018. No-u-turn sampling for fast Bayesian inference in ADMB and TMB: Introducing the Adnuts and Tmbstan r Packages. PloS One, 13(5).

Myers, R.A., Bowen, K.G., and Barrowman, N.J. 1999. Maximum reproductive rate of fish at low population sizes. Canadian Journal of Fisheries and Aquatic Sciences, 56, 2404–2419.

Pearsall, I.A., and Fargo, J.J. 2007. Diet composition and habitat fidelity for groundfish in Hecete Strait, British Columbia. Canadian Technical Report of Fisheries Aquatic Sciences.

Pedersen, N.G. 1975. Recent investigations of Petrale Sole off Washington and British Columbia. Wash. Dept. Fish. Tech. Rept. 17372.

Piner, K.R., Lee, H.H., and Maunder, M. N. 2016. Evaluation of using random-at-length observations and an equilibrium approximation of the population age structure in fitting the von Bertalanffy growth function. Fisheries Research, 180, 128-137.

Powell, A., Clarke, M. E., Haltuch, M. A., Fruh, E., Anderson, J., Whitmire, C. E., and Johnson, M.M. 2022. First autonomous underwater vehicle observations of a potential Petrale Sole (*Eopsetta jordani*) spawning aggregation off the US West Coast. Frontiers in Marine Science, 9, 834839.

Punt, A.E., Castillo-Jordán, C., Hamel, O.S., Cope, J.M., Maunder, M.N., and Ianelli, J.N. 2021. Consequences of error in natural mortality and its estimation in stock assessment models. Fisheries Research, 233, 105759.

Reilly, P.N., Wilson-Vandenberg, D., Lea, R.N., Wilson, C., and Sullivan, M. 1994. Recreational angler’s guide to the common nearshore fishes of Northern and Central California. California Department of Fish; Game.

Santa Cruz, F., Parada, C., Haltuch, M., Wallace, J., Cornejo-Guzman, S., and Curchitser, E. 2023. Petrale sole transboundary connectivity and settlement success: a biophysical approach. Frontiers in Marine Science, 10, 1155227.

Starr, P.J. 2009. Petrale Sole (*Eopsetta jordani*) in British Columbia, Canada: Stock Assessment for 2006/07 and Advice to Managers for 2007/08. DFO Can. Sci. Advis. Sec. Res. Doc. 2009/070. v + 134 p.

Starr, P.J. and Fargo, J. 2004. Petrale sole stock assessment for 2003 and recommendations for management in 2004. DFO. Can. Sci. Advis. Sec. Res. Doc. 2004/036. ii + 86 p.

Starr, P.J. and Haigh, R. 2021. Redstripe Rockfish (Sebastes proriger) stock assessment for British Columbia in 2018. DFO Can. Sci. Advis. Sec. Res. Doc. 2021/014. vii + 340 p.

Starr, P.J. and Haigh, R. 2022. Bocaccio (*Sebastes paucispinis*) stock assessment for British Columbia in 2019, including guidance for rebuilding plans. DFO Can. Sci. Advis. Sec. Res. Doc. 2022/001. vii + 292 p.

Starr, P.J. and Haigh, R. 2023. Canary Rockfish (*Sebastes pinniger*) Stock Assessment for British Columbia in 2022. DFO Can. Sci. Advis. Sec. Res. Doc. 2023/070. vi + 293 p.

Stewart, I. J., and Hamel, O. S. 2014. Bootstrapping of sample sizes for length-or age-composition data used in stock assessments. Canadian Journal of Fisheries and Aquatic Sciences, 71(4), 581-588.

Taylor, I.G., Gertseva, V., and Tolimieri, N. 2023. Status of petrale sole (*Eopsetta jordani*) along the U.S. West Coast in 2023. Pacific Fishery Management Council, Portland, Oregon. 174 p.

Taylor, I.G., Doering, K.L., Johnson, K.F., Wetzel, C.R., Stewart, I.J. 2021. Beyond visualizing catch-at-age models: Lessons learned from the r4ss package about software to support stock assessments. Fisheries Research, 239, 103924.

Then, A.Y., Hoenig, J.M., Hall, N.G., and Hewitt, D.A. 2015. Evaluating the predictive performance of empirical estimators of natural mortality rate using information on over 200 fish species. ICES Journal of Marine Science 72(1), 82–92.

Thorson, J.T., Jensen, O.P., and Zipkin, E.F. 2014. How variable is recruitment for exploited marine fishes? A hierarchical model for testing life history theory. Canadian Journal of Fisheries and Aquatic Sciences, 71(7), 973-983.

Trijoulet, V., Albertsen, C.M., Kristensen, K., Legault, C.M., Miller, T.J. and Nielsen, A. 2023. Model validation for compositional data in stock assessment models: calculating residuals with correct properties. Fisheries Research, 257, 106487.

Vehtari, A., Gelman, A., Simpson, D., Carpenter, B. and Bürkner, P.C. 2021. Rank-normalization, folding, and localization: An improved R^for assessing convergence of MCMC (with discussion). Bayesian analysis, 16(2), 667-718.

Wald, A. and Wolfowitz, J., 1940. On a test whether two samples are from the same population. The Annals of Mathematical Statistics, 11(2), 147-162.

Waterhouse, L., Sampson, D.B., Maunder, M., and Semmens, B.X. 2014. Using areas-as-fleets selectivity to model spatial fishing: Asymptotic curves are unlikely under equilibrium conditions. Fisheries Research. 158, 15-25.

Wetzel, C.R. 2019. Status of petrale sole (*Eopsetta jordani*) along the US west coast in 2019. Pacific Fishery Management Council, 7700.

Yin, Y. and Sampson, D.B. 2004. Bias and precision of estimates from an age-structured stock assessment program in relation to stock and data characteristics. North American Journal of Fisheries Management, 24(3), 865-879.

APPENDIX A. FISHERY AND CATCH HISTORY

A.1. FISHERY HISTORY

A.1.1. 1930's – 1960's

Ketchen and Forrester (1966) provide a detailed history of the early years of the Petrale Sole fishery in British Columbia, which we recap in this section.

Both US and Canadian trawl vessels targeted Petrale Sole in BC waters starting in the 1930s. In the early 1930s, the Canadian fleet stayed close to southern BC ports in the Strait of Georgia, while the US fleet in Washington remained south of the Canada-US border.

By 1938, both US and Canadian vessels had expanded their operations to the lower west coast of Vancouver Island (Area 3C), with Swiftsure Bank, the entrance to Juan de Fuca Strait, and La Perouse Bank being the most heavily fished. The trawl fishery during this period was focused on food fish, with Petrale Sole being the most commonly targeted species due to its relatively large size and high price compared to most other flatfish species.

Between 1938 and 1943, fishing for Petrale Sole in southern portions of Area 3C intensified and vessels began to move northward up the Vancouver Island coast. These increases were largely driven by the US trawl fleet. While the Canadian fleet was fishing Petrale Sole in these areas, the majority of Petrale Sole catch during this period was taken by the larger US fleet (Figure A-1).

By 1944, the fishery had expanded into Area 3D on northern Vancouver Island. In subsequent years, both the Canadian and US fleets continued to expand northward into Queen Charlotte Sound and Hecate Strait, all the way up to the Alaska border. Petrale Sole catches peaked in 1948, with an especially high catch that year due to the discovery of a very productive fishing area in the southern part of Area 5D.

Between 1949 and 1953, there was a decline in Petrale Sole catch for both Canadian and US fleets in Canadian waters, with the decline being sharpest for the Canadian fleet.

In March of 1953, US vessels discovered dense concentrations of Petrale Sole winter spawning aggregations in Area 3D at depths of 170-250 meters. Prior to 1953, fishing operations for Petrale were limited to relatively shallow grounds (<183 m) during spring to early-autumn months, when fish were not in spawning condition. The US fleet fished these deepwater concentrations heavily until the winter of 1957-58, at which time an international agreement was reached between Canada and the US to cease winter fishing, especially for Petrale Sole. The Canadian fleet did not take part in the deepwater winter Petrale fishery during the 1950s. Instead, they continued to fish shallower habitats during summer months.

By 1962, catches of Petrale Sole in BC, as well as along the US coast to the south, had declined substantially compared to the 1940s, with Petrale less frequently targeted due to poor catch rates.

A.1.2. 1960's – 1995

Throughout the 1960s and into the 1970s, Petrale Sole abundance continued to be perceived as low compared to the 1940s (Pedersen 1975), and catches remained lower than in the earlier time period. In 1967, the Canada-US agreement prohibiting winter fishing ended (Sampson and Lee 1999, cited in Haltuch et al. 2013). US vessels continued to catch Petrale Sole in Canadian waters until 1977, at which time US vessels were excluded based on the establishment of Canada's 200 nautical mile (nmi) Economic Exclusion Zone (EEZ) on January 1, 1977.

Landings of Petrale Sole increased in the 1980s and into the early 1990s. Increased catch during this period occurred for several groudfish species in anticipation of individual transferable quote (ITQ) management. Allocation of quota species to individual license holders was partly based on landings during the qualifying period of 1988-1992.

Seasonal restrictions and trip limits were used to reduce fishing pressure on Petrale Sole spawning aggregations throughout the 1980s and early 1990s (Table A.1). Only incidental catches of Petrale Sole were permitted between January 1 and March 31, with trip limits placed on incidental catch during this period. Targeted fishing without trip limits was permitted after March 31. Winter trip limits were reduced substantially starting in 1992. Between 1982 and 1991, trip limits varied between 15 t and 20 t. They were reduced to 4.5 t starting in 1992.

Trip limits in the late 1980s and early 1990s are believed to have influenced fisher behaviour. Limits were perceived to be overly restrictive by trawl fishers due to strong catch rates for Petrale Sole, which lead to some Petrale Sole catch being put into Dover Sole bins at landing (Brian Mose, Canadian Groundfish Research and Conservation Society, pers. comm). This misreporting would have led to an underestimate of Petrale Sole catch starting at the very end of the 1980s and ending with the introduction of at-sea observers in 1996 (Brian Mose, pers. comm).

A.1.3. 1996 – present

Between January 1996 and March 1997, no directed fishing was permitted on Petrale Sole, regardless of month. While management plans indicated that monthly bycatch limits for Petrale Sole would be used, the value of these limits is not documented in management plans.

The introduction of ITQs in 1996 lead to the establishment of the first coastwide (Areas 3CD, 5A-E) Total Allowable Catch (TAC) for Petrale Sole for the 1997 – 1998 fishing year, which was set at 479 t. A series of incremental TAC increases brought the TAC up to 900 t starting in the 2014-2015 fishing year (Table A.1). The TAC has remained at 900 t since this time.

Table A – 1. Summary of seasonal catch limit, trip limit, or TAC management measures applied to Petrale Sole.

Year(s)	Type(s)	Management Measure	TAC
1957 – 1967 *Jan 1 to Dec 31 Fishing Year*	Seasonal Limit Trip Limit	No directed landings of winter aggregations of Petrale Sole from Dec 20 to Apr 15. Incidental catch of Petrale Sole up to 1360 kg (3000 lb) per trip permitted to a maximum of two trips per month during closed season.	-
1967 – 1979	-	No information for this time period.	-
1979 – 1980	TAC Seasonal Limit Trip Limit	Trip limits of 1.4 t (3,100 lb) for incidental catch between January 1 and April 15. Targeted fishing permitted after April 15 to a maximum annual quota of 500 t for areas 3CD.	500 t
1981	TAC Seasonal Limit Trip Limit	Maximum of 100 t of the annual quota permitted in areas 3CD as incidental catch between Jan 1 and Apr 15, with a vessel trip limit of 6.8 t (15,000 lb). Thereafter, a 500 t quota in areas 3CD was permitted as targeted fishing.	600 t
1982	Seasonal Limit Trip Limit Trips	Incidental catch of Petrale Sole was permitted coastwide between January 1 and March 31, with a trip limit of 15 t (33,100 lb) of incidental catch per boat to a maximum of two trips per month during this period. Targeted fishing allowed after March 31.	-

Year(s)	Type(s)	Management Measure	TAC
1983 – 1986	Seasonal Limit Trip Limit Trips	Only incidental catch of Petrale Sole permitted between January 1 and March 31, with a trip limit of 20 t (44,100 lb) of incidental catch per vessel to a maximum of two trips per month during this period. Targeted fishing allowed after March 31.	-
1987 – 1991	Seasonal Limit Trip Limit	Petrale Sole trip limit of 20 t (44,100 lb) of catch per boat permitted between January 1 and March 31. Targeted fishing allowed after March 31.	-
1992 – 1995	Seasonal Limit Trip Limit License Limit	Petrale Sole trip limit of 4.5 t (10,000 lb) of catch per vessel allowed between Jan 1 and Mar 31. Targeted fishing allowed after March 31.	-
1996 - 1997 *Jan 1996-Mar 1997 Fishing Year*	Fishing Limit	Only incidental catch of Petrale Sole permitted. The management plan stated that a calendar-month bycatch limit shall be determined for Petrale Sole but actual values were not stated within the plan; possibly values were specified in Conditions of Licence.	-
1997-1998 to 2003-2004 *Start Apr 1-Mar 31 Fishing Year*	TAC Fishing Limit	Coastwide TAC areas 3CD, 5A-E. Petrale Sole limit of 200 lb per month in Area 4B (Strait of Georgia).	479 t
2004 - 2005 To 2006 – 2007	TAC Fishing Limit	Coastwide TAC areas 3CD, 5A-E. Petrale Sole limit of 200 lb per month in Area 4B (Strait of Georgia).	600 t
2007 – 2008 to 2013 – 2014 *Note: 2008-2009 was first year of Feb 21 – Feb 20 Fishing Year*	TAC Fishing Limit	Coastwide TAC areas 3CD, 5A-E. Petrale Sole limit of 200 lb per month in Area 4B (Strait of Georgia).	700 t
2012 - 2013 to 2013 – 2014	TAC Fishing Limit	Coastwide TAC areas 3CD, 5A-E. Petrale Sole limit of 200 lb per month in Area 4B (Strait of Georgia).	750 t
2014 – 2015 to 2023 – 2024	TAC Fishing Limit	Coastwide TAC areas 3CD, 5A-E. Petrale Sole limit of 200 lb per month in Area 4B (Strait of Georgia).	900 t

A.2. CATCH DATA

Figure A -1 shows the catch time series used in the current stock assessment, separated out by fishing fleet (Canada vs. US). Area- and gear-specific patterns in Canadian catch are shown in Figure A - 2, while the spatial distribution of catch-per-unit-effort in more recent years (≥1996) is shown in Figure A - 3. Almost all Petrale Sole catch is taken in bottom trawl fisheries (Figure A - 2); however, a small amount is occasionally taken by other gear types. Catch in DFO Management Area 4B (Strait of Georgia) has always been low and has been concentrated in a few locations in the most northern and southern portions of Area 4B since 1996 (Figures A - 2, A - 3). We do not present catch statistics for Area 4B beyond these figures, but note that Starr (2009) summarized available data up to 2006. Catches have mostly been <1 tonne per year in this area since the 1990s.

A.2.1. Retained Catch

Sources of retained catch data for Petrale Sole vary over time and among Canadian and US fishing fleets. Some historical catches used in this assessment, including catches prior to 1954 and those from US vessels fishing in Canadian waters, are not archived in DFO databases. In these cases, we use catch values taken from previously published reports, all of which are re-produced in this appendix (e.g., Tables A - 2, A - 3). We break out the description of catch data into three different periods below based on available data sources for each period.

A.2.1.1. 1938 – 1953

Retailed catch values for 1938 to 1953 are taken from Ketchen and Forrester (1966). The collection of catch statistics for this time period pre-dates the establishment of the Pacific Marine Fisheries Commission (PMFC) in 1956, at which time an agreement was reached between Canada and US on the definition of statistical areas as well as mechanisms for sharing data among countries. As a result, Ketchen and Forrester (1966) relied on a variety of information sources to compile catch estimates for this time period, including regional catch summaries, personal communications, infilling to assign catch to statistical areas based on effort distributions, and/or reconstructions of Petrale Sole catch based on records of “sole landings”. While the methods used in each area are documented in Ketchen and Forrester (1966), documentation is not sufficient to reproduce. As a result, catch statistics from this time period are believed to be informative of general temporal patterns, but highly uncertain.

Based on catch tables presented in Ketchen and Forrester (1966), we compiled estimates of retained catch for Petrale Sole in Canadian waters for the years 1938 – 1953 (Table A - 2). While we only use total coastwide catch from both US and Canadian fleets combined when fitting the current stock assessment model, we provide catch by fleet and statistical area in Table A - 2.

A.2.1.2. 1954 - 1995

Retained catch from Canadian fisheries during this period are archived by the Groundfish Data Unit (Fisheries and Oceans Canada, Science Branch, Pacifc Region) and housed in the GFCatch database (trawl and trap) and PACHARVHL database (hook and line). We used the gfdata R package to extract catch from GFcatch. The gfdata package was developed as a reproducible tool to support the Groundfish Data Synopsis Report (Anderson et al. 2019), but note that only users with access to DFO’s Pacific Biological Station network and permissions to access the groundfish databases can extract data). Detailed descriptions of the database queries used to extract catch data are available from Appendix C of Anderson et al. 2019.

Retained catch from US fisheries between 1954 and 1976 was taken from Fargo (1999; Table A-3). Fargo (1999) provided separate catch tables for Area 3C and the rest of the BC coast (Areas 3D, 5A-D) based on their assumption of two discrete Petrale Sole populations in BC. Catch was presented as total catch (US and Canadian fleets combined) and catch from only the Canadian fleet, which allowed us to calculate catches from US fleets as the difference between the two. This is the same source of US catch used in the last Petrale Sole assessment (Starr 2009). While Fargo (1999) summarized catch as far back as 1944, we relied on the Ketchen and Forrester (1966) estimates of US catch described above prior to 1954, and only use US catch from Fargo starting in 1954. A comparison on US catch estimates for 1944 – 1953 from Fargo (1999) and Ketchen and Forrester (1966) showed high agreement in almost all years.

Fargo (1999) reported zero catch from US fisheries in Canadian waters starting in 1977, which coincides with the implementation of Canada's 200 nmi EEZ in 1977 and the cessation of US fishing in Canadian waters.

A.2.1.3. 1996 - 2023

As with the previous time period, estimates of retained catch for this period are archived in relational databases by the Groundfish Data Unit. Retained catch values for 1996 – 2007 are maintained in the PacHarvest database (trawl), the PACHARVSABLE database (trap and longline) and the PACHARVHL database (hook and line). Catches from all gear types for 2007 - 2023 are maintained in the GFFOS database. The gfdata R package cited above was also used to extract catch data for 1966-2023, with detailed descriptions of the methods documented in Appendix C of Anderson et al. 2019.

A.2.2. Discarded Catch

Discarded catch values from 1996 – 2023 were taken from the GFFOS catch database using the gfdata R package. Reported discard weights are considered unreliable prior to the start of the 100% observer coverage for the bottom trawl fishery in 1996. Discards prior to 1996 were estimated by applying the average discard ratio (amount discarded divided by amount landed) between 1996 and 2023 to landed catch values in all earlier years. The average ratio used was 5.5%.

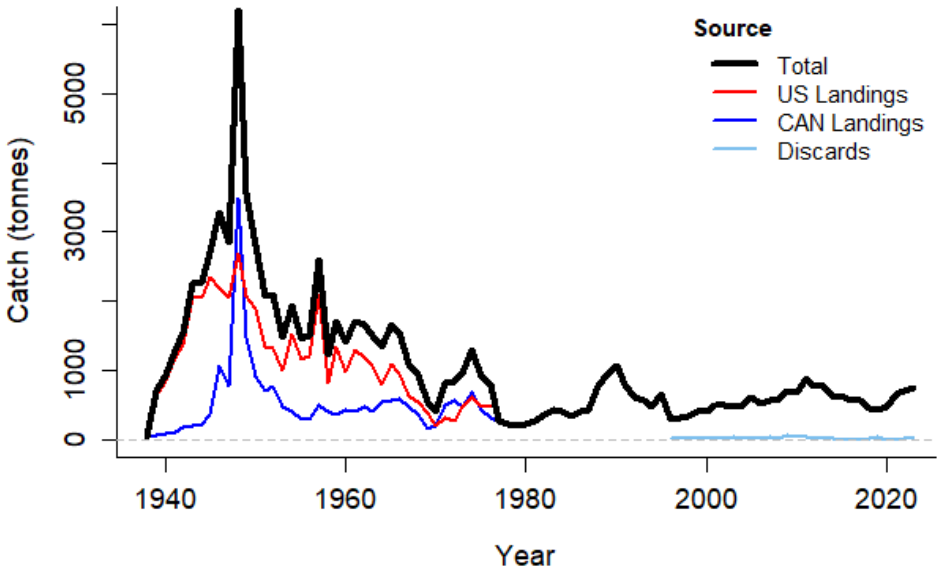


Figure A - 1. Petrale Sole catch (tonnes) from 1938 to 2023.

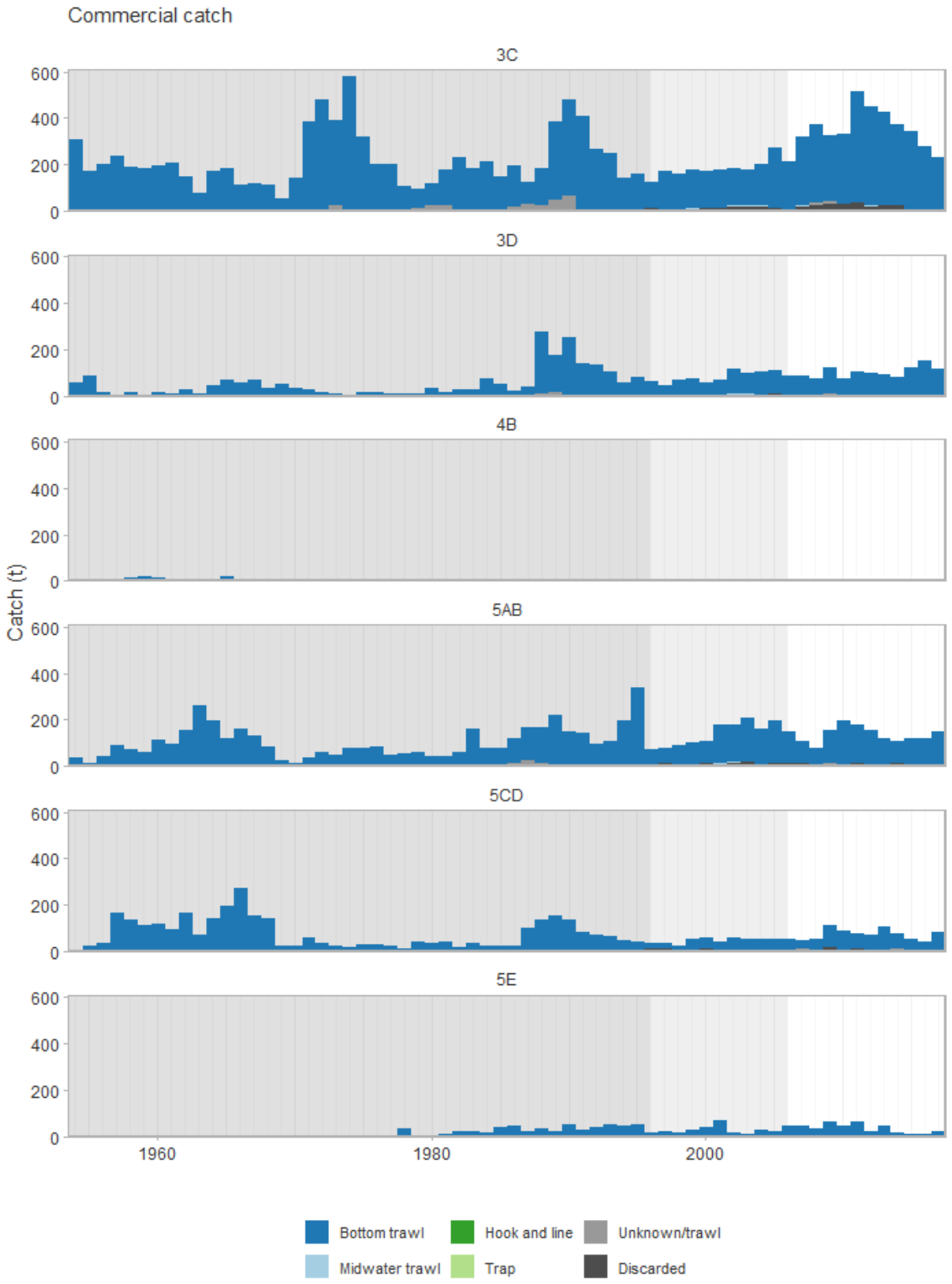


Figure A - 2. Petrale Sole catch by area and gear type from 1954 to 2023.

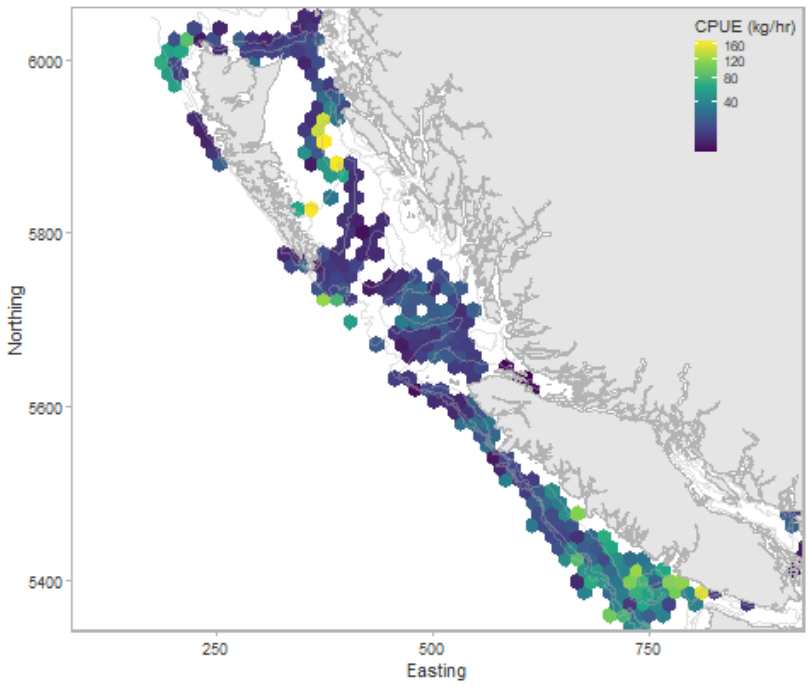


Figure A - 3. Average fishery catch-per-unit-effort (CPUE; kg/hr) of Petrale Sole over space from 1996 to 2023.

Table A - 2. Retained catch estimates for Canadian and US vessels fishing in Canadian waters from 1938 to 1953. Taken from Ketchen and Forrester (1966).

Year	Canadian Trawl Fleet					US Trawl Fleet					Can + US Total
	3C	3D	5AB	5CD	Total	3C	3D	5AB	5CD	Total	
1938	45	0	0	0	45	0	0	0	0	0	45
1939	68	0	0	0	68	640	0	0	0	640	708
1940	91	0	0	0	91	844	0	0	0	844	934
1941	113	0	0	0	113	1197	0	0	0	1197	1311
1942	181	0	0	0	181	1379	0	0	0	1379	1560
1943	204	0	0	0	204	2059	0	0	0	2059	2263
1944	181	45	0	0	227	1307	454	303	0	2063	2290
1945	163	97	87	20	366	555	174	1447	174	2349	2715
1946	366	183	341	194	1084	540	440	916	299	2195	3279
1947	119	56	124	487	787	508	413	862	281	2064	2850
1948	627	71	312	2483	3493	693	872	608	527	2700	6193
1949	502	95	172	716	1486	676	221	257	927	2081	3566
1950	492	147	130	157	926	362	546	439	542	1890	2816
1951	293	81	104	242	719	501	224	222	400	1347	2067
1952	528	87	80	82	777	419	178	225	492	1315	2092
1953	380	13	49	30	472	367	222	401	16	1007	1479

Table A - 3. Retained catch estimates for US vessels fishing in Canadian waters from 1954 to 1976. Taken from Fargo (1999). Note that catch is reported as Area 3C north in Fargo (1999), which is the Canadian portion of PFMC Area 3C with Cape Flattery Spit removed.

Year	US Trawl Fleet		
	3C[1]	3D5ABCD	Total
1954	385	1141	1526
1955	273	890	1163
1956	412	804	1216
1957	429	1671	2100
1958	465	367	832
1959	913	428	1341
1960	800	187	987
1961	953	358	1311
1962	715	472	1187
1963	592	492	1084
1964	389	408	797
1965	540	557	1097
1066	422	528	950
1967	155	480	635
1968	123	439	562
1969	90	297	387
1970	56	149	205
1971	157	162	319
1972	135	135	270
1973	124	354	478
1974	218	408	626
1975	170	318	488
1976	281	197	478

LITERATURE CITED

Anderson, S.C., Keppel, E.A., and Edwards, A.M. 2019. A reproducible data synopsis for over 100 species of British Columbia groundfsh. DFO Can. Sci. Advis. Sec. Res. Doc. 2019/041. vii + 321 p.

Fargo, J. 1999. Flatfish Stock Assessments for the west coast of Canada for 1998 and Recommended Yield Options for 1999. DFO. Can. Stock. Assess. Sec. Res. Doc. 1999/17. 51 p.

Haltuch, M. A., Ono, K., and Valero, J. L. 2013. Status of the U.S. petrale sole resource in 2012. Portland, OR: Pacific Fishery Management Council.

Ketchen, K.S., and C.R. Forrester. 1966. Population dynamics of Petrale Sole (*Eopsetta jordani*) in waters off western Canada. Fish. Res. Board. Can. Bull. 153: 95 p.

Pedersen, N.G. 1975. Recent investigations of Petrale Sole off Washington and British Columbia, Wash. Dept. Fish. Tech. Rept. 17372

Sampson, D., and Lee, Y. 1999. An assessment of the stocks of petrale sole off Washington, Oregon, and Northern California in 1998. Pacific Fishery Management Council, 7700 Ambassador Place NE, Suite 200, Portland, OR 97220.

Starr, P.J. 2009. Petrale Sole (*Eopsetta jordani*) in British Columbia, Canada: Stock Assessment for 2006/07 and Advice to Managers for 2007/08. DFO Can. Sci. Advis. Sec. Res. Doc. 2009/070. V + 134 p.

APPENDIX B. BIOLOGICAL ANALYSES

B.1. VON BERTALANFFY GROWTH MODEL

We used a von Bertalanffy growth model to characterize mean length at age:

$$\hat{L}_{s,a} = L_{\infty_s}\left(1 - e^{-k_s(a-t_{0_s})}\right)$$

Eq. B - 1

where a represents age, s denotes sex, and L_{∞_s}, k_s, and t_{0_s} represent sex-specific von-Bertalanffy growth parameters. The model also estimated a coefficient of variation of length at age for each sex (CV_s). The model was fit to data in Template Model Builder (TMB; Kristensen et al. 2016) using a robust log likelihood function that assumed a mixed probability density of the normal distribution and the t-distribution for length at age:

$$LL = \sum_i log\left(\frac{\left((1-p)\phi\left(\frac{L_{s_i,a_i} - \hat{L}_{s_i,a_i}}{CV_{s_i}\hat{L}_{s_i,a_i}}\right) + p\psi\left(\frac{L_{s_i,a_i} - \hat{L}_{s_i,a_i}}{CV_{s_i}\hat{L}_{s_i,a_i}}\right)\right)}{CV_{s_i}\hat{L}_{s_i,a_i}}\right)$$

Eq. B - 2

where i represents an individual fish observation, ϕ denotes the probability density function (pdf) of the standard normal, ψ denotes the pdf of the t-distribution with 3 degrees of freedom, and p denotes the mixture of t-distribution to normal-distribution and was set to 0.05. The robust distribution was used to avoid sensitivity to outliers in length-age data.

All available pairs of length and age observations from surveys were used for parameter estimation, without distinguishing year or survey series. Estimated model fits and parameters for the coastwide Petrale Sole stock (Areas 3CD, 5ABCDE combined), which we used for the stock assessment, are shown in Figure B - 1 and Table B - 1. Females are estimated to grow larger than males.

In addition to the coastwide model fit, we looked at variation in parameter estimates from models fit to smaller spatial units (Figure B - 2; west coast Vancouver Island = Areas 3CD, Queen Charlotte Sound = Areas 5AB, Hecate Strait = Areas 5CD). Age sample sizes for west coast Haida Gwaii (Area 5E) were not large enough to reliably estimate length-at-age relationships (N = 13 for females and 47 for males). We found no consistent differences in growth parameters between regions that would support smaller-scale stock delineation.

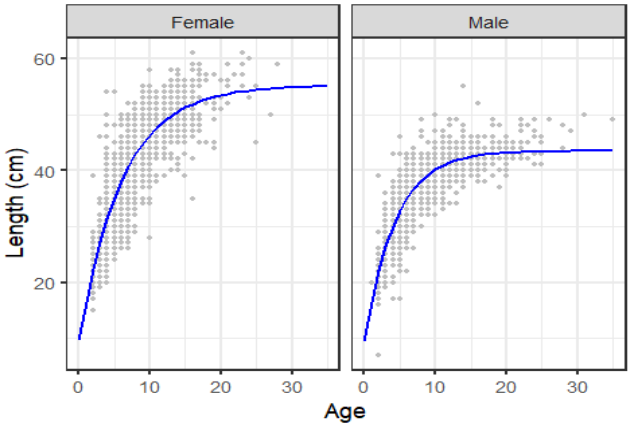


Figure B - 1. Predicted mean length at age for female and male Petrale Sole.

Table B - 1. Coastwide parameter estimates for von Bertalanffy growth along with associated sample size and standard errors for Petrale Sole.

Sex	N	L_∞	$SE_{L\infty}$	k	SE_k	t_0	SE_{t0}	CV	SE_{CV}
Female	2334	55.155	0.609	0.164	0.006	-1.158	0.100	0.104	0.002
Male	2100	43.475	0.268	0.233	0.007	-1.038	0.099	0.089	0.002

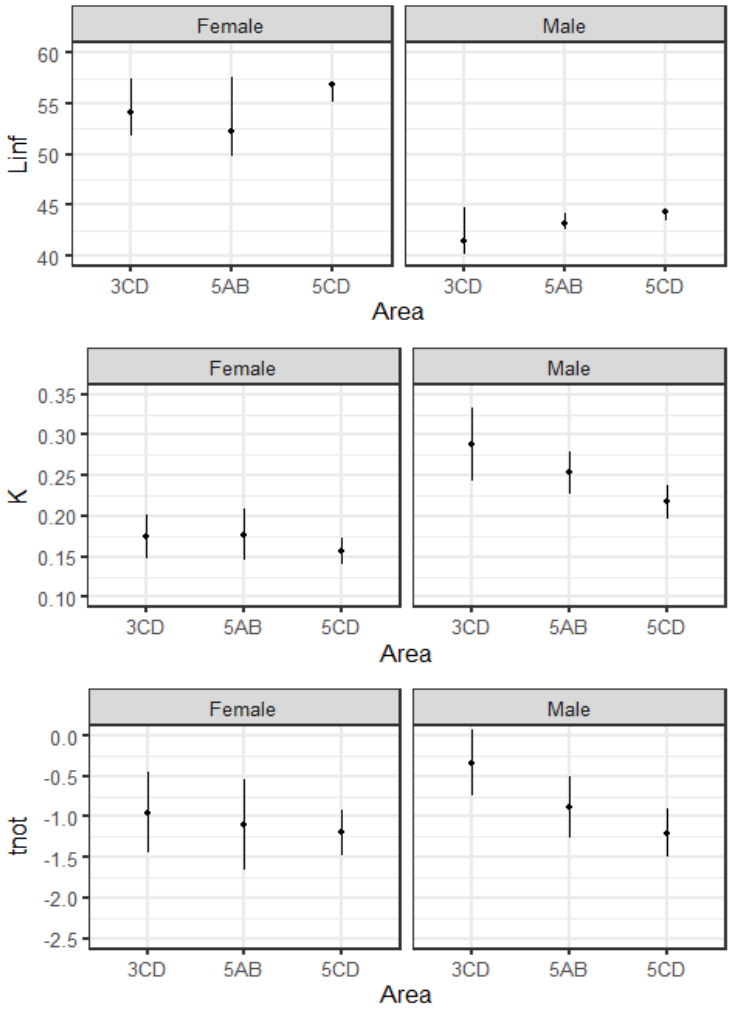


Figure B - 2. Estimated von Bertalanffy growth parameters, by sex and area groupings. Error bars show +/- 1.96 standard deviations around parameter estimates.

B.2. WEIGHT-LENGTH MODEL

We parameterized mean weight at length using the following model:

$$log(\widehat{W}_s) = log(\alpha_s) + \beta_s log(L_s)$$

Eq. B - 3

where, L_s denotes the length of a fish sex s, and α_s and β_s are sex-specific length-weight parameters. A standard deviation parameter was also estimated for each sex (σ_s). The model was fit as a linear regression to log length and log weight pairs using all available observations from research surveys, without distinguishing year or survey series. TMB was used to fit weight-length models to data using the same robust log likelihood used in the von Bertalanffy model:

$$LL = \sum_i log\left(\frac{\left((1-p)\phi\left(\frac{log(W_{s_i}) - log(\widehat{W}_{s_i})}{\sigma_{s_i}}\right) + p\psi\left(\frac{log(W_{s_i}) - log(\widehat{W}_{s_i})}{\sigma_{s_i}}\right)\right)}{\sigma_{s_i}}\right)$$

Eq. B - 4

Estimated model fits and parameters for the coastwide Petrale Sole stock (Areas 3CD, 5ABCDE combined), which we used in the stock assessment model, are shown in Figure B - 3 and Table B - 2.

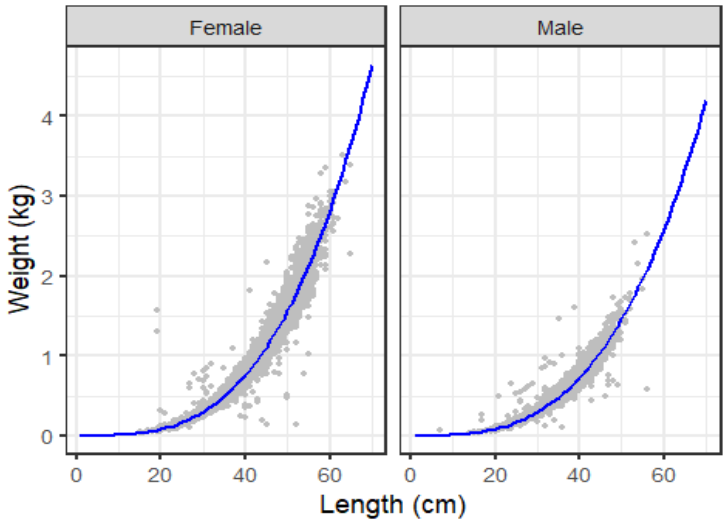


Figure B - 3. Regression analyses showing fitted length-weight models and length-weight pairs, for all Petrale Sole specimens collected from research surveys.

Table B - 2. Coastwide parameter estimates for length-weight parameters along with associated sample size and standard errors.

Sex	N	α	$SE_{log(\alpha)}$	β	SE_{β}	σ_s	$SE\sigma_s$
Female	12,250	4.96E-06	6.95E-08	3.236	0.004	0.087	0.001
Male	10,576	6.94E-06	1.19E-07	3.134	0.005	0.085	0.001

We also fit the length-weight model to smaller spatial units to look for evidence of variation in growth patterns among regions. Results showed that estimated alpha parameters tended to be larger in northern areas (Areas 5CD and 5E) compared to more southern areas (Areas 3CD and 5AB), while estimated beta parameters tended to be smaller in northern areas compared to southern areas. However, these differences were small and overall weight-length relationships were similar among regions.

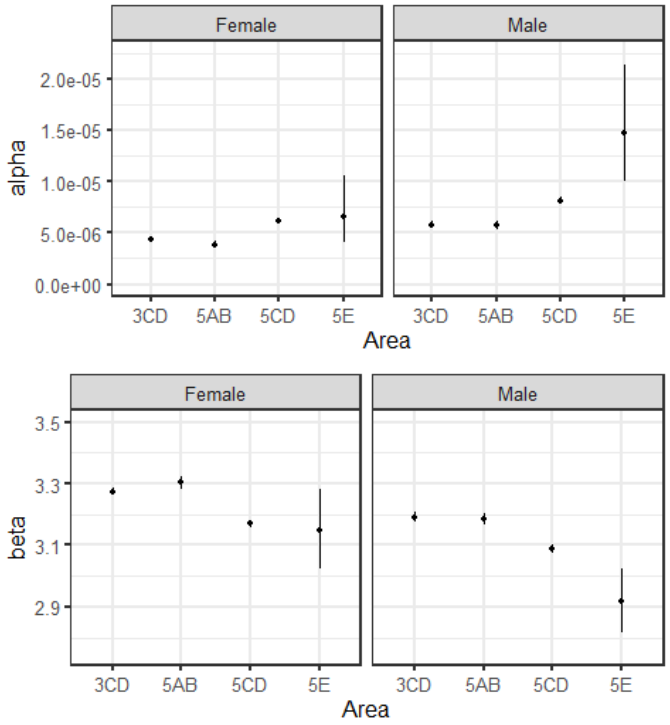


Figure B - 4. Weight-length relationship parameters by sex and area grouping. Error bars show +/- 1.96 standard deviations around parameter estimates.

B.3. MATURITY

Maturity analyses used all available fishery and survey samples with maturity convention code recorded as “Flatfish” or “Port Samples”. Flatfish maturity is assigned using a scale of 1 to 7, with codes >2 considered mature (Figure B - 5; Anderson et al. 2019). Ripe and spawning females are predominantly observed in winter months, from December to April. During spring and early-summer, the majority of samples from both sexes are in the resting stage, with gonads starting to develop for reproduction in late-summer and through the fall. Surveys rarely cover the spawning period, so fishery samples were also included in this analysis.

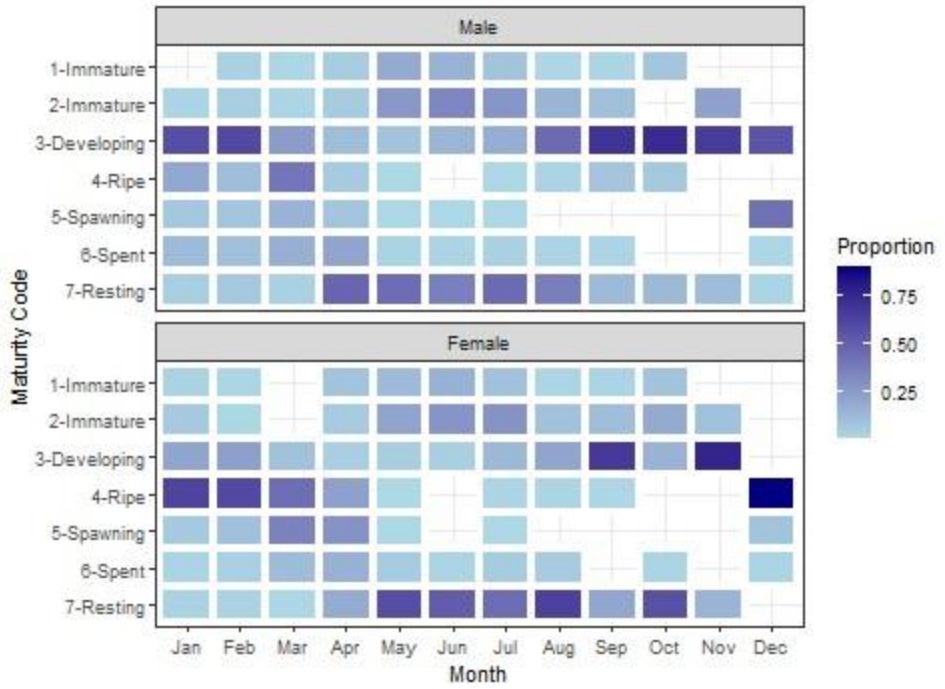


Figure B - 5. Proportion of maturity codes assigned to each of the seven maturity codes within each month. All available Petrale Sole specimens sampled from commercial fisheries and research surveys were used to calculate monthly proportions.

Maturity ogives describing the proportion of mature fish at a given age were fit as logistic regressions to individual sampled specimens categorized as a Bernoulli variable of mature (y_i = 1) or immature ($y_i = 0$). Specimens with a maturity code of 1 or 2 were classified as immature, while maturity codes of 3 to 7 were classified as mature.

We use the same logistic regression approach as Anderson et al. (2019):

$$y_i = \text{Binomial}(\pi_i)$$

$$logit(\pi_i) = B_0 + B_1 x_i$$

Eq. B - 5

where y_i is the indicator of mature (1) or immature (0) for fish i, π_i represents the expected probability of fish i being mature, B_0 and B_1 are estimated logistic regression parameters, and x_i represents the age of specimen *i*. Maturity ogives for males and females, as well as associated parameter estimates, are shown in Figure B - 6.

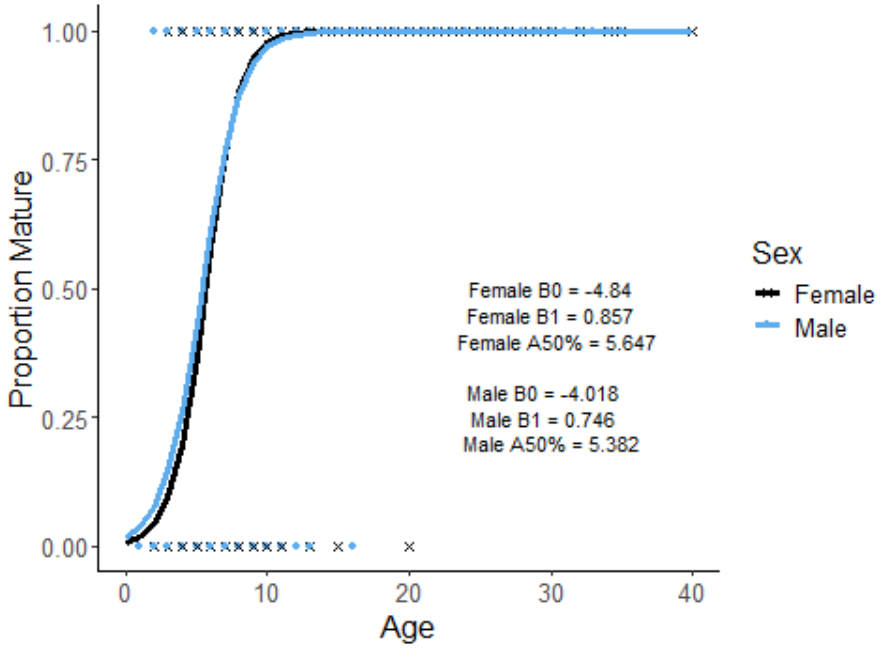


Figure B - 6. Sex-specific estimated proportion mature at age (lines) with data points used to fit maturity model.

B.4. AGE AND LENGTH COMPOSITION

B.4.1. Age and Length Composition Expansion

Age and length composition data were expanded from raw samples to stock wide proportions caught at age or length. For commercial data, within each quarter commercial ages or lengths were weighted by the catch weight of Petrale Sole in tows that were sampled. Quarterly commercial ages or lengths were then weighted by the commercial catch weight of Petrale Sole from all tows within each quarter. For the survey data, within each survey stratum survey ages or lengths were weighted by the catch density (t/km^2) of Petrale Sole in sampled tows. Stratum survey ages or lengths were then weighted by stratum areas (km^2) in the survey. The mathematics regarding this expansion procedure have been well documented in other assessments, hence we refer readers to those documents for detailed methods and equations (Holt et al. 2016; Starr and Haigh, 2023). The gfplot package in R (Anderson et al. 2024) was used for the expansions. Length composition data were only used in the Length+CAAL sensitivity model.

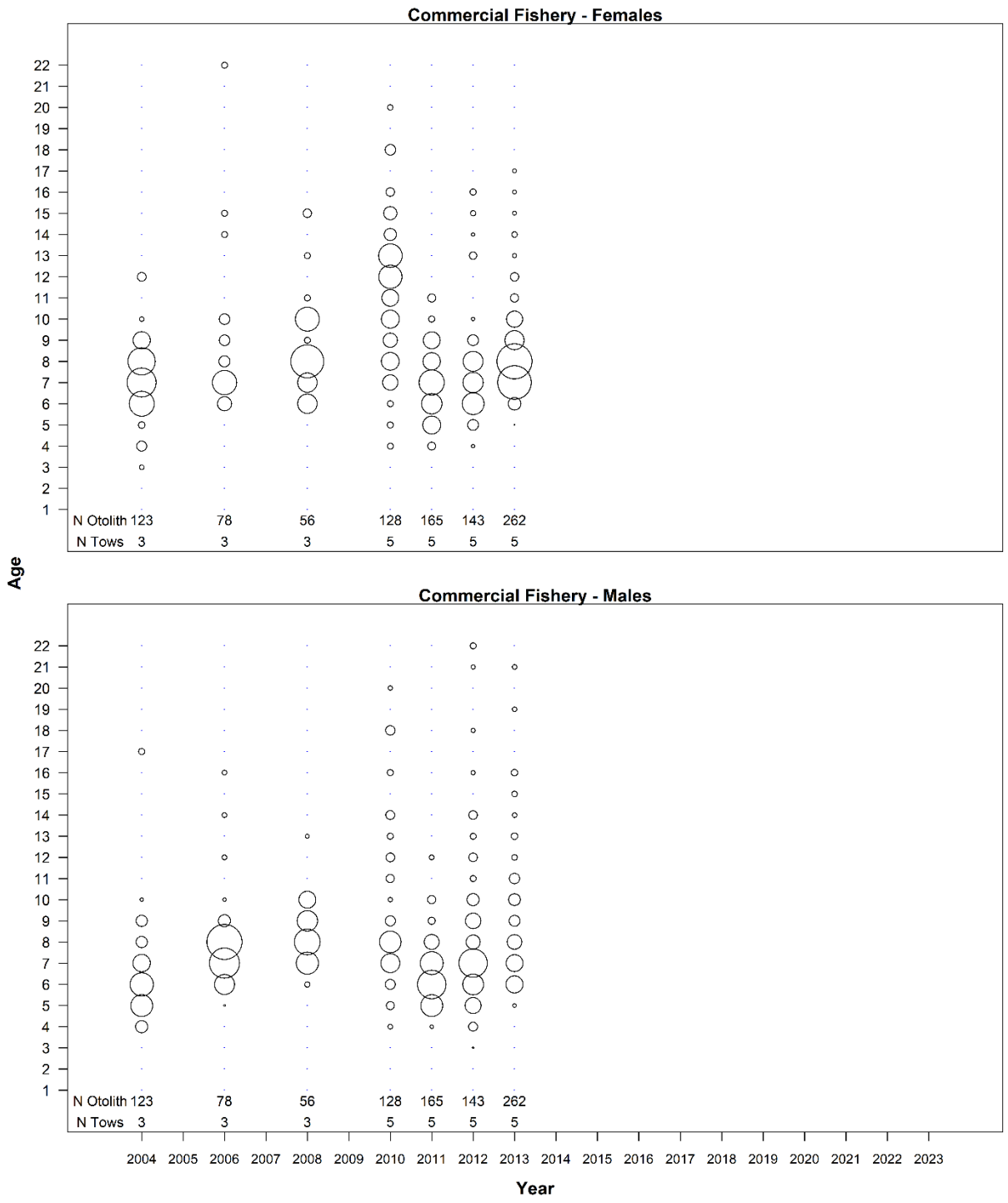


Figure B - 7. The expanded age composition data for the commercial fishery for the years in which there were three or more tows sampled with aged otoliths. The label "N Otolith" refers to the number of otoliths read in each year and "N Tows" refers to the number of tows sampled.

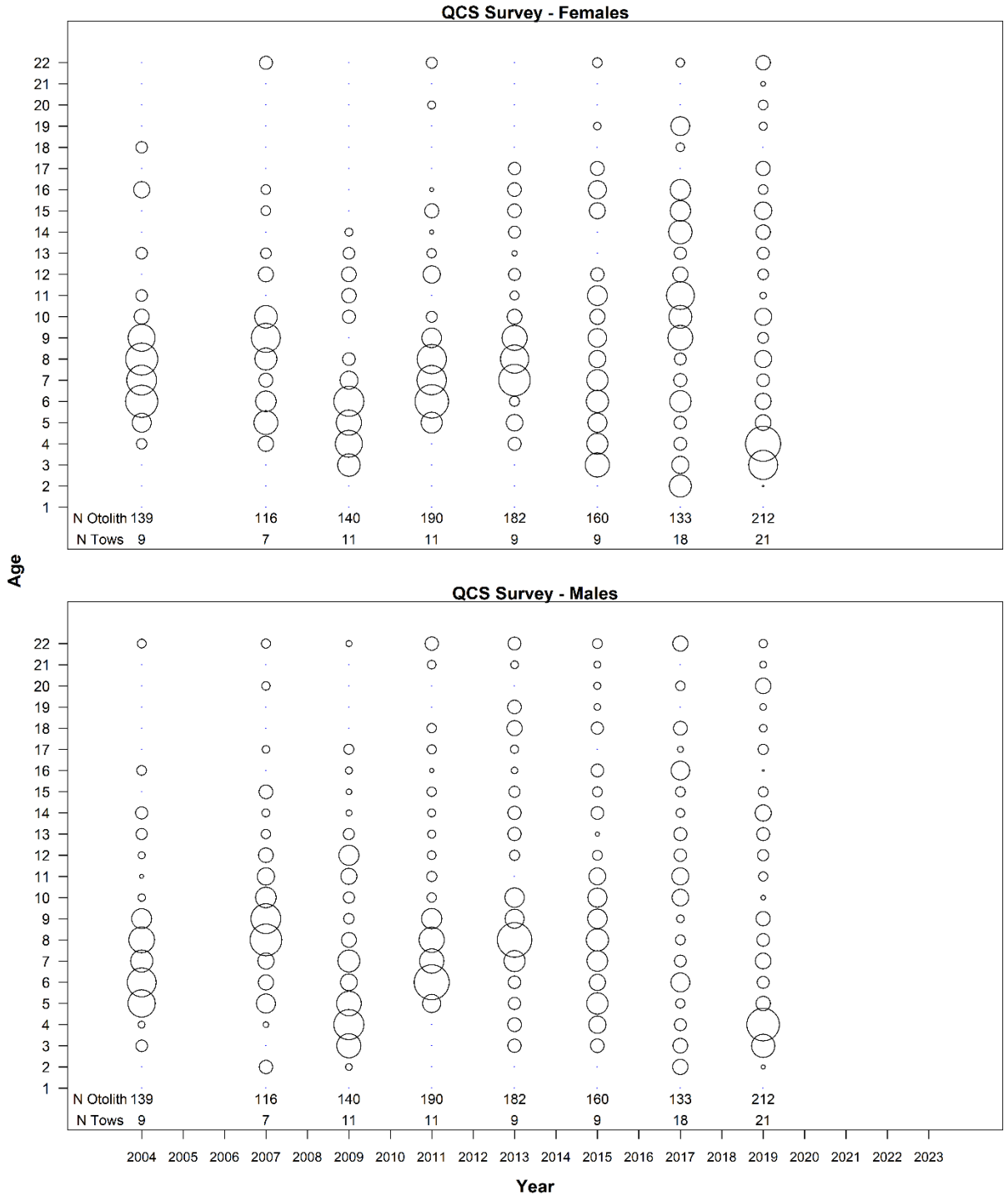


Figure B - 8. The expanded age composition data for the Queen Charlotte Sound (QCS) survey. The label "N Otolith" refers to the number of otoliths read in each year and "N Tows" refers to the number of tows sampled.

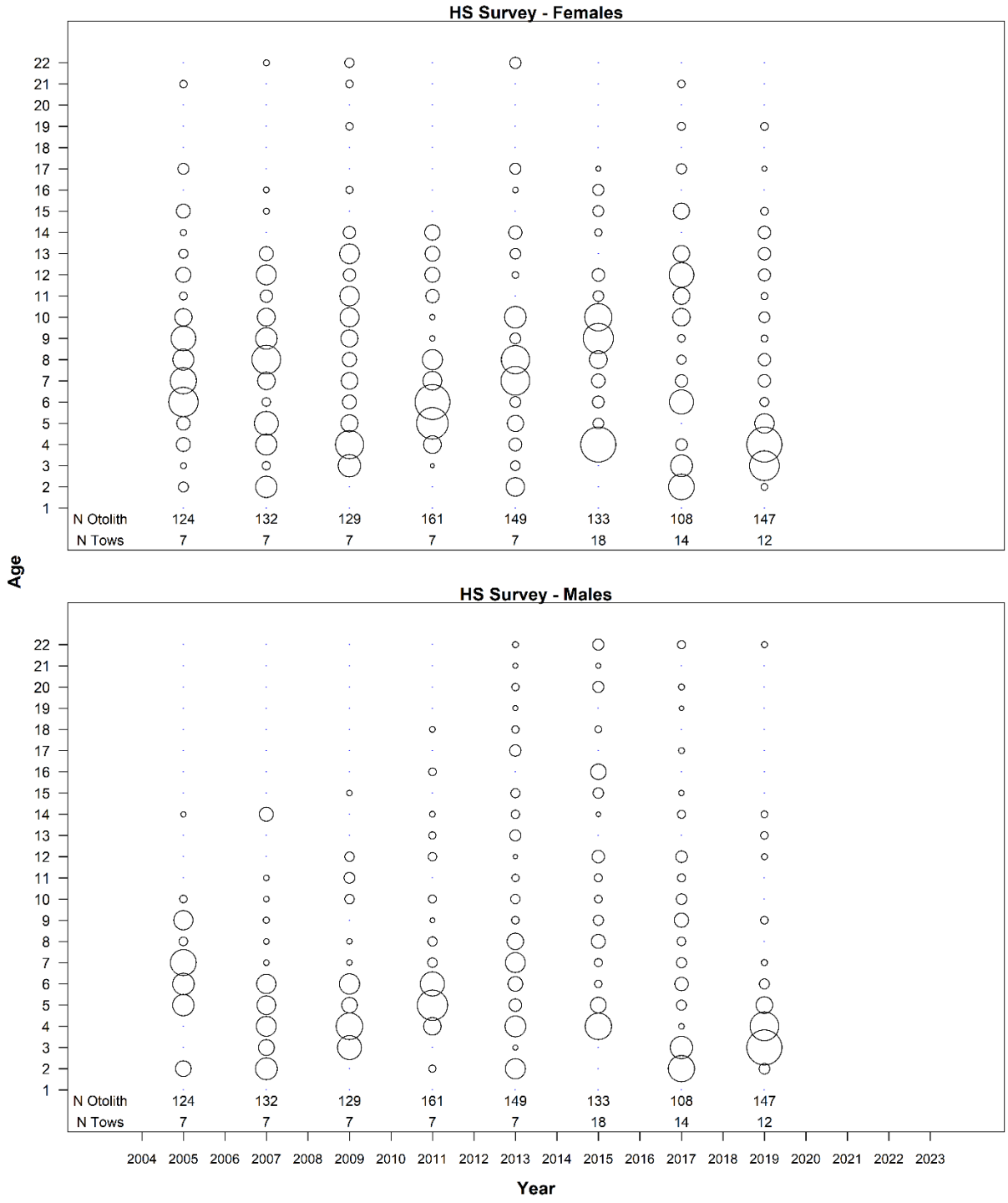


Figure B - 9. The expanded age composition data for the Hecate Strait (HS) survey. The label "N Otolith" refers to the number of otoliths read in each year and "N Tows" refers to the number of tows sampled.

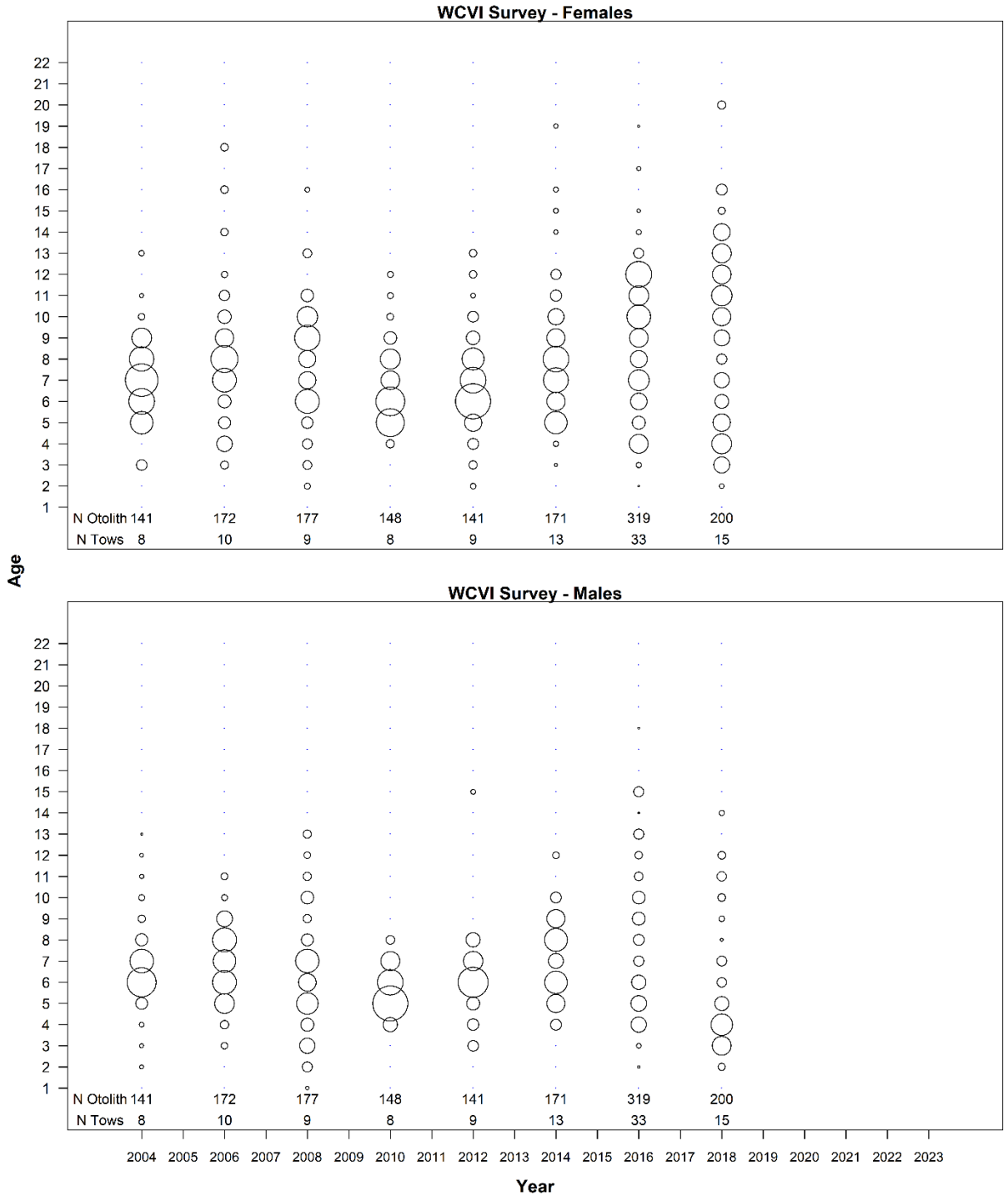


Figure B - 10. The expanded age composition data for the West Coast Vancouver Island (WCVI) survey. The label "N Otolith" refers to the number of otoliths read in each year and "N Tows" refers to the number of tows sampled.

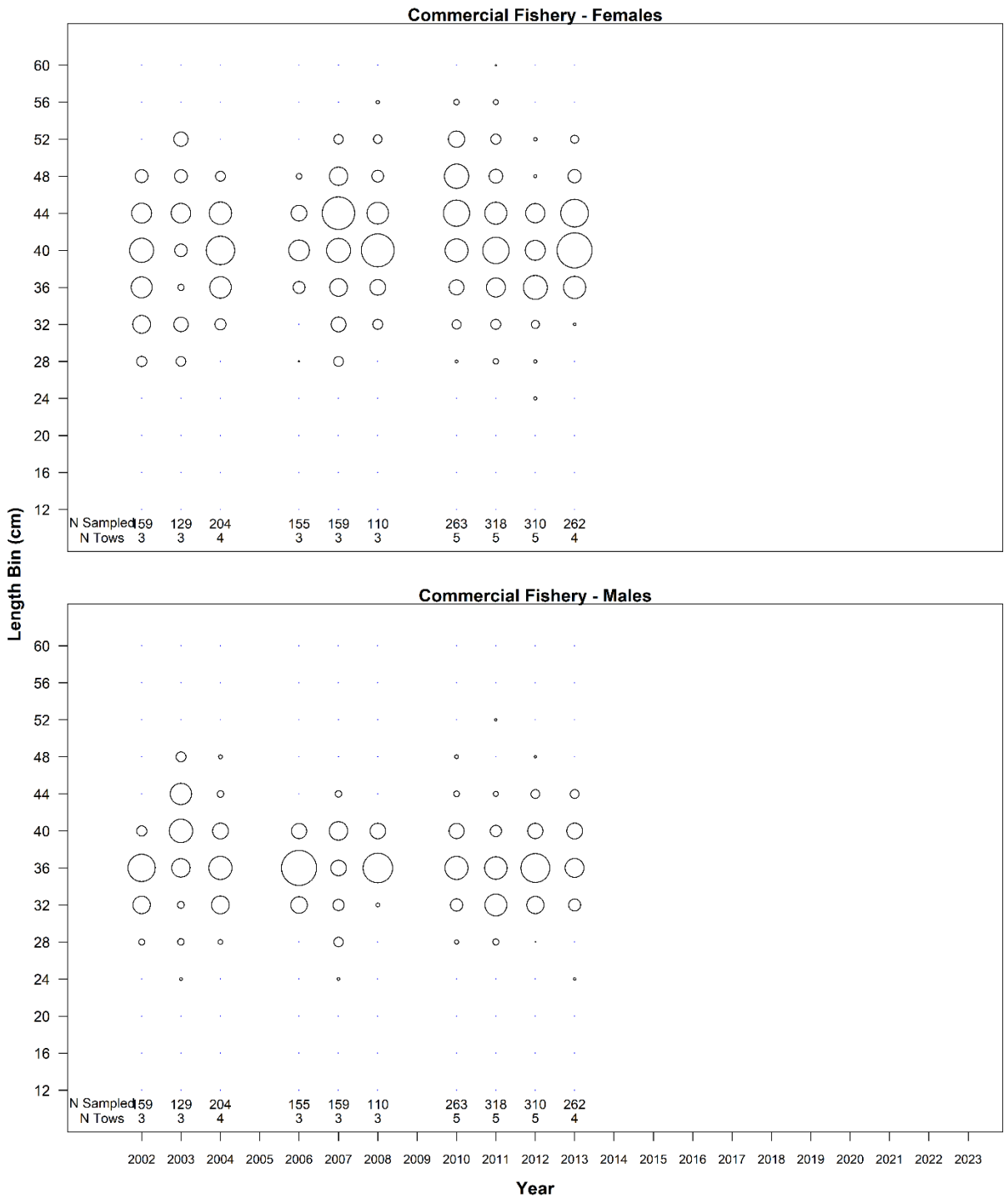


Figure B - 11. The expanded length composition data for the commercial fishery for the years in which there were three or more tows sampled with lengths. The label "N Sampled" refers to the number of fish sampled in each year and "N Tows" refers to the number of tows sampled.

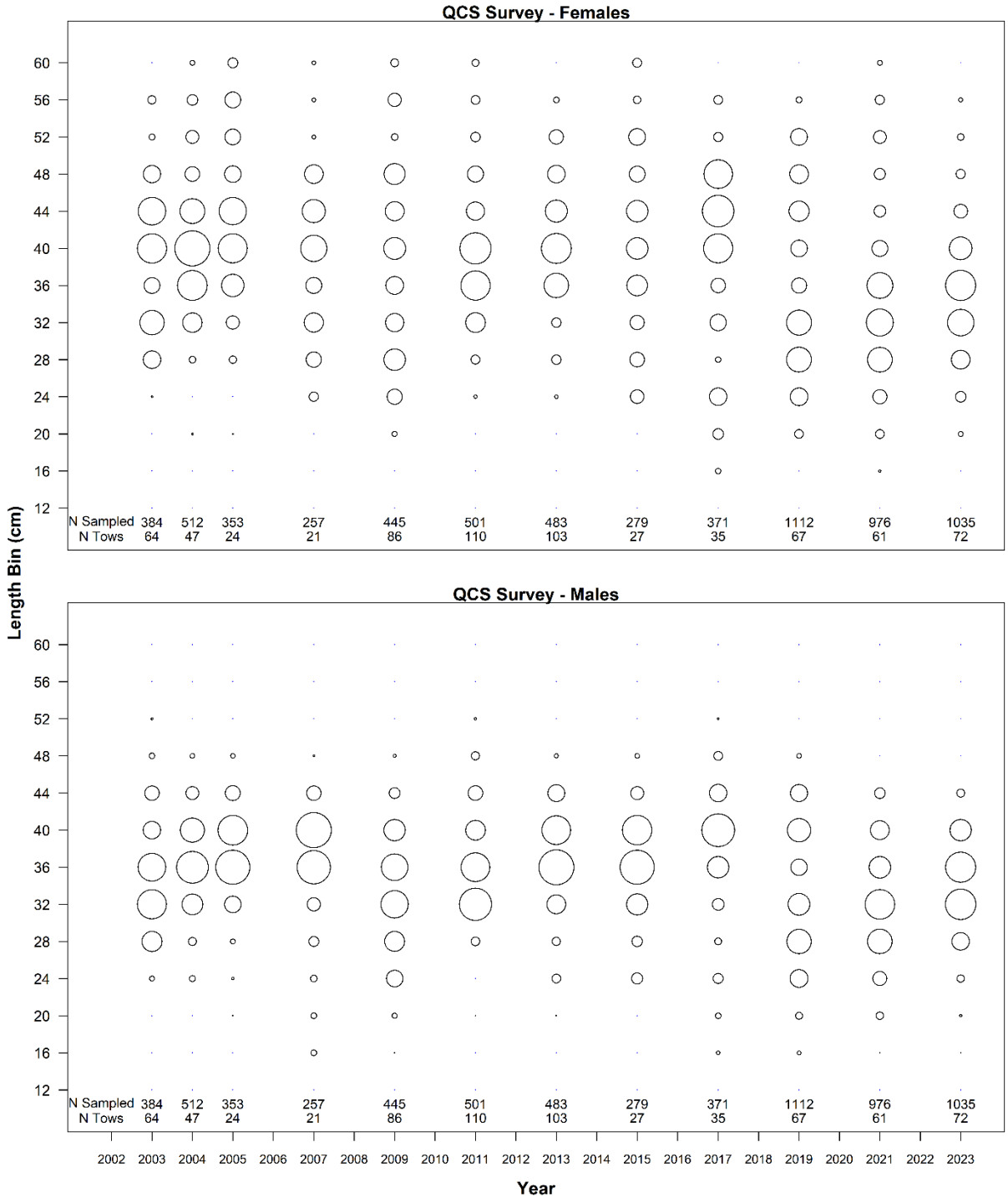


Figure B - 12. The expanded length composition data for the Queen Charlotte Sound (QCS) survey. The label "N Sampled" refers to the number of fish sampled in each year and "N Tows" refers to the number of tows sampled.

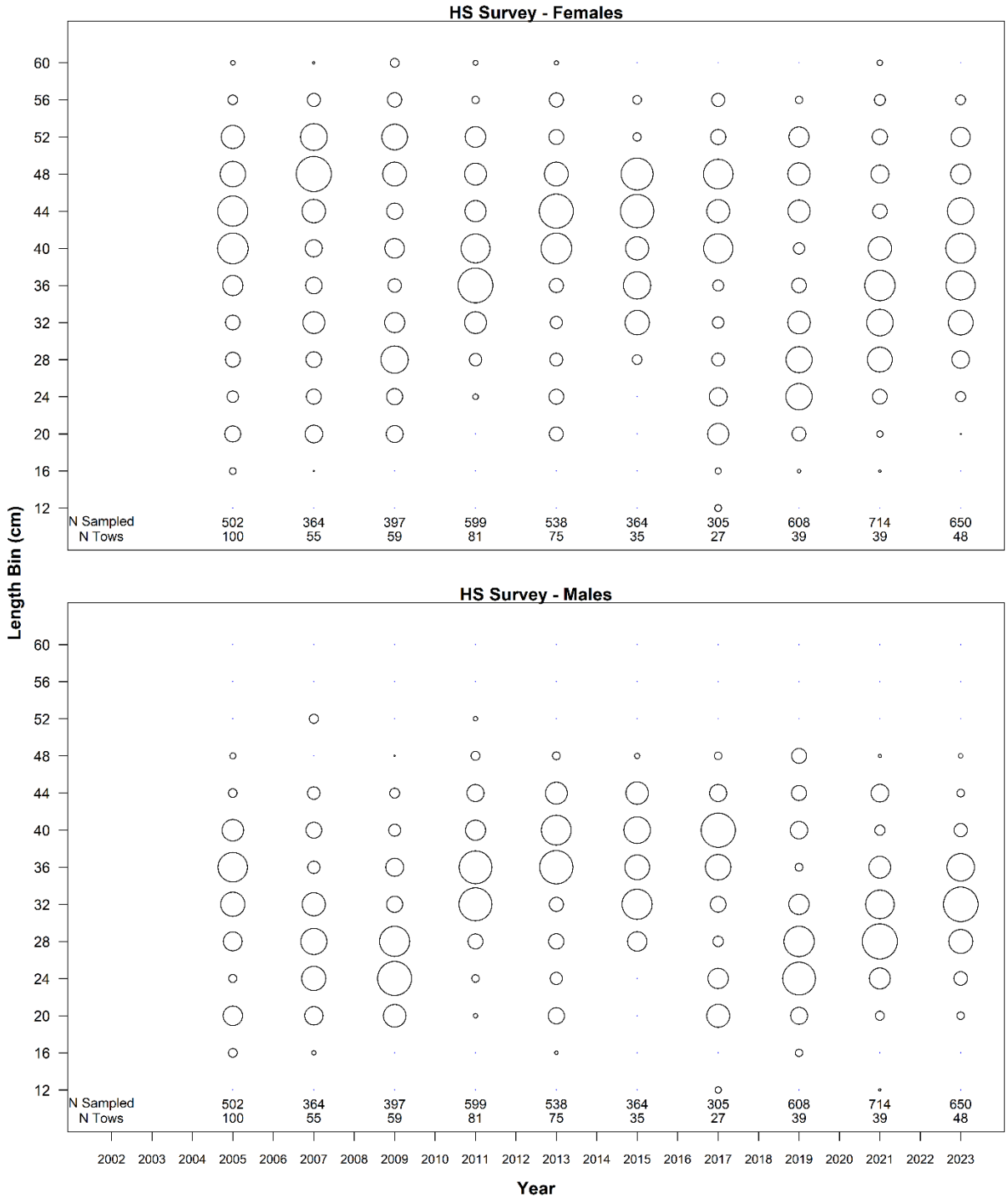


Figure B - 13. The expanded length composition data for the Hecate Strait (HS) survey. The label "N Sampled" refers to the number of fish sampled in each year and "N Tows" refers to the number of tows sampled.

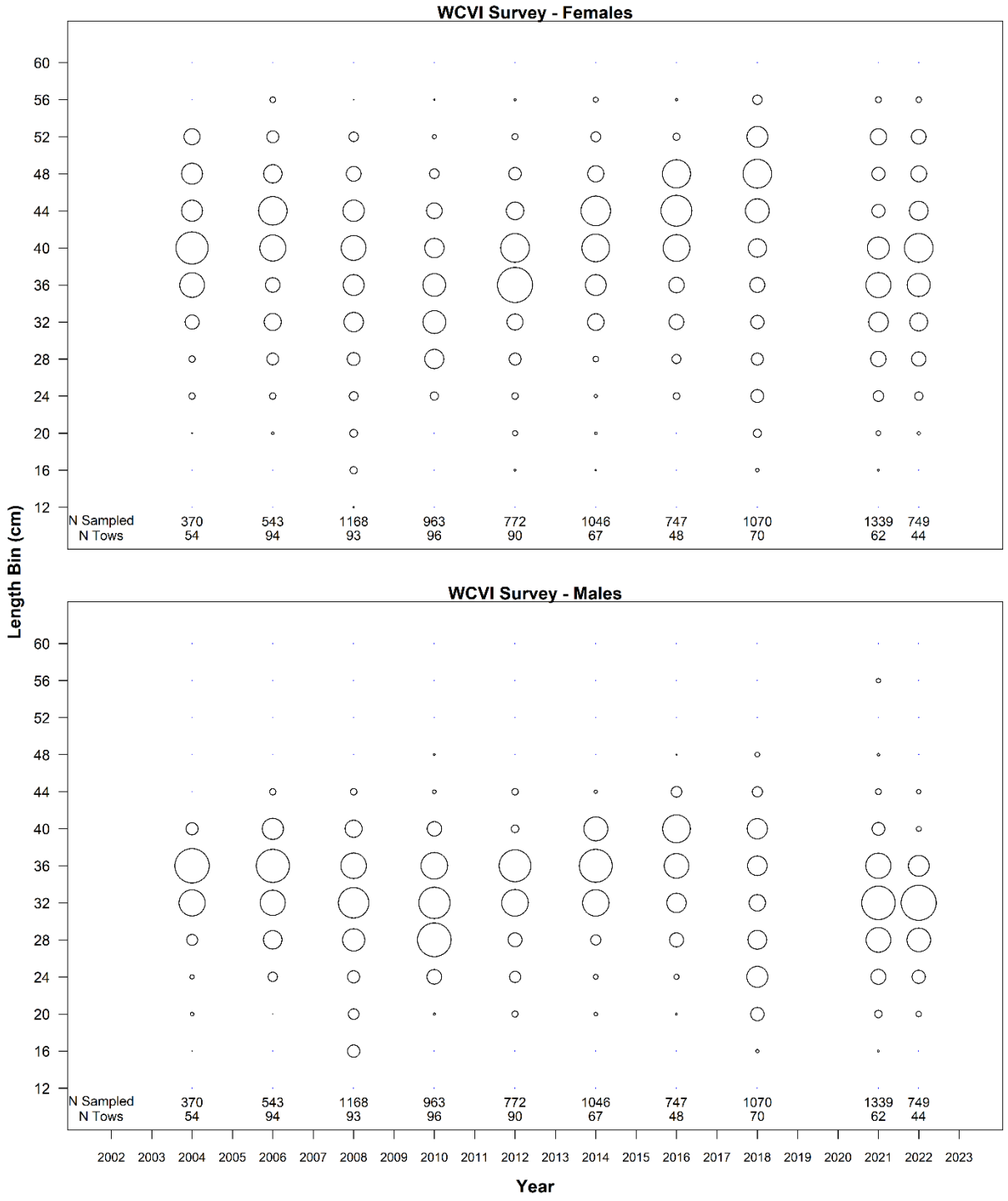


Figure B - 14. The expanded length composition data for the West Coast Vancouver Island (WCVI) survey. The label "N Sampled" refers to the number of fish sampled in each year and "N Tows" refers to the number of tows sampled.

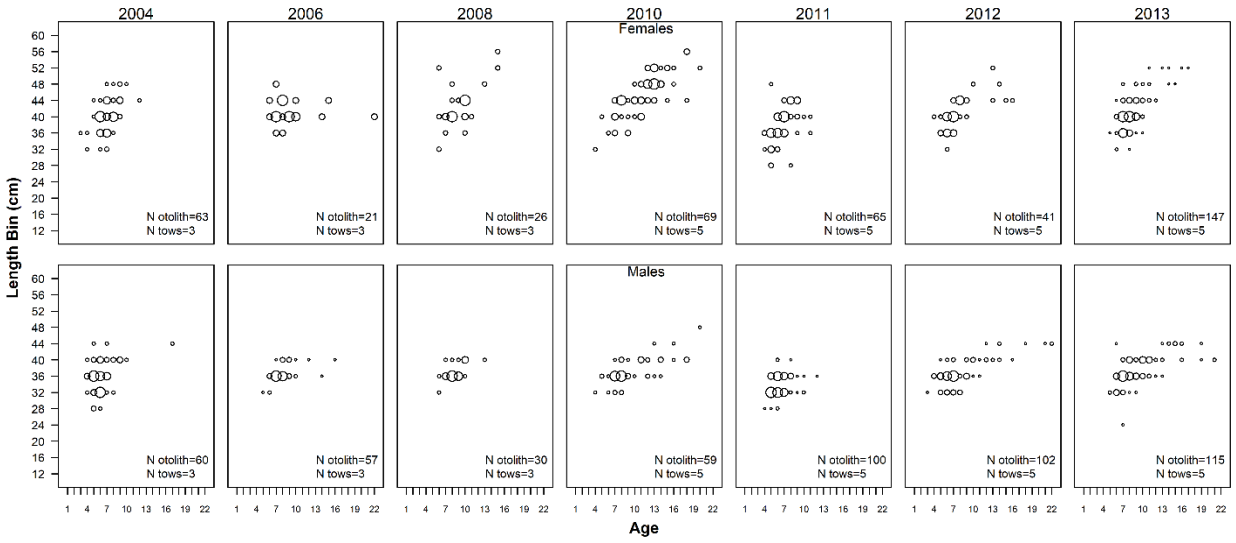


Figure B - 15. The conditional age-at-length composition data for the commercial fishery for the years in which there were three or more tows sampled with ages. The label "N Otolith" refers to the number of otoliths read in each year and "N Tows" refers to the number of tows sampled.

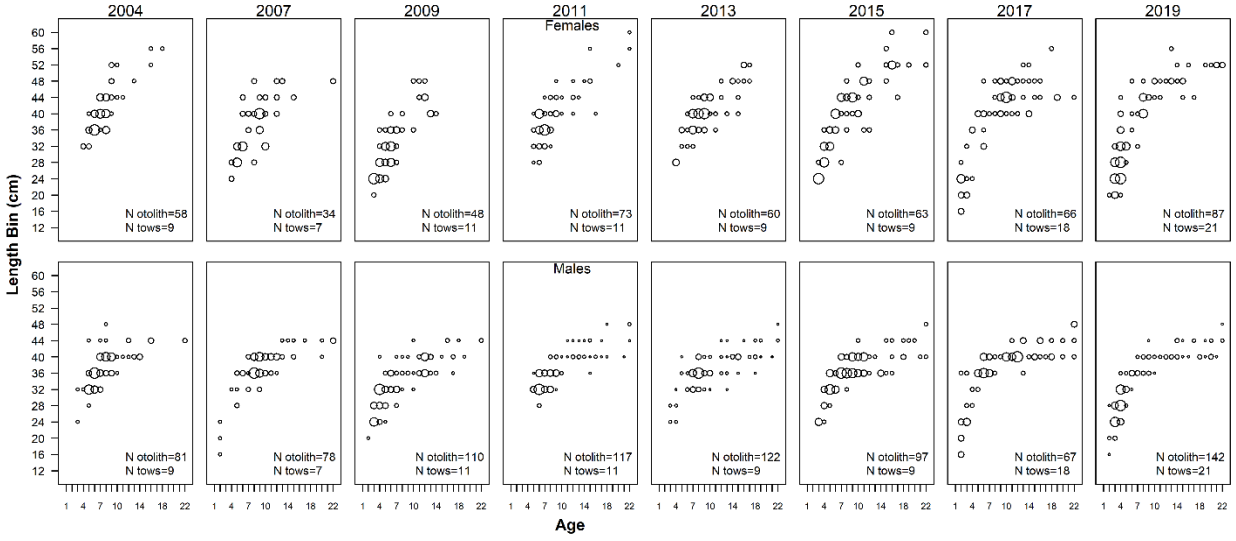


Figure B - 16. The conditional age-at-length composition data for the Queen Charlotte Sound survey. The label "N Otolith" refers to the number of otoliths read in each year and "N Tows" refers to the number of tows sampled.

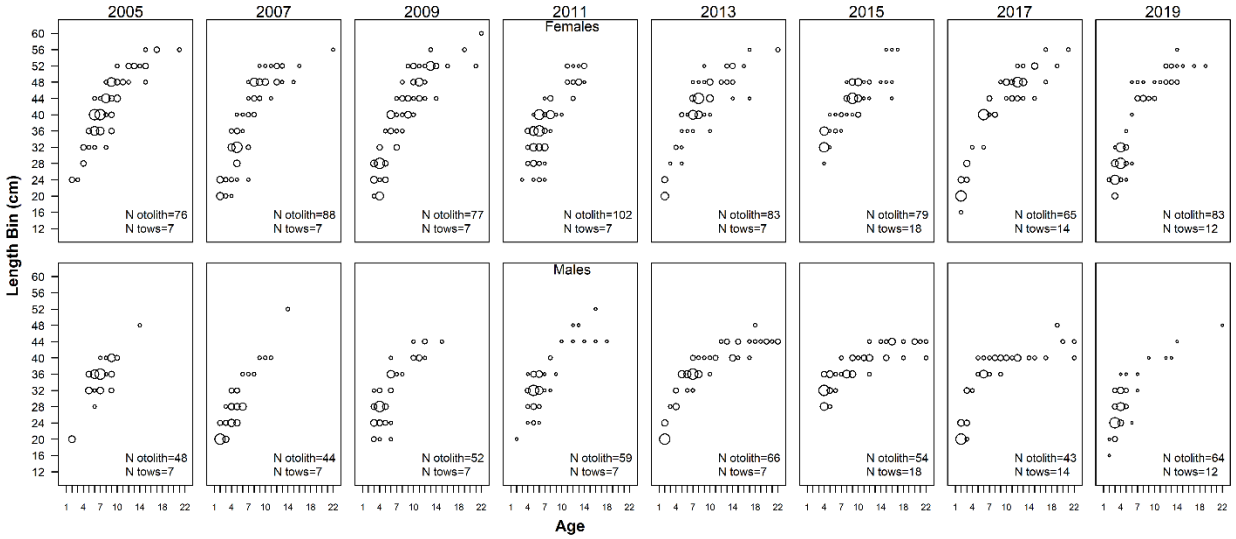


Figure B - 17. The conditional age-at-length composition data for the Hecate Strait survey. The label "N Otolith" refers to the number of otoliths read in each year and "N Tows" refers to the number of tows sampled.

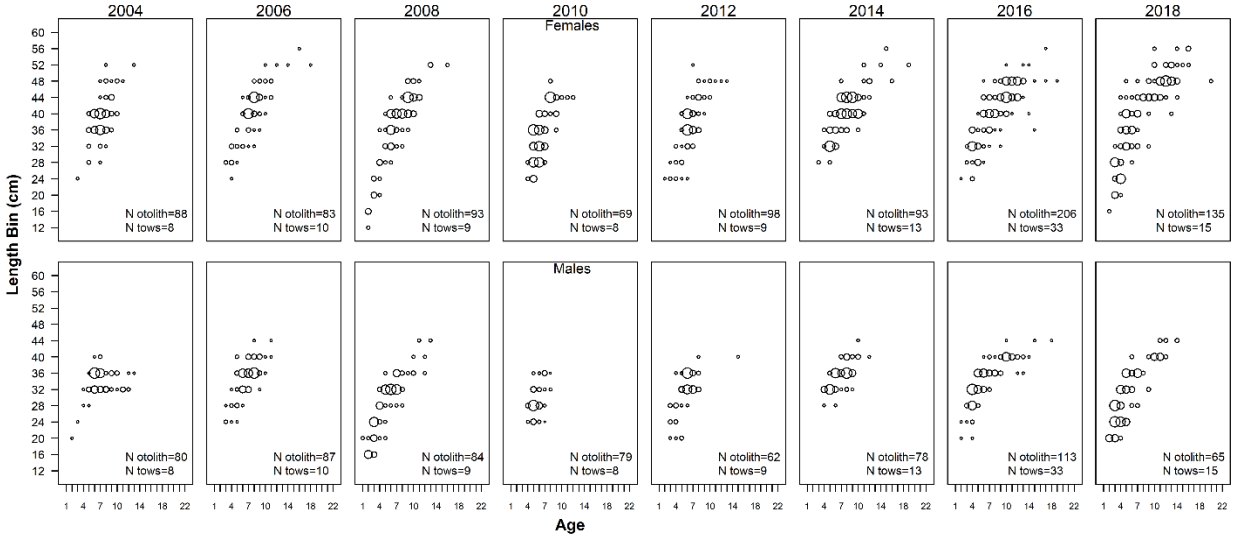


Figure B - 18. The conditional age-at-length composition data for the West Coast Vancouver Island survey. The label "N Otolith" refers to the number of otoliths read in each year and "N Tows" refers to the number of tows sampled.

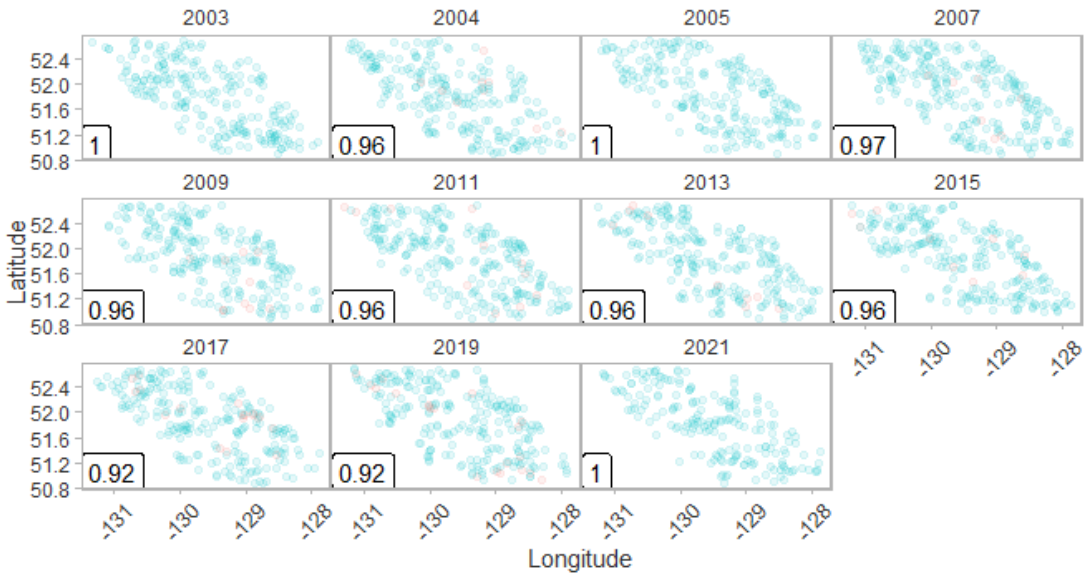


Figure B - 19. Samples from the Queen Charlotte Sound Synoptic Survey from 2003 to 2021 with samples with age data in red and samples without age data in blue. The number in the left corner is the proportion of samples without age data for each year.

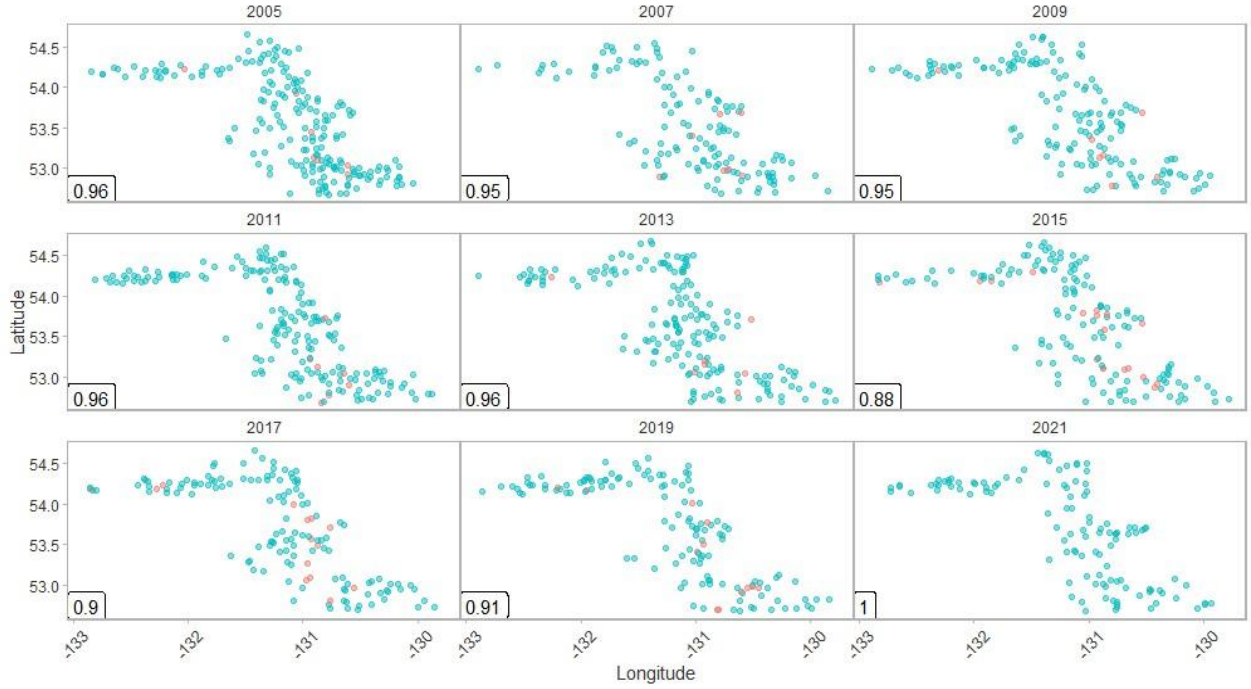


Figure B - 20. Samples from the Hecate Strait Synoptic Survey from 2005 to 2021 with samples with age data in red and samples without age data in blue. The number in the left corner is the proportion of samples without age data for each year.

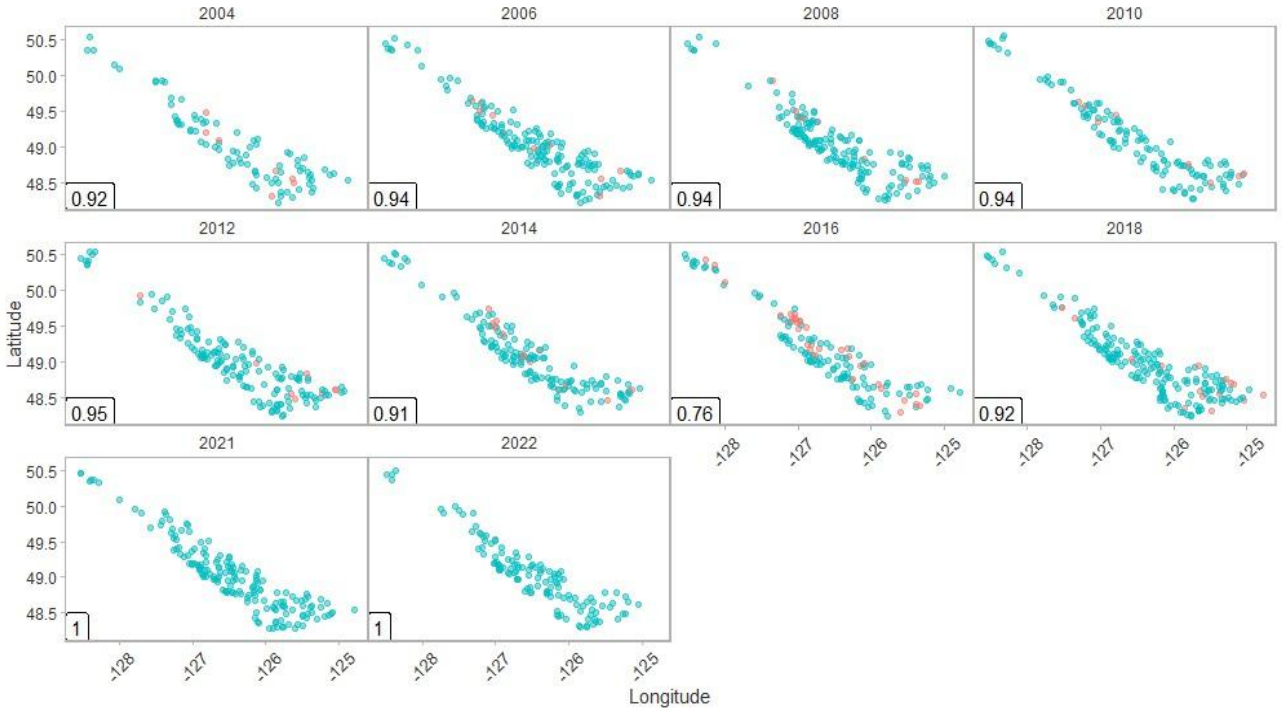


Figure B - 21. Samples from the West Coast Vancouver Island Synoptic Survey from 2004 to 2022 with samples with age data in red and samples without age data in blue. The number in the left corner is the proportion of samples without age data for each year.

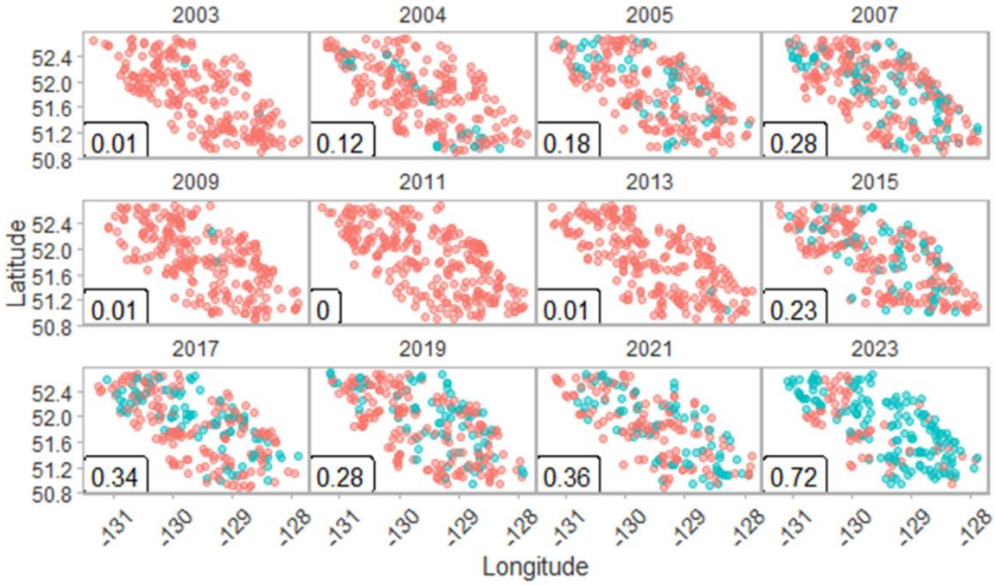


Figure B - 22. Samples from the Queen Charlotte Sound Synoptic Survey from 2003 to 2023 with samples with length data in red and samples without length data in blue. The number in the left corner is the proportion of samples without length data for each year.

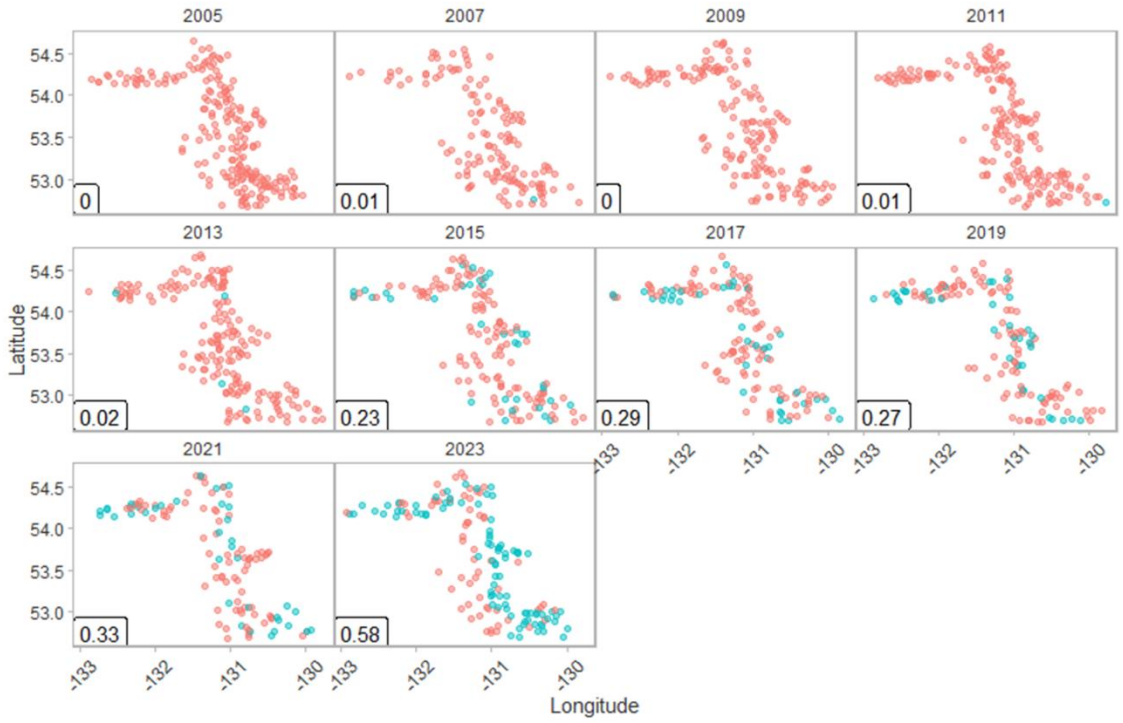


Figure B - 23. Samples from the Hecate Strait Synoptic Survey from 2005 to 2023 with samples with length data in red and samples without length data in blue. The number in the left corner is the proportion of samples without length data for each year.



Figure B - 24. Samples from the West Coast Vancouver Island Synoptic Survey from 2004 to 2022 with samples with length data in red and samples without length data in blue. The number in the left corner is the proportion of samples without length data for each year.

B.4.2. Bootstrapping For Input Sample Sizes

A bootstrapping procedure was conducted to determine input sample sizes as a measure of the sampling variance for the composition datasets. This procedure roughly followed the methods of Stewart and Hamel (2014). For the commercial age composition data, the procedure was as follows:

1. Within each year, resample with replacement the tows that had specimen samples that were aged and sexed.
2. Within each resampled tow, resample with replacement the specimen samples that were aged and sexed.
3. Redo expansion (B.4.1) to obtain bootstrapped estimate of annual age composition.

   Calculate the realized sample size (McAllister and Ianelli, 1997) using

$$R = \frac{\sum_b \left(P_b(1-P_b)\right)}{\sum_b (P_b - B_b)^2}$$

Eq. B - 6

4. where *P* refers to the observed composition, *b* the age (or length) bin, and *B* the bootstrapped estimate.
5. Repeat steps 1-4 10,000 times and calculate the harmonic mean of *R* in each year (across the 10,000 simulations).

The recommendation for the harmonic mean comes from Stewart and Hamel (2014) who tested a suite of estimators for calculating input sample size and determined the harmonic mean minimized bias in simulation tests. For the survey data, the procedure was nearly identical with the exception that for step 1, tows were resampled with replacement within a strata within a year. The commercial tows were resampled within a year rather than within each quarter given a large amount of variability in the number of tows sampled each quarter. The resampling of tows within each year allows that variability to be captured in the bootstrap procedure.

For calculating input sample sizes of the length compositions, similar procedures were followed simply replacing age with length in the above steps. For the conditional age-at-length data, the procedure simply omitted step 3 involving the expansion as the data were treated as random draws of age at length (and not expanded).

Table B - 3. Input sample size estimates from the bootstrap procedure for the age-composition data.

Year	Commercial Fishery	Queen Charlotte Sound Survey	Hecate Strait Survey	West Coast Vancouver Island Survey
2004	27.72	55.17	-	55.11
2005	-	-	63.79	-
2006	19.25	-	-	80.94
2007	-	64.02	44.72	-
2008	22.07	-	-	54.29
2009	-	72.09	75.26	-
2010	52.89	-	-	77.93
2011	33.98	88.60	75.43	-
2012	27.17	-	-	63.30
2013	44.08	91.04	41.80	-
2014	-	-	-	60.26
2015	-	62.96	55.40	-
2016	-	-	-	72.49
2017	-	47.78	43.17	-
2018	-	-	-	68.50
2019	-	83.71	50.75	-

Table B - 4. Input sample size estimates from the bootstrap procedure for the length-composition data.

Year	Commercial Fishery	Queen Charlotte Sound Survey	Hecate Strait Survey	West Coast Vancouver Island Survey
2002	26.62	-	-	-
2003	17.38	107.49	-	-
2004	43.25	121.55	-	95.01
2005	-	107.15	131.71	-
2006	24.87	-	-	163.60
2007	41.07	71.57	97.59	-
2008	17.42	-	-	214.30
2009	-	133.08	71.45	-
2010	55.42	-	-	236.27
2011	36.64	125.79	195.78	-
2012	43.72	-	-	157.00
2013	34.14	141.94	123.80	-
2014	-	-	-	213.12
2015	-	68.01	130.17	-
2016	-	-	-	137.27
2017	-	107.63	86.46	-
2018	-	-	-	191.35
2019	-	258.61	100.51	-
2020	-	-	-	-
2021	-	214.09	169.09	191.51
2022	-	-	-	212.38
2023	-	196.76	170.42	-

Table B - 5. Input sample size estimates from the bootstrap procedure for the conditional age-at-length composition data, separated by sex.

Commercial Fishery

Year	Sex	Length Bin (cm)											
		16	20	24	28	32	36	40	44	48	52	56	60
2004	F	0	0	0	0	1.6	6	5	2.4	3.5	0	0	0
	M	0	0	0	0.99	8.2	8.9	8.2	1.5	0	0	0	0
2006	F	0	0	0	0	0	1.1	4.5	3.4	0	0	0	0
	M	0	0	0	0	1.1	15.8	7.5	0	0	0	0	0
2008	F	0	0	0	0	0	1.3	8.1	3.1	1.4	1.3	0	0
	M	0	0	0	0	0	18.3	4.6	0	0	0	0	0
2010	F	0	0	0	0	0.6	2.6	4.29	13.9	8.7	6.8	0	0
	M	0	0	0	0	3.6	16.6	8.9	1.3	0	0	0	0
2011	F	0	0	0	2	5.1	9.4	5.9	3.7	0	0	0	0
	M	0	0	0	2.1	19.4	13.5	2.1	0	0	0	0	0
2012	F	0	0	0	0	0	5.7	10.1	5	1.3	0	0	0
	M	0	0	0	0	12	18.7	8.6	8.2	0	0	0	0
2013	F	0	0	0	0	1.5	18.9	19.3	16.3	3.8	2.40	0	0
	M	0	0	0	0	6.1	15.6	10.5	4.5	3.8	2.4	0	0

Queen Charlotte Sound Survey

Year	Sex	Length Bin (cm)											
		16	20	24	28	32	36	40	44	48	52	56	60
2004	F	0	0	0	0	2	9.6	10.4	6.7	1.10	2.9	1.5	0
	M	0	0	0	0	10.5	14.5	16.5	5.7	0	0	0	0
2007	F	0	0	0	2.9	4	1	5.3	2.8	2.7	0	0	0
	M	0	0	0	0	3.4	15	15.6	4.3	0	0	0	0
2009	F	0	0	5.1	5.4	4.1	4.2	2.4	1.6	1.5	0	0	0
	M	0	0	7	8.2	13.5	15.9	11.1	4.1	0	0	0	0
2011	F	0	0	0	1	5	13.5	13.3	5.9	2.64	0	0.9	0
	M	0	0	0	0	25	19.8	11	4	1.3	0	0	0
2013	F	0	0	0	0	1.5	7.1	14.5	4.8	3.1	1.3	0	0
	M	0	0	2	1.6	11.2	39.8	14.7	3.9	0	0	0	0
2015	F	0	0	0.5	2.8	2.1	3.8	4.4	7.7	2.30	3.20	0	0.9
	M	0	0	3.5	2.3	8.3	17.6	14.3	3	0	0	0	0
2017	F	0	1.8	4.4	0	1.6	2	8.6	11.2	10	1	0	0
	M	0	0	3.1	1	1	8.9	19.6	4.1	0	0	0	0
2019	F	0	3.3	5.2	7.1	7.6	2.1	5.9	6.4	7.1	4.9	0	0
	M	0	3	12	12.6	12.4	10.9	17.8	6.5	0	0	0	0

Hecate Strait Survey

Year	Sex	Length Bin (cm)											
		16	20	24	28	32	36	40	44	48	52	56	60
2005	F	0	0	1.3	0	2.5	6.1	7.5	7.2	5.9	3.6	2.2	0
	M	0	0	0	0	4.5	13.4	4.3	0	0	0	0	0
2007	F	0	3.4	5.2	0	3.9	3.4	2.7	3.4	12.6	5.5	0	0
	M	0	5.6	6.2	5.1	1.9	1.5	1.5	0	0	0	0	0
2009	F	0	2	2.5	12.8	1.9	2.6	4.4	6.5	5.8	9	1	0
	M	0	4.2	9.4	10.1	2.3	3.1	4.3	2.7	0	0	0	0
2011	F	0	0	2.6	3.8	11.7	12.2	10.8	2.7	4.3	3.1	0	0
	M	0	0	1.9	3.4	9.5	4.4	0	2.1	0.9	0	0	0
2013	F	0	0	0	0.9	1.3	1.9	7.7	11.2	7.7	3.2	1.5	0
	M	0	0	0	1.5	2	12.7	8.2	8.9	0	0	0	0
2015	F	0	0	0	0	8.8	4.4	5.1	12.8	10.7	0	1.7	0
	M	0	0	0	2.7	7	8.6	8.9	5.6	0	0	0	0
2017	F	0	0	2.2	0	1	0	4.5	5.4	12.1	3	1.3	0
	M	0	4.3	2.6	0	1.5	3.3	11.3	1.2	0	0	0	0
2019	F	0	0	6.9	12.7	8.5	0	0	7	6.4	4	0	0
	M	0	3.6	8.9	10.7	7.3	1.7	1.7	0	0	0	0	0

West Coast Vancouver Island Survey

Year	Sex	Length Bin (cm)											
		16	20	24	28	32	36	40	44	48	52	56	60
2004	F	0	0	0	1.4	2.7	18.5	19.2	4.6	3.6	0.9	0	0
	M	0	0	0	1.1	34.3	26.3	1.4	0	0	0	0	0
2006	F	0	0	0	3.2	5.2	3.5	10.3	15.9	4.3	2	0	0
	M	0	0	1.9	3.4	9	21.1	8.5	0.9	0	0	0	0
2008	F	0	3.4	1.6	2.4	4.9	7.8	13.1	10.3	1.9	1.5	0	0
	M	9.8	4.3	2.2	4	25.7	6.6	1	1.5	0	0	0	0
2010	F	0	0	2.4	4.3	8.7	9	4	5.5	0	0	0	0
	M	0	0	9.2	16.1	7.6	8.3	0	0	0	0	0	0
2012	F	0	0	3.8	2.8	6.3	15.8	15.3	5.5	3.7	0	0	0
	M	0	4.1	1.9	3.2	18.8	10.8	1	0	0	0	0	0
2014	F	0	0	0	0.9	7.9	6.5	20.5	14.6	2.7	1.5	0	0
	M	0	0	0	1	12.9	17.2	5.4	0	0	0	0	0
2016	F	0	0	2	6.3	12.7	11.7	25.8	31.6	26.7	1.6	0	0
	M	0	1	1.6	10.2	18.2	20.9	16.4	1.6	0	0	0	0
2018	F	0	3	6.4	4.5	7.2	9.9	8.5	14.5	20.1	5.8	2.8	0
	M	0	5.3	9.1	5.7	7	9.6	5.6	1.7	0	0	0	0

B.5. AGEING ERROR

We used double-read precision data collected by the Sclerochronology Lab (SCL) at DFO's Pacific Biological Station to estimate an ageing error matrix for Petrale Sole in BC. Approximately 25% of Petrale Sole otoliths used to develop age composition inputs for the current assessment were read by two independent age-readers: a primary reader and then a secondary 'precision' reader (Figure B - 25). Of the 1121 double-read otoliths available, both readers agreed on an age for 41% of the otoliths and were within one year of each other for 81% of otoliths. We did not find any evidence of temporal patterns in the distribution of differences among readers during data explorations.

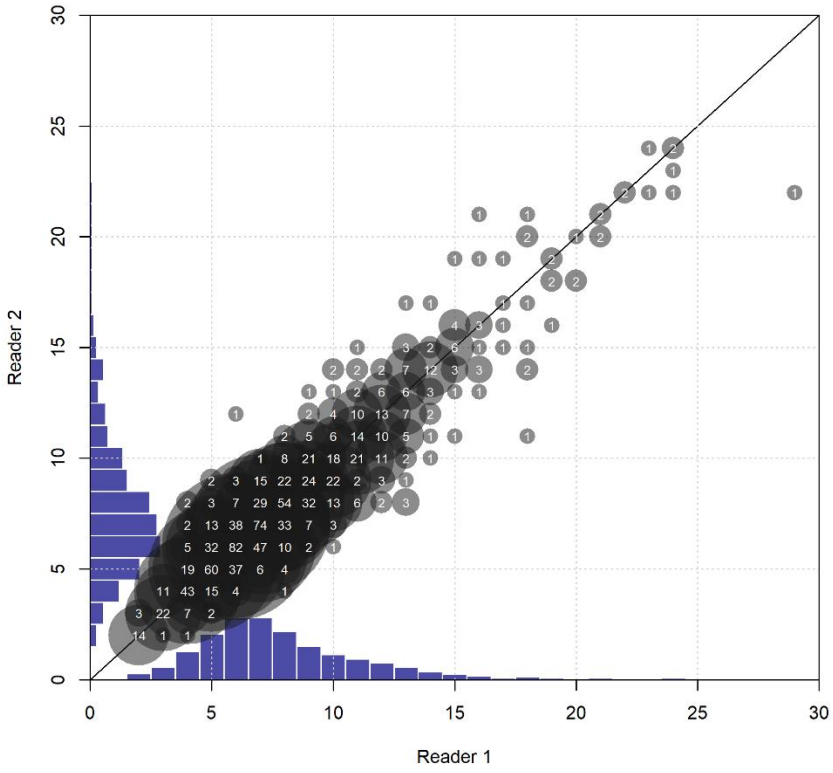


Figure B - 25. Age estimates from a primary reader (Reader 1) vs. a secondary 'precision' reader (Reader 2) for Petrale Sole, were sample sizes falling into each combination of Reader 1 vs. Reader 2 ages shown numerically and by dot size. Purple histrograms show the relative number of estimates at each age for each reader. Plot created using `nwfscAgeingError` *package cited in text.*

We estimated ageing error using the ageing error package for R '`nwfscAgeingError`' (version 1.3.2, Punt et al. 2008, Thorson et al., 2012), with age-reading error standard deviation modelled using the same 3-parameter non-linear model as Richards et al. (1992). The Punt et al. (2008) method extends the method developed by Richards et al. (1992) to allow for both ageing bias and ageing imprecision to be quantified; however, we do not have samples of known-age Petrale in BC. As a result, both readers (the primary reader and the precision reader) are assumed to be unbiased. We also assume that both readers have the same curvilinear standard deviation, and just estimate a single standard deviation at age to be represented in the ageing error matrix.

The nwfscAgeingError package models the probability of reader *i* assigning a fish an estimated age of *a*' given that the true age of the fish is *a* as follows:

$$P^i(a'|a,\emptyset) = exp\left(\frac{-\left(a' - b_a^i(\emptyset)\right)^2}{2\left(\sigma_a^i(\emptyset)\right)^2}\right)$$

Eq. B - 7

where, b_a^i is the expected age when reader *i* determines the age of a fish of true age *a*, σ_a^i is the ageing error standard deviation of reader *i* for a fish of age *a*, and $\emptyset$ is a vector of parameters that determines the ageing error matrix. Because we assume that ageing estimates are unbiased, b_a^i is set to *a* in the above equation. $P^i(a'|a,\emptyset)$ is set to zero for *a*' less than 1 and *a*' greater than a pre-specified maximum age. For Petrale Sole in BC, we set the maximum age to 36 years, which was the maximum precision age documented in the database.

Age-reading error standard deviation, σ_a, is modelled using a 3-parameter curvilinear model:

$$\sigma_a = \begin{cases} \sigma_1 + (\sigma_A - \sigma_1)\dfrac{1 - e^{-\alpha(a-1)}}{1 - e^{-\alpha(A-1)}} & \alpha \neq 0 \\ \sigma_1 + (\sigma_A - \sigma_1)\dfrac{a-1}{A-1} & \alpha = 0 \end{cases}$$

Eq. B - 8

where, σ_1 is the age reading error standard deviation for a pre-specified minimum age of 1, σ_A is the age reading error standard deviation for the maximum age *A*, and the α parameter controls the extent of nonlinearity between age and the age reading standard deviation, with the relationship becoming more linear as α trends towards zero.

Parameter values in $\emptyset$ (where, $\emptyset$=$\{\alpha, \sigma_1, \sigma_A\}$) are estimated by maximizing the following likelihood function:

$$L(\mathbf{A}'|\mathbf{A}) = \prod_{j=1}^{J}\prod_{i=1}^{I} P^i\left(a'_{i,j}|a_j,\emptyset\right)$$

Eq. B - 9

where, **A**' is the entire matrix of observed age readings, $a'_{i,j}$ is the observed age of fish *j* by reader *i* and a_j is the true age of fish *j*.

The final fitted model predicted an almost linear relationship between age and age reading error standard deviation (Figure B - 26). The CV of age reading error was approximately 14% at age 1, 12% at age 2, and 10-11% for all other ages.

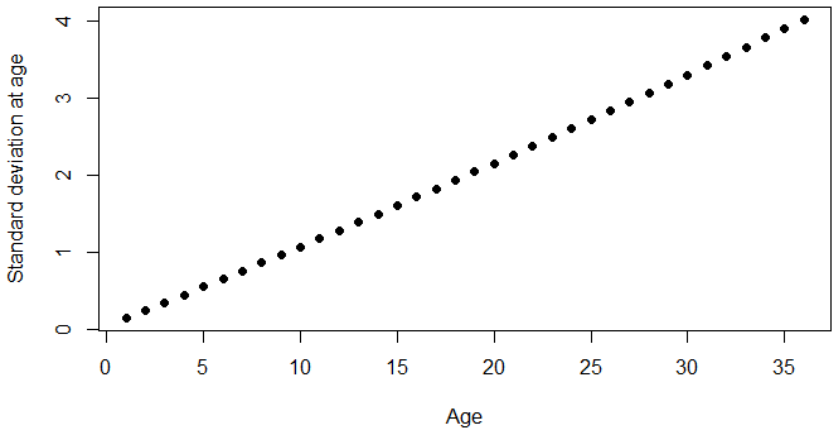


Figure B - 26. Predicted age reader error standard deviation at age for Petrale Sole in BC.

LITERATURE CITED

Anderson, S.C., Keppel, E.A., Edwards, A.M., and Grandin, C. 2024. gfplot: Data Extraction and Plotting for DFO PBS Groundfish Stocks . R package version 0.2.1, commit 66ca660b993304fe19bd387edd1ff7ebf711d396.

Holt, K.R., Starr, P.J., Haigh, R. and Krishka, B. 2016. Stock Assessment and Harvest Advice for Rock Sole (*Lepidopsetta spp.*) in British Columbia. DFO Can. Sci. Advis. Sec. Res. Doc. 2016/009. ix + 256 p.

Kristensen, K., Nielsen, A., Berg, C.W., Skaug, H., and Bell, B.M. 2016. TMB: automatic differentiation and laplace approximation. Journal of Statistical Software, 70, 1–21.

McAllister, M. K., and Ianelli, J. N. 1997. Bayesian stock assessment using catch-age data and the sampling-importance resampling algorithm. Canadian Journal of Fisheries and Aquatic Sciences, 54(2), 284-300.

Punt, A.E., Smith, D.C., KrusicGolub, K., and Robertson, S. 2008. Quantifying age-reading error for use in fisheries stock assessments, with application to species in Australia's southern and eastern scalefish and shark fishery. Canadian Journal of Fisheries and Aquatic Sciences, 65, 1991–2005.

Richards, L.J., Schnute, J.T., Kronlund, A.R., and Beamish, R.J. 1992. Statistical models for the analysis of ageing error. Canadian Journal of Fisheries and Aquatic Sciences, 49, 1801–1815.

Starr, P.J. and Haigh, R. 2023. Canary Rockfish (*Sebastes pinniger*) Stock Assessment for British Columbia in 2022. DFO Can. Sci. Advis. Sec. Res. Doc. 2023/070. vi + 293 p.

Stewart, I. J., and Hamel, O.S. 2014. Bootstrapping of sample sizes for length-or age-composition data used in stock assessments. Canadian Journal of Fisheries and Aquatic Sciences, 71(4), 581-588.

Thorson, J.T., Stewart, I.J., and Punt, A.E. 2012. nwfscAgeingError: a user interface in R for the Punt et al. (2008) method for calculating ageing error and imprecision.

APPENDIX C. COMMERCIAL FISHERY CPUE STANDARDIZATION

Relative indices of abundance based on commercial trawl fishery catch-per-unit-effort (CPUE) were developed using a GLMM (generalized linear mixed effect model) based on a Tweedie distribution that standardized CPUE for depth, fishing locality (defined spatial regions, see Anderson et al. 2019 for locality map), month, vessel, and latitude. We followed the Tweedie standardization methods documented in Anderson et al. (2019) and applied to recent stock assessments for Pacific Cod (*Gadus macrocephalus,* Forrest et al. 2020) and Arrowtooth Flounder (*Atheresthes stomias*, Grandin et al. 2026) in BC. Code used to fit Tweedie GLMM models to Petrale Sole catch and effort data were provided by Sean Anderson (pers. comm, Fisheries and Oceans Canada, Pacific Biological Station; code available upon request).

C.1. FLEET DEFINTION

The level of data available for GLMM analyses of trawl fishery CPUE in BC data differs over time. We defined two time periods based on data availability: Historical (1954 – 1995) and Modern (1996 – present), for our Petrale Sole analysis, which was the same approach used for Pacific Cod (Forrest et al. 2020). The year 1996 was used as a break-point for the two time periods because it was the start of quota management and 100% at-sea observer coverage for the BC trawl fishery, which changed fishing behaviour of the fleet significantly. The number of DFO fishing localities represented in the CPUE dataset increased markedly in 1991, which corresponds to the start of catch and effort reporting on a tow-by-tow basis. However, an additional break-point at 1991 was not considered because the 1991 – 1995 time series would be short.

The definitions of the fishing fleet for both time periods are described below, including the data sources available for each period. Catch and effort data from all seven Groundfish Management Areas included in the current coastwide definition of the stock were used to calculate CPUE indices (Areas 3CD, 5ABCDE).

C.1.1. Historical Fleet: 1954 – 1995

Prior to 1991, commercial catch and effort data from groundfish trawl fisheries were collected via dockside interviews and are only available to the level of trip and fishing locality. Logbook records are available from 1991 onwards, which distinguishes catch and effort to the fishing event (i.e., trawl set) level. However, in order to combine 1991 – 1995 data with the pre-1991 data, fishing event data from 1991 – 1995 were aggregated to the locality-trip level. During the Historical time period, the variables depth, date, and locality were available as model covariates.

C.1.2. Modern Fleet: 1996 - 2023

Since 1996, commercial catch and effort data have been recorded to the fishing event level with catches monitored via on-board observers or electronic video monitoring. The higher data resolution for this time period included two additional variables that were used to standardize CPUE: latitude and a unique vessel ID. As a result, the variables depth, date, locality, latitude, and vessel were available as model covariates during the Modern time period.

When defining the Modern fleet, we used criteria similar to other Pacific Groundfish assessments. Vessels included in the standardization analysis were required to have caught Petrale Sole in at least 100 tows between 1996 and 2023, and to have passed a threshold of at least five trips that caught Petrale Sole for at least five years.

C.2. STANDARDIZATION PREDICTORS

The following description of predictor variables used for the Tweedie GLMM has been reproduced from Anderson et al. 2019.

For depth and latitude, we binned the values into a sequence of bands to allow for nonlinear relationships between these predictors and CPUE (e.g., Maunder and Punt 2004). For depth, we binned trawl depth into bands 25m wide. For latitude, we used bands that were 0.1 degrees wide. To ensure sufficient data to estimate a coefficient for each factor level, we limited the range of depth bins to those that fell within the 0.1% to 99.9% cumulative probability of positive observations and then removed any factor levels (across all predictors) that contained fewer than 0.1% of the positive observations.

Predictors that are treated as factors in a statistical model need a reference or base level — a level from which the other coefficients for that variable estimate a difference. The base level then becomes the predictor value that is used in the prediction for the standardized index. We chose the most frequent factor level as the base level — a common choice for these types of models (Maunder and Punt 2004). For example, we set the base month as the most common month observed in the dataset filtered for only tows where the species was caught. This choice of base level only affected the intercept or relative magnitude of our index because of the form of our model (discussed below) and makes no functional difference in the commercial CPUE time series presented in this report since they are all scaled to that same maximum and displayed without units.

The following description of the Tweedie GLMM has been reproduced, with permission, from Anderson et al. 2019.

The Tweedie distribution has a mean parameter as well as two additional parameters: a power parameter ρ and a dispersion parameter φ. If $1 < \rho < 2$ then the Tweedie distribution represents a compound distribution between the Poisson ($p = 1$) and the Gamma distribution ($p = 2$). In fact, the Tweedie is alternatively referred to as the compound-Poisson-Gamma distribution in this bounded case. We note, however, that the compound-Poisson-Gamma distribution is often used to refer to a re-parameterization in which the Poisson and Gamma components are fit so that they are not assumed to have the same predictive coefficients as they are in the Tweedie distribution (e.g., Foster and Bravington 2013, Lecomte et al. 2013).

We fit the Tweedie GLMM (generalized linear mixed effects model) as

$$y_i \sim \text{Tweedie}(\mu_i, \rho, \varphi), \quad 1 < \rho < 2,$$
$$\mu_i = exp\left(\mathbf{X}_i\beta + \alpha_{j[i]}^{locality} + \alpha_{k[i]}^{locality-year} + \alpha_{l[i]}^{vessel}\right)$$
$$\alpha_j^{\text{locality}} \sim \text{Normal}\left(0, \sigma^2_{\alpha\ \text{locality}}\right)$$
$$\alpha_k^{\text{locality - year}} \sim \text{Normal}\left(0, \sigma^2_{\alpha\ \text{locality - year}}\right)$$
$$\alpha_l^{\text{vessel}} \sim \text{Normal}\left(0\ \sigma^2_{\alpha\ \text{vessel}}\right)$$

Eq. C - 1

where, *i* represents a single trip (historical data) or tow (modern data), y_i represents the catch (kg) per unit effort (hours trawled), $\mathbf{X}_i$ represents a vector of fixed-effect predictors (historical: depth bins, months; modern: depth bins, months, latitude bins), β represents a vector of coefficients, and μ_i represents the expected CPUE in a trip or tow. The random effects intercepts (α symbols) are allowed to vary from the overall intercept by locality *j* ($\alpha_j^{\text{locality}}$), locality

– year k ($\alpha_k^{\text{locality - year}}$), and vessel *l* ($\alpha_l^{\text{vessel}}$) (for the modern dataset only), and are constrained by normal distributions with respective standard deviations denoted by σ parameters. By including the locality-year interactions, we allow the individual localities to have unique CPUE trends (somewhat constrained by the random effect distribution) while estimating the overall average trend.

We can then calculate the standardized estimate of CPUE for year *t*, μ_t, as

$$\mu_t = \exp(\mathbf{X}_t \beta)$$

Eq. C - 2

where $\mathbf{X}_t$ represents a vector of predictors set to the reference (*r*) levels with the year set to the year of interest. Because each of the α random intercepts is set to zero, the index is predicted for an average locality, locality-year, and vessel. We estimated the fixed effects with maximum marginal likelihood while integrating over the random effects with the statistical software Template Model Builder (TMB) via the R package glmmTMB. We used standard errors (*SE*) as calculated by TMB on $log(\mu_t)$ via the generalized delta method. We then calculated the 95% Wald confidence intervals as $exp(\mu_t \pm 1.96 SE_t)$. For comparison, we calculated an unstandardized time series by summing the catch each year and dividing it by the summed effort each year (the dashed lines on the figure pages).

C.3. RESULTS

C.3.1. Historical CPUE (1954-1995)

The raw Petrale Sole catch shows variable trends through time between 1954 and 1995, while effort shows an increasing pattern towards the end of the time period (Figure C - 1). The majority of the Petrale Sole catch during this period came from depths of 50-225 m; however, small portions of catch came from deeper depths extending up to 450 m (Figure C - 2).



Figure C - 1. Raw time series of Petrale Sole catch and total hours trawled (regardless of species caught) for the Historical time period, which covered the years 1955 to 1995 as shown on the x-axis.

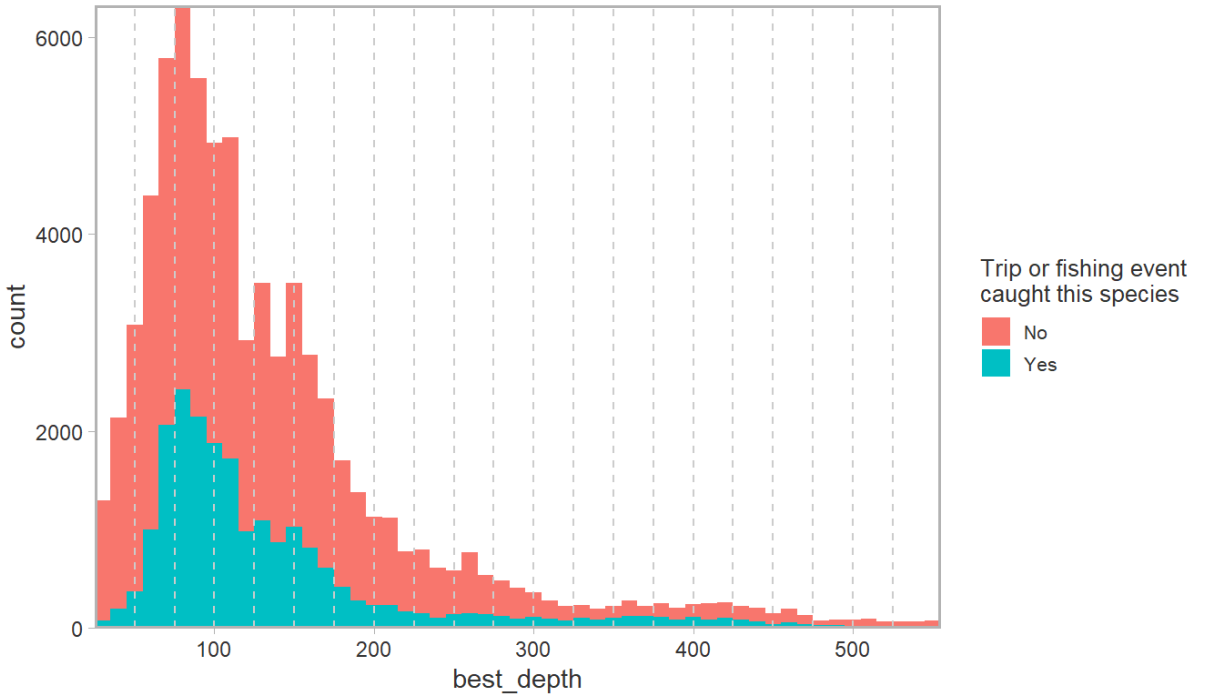


Figure C - 2. The depth distribution (in meters) for fishing trips that caught Petrale Sole, or did not catch Petrale Sole, during the Historical time period (1954-1995).

Temporal patterns were apparent in the depth, month, and locality of fishing over the Historical period (Figure C - 3). We see an increase in the depths fished by the trawl fishery starting in the early 1980's, with a subsequent increase in the 1990s. There is also increased fishing during winter months throughout the 1980s and early 1990s, with Petrale Sole frequently encountered during winter months. Specific localities fished fluctuated over time, with an increase in the number of localities fished throughout the time period.

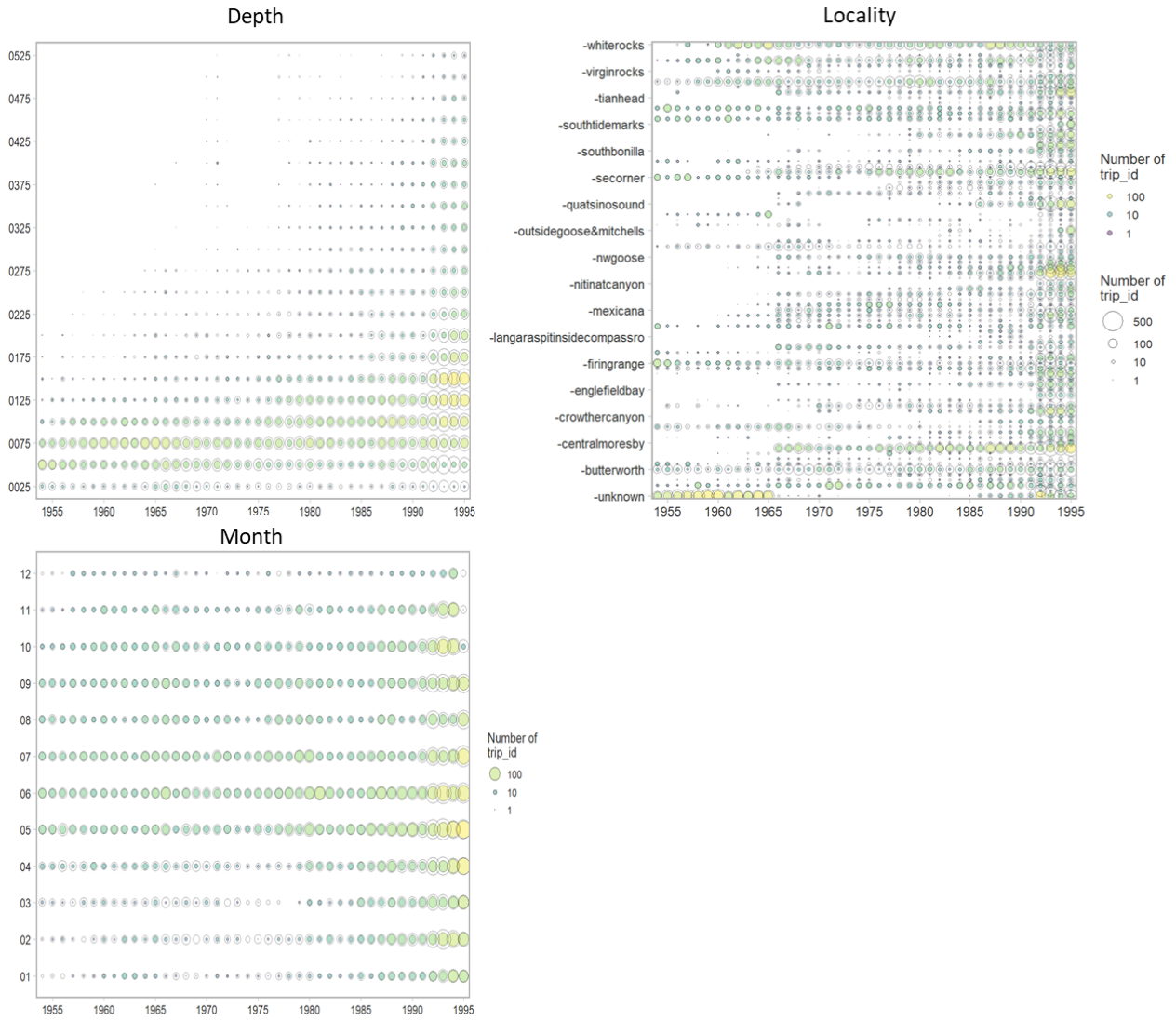


Figure C - 3. Distribution of predictors (depth, locality, and month) in CPUE standardization models for the Historical time period (1954-1995). Area of outermost circles represents the number of trips ('trip_id') for that predictor value and year combination. Area and shading of innermost circles represents the number of trip-locality combinations for that predictor value and year combination that caught Petrale Sole.

Coefficient plots were used to examine the contribution of all fixed and random effect parameters to the GLMM standardization (Figure C - 4 to Figure C - 6). Strong patterns were apparent in the fixed coefficients for both depth and month.

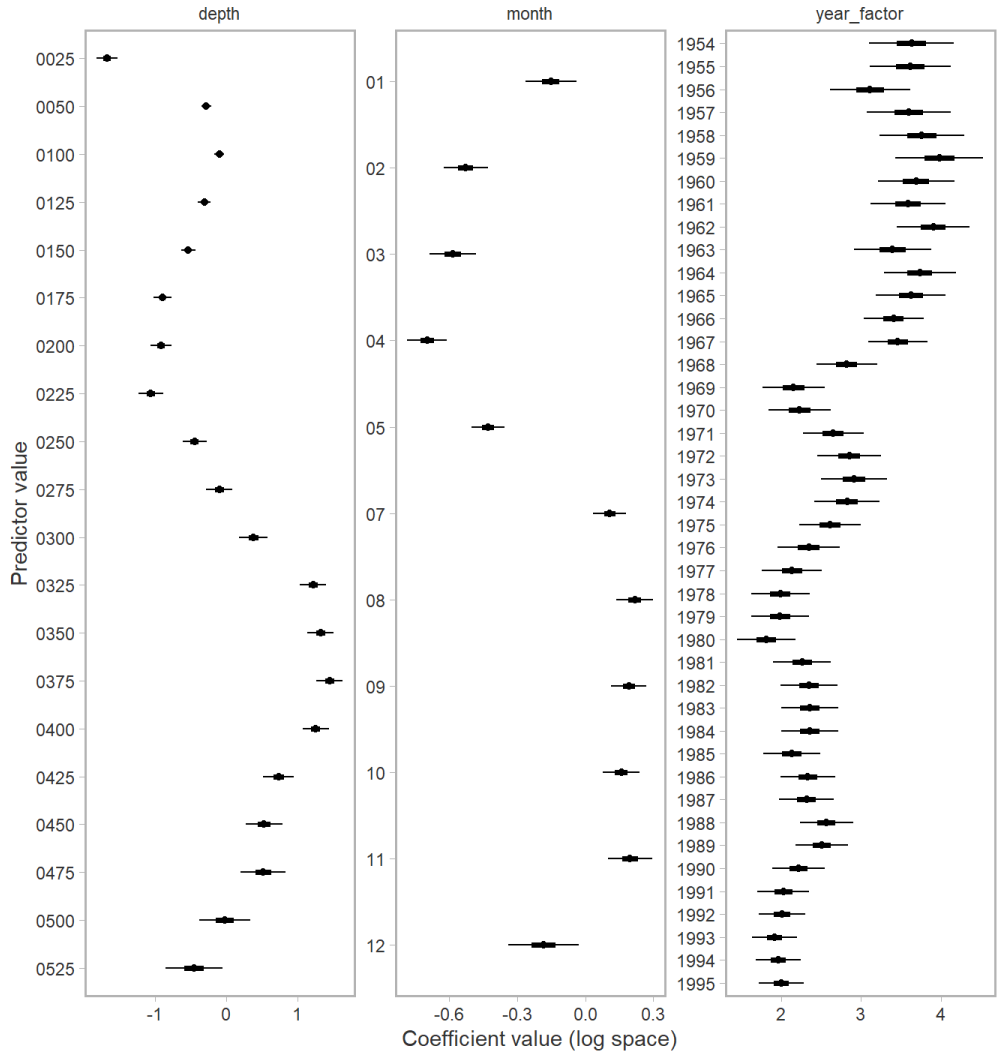


Figure C - 4. Fixed effect coefficients for Historical commercial CPUE standardization model. In all cases, the values are with respect to the reference (most common) factor level (the missing factor level in each plot). Dots represent the mean while thick and thin line segments represent the 50% and 95% Wald confidence intervals, respectively.

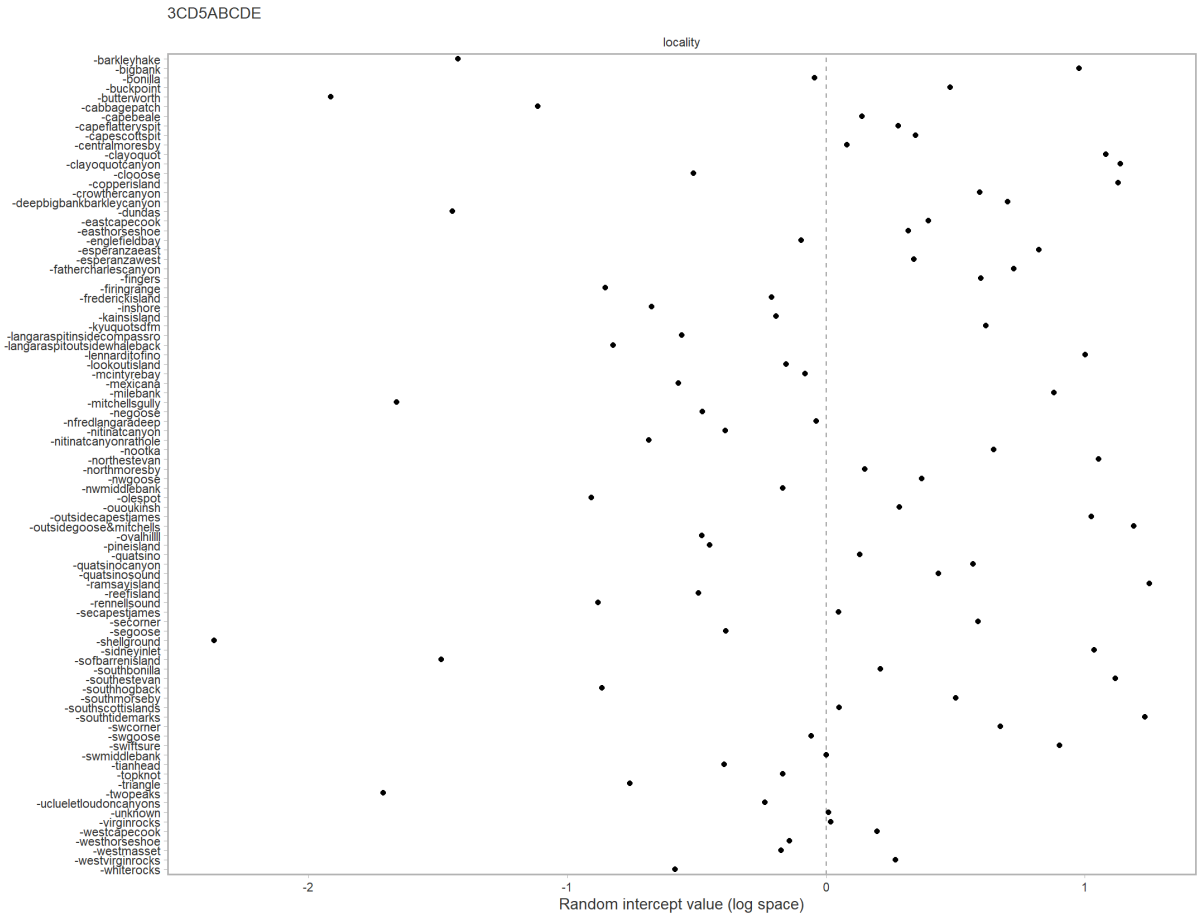


Figure C - 5. Locality random effects for the Historical commercial CPUE standardization model.



Figure C - 6. Random intercept values for the locality-year interaction effect in the Historical standardization model. Panel labels represent locality names. Years on the x-axis extend from 1954 – 1995.

A comparison of the final, standardized CPUE index with an unstandardized index of nominal CPUE is shown in Figure C - 7. The standardization process increases the CPUE at the early part of the Historical time series, during which time fewer fishing trips occurred at deeper (>250 m) depths during the winter months. This result is as expected given that encounters with spawning aggregations are known to be highest at these deeper depths during the winter. The standardization also reduced CPUE somewhat during the early 1970s compared to the unstandardized index.

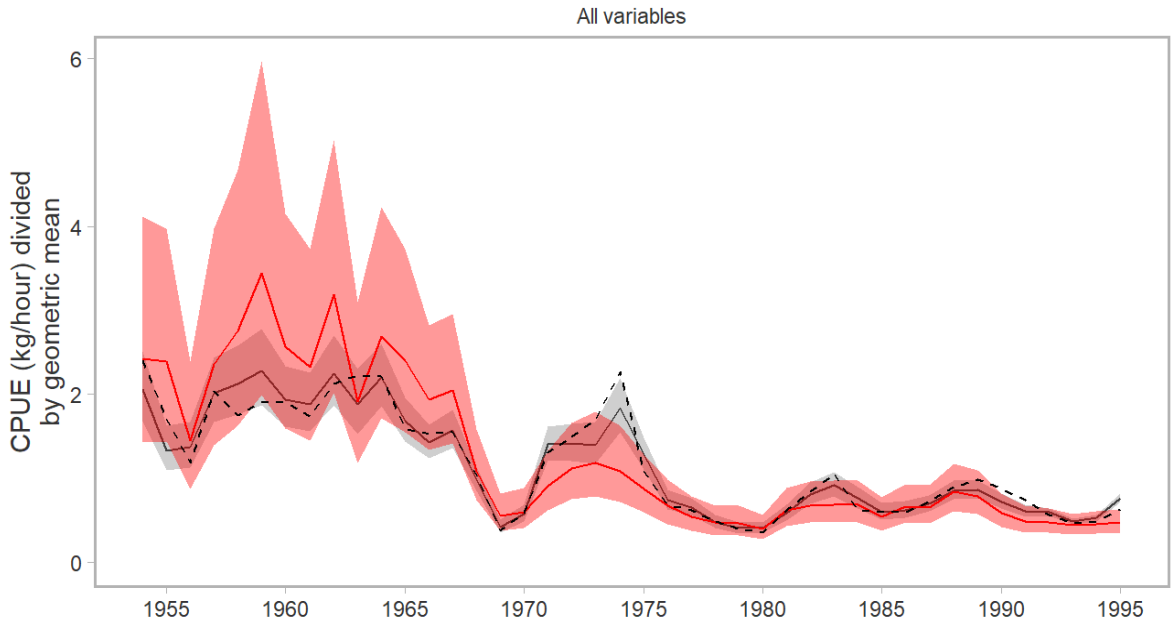


Figure C - 7. Commercial CPUE indices for the historical time period which covered the years 1955 to 1995 as shown on the x-axis.. The red line is the standardized version, the black solid line is a version with only a year predictor with the Tweedie observation model, and the dashed line is the summed catch for the species divided by effort. The ribbons indicate the 95% (Wald) confidence intervals.

Table C - 1. Commercial CPUE (kg / hour) index values for the Historical full standardization model. Lower and Upper show the upper and lower bounds of the 95% (Wald) confidence intervals.

Year	CPUE	Lower	Upper
1954	37.74	22.25	64.03
1955	37.13	22.34	61.73
1956	22.50	13.62	37.15
1957	36.56	21.66	61.71
1958	42.87	25.31	72.60
1959	53.50	30.92	92.58
1960	39.95	24.76	64.46
1961	36.18	22.61	57.89
1962	49.48	31.36	78.07
1963	29.73	18.36	48.14
1964	41.83	26.65	65.65
1965	37.34	24.07	57.93
1966	30.18	20.77	43.86
1967	31.76	21.97	45.92

Year	CPUE	Lower	Upper
1968	16.80	11.49	24.56
1969	8.65	5.84	12.81
1970	9.32	6.32	13.73
1971	14.18	9.71	20.72
1972	17.33	11.65	25.80
1973	18.42	12.17	27.88
1974	16.85	11.25	25.25
1975	13.59	9.24	19.99
1976	10.45	7.09	15.38
1977	8.48	5.84	12.31
1978	7.33	5.08	10.59
1979	7.31	5.09	10.49
1980	6.15	4.28	8.84
1981	9.60	6.72	13.71
1982	10.46	7.34	14.91
1983	10.61	7.44	15.15
1984	10.60	7.41	15.17
1985	8.47	5.94	12.08
1986	10.33	7.36	14.51
1987	10.16	7.23	14.27
1988	13.06	9.40	18.16
1989	12.29	8.89	17.00
1990	9.20	6.63	12.77
1991	7.61	5.50	10.52
1992	7.49	5.60	10.01
1993	6.83	5.16	9.04
1994	7.13	5.37	9.47
1995	7.42	5.58	9.86

C.3.2. Modern CPUE (1996 – 2023)

The raw Petrale Sole catch shows a variable, but generally increasing, trend through time between 1996 and 2023, while effort shows a declining trend over the same period (Figure C - 8). The majority of the Petrale Sole catch during this period came from depths of 50-450 m (Figure C - 9). A higher portion of Petrale Sole catch came from depths >250 m for the Modern time period compared to the Historical time period, which coincides with the removal of winter trip limits for Petrale Sole after Individual Transferable Quotas (ITQs) were introduced in 1996.

The distribution of fishing events among depth, month, and locality, as well as the distribution of fishing events that encountered Petrale Sole, was more constant over time for the Modern time period compared to the Historical time period (Figure C - 10). The distribution of fishing events and Petrale Sole encounters among latitudinal bands were also relatively constant over time. There were patterns in the number of vessels fishing over time, with fewer vessels at the end of the time period compared to 1996. Petrale Sole catch therefore became more concentrated among fewer vessels over time.

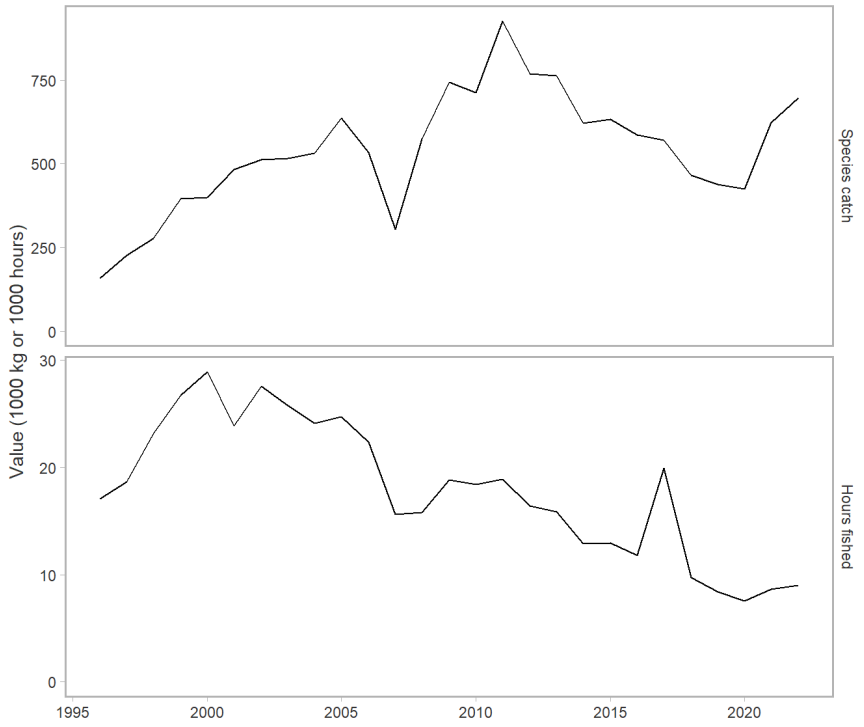


Figure C - 8. Raw time series of Petrale Sole catch and total hours trawled (regardless of species caught) for Modern time period, which covers the years 1996 to 2023 as shown on the x-axis.

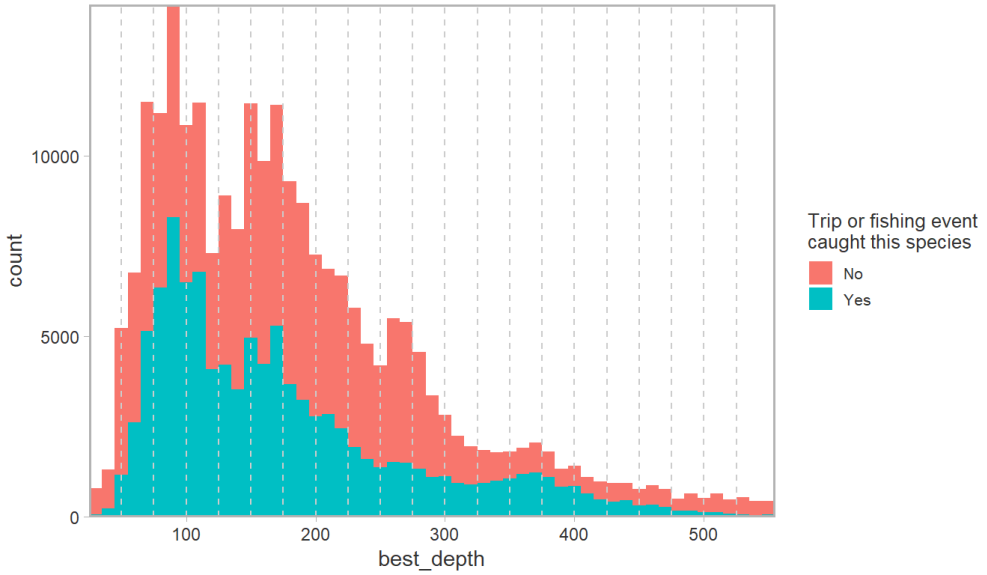


Figure C - 9. The depth distribution for trawl fishing events that caught Petrale Sole, or did not catch Petrale Sole, during the Modern time period (1996-2023).

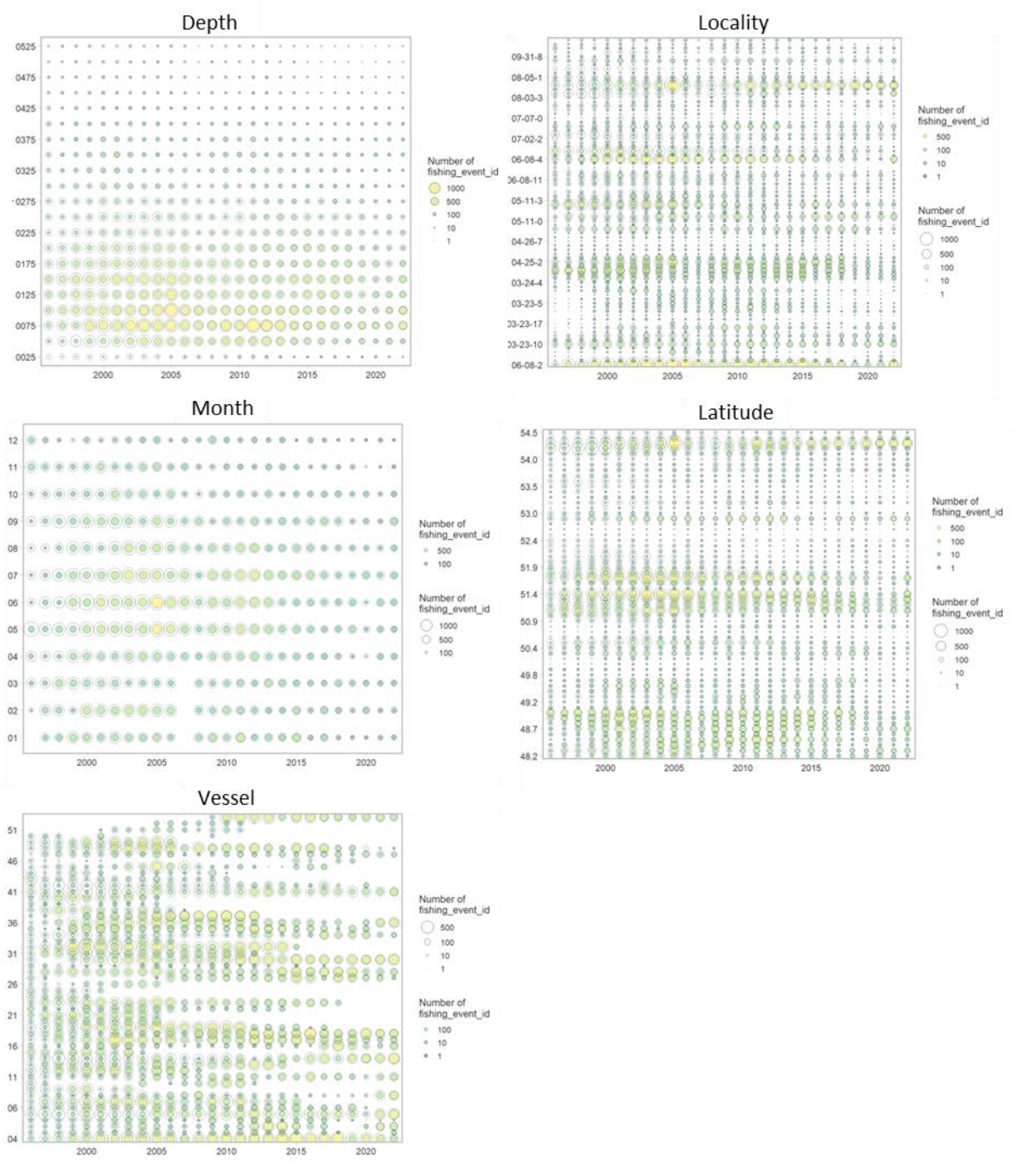


Figure C - 10. Distribution of predictors (depth, locality, month, latitude, vessel) in CPUE standardization models for the Modern time period (1996-2023). Area of outermost circles represents the number of trawl tows ('fishing_event_id') for that predictor value and year combination. Area and shading of innermost circles represents the number of trip-locality combinations for that predictor value and year combination that caught Petrale Sole.

Coefficient plots were used to examine the contribution of all fixed and random effect parameters to the GLMM standardization (Figure C - 11 - Figure C - 13). Strong patterns were apparent in the fixed coefficients for depth, month, and latitude.

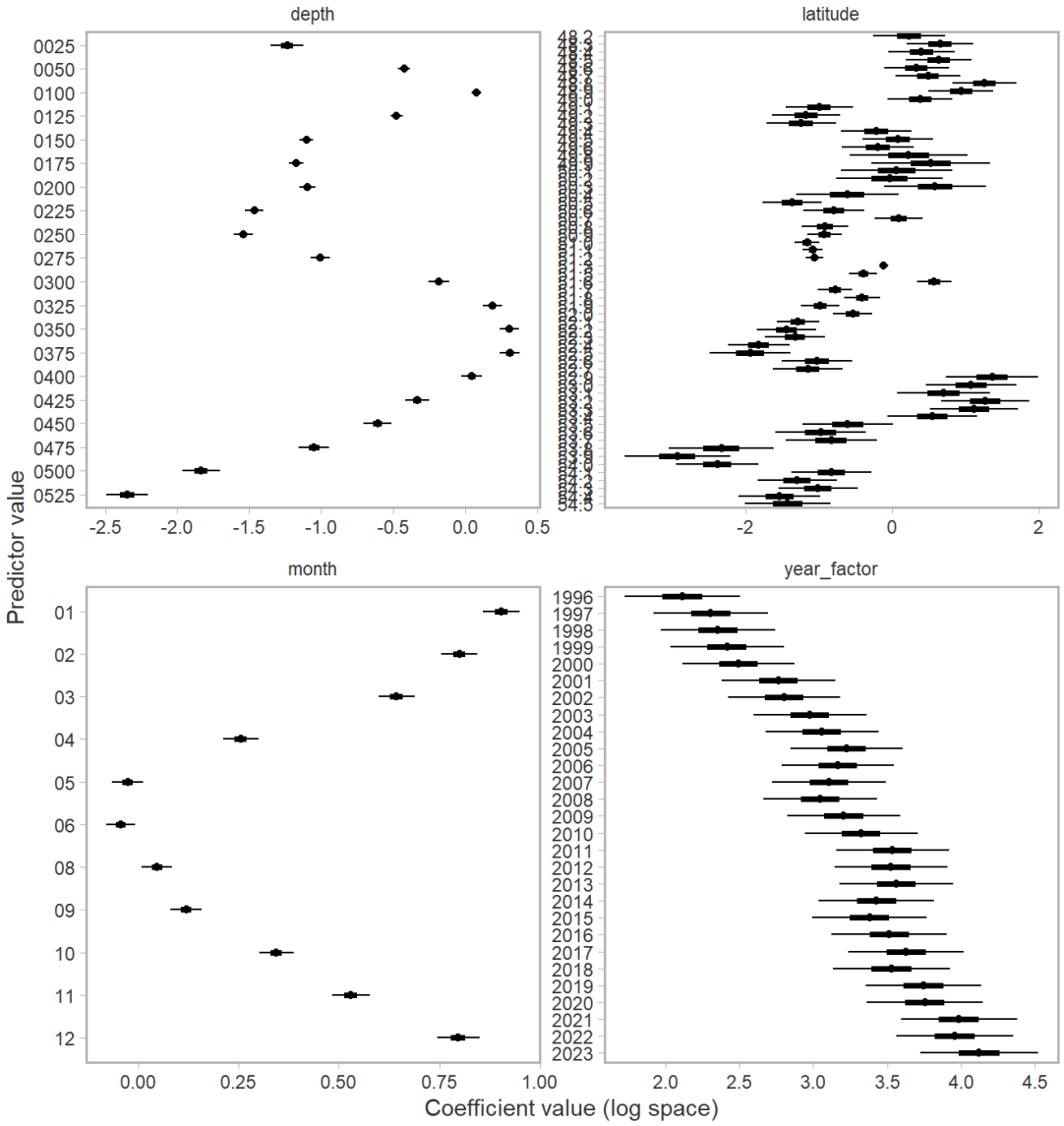


Figure C - 11. Fixed effect coefficients for Modern commercial CPUE standardization model. In all cases, the values are with respect to the reference (most common) factor level (the missing factor level in each plot). Dots represent the mean while thick and thin line segments represent the 50% and 95% Wald confidence intervals, respectively.

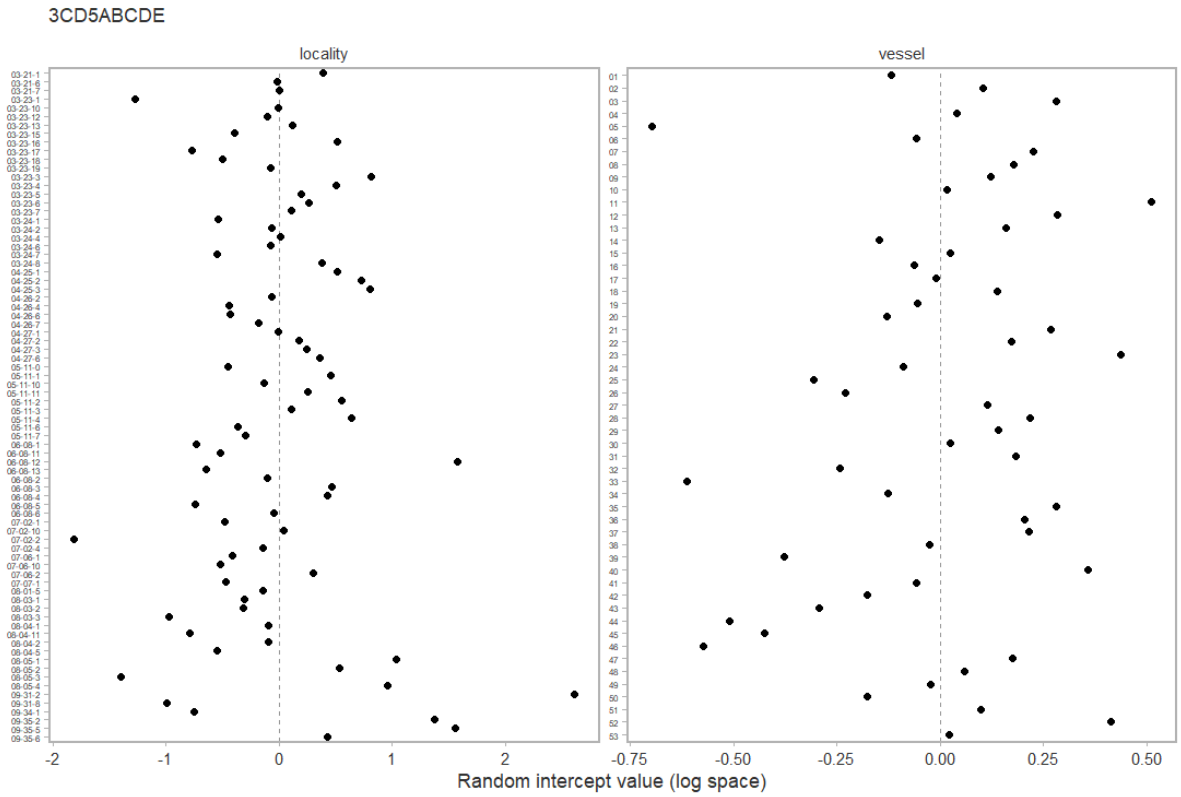


Figure C - 12. Locality random effects for the Modern commercial CPUE standardization model.

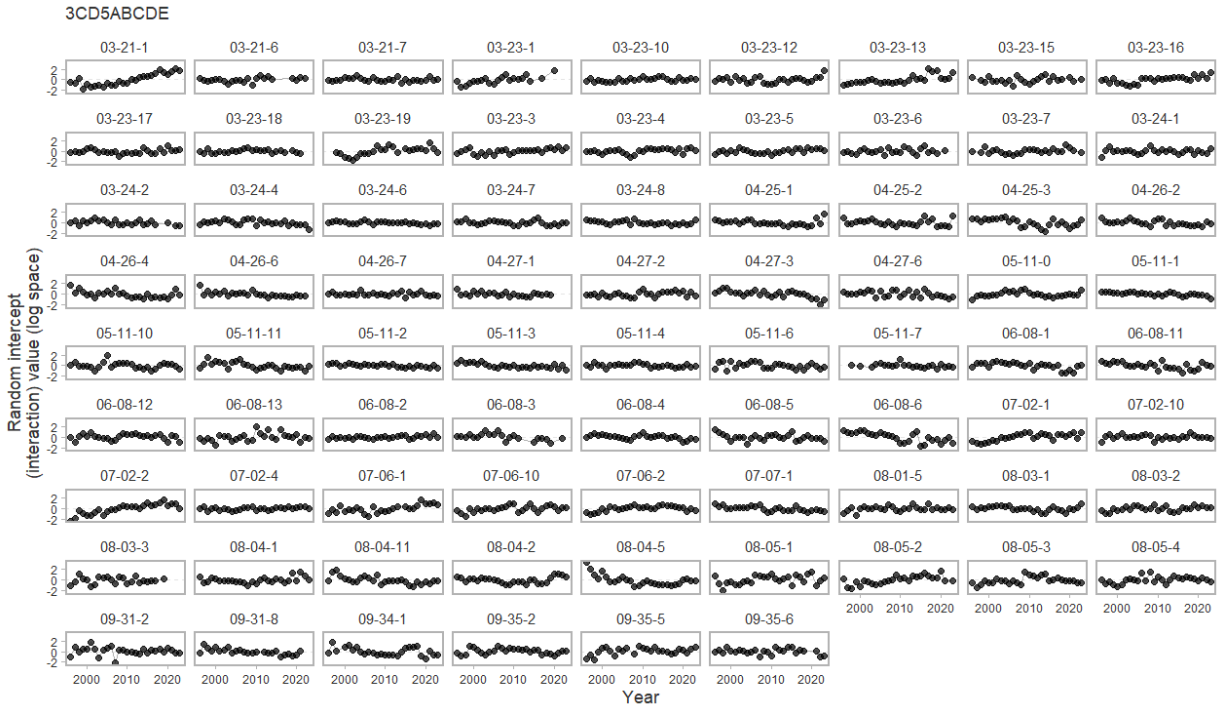


Figure C -13. Random intercept values for the locality-year interaction effect in the Modern standardization model. Panel labels represent locality codes. Years on the x-axis extend from 1996-2023.

The standardization process did not have a large impact on the shape of the Modern CPUE time series, although the time series was slightly smoothed (Figure C - 14). The low impact of standardization is likely indicative that there have not been systematic changes in the standardization factors included in the model over the Modern time period.

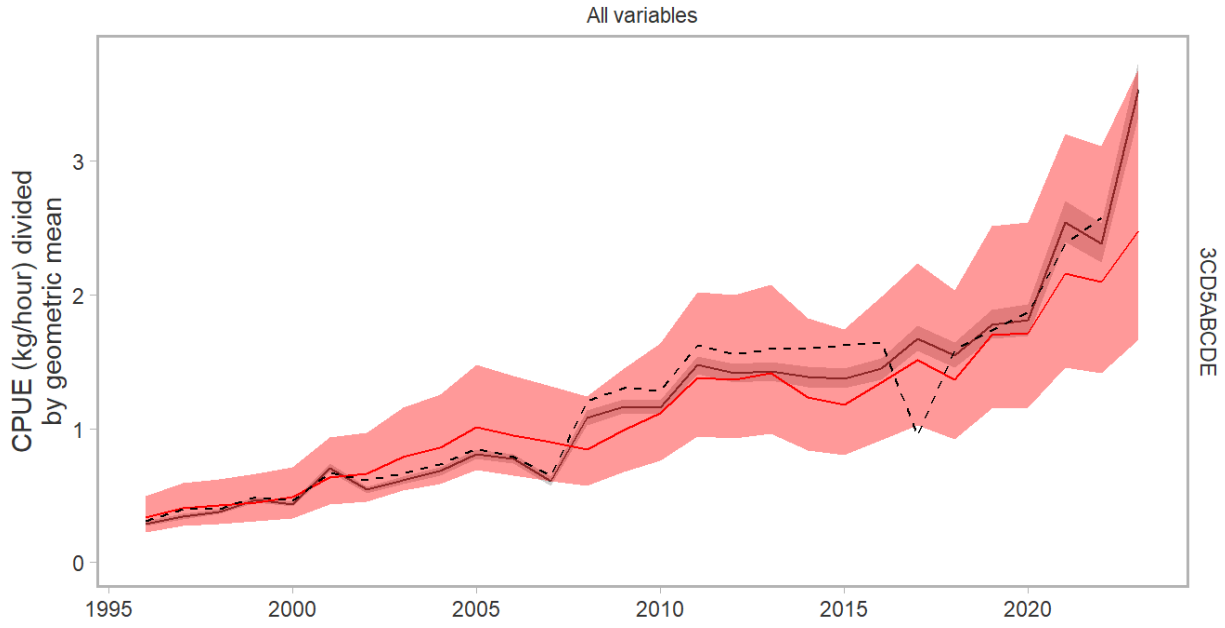


Figure C - 14. Commercial CPUE indices for the Modern time period, which covers years 1996 – 2023 as shown on the x-axis. The red line is the standardized version, the black solid line is a version with only a year predictor with the Tweedie observation model, and the dashed line is the summed catch for the species divided by effort. The ribbons indicate the 95% (Wald) confidence intervals.

Table C - 2. Commercial CPUE (kg / hour) index values for the Modern full standardization model. Lower and Upper show the upper and lower bounds of the 95% (Wald) confidence intervals.

Year	CPUE	Lower	Upper
1996	8.28	5.59	12.26
1997	10.03	6.79	14.80
1998	10.53	7.15	15.50
1999	11.20	7.62	16.46
2000	12.10	8.26	17.73
2001	15.86	10.81	23.26
2002	16.49	11.26	24.15
2003	19.64	13.41	28.75
2004	21.31	14.55	31.19
2005	25.17	17.20	36.84
2006	23.70	16.18	34.72

Year	CPUE	Lower	Upper
2007	22.32	15.19	32.79
2008	21.04	14.33	30.89
2009	24.68	16.85	36.16
2010	27.78	18.94	40.73
2011	34.32	23.41	50.32
2012	33.97	23.15	49.85
2013	35.24	23.98	51.79
2014	30.77	20.85	45.41
2015	29.39	19.92	43.37
2016	33.57	22.75	49.52
2017	37.62	25.45	55.62
2018	34.09	22.96	50.61
2019	42.35	28.60	62.70
2020	42.71	28.78	63.37
2021	53.81	36.31	79.74
2022	52.24	35.15	77.63
2023	61.71	41.40	91.99

LITERATURE CITED

Anderson, S.C., Keppel, E.A., and Edwards, A.M. 2019. A reproducible data synopsis for over 100 species of British Columbia groundfsh. DFO Can. Sci. Advis. Sec. Res. Doc. 2019/041. vii + 321 p.

Anderson, S.C., Ward, E.J., English, P.A., Barnett, L.A., and Thorson, J.T. 2024. sdmTMB: an R package for fast, flexible, and user-friendly generalized linear mixed effects models with spatial and spatiotemporal random fields. BioRxiv, 2022.03.24.485545.

Forrest, R.E., Anderson, S.C., Grandin, C.J., and Starr, P.J. 2020. Assessment of Pacific Cod (*Gadus macrocephalus*) for Hecate Strait and Queen Charlotte Sound (Area 5ABCD), and West Coast Vancouver Island (Area 3CD) in 2018. DFO Can. Sci. Advis. Sec. Res. Doc. 2020/070. v + 215 p.

Foster, S.D., and Bravington, M.V. 2013. A Poisson–Gamma model for analysis of ecological non-negative continuous data. Environmental and Ecological Statistics, 20(4), 533-552.

Grandin, C.J., Anderson, S.C., and English, P.A. 2026. Arrowtooth Flounder (*Atheresthes stomias*) Stock Assessment for the West Coast of British Columbia in 2021. DFO Can. Sci. Advis. Sec. Res. Doc. 2024/071. v + 142 p.

Lecomte, J.-B., Benoît, H.P., Ancelet, S., Etienne, M.-P., Bel, L., and Parent, E. 2013. Compound Poisson-gamma vs. Delta-gamma to handle zero-infated continuous data under a variable sampling volume. Methods in Ecology and Evolution 4(12), 1159–1166.

Maunder, M.N., and Punt, A.E. 2004. Standardizing catch and effort data: A review of recent approaches. Fisheries Research, 70(2), 141–159.

Thorson. 2018. Three problems with the conventional delta-model for biomass sampling data, and a computationally efficient alternative. Canadian Journal of Fisheries Aquatic Sciences. 75, 1369 – 1382.

APPENDIX D. SURVEY INDICES

Four different survey biomass indices were used for stock assessment modelling. Three of these surveys are part of DFO's ongoing Groundfish Synoptic Bottom Trawl Surveys, which have operated off Canada's west coast since around 2003-2005. These surveys operate as three distinct surveys in different portions of the coast (West Coast Vancouver Island, Queen Charlotte Sound, and Hecate Strait) and typically occur biennially, with different surveys conducted in alternating years. We developed biomass indices for each of the three synoptic trawl surveys using geostatistical models previously developed and applied to BC groundfish species (Anderson et al. 2019). All three of these survey indices were used as part of the base ensemble model for this assessment. The fourth survey index series used is from the US National Oceanic and Atmospheric Administration (NOAA's) historical Triennial trawl survey (also called the NMFS Triennial survey), which operated in Canadian waters off Vancouver Island between 1980 and 2001. This data series was not used as part of the base ensemble model but was considered as a sensitivity analysis.

D.1. DFO SYNOPTIC TRAWL SURVEYS: GEOSTATISTICAL MODELLING

D.1.1. Methods

Survey datasets for each of the three synoptic trawl surveys were extracted from DFO databases using the gfdata R package, which was developed as a reproducible tool to support the Groundfish Data Synopsis Report (Anderson et al. 2019; Figures D – 1, D– 2, and D – 3). Survey data are also publicly available through DFO's Open Government data portal.

The expected spatial trawl biomass densities were modelled using geostatistical spatiotemporal GLMMs (generalized linear mixed effect models; Anderson et al. 2024), applied to data from each of the three synoptic trawl surveys independently. In these spatiotemporal models, random effects are used to explain spatial and/or spatiotemporal components. Spatial random effects are constant over time, and spatiotemporal random effects vary through time. Petrale Sole indices for the three synoptic surveys were estimated with sdmTMB (Anderson et al. 2024). sdmTMB has many advantages, such as flexible user-friendly interface, fast estimation, simple out-of-sample cross validation, and usefulness for large and complex data. sdmTMB implements Stochastic Partial Differential Equation (SPDE) approximation to Gaussian random fields with Gaussian Markov random fields (Lindgren et al. 2011). The Laplace approximation, implemented in Template Model Builder (TMB; Kristensen et al. 2016), is used to integrate over random effects. The formulation of these models is:

$$g(\mu_{s,t}) = X_{s,t}\beta + \omega_s + \epsilon_{s,t}$$

Eq. D - 1

where *g()* represents a link function; $\mu_{s,t}$ is the expected value of the density at location *s* and time *t*, $X_{s,t}$ is a matrix of covariates, β is a vector of fixed-effect coefficients, ω_s is the spatial random effect at location *s*, and $\epsilon_{s,t}$ is the spatiotemporal random effect at location *s* and time *t.*

For each synoptic trawl survey, spatiotemporal models were fit with and without a depth covariate and with Tweedie, delta-lognormal, and delta-gamma families. The effect of depth was included via a spline function, because the depth effect is expected to be non-linear. Model convergence was confirmed by checking gradients and Hessian matrices. We constructed our triangulation meshes in order to implement the SPDE such that the minimum allowed distance between vertices in the mesh was 10 km for each of the Synoptic Surveys. The best model for each survey was determined with AIC. Biomass was then predicted onto each of the synoptic

survey grids and aggregated to determine survey indices. Biomass estimates are a sum of the product of the population density across grid cells, and uncertainty is a function of uncertainty in the predictions across grid cells.

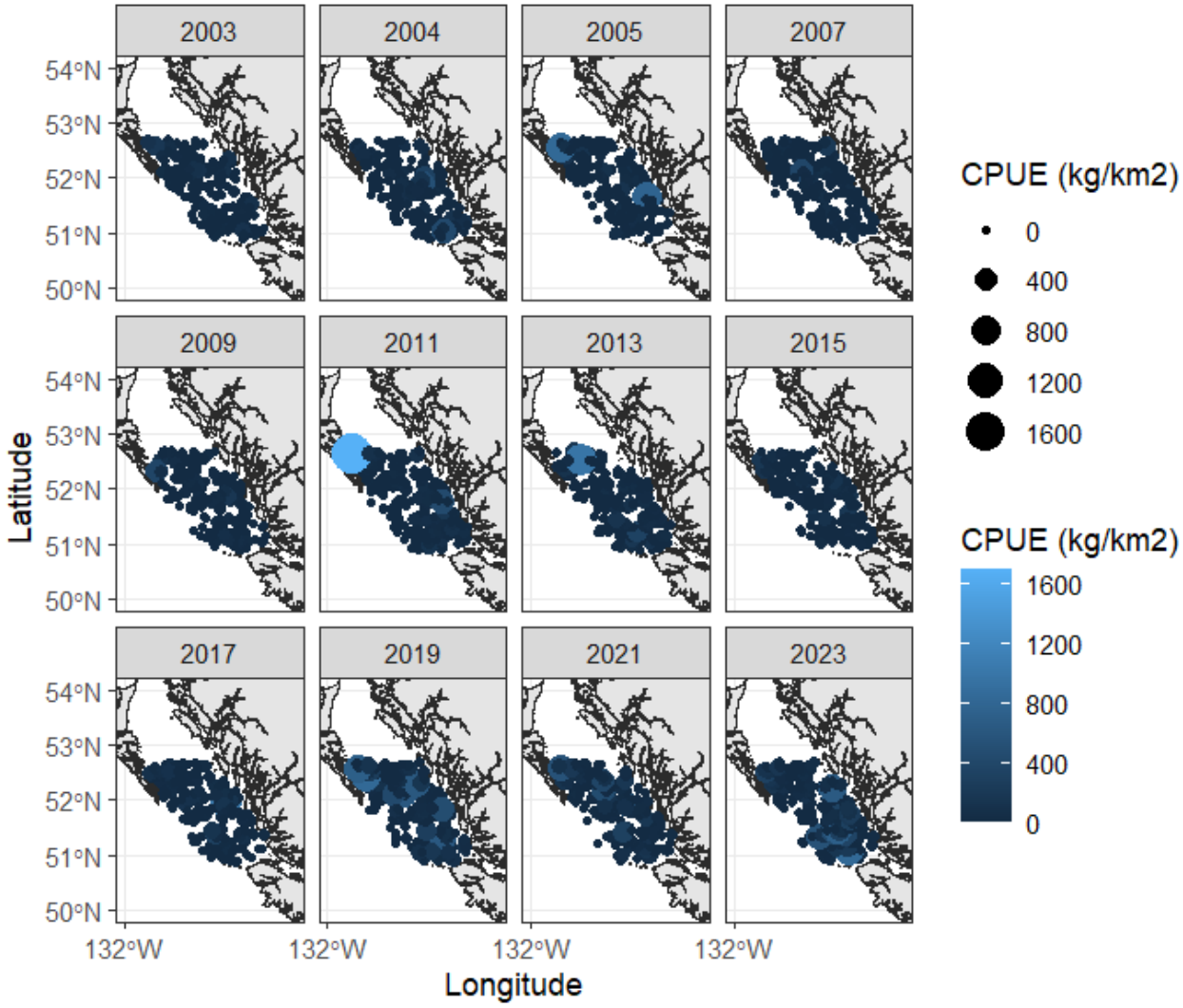


Figure D - 1. Survey data bubble plot for Queen Charlotte Sound Synoptic trawl survey. The area and colour of circles corresponds to the catch-per-unit-effort (CPUE) for a given set in each year.

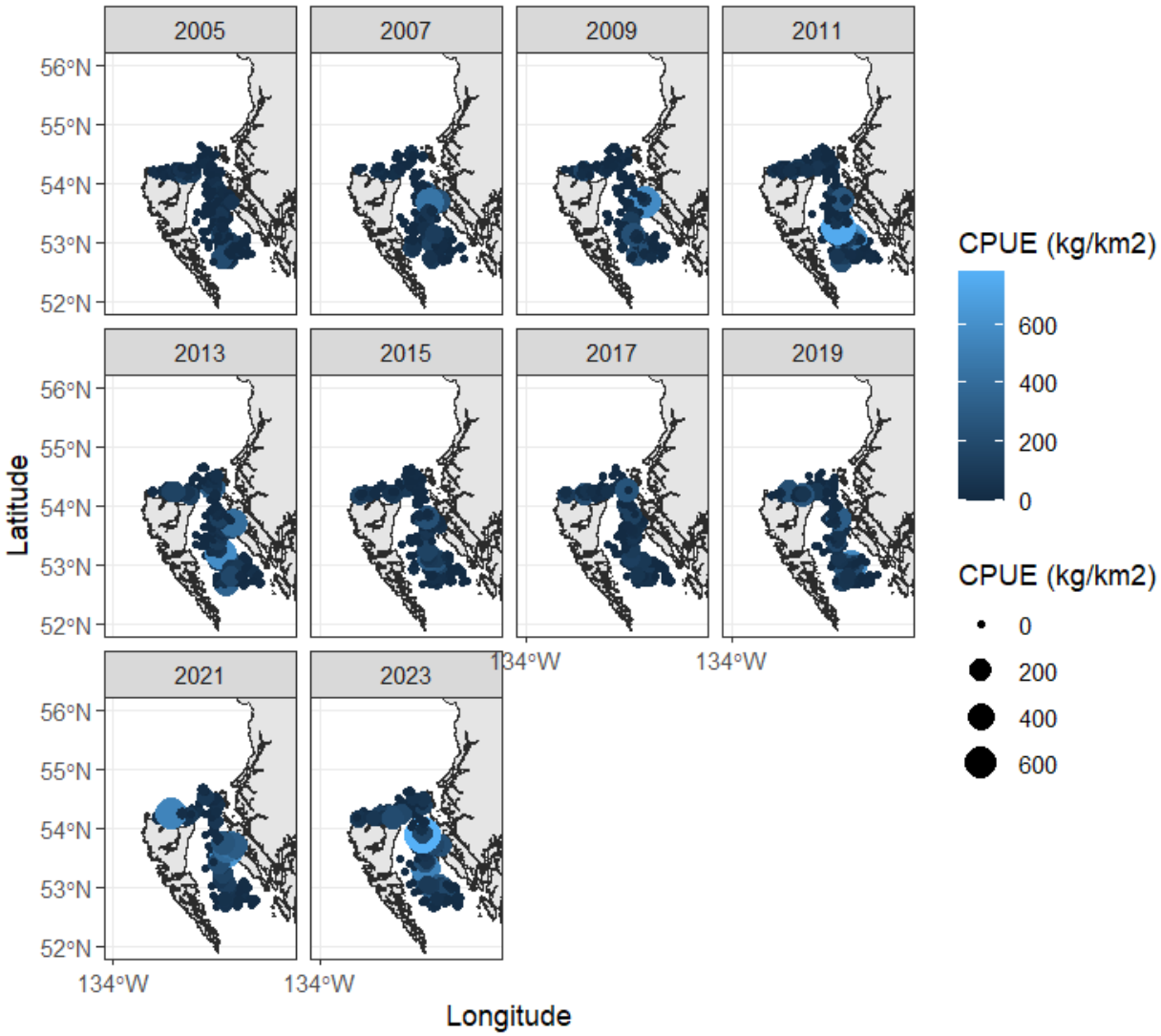


Figure D - 2. Survey data bubble plot for Hecate Strait Synoptic trawl survey. The area and colour of circles corresponds to the catch-per-unit-effort (CPUE) for a given set in each year.

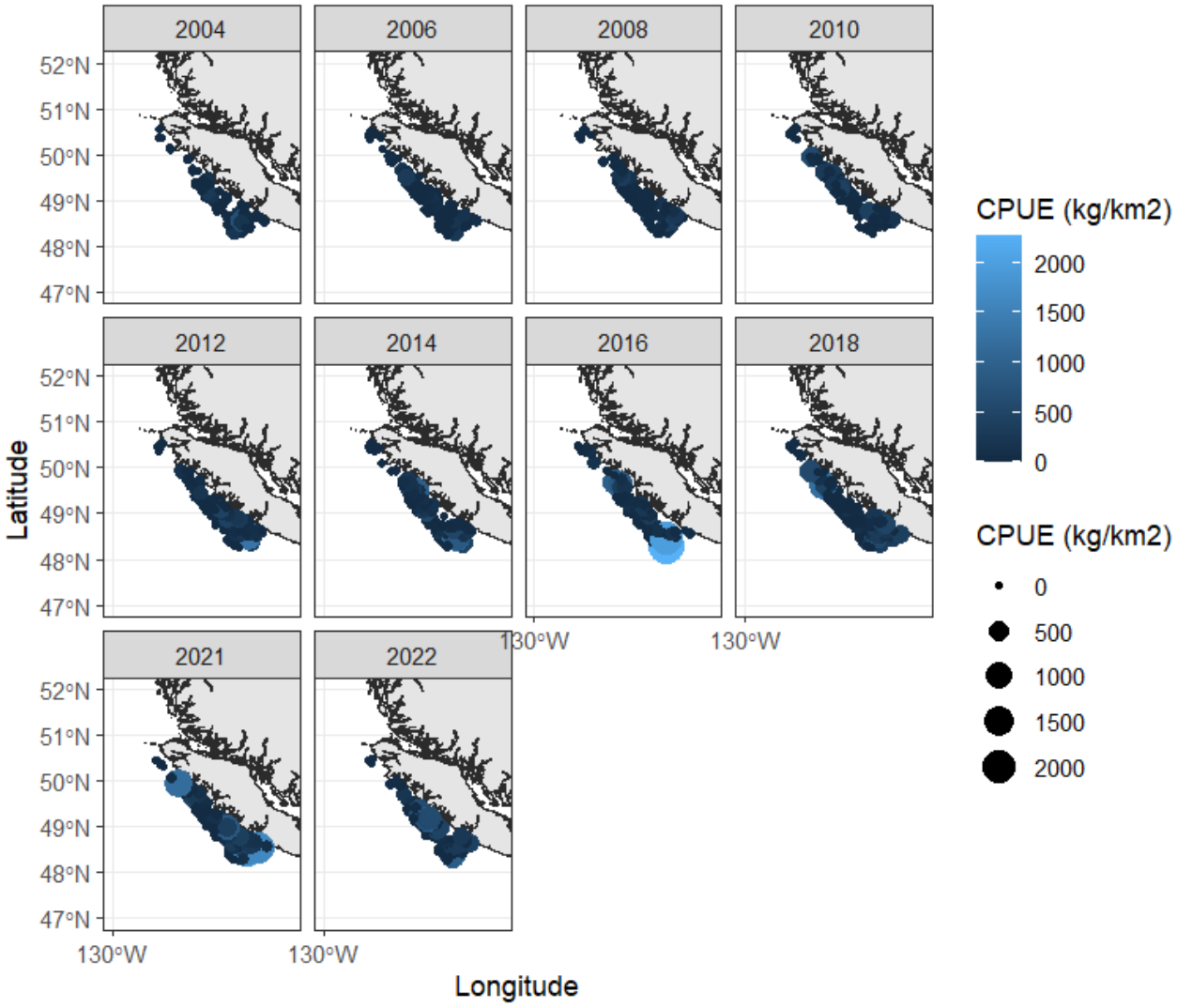


Figure D - 3. Survey data bubble plot for the West Coast Vancouver Island Synoptic trawl survey. The area and colour of circles corresponds to the catch-per-unit-effort (CPUE) for a given set in each year.

D.1.2. Results

The delta-gamma model with depth was the best model for the QCS Synoptic Survey index. The delta-lognormal model with depth was the best model for the HS Synoptic Survey index. The Tweedie model with depth was the best model for the WCVI Synoptic Survey index. Both modelled and design-based survey indices for QCS and HS showed similar increasing trends over most years (Figures D – 4, D – 5, and D – 6 and Tables D – 1, D -2, and D – 3), while he modelled and design-based indices for the WCVI survey show more variable trends over the last decade (Figure D – 6). The CV for the modelled QCS survey index decreased over time (Table D – 1). The modelled indices for the surveys had lower CVs than the design-based indices (Figures D – 4, D – 5, and D– 6). Areas of high and low estimated biomass stayed roughly the same over time, with the high biomass areas increasing in biomass over time (Figures D – 7, D – 8, and D – 9).

Table D - 1. Estimated biomass index and CV for the Queen Charlotte Sound Synoptic Survey.

Year	Biomass Index	CV
2003	266.11	0.16
2004	291.45	0.16
2005	267.58	0.16
2007	193.83	0.13
2009	248.26	0.14
2011	394.99	0.12
2013	377.56	0.12
2015	301.48	0.14
2017	431.05	0.11
2019	851.88	0.10
2021	808.20	0.10
2023	896.80	0.09

Table D - 2. Estimated biomass index and CV for the Hecate Strait Synoptic Survey.

Year	Biomass Index	CV
2005	149.77	0.13
2007	212.68	0.17
2009	149.15	0.16
2011	361.77	0.14
2013	396.09	0.14
2015	280.49	0.15
2017	280.89	0.15
2019	275.87	0.14
2021	502.56	0.14
2023	579.86	0.13

Table D - 3. Estimated biomass index and CV for the West Coast Vancouver Island Synoptic Survey.

Year	Biomass Index	CV
2004	331.90	0.18
2006	299.86	0.13
2008	471.35	0.12
2010	537.19	0.12
2012	629.49	0.12
2014	1124.87	0.13
2016	1313.15	0.18
2018	745.11	0.11
2021	1596.63	0.10
2022	979.84	0.12

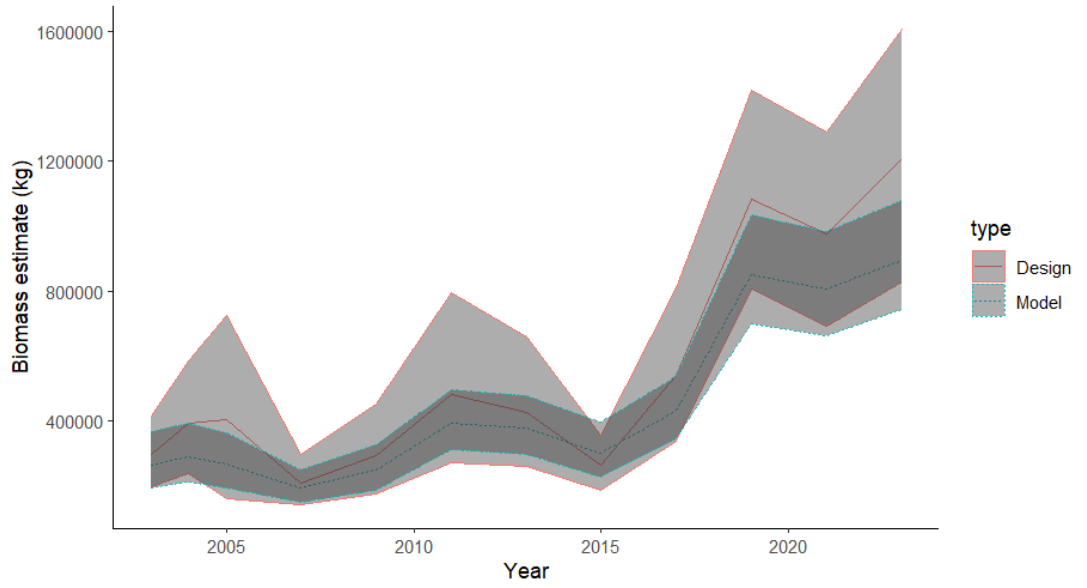


Figure D - 4. Modelled geostatistical index for Queen Charlotte Sound Synoptic trawl survey compared to the design-based index. Shaded portions represent 95% confidence intervals.



Figure D - 5. Modelled geostatistical index for Hecate Strait Synoptic trawl survey compared to the design-based index. Shaded portions represent 95% confidence intervals.

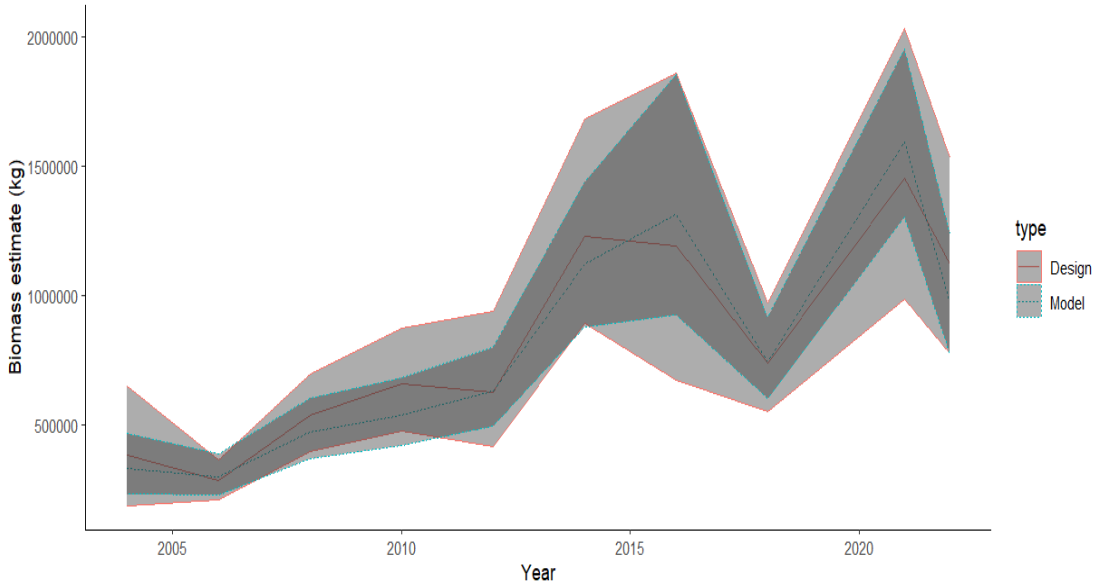


Figure D - 6. Modelled geostatistical index for West Coast Vancouver Island Synoptic trawl survey compared to the design-based index. Shaded portions represent 95% confidence intervals.

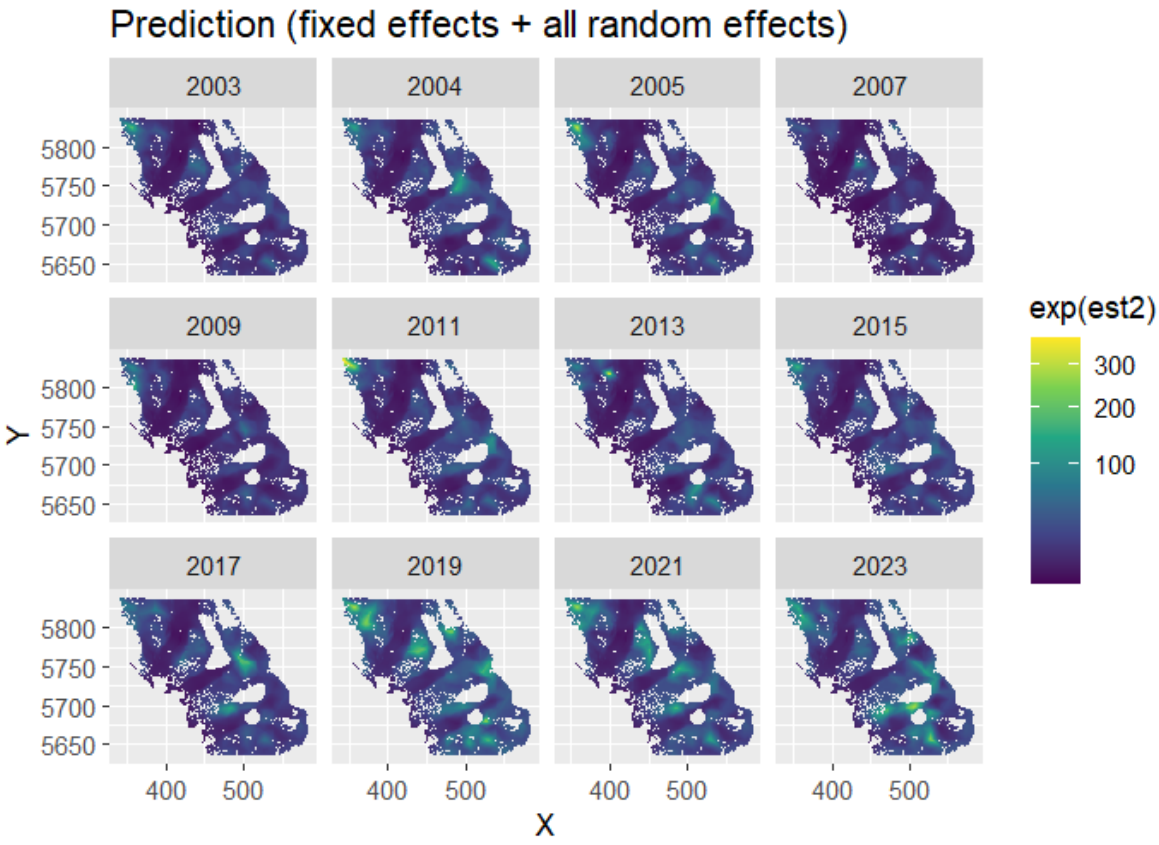


Figure D – 7. Predicted biomass (est2) across space from 2003 to 2023 using data from the Queen Charlotte Sound Synoptic Survey.

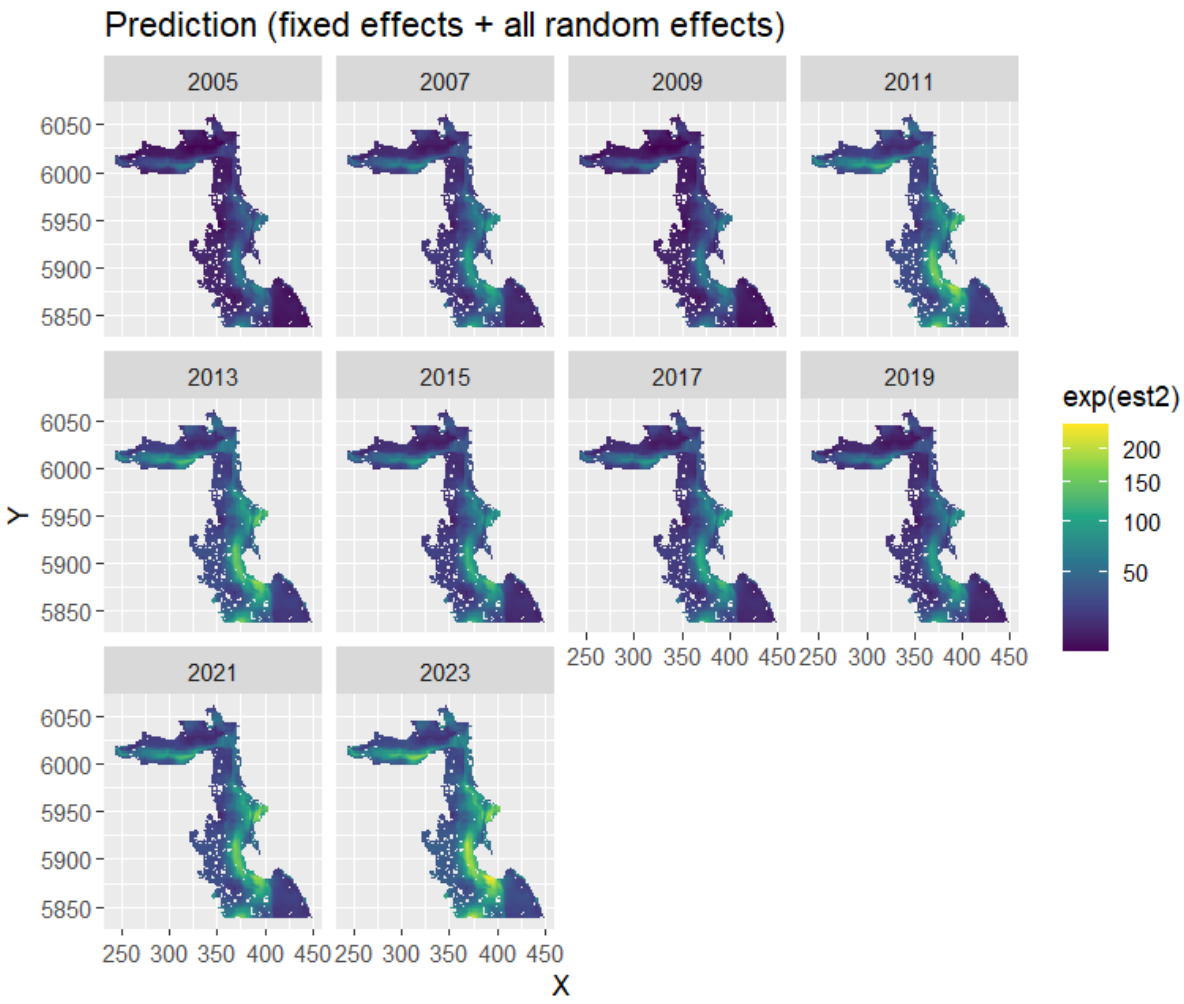


Figure D - 8. Predicted biomass (est2) across space from 2005 to 2023 using data from the Hecate Strait Synoptic Survey.

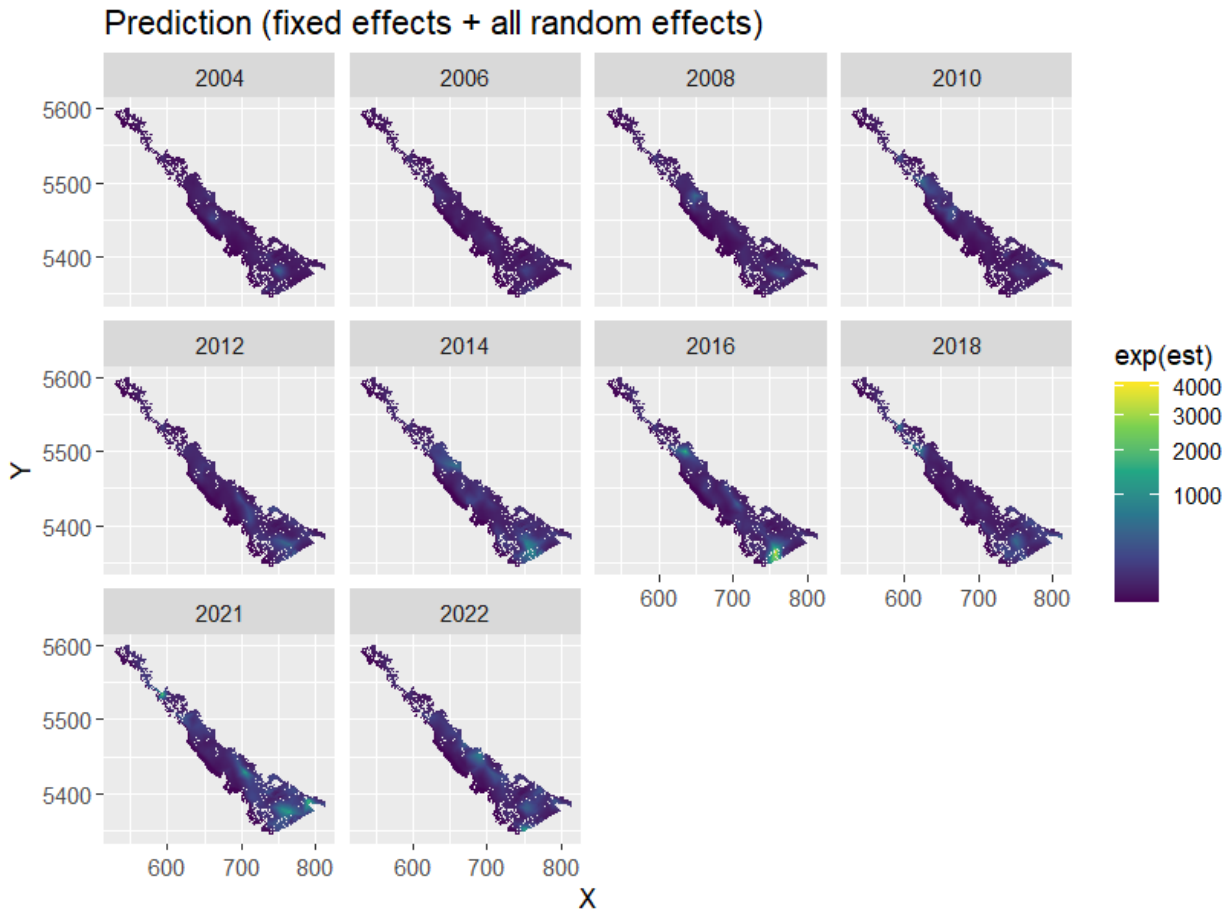


Figure D - 9. Predicted biomass (est2) across space from 2004 to 2022 using data from the West Coast Vancouver Island Synoptic Survey.

D.2. NOAA TRIENNIAL TRAWL SURVEY

The NOAA Triennial trawl survey (also called the NMFS trawl survey) covered the Vancouver region defined by the INFPC (International Convention for the High Seas Fisheries of the North Pacific Ocean), which included waters in both the Canada and the US. The survey operated in Canada for seven years between 1980 and 2001, with tows occurring along the southern portion of Vancouver Island in DFO Groundfish Areas 3C and the southern part of 3D. A design-based biomass index for the Canadian portion of the survey was developed for Petrale Sole by Starr and Fargo (2004), and applied to the subsequent 2006 assessment (Starr 2009). Their analysis was confined to strata that that covered depth ranges between 55 and 366 m that had been consistently fished over the seven years. Detailed description of the methods and results used to develop the index are presented in Starr and Fargo (2004). The index values used in the current assessment (Table D - 4) were provided by P. Starr (pers. Comm, Canadian Groundfish and Research Conservation Society).

Table D - 4. Biomass index and CV for the NOAA Triennial Trawl Survey (only considering Canadian tows; provided by P. Starr, Canadian Groundfish and Research Conservation Society).

Year	Biomass Index	CV
1980	392	0.315
1983	536	0.330
1989	976	0.202
1992	362	0.193
1995	689	0.223
1998	579	0.234
2001	820	0.281

LITERATURE CITED

Anderson, S.C., Keppel, E.A., and Edwards, A.M. 2019. A reproducible data synopsis for over 100 species of British Columbia groundfsh. DFO Can. Sci. Advis. Sec. Res. Doc. 2019/041. vii + 321 p.

Anderson, S.C., Ward, E.J., English, P.A., Barnett, L.A., and Thorson, J.T. 2024. sdmTMB: an R package for fast, flexible, and user-friendly generalized linear mixed effects models with spatial and spatiotemporal random fields. BioRxiv, 2022.03.24.485545.

Kristensen K., Nielsen A., Berg C.W., Skaug H., and Bell B.M. 2016. TMB: automatic differentiation and laplace approximation. Journal of Statistical Software, 70, 1–21.

Lindgren, F., Rue, H., and Lindstrom, J. 2011. An explicit link between Gaussian fields and Gaussian Markov random fields: The stochastic partial differential equation approach. Journal of the Royal Statistical Society: Series B (Statistical Methodology). 73(4), 423–498.

Starr, P.J. 2009. Petrale Sole (*Eopsetta jordani*) in British Columbia, Canada: Stock Assessment for 2006/07 and Advice to Managers for 2007/08. DFO Can. Sci. Advis. Sec. Res. Doc. 2009/070. v + 134 p.

Starr, P.J., and Fargo, J. 2004. Petrale sole stock assessment for 2003 and recommendations for management in 2004. DFO. Can. Sci. Advis. Sec. Res. Doc. 2004/036. ii + 86 p.

APPENDIX E. STOCK SYNTHESIS MODEL STRUCTURE

Stock Synthesis (SS; Methot and Wetzel 2013; Stock Synthesis (SS3) Website) was used to estimate parameters in the model, stock size, and reference points for Petrale Sole in DFO combined areas 3CD5ABCDE. SS is an age-structured population dynamics model framework that can use a wide range of data sources, including length data. SS has been used for many other stock assessments in the region (Edwards et al. 2022; Starr and Haigh 2023; DFO 2024b, to name a few). SS is also commonly used in the U.S. West Coast, Europe, Australia, and for international stocks.

The model for Petrale Sole was two-sex, assumed one aggregated fleet, and used both age and length data. Model structure was selected to balance realism and parsimony. Given the availability and magnitude of historical catch data, the first year of the assessment was in 1938, which is the first year of recorded catches for Petrale Sole. As a result, the stock was assumed to be beginning at an unfished state in 1938.

A von Bertalanffy growth model was assumed, and maturity was age logistic. Fecundity-at-age was assumed to be proportional to weight-at-age and spawning stock biomass was assumed to be made up of only females. Growth and maturity-at-age parameters were fixed, constant over time, and determined via the methods described in Appendices B.1, B.2, & B.3. Annual recruitment was treated as stochastic and estimated as annual lognormal deviations from mean recruitment, where mean recruitment is calculated from the Beverton-Holt stock recruitment curve. Fraction female at the time of recruitment was assumed to be 0.5. The standard deviation of the natural log of recruitment deviations was fixed at 0.636, which was the recruitment SD estimated for flatfish in Thorson et al. (2014). Thorson et al. (2014) developed a hierarchical model explaining recruitment variability, which was applied to data from 154 fish populations.

Selectivity-at-age was assumed to be asymptotic (forced from a double normal parameterization) and time invariant for the fishery and surveys. Male selectivity parameters were offset from female selectivity parameters. For the fishery and each of the surveys, the selectivity peak (beginning age for the plateau), selectivity ascending width, and male offset for the selectivity peak were estimated. Multinomial likelihoods were used to fit age compositions. Dirichlet-multinomial error was considered but resulted in negligible down weighting. As a result, multinomial likelihoods were used for the base model with input sample sizes determined from bootstrapping, and Dirichlet-multinomial error is presented as a sensitivity.

Fishing mortality was calculated using a hybrid method that uses Pope's approximation for initial values that are iteratively adjusted by Baranov continuous fishing mortality values to closely approximate the observed catch. A maximum fishing mortality of 4 was assumed. An analytical solution was used for catchability. In the analytical solution, the units of CPUE are treated as dimensionless so that catchability is adjusted within each model iteration to maintain a mean difference of zero between observed and expected vulnerable biomass across all years. This reduced the number of parameters to estimate and is commonly used in stock assessments that use Stock Synthesis. For each of the indices, a parameter was estimated as an additional SD that was added to the input standard deviation of the index variability (from the standardization procedure).

An informative prior was applied to steepness and broad uninformative priors were applied to Ln(R0) and selectivity parameters to aid in model stability. An even more uninformative prior on Ln(R0) was used for the highM scenario than the baseM and lowM scenarios, which resulted in better Markov Chain Monte Carlo (MCMC) diagnostics. Ln(R0) is estimated to inform the magnitude of the initial stock size. The steepness prior was based on the Rock Sole steepness prior (Holt et al. 2016) and assumed a beta distribution with a mean of 0.85 and a CV of 10%.

Steepness is defined as the proportion of the unfished recruitment produced when female spawning stock biomass is 20% of B0 (Francis 1992).

The base model used an ensemble approach, where the posteriors from three models are combined due to uncertainty in natural mortality (M). The differences in the models is the M assumption, where one model assumed female and male Ms of 0.124 (low), another model assumed Ms of 0.154 (middle), and another model assumed Ms of 0.184 (high). The medium level of 0.154 for M was based on maximum age (Hamel and Cope 2022).

Several large ages (>26) were observed for both females and males, suggesting that M may not be that different between sexes.

The total number of parameters estimated was 99. Parameters for R0, steepness, extra standard deviations for the survey indices, selectivity, and recruitment deviations were estimated in the ensemble base model. Recruitment deviations were estimated with a sum-to-zero constraint. Main recruitment deviations began in 1986, as this is the earliest that age composition data could inform recruitment deviations, and ended in 2019, which was the last year of age composition data. Early recruitment deviations began in 1938. Minimum and maximum values for recruitment deviations were -5 and 5, respectively. SS3 files are available at Zenodo.

Table E - 1. Petrale Sole stock assessment model specifications.

Model Specification	**Base Model**
Starting year	1938
Gender	2
Ages	1-22 ages
Fishing mortality method	Hybrid
Maximum F	4
Catchability	Analytical estimate
Selectivity	Double normal but fixed at asymptotic

Table E - 2. List of fixed parameters in the assessment model.

Parameter	Value
Female natural mortality	0.154
Female length at minimum age	16.43
Female asymptotic length in von-Bertalanffy growth equation (cm)	55.16
Female growth coefficient (K) in the von-Bertalanffy growth equation	0.16
Female variability in size at age 1	0.19
Female variability in size at ages 22+	0.08
Coefficient to convert length in cm to weight in kg for females	4.96e-6
Exponent to convert length to weight for females	3.24
Maturity logistic inflection where female maturity-at-age is a logistic function	5.70
Logistic slope for female maturity-at-age	-0.77
a parameter in fecundity relationship (fecundity = wt $*$ (a + b $*$ wt))	1
b parameter in fecundity relationship (fecundity = wt $*$ (a + b $*$ wt))	0
Male natural mortality	0.154
Male length at minimum age	16.45
Male asymptotic length in von-Bertalanffy growth equation (cm)	43.47
Male growth coefficient (K) in the von-Bertalanffy growth equation	0.23
Male variability in size at age 1	0.14
Male variability in size at ages 22+	0.05
Coefficient to convert length in cm to weight in kg for males	6.94e-6
Exponent to convert length to weight for males	3.13
Fraction female at the time of recruitment	0.5
Standard deviation of natural log recruitment	0.636
Autocorrelation in recruitment	0
Fishery selectivity top (width of plateau)	0
Fishery selectivity descending width	200
Fishery selectivity at first bin	-999
Fishery selectivity at last bin	-999
Male offset for fishery selectivity top	0
Male offset for fishery ascending width	0
Male offset for fishery descending width	0
Male apical fishery selectivity	1
QCS survey selectivity top (width of plateau)	0
QCS survey selectivity descending width	200

Parameter	Value
QCS survey selectivity at first bin	-999
QCS survey selectivity at last bin	-999
Male offset for QCS survey selectivity top	0
Male offset for QCS survey ascending width	0
Male offset for QCS survey descending width	0
Male apical QCS survey selectivity	1
HS survey selectivity top (width of plateau)	0
HS survey selectivity descending width	200
HS survey selectivity at first bin	-999
HS survey selectivity at last bin	-999
Male offset for HS survey selectivity top	0
Male offset for HS survey ascending width	0
Male offset for HS survey descending width	0
Male apical HS survey selectivity	1
WCVI survey selectivity top (width of plateau)	0
WCVI survey selectivity descending width	200
WCVI survey selectivity at first bin	-999
WCVI survey selectivity at last bin	-999
Male offset for WCVI survey selectivity top	0
Male offset for WCVI survey ascending width	0
Male offset for WCVI survey descending width	0
Male apical WCVI survey selectivity	1

Table E - 3. List of phases, bounds, and priors for estimated parameters in the assessment model. Estimated values are available in the main text in Section 3.1.1.

Parameter	Phase	Bounds	Prior (Exp. Val, SD)
Log of virgin recruitment level	1	(7,15)	baseM and lowM: Normal(11,6) highM: Normal(11,10)
Steepness	5	(0.2,1)	Beta(0.85,0.1)
Extra standard error for QCS survey index	4	(0,0.4)	None
Extra standard error for HS survey index	4	(0,0.4)	None
WCVI survey index	4	(0,0.4)	None
Fishery selectivity peak (beginning age for the plateau)	3	(2,17)	Normal(9,2)
Fishery selectivity ascending width	3	(-10,10)	Normal(2.8,3)
Male offset for fishery selectivity peak	3	(-5,5)	Normal(0,3)
QCS survey selectivity peak (beginning age for the plateau)	3	(2,17)	Normal(8,2)
QCS survey selectivity ascending width	3	(-10,10)	Normal(3.9,3)
Male offset for QCS survey selectivity peak	3	(-5,5)	Normal(0,3)
HS survey selectivity peak (beginning age for the plateau)	3	(2,17)	Normal(4,2)
HS survey selectivity ascending width	3	(-10,10)	Normal(2.8,3)
Male offset for HS survey selectivity peak	3	(-5,5)	Normal(0,3)
WCVI survey selectivity peak (beginning age for the plateau)	3	(2,17)	Normal(6,2)
WCVI survey selectivity ascending width	3	(-10,10)	Normal(3.7,3)
Male offset for WCVI survey selectivity peak	3	(-5,5)	Normal(0,3)

LITERATURE CITED

DFO. 2024. Pacific Ocean Perch (*Sebastes alutus*) Stock Assessment for British Columbia in 2023. DFO Can. Sci. Advis. Sec. Sci. Advis. Rep. 2024/012.

Edwards, A.M., Berger, A.M., Grandin, C.J. and Johnson, K.F. 2022. Status of the Pacifc Hake (whiting) stock in U.S. and Canadian waters in 2022. Prepared by the Joint Technical Committee of the U.S. and Canada Pacifc Hake/Whiting Agreement, National Marine Fisheries Service and Fisheries and Oceans Canada. 238 p.

Francis, R. I. C. 1992. Use of risk analysis to assess fishery management strategies: a case study using orange roughy (*Hoplostethus atlanticus*) on the Chatham Rise, New Zealand. Canadian Journal of Fisheries and Aquatic Sciences, 49(5), 922-930.

Hamel, O. S. and Cope, J. M. 2022. Development and considerations for application of a longevity-based prior for the natural mortality rate. Fisheries Research, 256, 106477.

Methot Jr, R.D. and Wetzel, C.R. 2013. Stock synthesis: a biological and statistical framework for fish stock assessment and fishery management. Fisheries Research, 142, 86-99.

Starr, P.J. and Haigh, R. 2023. Canary Rockfish (*Sebastes pinniger*) Stock Assessment for British Columbia in 2022. DFO Can. Sci. Advis. Sec. Res. Doc. 2023/070. vi + 293 p.

Thorson, J.T., Jensen, O. P. and Zipkin, E.F. 2014. How variable is recruitment for exploited marine fishes? A hierarchical model for testing life history theory. Canadian Journal of Fisheries and Aquatic Sciences, 71(7), 973-983.

APPENDIX F. MCMC DIAGNOSTICS

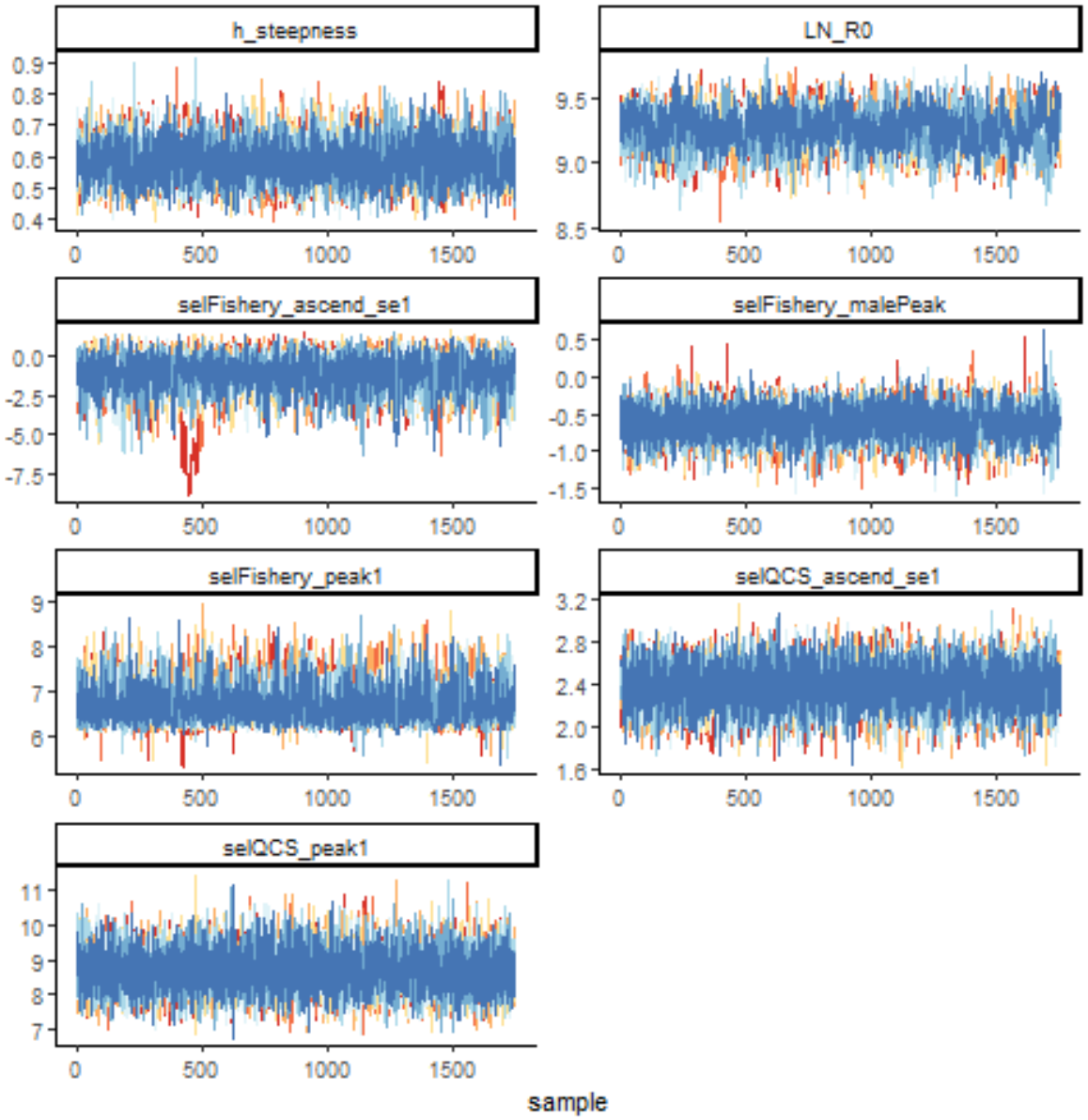


*Figure F - 1. MCMC traces for a first subset of estimated parameters from the **baseM** model with M = 0.154. Samples from each of the eight chains are shown with a different colour. Abbreviations: h_steepness = Beverton-Holt steepness parameter, LN_R0 = log of unfished recruitment, selFishery_peak1 = fishery selectivity peak, selFishery_ascend_se1 = ascending width for fishery selectivity, selFishery_malePeak = male offset for fishery selectivity peak, selQCS_peak1 = selectivity peak for the QCS synoptic survey, and selQCS_ascend_se1 = ascending width for QCS survey selectivity.*

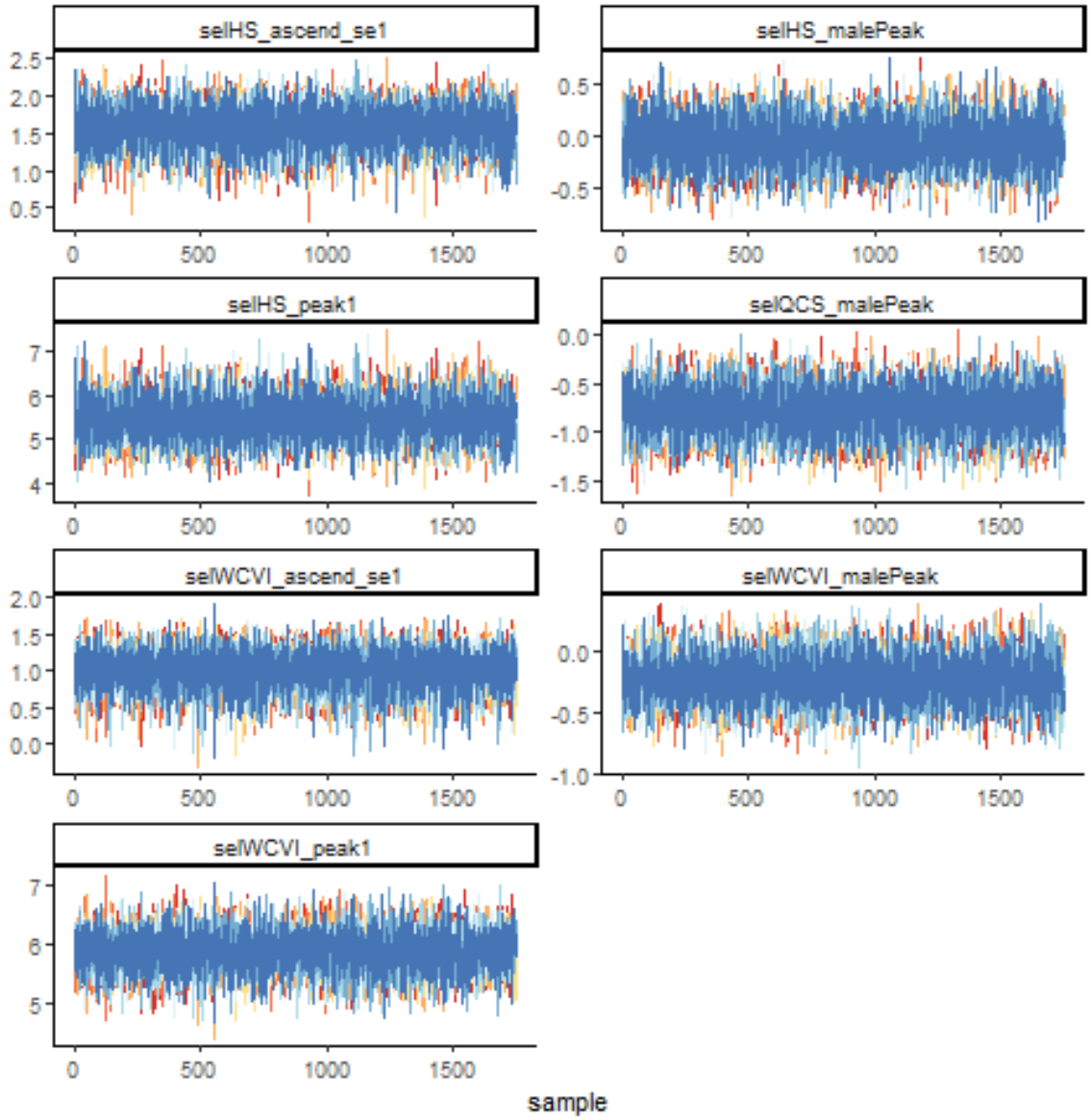


*Figure F - 2. MCMC traces for a second subset of estimated parameters from the **baseM** model with M = 0.154. Samples from each of the eight chains are shown with a different colour. Abbreviations: selHS_peak1 = selectivity peak for the HS synoptic survey, selHS_ascend_se1 = ascending width for HS survey selectivity, selHS_malePeak = male offset for HS survey selectivity peak, selWCVI_peak1 = selectivity peak for the WCVI synoptic survey, selWCVI_ascend_se1 = ascending width for WCVI survey selectivity, selWCVI_malePeak = male offset for WCVI survey selectivity peak.*

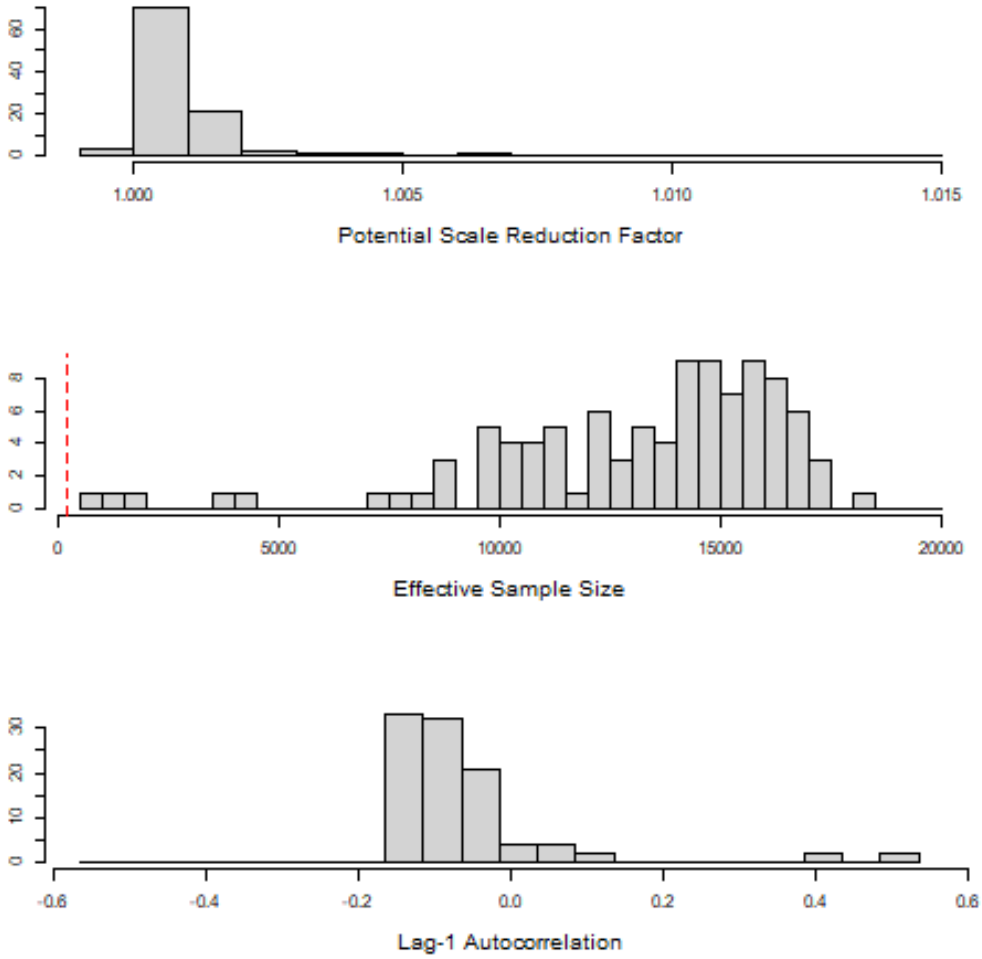


*Figure F - 3. Distributions of MCMC convergence diagnostics for all estimated parameters in the **baseM** model with M = 0.154. Diagnostics shown from top to bottom are: between chain relative standard error ($\hat{R}$), effective sample size, and within chain lag-1 autocorrelation. Red vertical lines show minimum threshold for $\hat{R}$ ($\hat{R}$ = 1.01) and effective sample size (400).*

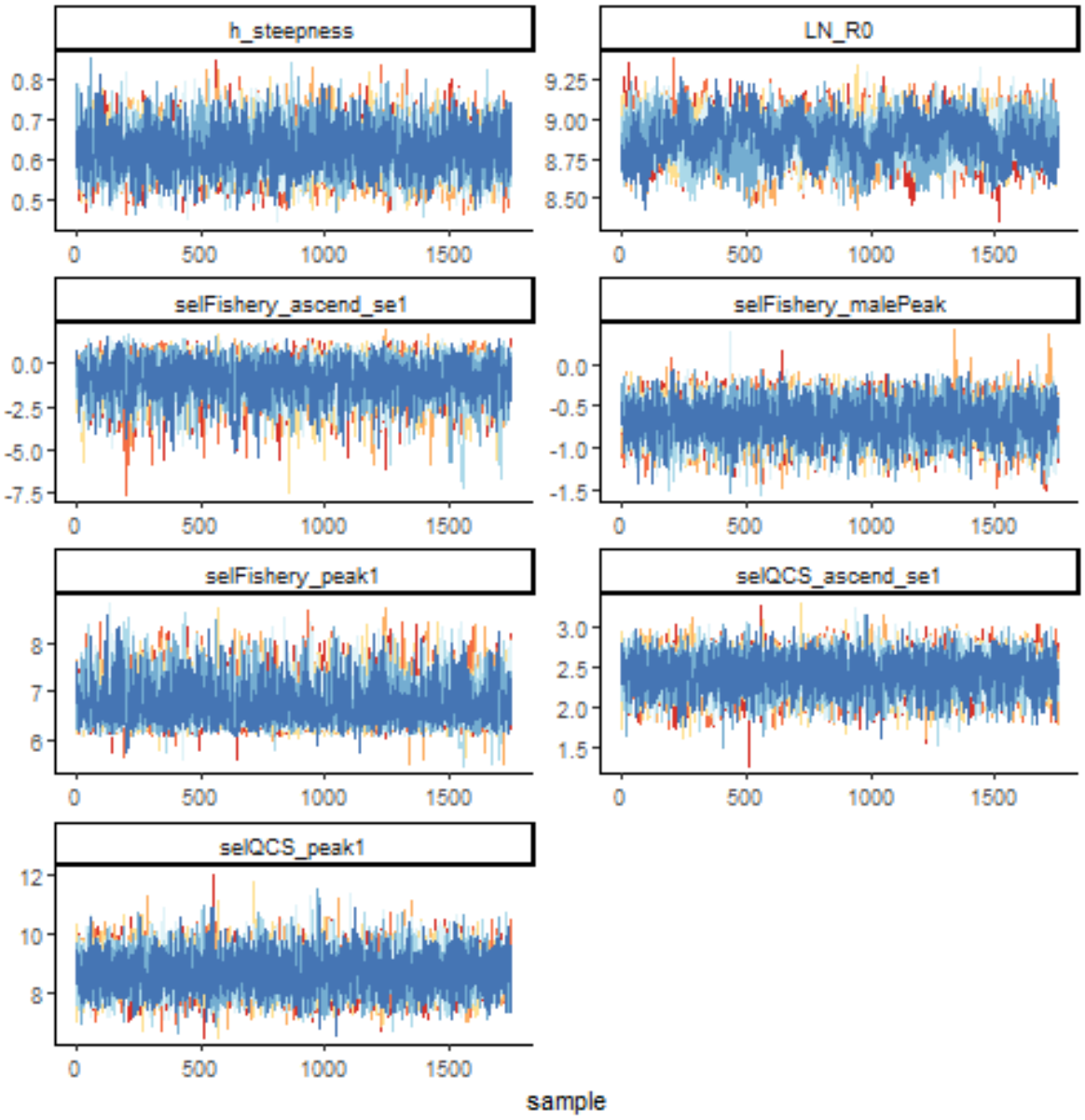


*Figure F - 4. MCMC traces for a first subset of estimated parameters from the **lowM** model with M = 0.124. Samples from each of the eight chains are shown with a different colour. See caption for Figure F – 2 for parameter abbreviations.*

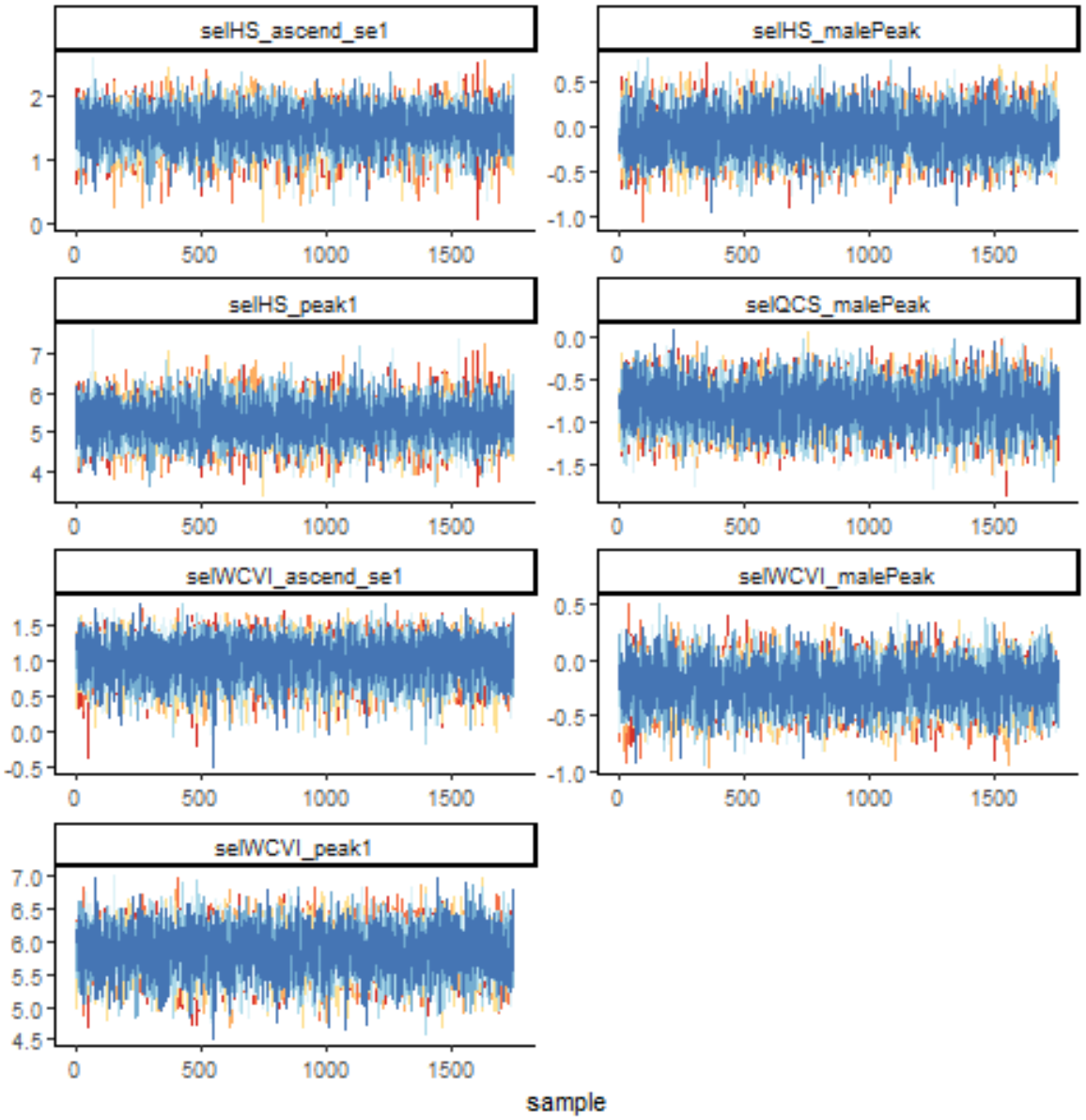


*Figure F - 5. MCMC traces for a second subset of estimated parameters from the **lowM** model with M = 0.124. Samples from each of the eight chains are shown with a different colour. See caption for Figure F - for parameter abbreviations.*

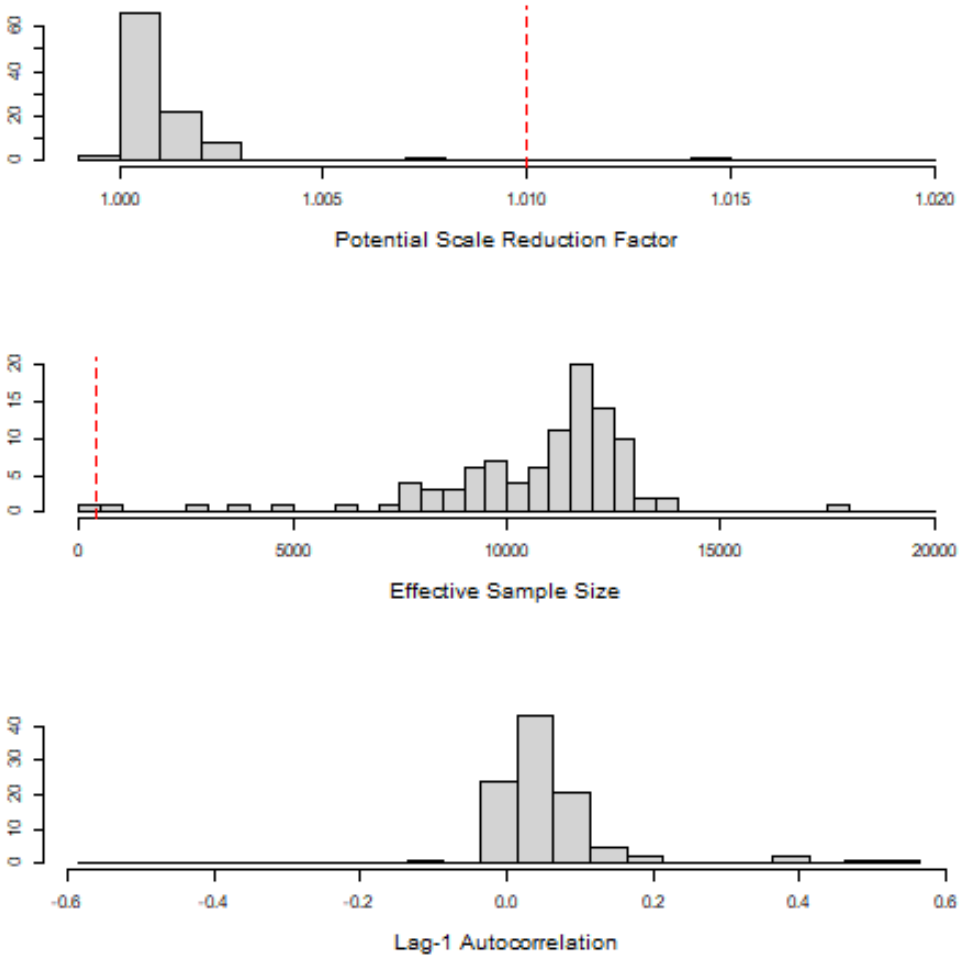


*Figure F - 6. Distributions of MCMC convergence diagnostics over all estimated parameters in the **lowM** model with M = 0.124. Diagnostics shown from top to bottom are: between chain relative standard error ($\hat{R}$), effective sample size, and within chain lag-1 autocorrelation. Red vertical lines show minimum threshold for $\hat{R}$ ($\hat{R}$ = 1.01) and effective sample size (400).*

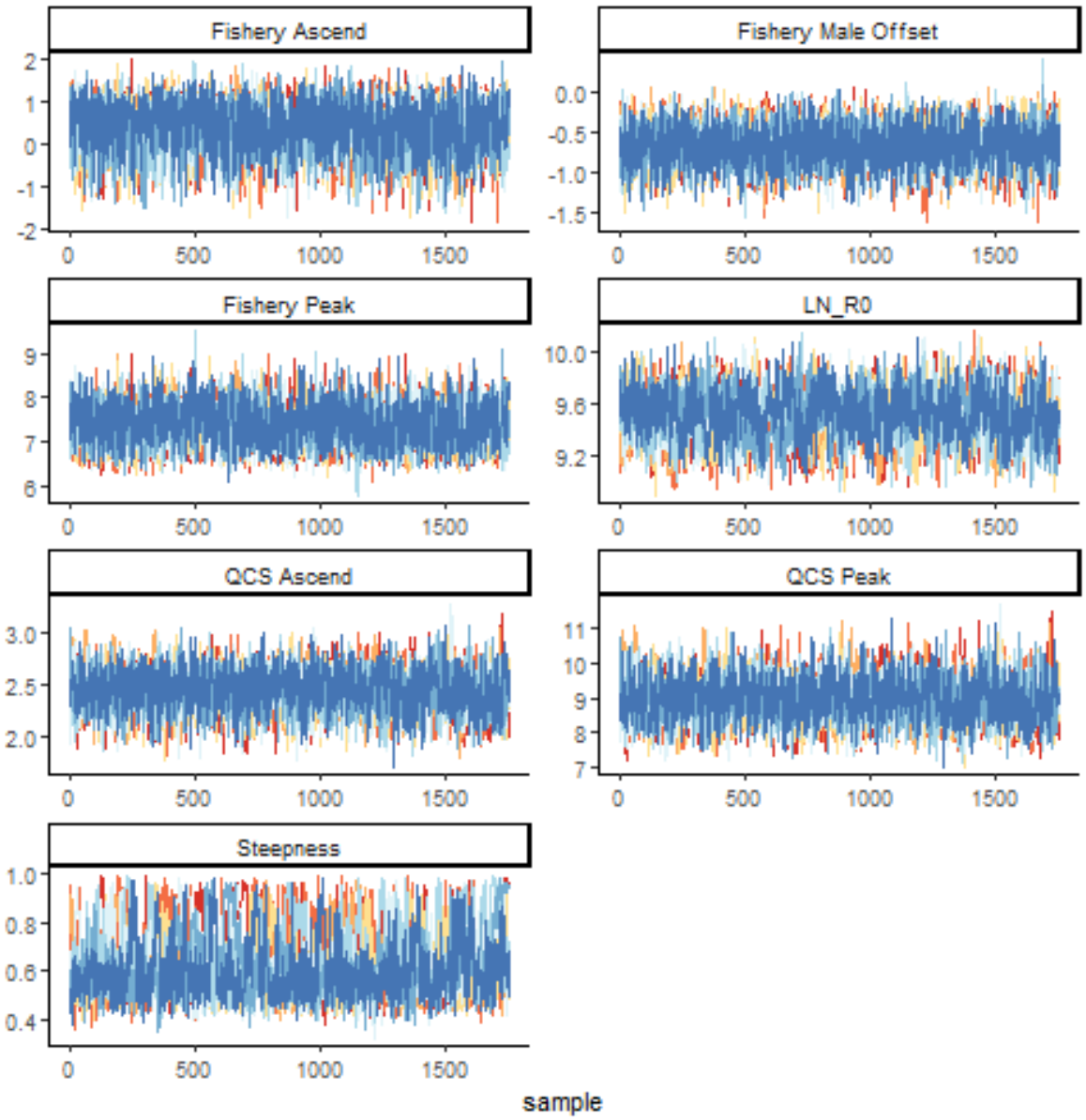


*Figure F - 7. MCMC traces for a first subset of estimated parameters from the **highM** model with M = 0.184. Samples from each of the eight chains are shown with a different colour. See caption for Figure F - 2 for parameter abbreviations.*

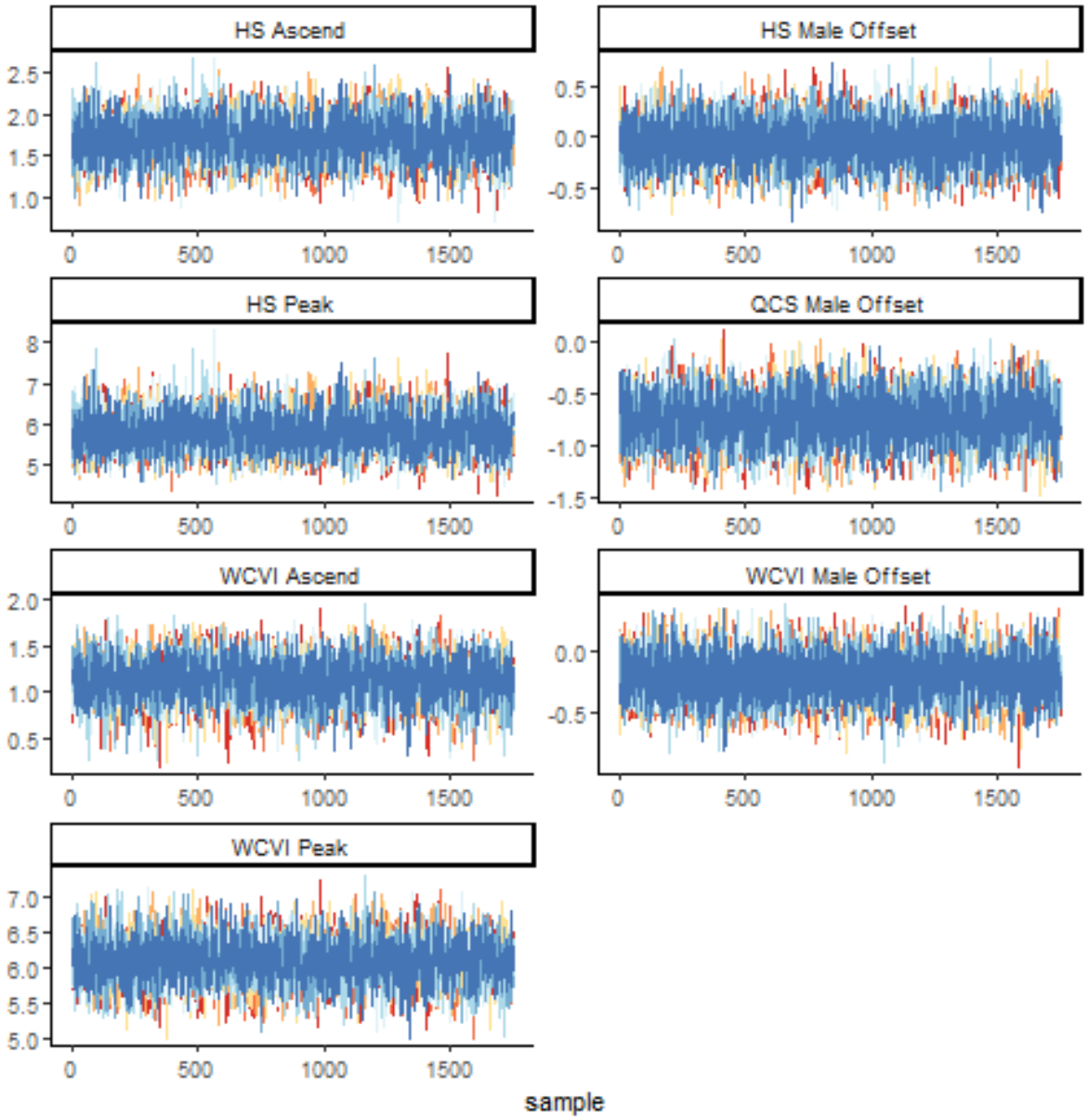


*Figure F - 8. MCMC traces for a second subset of estimated parameters from the **highM** model with M = 0.184. Samples from each of the eight chains are shown with a different colour. See caption for Figure F - for parameter abbreviations.*

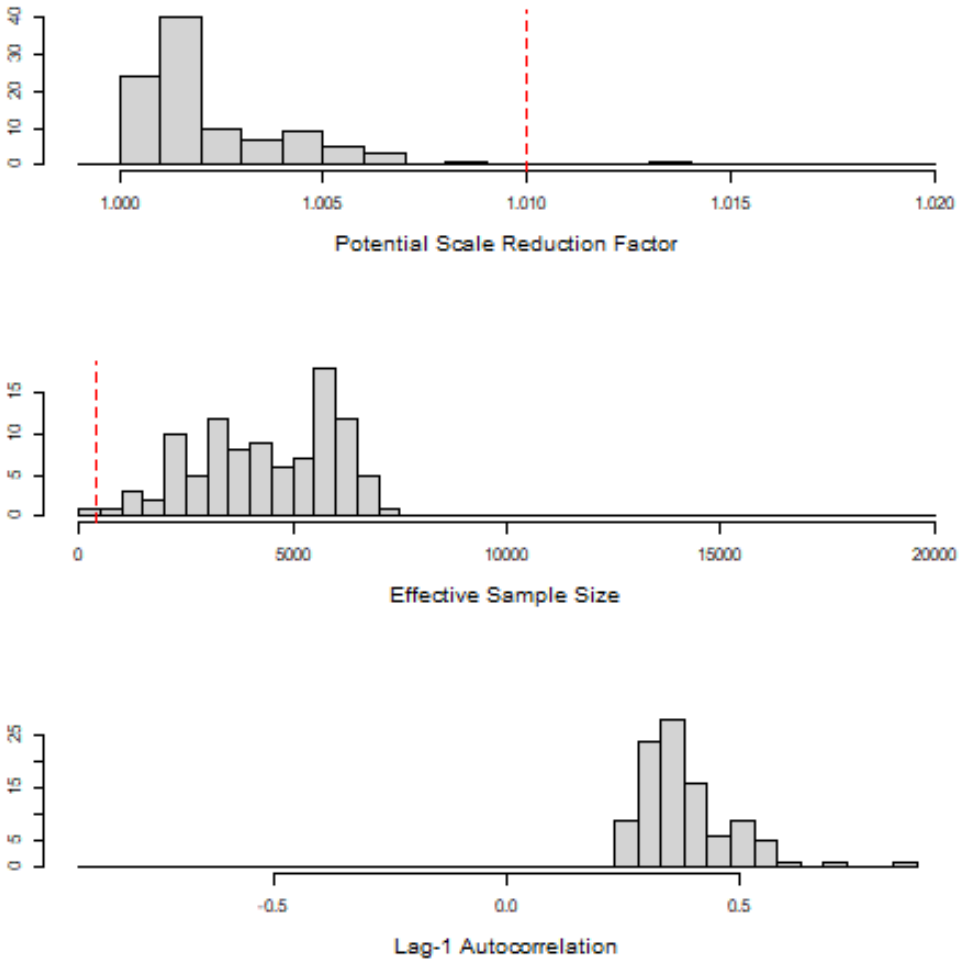


*Figure F - 9. Distributions of MCMC convergence diagnostics over all estimated parameters in the **highM** model with M = 0.184. Diagnostics shown from top to bottom are: between chain relative standard error ($\hat{R}$), effective sample size, and within chain lag-1 autocorrelation. Red vertical lines show minimum threshold for $\hat{R}$ ($\hat{R}$ = 1.01) and effective sample size (400).*

APPENDIX G. SENSITIVITY ANALYSIS WITH MLE OUTPUTS

Some sensitivity analyses did not result in acceptable Maximum Likelihood Estimation (MLE) or Markov Chain Monte Carlo (MCMC) diagnostics, so they are summarized in this appendix with MLE outputs (Table G - 1). These sensitivities were compared the MLE version of the baseM model from the base ensemble model.

One sensitivity explored estimating natural mortality (“Estimated M”), as M was a key uncertainty, which was fixed at three different levels in an ensemble model in this assessment. In this sensitivity, M had a prior based on maximum age (Hamel and Cope 2022).

Two other sensitivities explored variations in the fixed recruitment variability (“sigma R”) value (Higher Sigma R and Lower Sigma R), as the base ensemble model assumed a fixed sigma R of 0.636.

Another sensitivity explored Francis weighting on the age composition data (“With Francis Weighting”) as an alternative to the base model approach that utilized multinomial likelihoods with fixed input sample sizes as well as to the Dirichlet-multinomial likelihood scenario tested as an MCMC sensitivity scenario (where the latter resulted in negligible down weighting).

We also tested a sensitivity without extra standard deviations on variability for survey indices (“Without Extra Survey SDs”), which was in contrast to the base ensemble model that estimated an extra standard deviation for each survey index.

Another sensitivity explored using standardized fishery CPUE as an index (“With CPUE”). In the base ensemble model, there was no information aside from catch until 2003. In this sensitivity, fishery CPUE was included as a source of information in the earlier years until present (1954 to 2023). We also tested a sensitivity with a modern CPUE index only (With Modern CPUE Only; 1996 to 2023), as the historical fishery CPUE index was more uncertain and more variables were available to standardized the modern fishery CPUE index. Appendix C describes the fishery CPUE standardization in detail.

We also tested a sensitivity where the model could estimate dome-shaped selectivity for each of the surveys. This more flexible selectivity assumption was explored due to the residual patterns in age composition fits for the surveys.

Table G - 1. Sensitivity analyses that compared MLE output.

Scenario label	Description
BaseM	Assumed M = 0.154
Estimated M	Estimated M
Higher Sigma R	Assumed a recruitment variation (sigma R) of 0.836
Lower Sigma R	Assumed a recruitment variation (sigma R) of 0.436
With CPUE	With fishery CPUE indices (historical and modern)
With Francis Weighting	With Francis weighting on age compositions
With Modern CPUE Only	With the modern fishery CPUE index only
Without Extra Survey SDs	Without extra standard deviations on variability for survey indices
Dome-shaped Selectivity	With the flexibility to estimate dome-shaped selectivity for each of the surveys

While all of these sensitivities described here were not reliable since their model performance was unstable and MCMC diagnostics were poor, the Without Extra Survey SDs and Dome-shaped Selectivity sensitivities resulted in the highest female spawning stock biomass (B), recruitment, and B/B_{MSY} ratio, while the With Francis Weighting sensitivity resulted in the lowest B, recruitment, and B/B_{MSY} ratio (Figures G - 1, G - 2, and G - 4). Recruitment and B was more variable under the With CPUE sensitivity. Including CPUE also resulted in slightly lower recruitment in the most recent years. The With CPUE sensitivity resulted in the highest fishing mortality in earlier years, and the Without Extra Survey SDs and Dome-shaped Selectivity sensitivities resulted in the lowest fishing mortality, although they were similar to the majority of MLE sensitivities (Figure G - 3). The With Francis Weighting sensitivity results in the highest fishing mortality and F/F_{MSY} ratio in recent years (Figure G – 3 and G - 5). The With CPUE sensitivity resulted in the highest steepness at 0.78, and the With Francis Weighting resulted in the lowest steepness at 0.59 (Table G – 3). Table G – 2 shows negative log likelihoods for each of the MLE sensitivities that had converged models (Lower Sigma R and With Francis Weighting), but both of these models, aside from the Base, had poor model diagnostics, so the likelihoods should be interpreted with caution. The Estimated M, Higher Sigma R, With CPUE, With Modern CPUE Only, and Without Extra Survey SDs models did not converge and thus their negative log likelihoods are not reported.

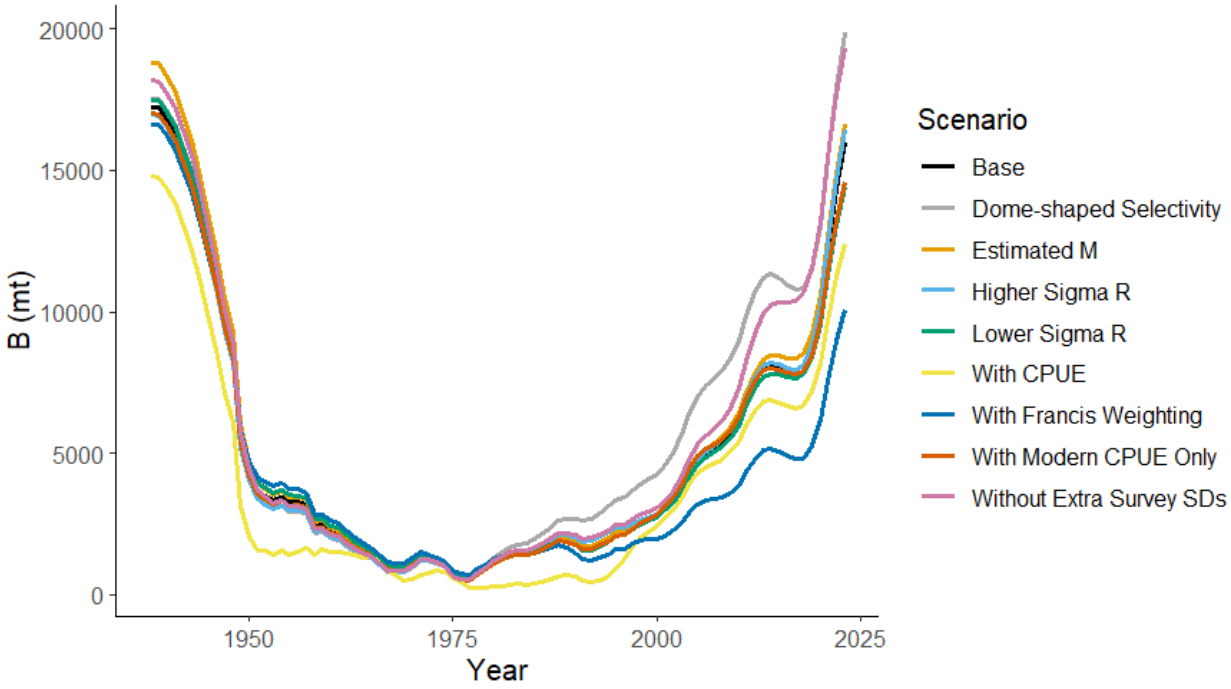


Figure G - 1. Estimated female spawning stock biomass from the model from the ensemble with natural mortality at 0.154 (baseM) and selected sensitives with maximum likelihood estimation.

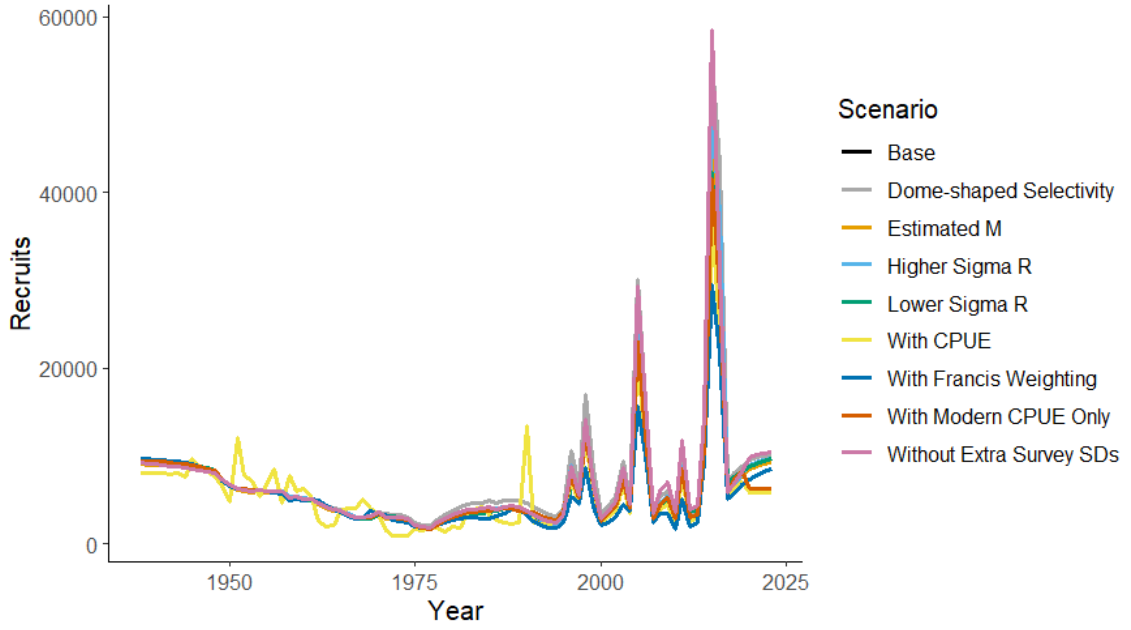


Figure G - 2. Estimated recruits from the model from the ensemble with natural mortality at 0.154 (baseM) and selected sensitives with maximum likelihood estimation.

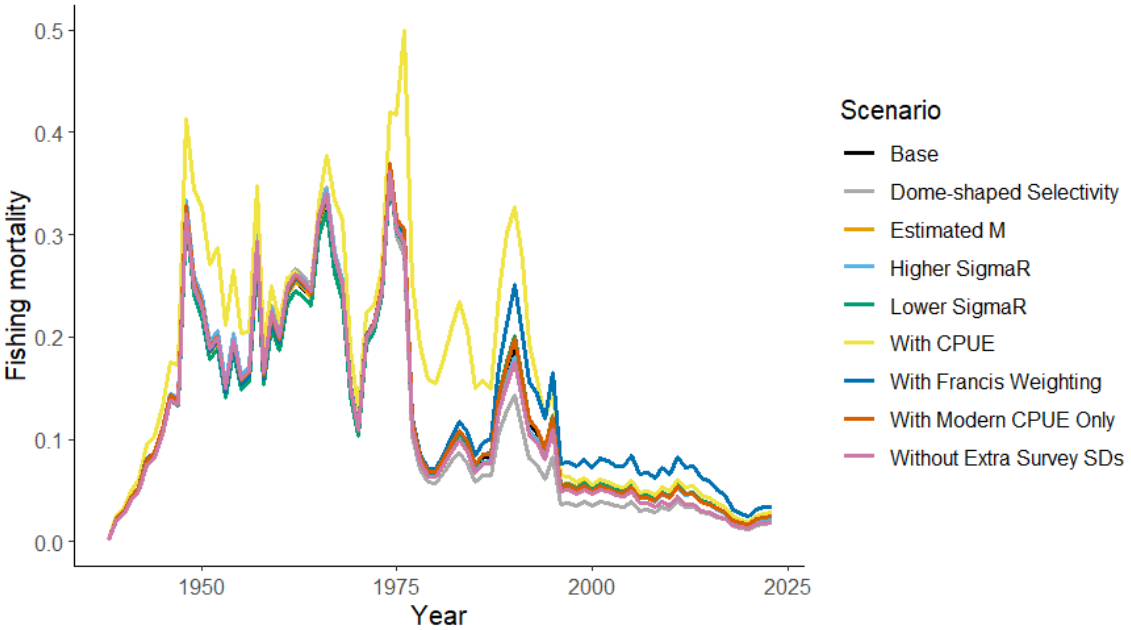


Figure G - 3. Estimated fishing mortality from the model from the ensemble with natural mortality at 0.154 (baseM) and selected sensitives with maximum likelihood estimation.

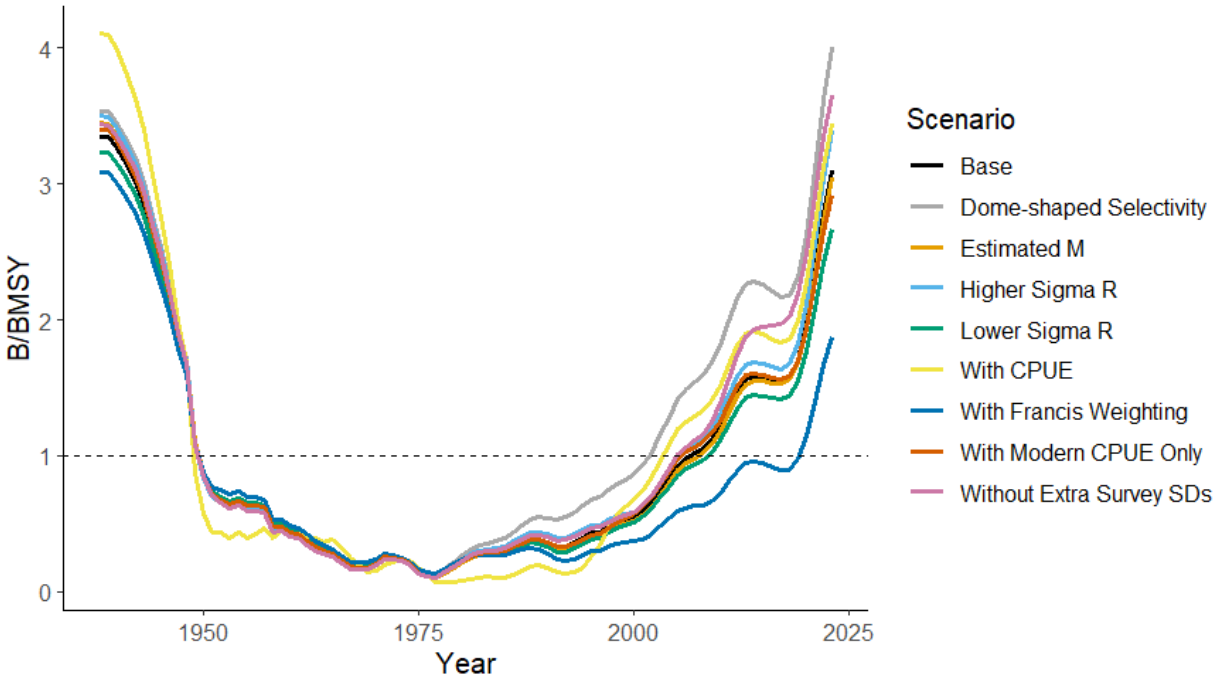


Figure G - 4. Estimated ratio of female spawning stock biomass to female spawning stock biomass at maximum sustainable yield (B/B_{MSY}) from the model from the ensemble with natural mortality at 0.154 (baseM) and selected sensitives with maximum likelihood estimation.

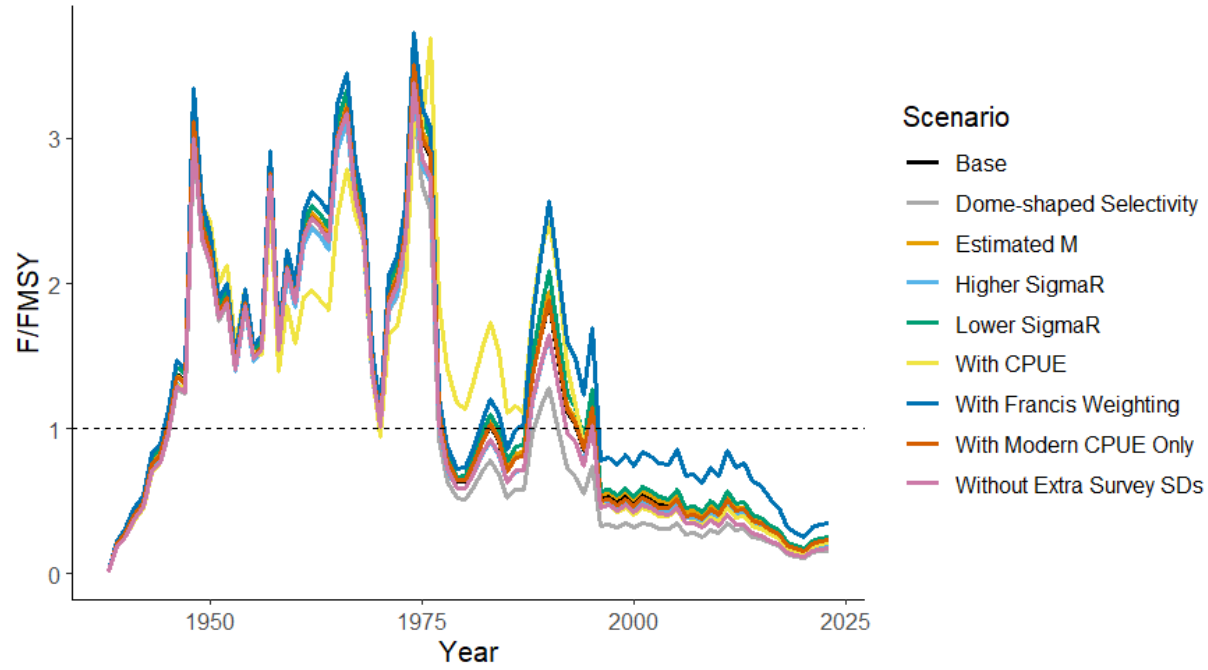


Figure G - 5. Estimated ratio of fishing mortality to fishing mortality at maximum sustainable yield (F/F_{MSY}) from the model from the ensemble with natural mortality at 0.154 (baseM) and selected sensitives with maximum likelihood estimation.

Table G - 2. Negative log likelihoods under the model from the ensemble with natural mortality at 0.154 (baseM) and selected sensitives with converged models with maximum likelihood estimation.

Likelihood	BaseM	Lower SigmaR	With Francis Weighting
Total	417.10	426.48	356.51
Catch	0.0043	0.0038	0.039
Survey	-25.63	-25.83	-24.83
Age compositions	429.16	435.76	369.65
Recruitment	9.20	11.86	7.33

Table G - 3. Estimated Ln(R0) and steepness parameters under the model from the ensemble with natural mortality at 0.154 (BaseM) and selected sensitives with maximum likelihood estimation.

Parameter	Base M	Estimated M	Higher Sigma R	Lower Sigma R	With CPUE	With Francis Weighting	With Modern CPUE Only	Without Extra Survey SDs	Dome-shaped Selectivity
Ln(R0)	9.19	9.15	9.18	9.21	9.04	9.16	9.18	9.24	9.21
Steepness	0.64	0.65	0.67	0.61	0.78	0.59	0.65	0.66	0.68

Table G – 4. Median estimated B_{MSY} and F_{MSY} from the model from the ensemble with natural mortality at 0.154 (BaseM) and selected sensitives with maximum likelihood estimation.

Reference Point	Base M	Estimated M	Higher Sigma R	Lower Sigma R	With CPUE	With Francis Weighting	With Modern CPUE Only	Without Extra Survey SDs	Dome-shaped Selectivity
B_{MSY}	5146	5457	4842	5408	3598	5387	4996	5284	4960
F_{MSY}	0.10	0.10	0.11	0.10	0.14	0.10	0.10	0.11	0.11

APPENDIX H. FITS TO LENGTH COMPOSITIONS FROM THE LENGTH AND CONDITIONAL-AGE-AT-LENGTH MODEL

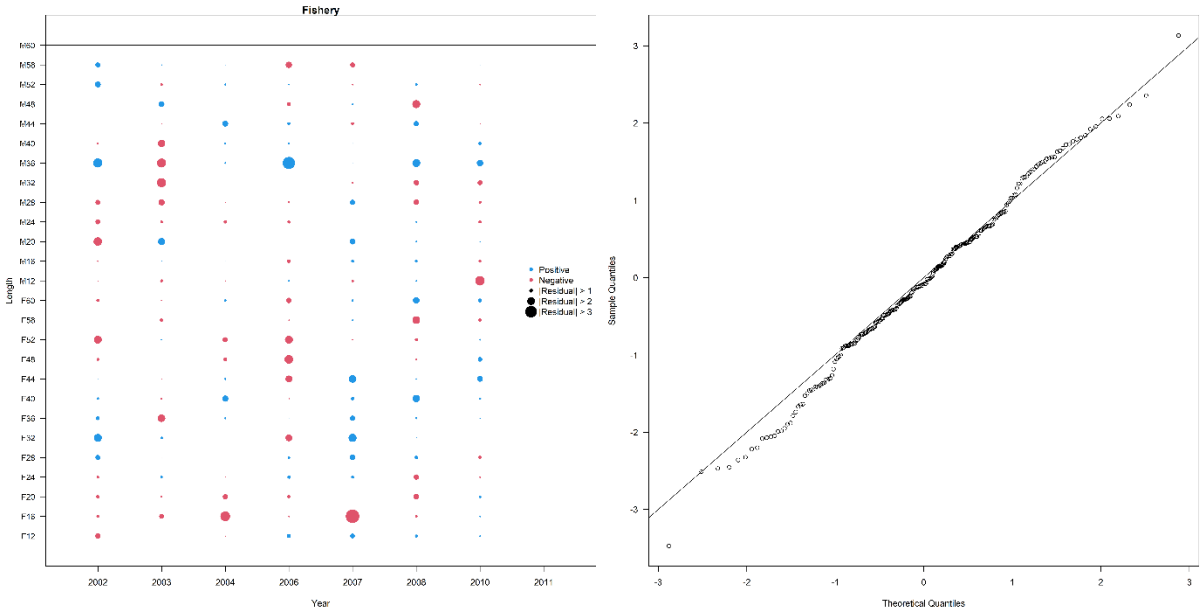


Figure H - 1. One-Step-Ahead (OSA) residuals for fits to the fishery length composition data for the length+CAAL assessment model. Depicted are the residuals at the medians of the posterior distribution. The length bins are labeled F12-F60 for females and M12-M60 for males. OSA residuals are calculated for the number of bins – 1, thus the final bin "M60" does not contain OSA residuals in this case.

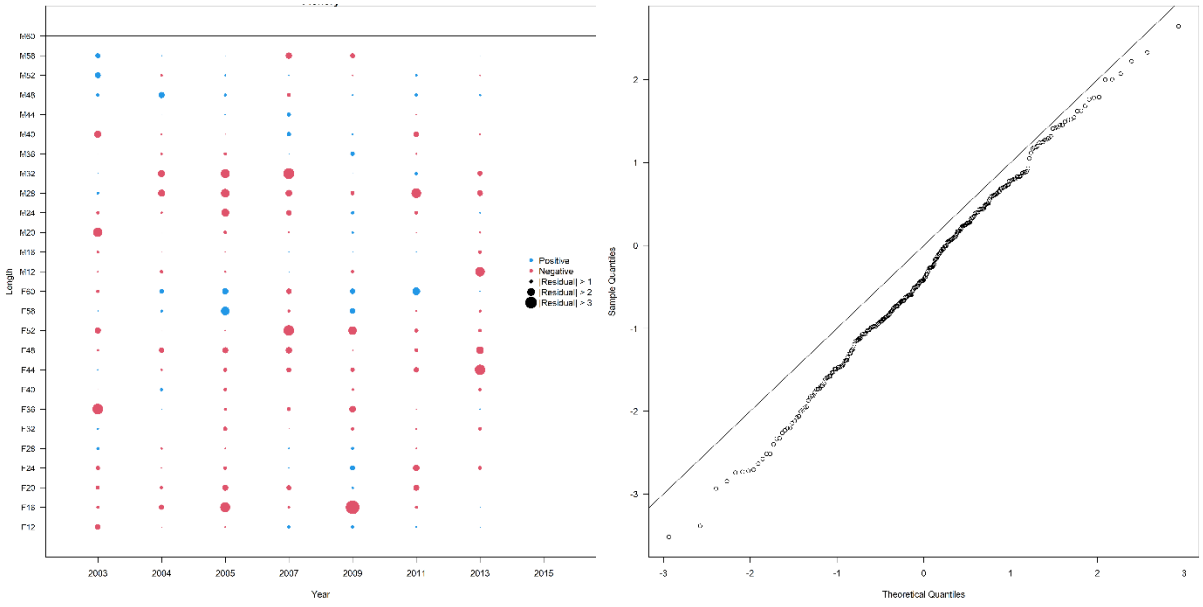


Figure H - 2. One-Step-Ahead (OSA) residuals for fits to the Queen Charlotte Sound Synoptic Survey length composition data for the length+CAAL assessment model. Depicted are the residuals at the medians of the posterior distribution. The length bins are labeled F12-F60 for females and M12-M60 for males. OSA residuals are calculated for the number of bins – 1, thus the final bin "M60" does not contain OSA residuals in this case.

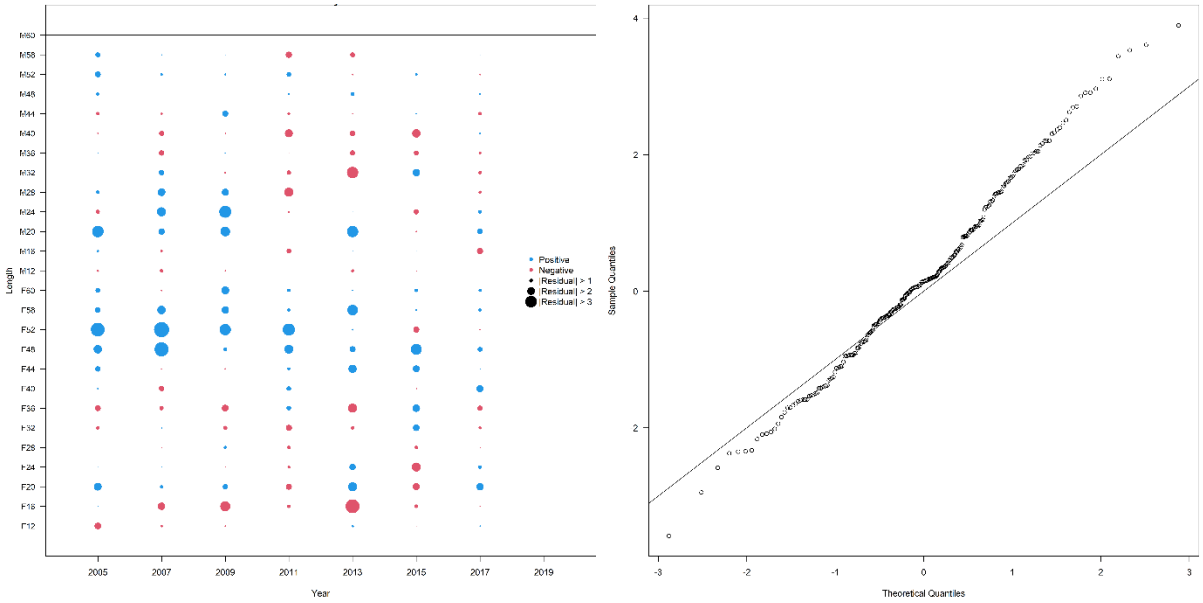


Figure H – 3. One-Step-Ahead (OSA) residuals for fits to the Hecate Strait Synoptic Survey length composition data for the length+CAAL assessment model. Depicted are the residuals at the medians of the posterior distribution. The length bins are labeled F12-F60 for females and M12-M60 for males. OSA residuals are calculated for the number of bins – 1, thus the final bin "M60" does not contain OSA residuals in this case.

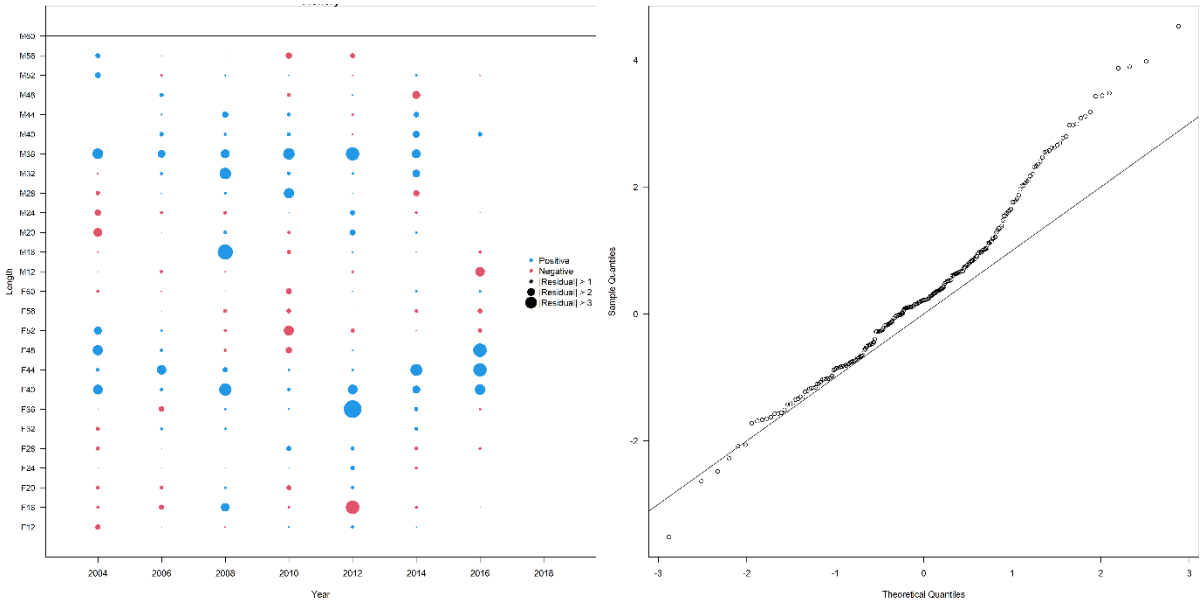


Figure H - 4. One-Step-Ahead (OSA) residuals for fits to the West Coast Vancouver Island Synoptic Survey length composition data for the length+CAAL assessment model. Depicted are the residuals at the medians of the posterior distribution. The length bins are labeled F12-F60 for females and M12-M60 for males. OSA residuals are calculated for the number of bins – 1, thus the final bin "M60" does not contain OSA residuals in this case.

APPENDIX I. TIME-SERIES REGRESSIONS BETWEEN ENVIRONMENTAL CONDITIONS AND SPECIES BIOLOGY

To examine how environmental conditions may affect Petrale Sole productivity, we used Bayesian time-series regressions to account for temporal autocorrelation and propagate uncertainty in the biological states.

I.1. ENVIRONMENTAL DATA SOURCES AND SPATIOTEMPORAL AGGREGATION

We selected a relevant subset of climate and biotic variables from those available in the *pacea* R package (Edwards et al. 2024). In addition to a variety of climatic and oceanographic indices, *pacea* aggregates outputs from the spatial British Columbia continental margin (BCCM) coupled physical-biogeochemical model by Peña et al. (2019) including dissolved oxygen concentration, temperature, pH, and salinity, as well as two biotic variables—phytoplankton from surface to 10 m and depth-integrated primary production (Figure I - 1). Each of the geochemical variables are estimated for sea surface and sea floor, as well as some intermediate depth strata. All variables are available as monthly means from 1993 to 2019 at a resolution of between 4 km^2 (on the continental shelf and slope) and 36 km^2 (further offshore) for all of Canada's Pacific Exclusive Economic Zone.

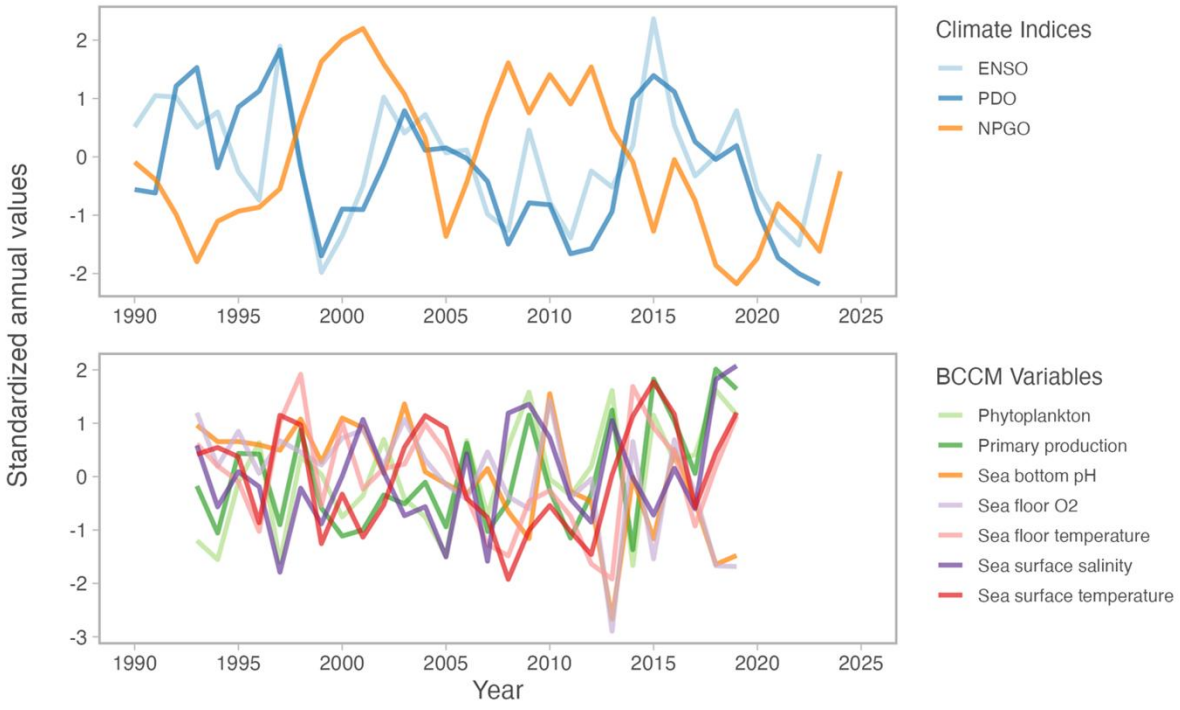


Figure I - 1. A sample of the possible climate indices and BCCM physical-biogeochemical model variables available in the pacea R package. Climate indices are available for more years than are shown here, but BCCM variables are not. BCCM variables are aggregated as annual means across all cells containing any of the depths occupied by Petrale Sole.

The climate index found to be important for other flatfish species on this coast is the Pacific Decadal Oscillation (PDO; Clark and Hare 2002, Stewart and Martell 2016). North Pacific Gyre Oscillation (NPGO) is another index of likely importance as an indicator of upwelling (Peña et al. 2019). Of the available BCCM variables, we selected temperature, oxygen, salinity, and the two biotic variables for the sea surface or sea floor, depending on life stage of interest. At an annual

scale and across all depths occupied by Petrale Sole, the highest correlations were among sea surface and sea floor temperature and between the two biotic variables, primary productivity and phytoplankton (Figure I - 2). Aside from these cases, the next strongest correlations were between PDO and sea surface temperature and between sea floor oxygen and phytoplankton. This latter relationship was negative, such that an increase in sea floor oxygen concentration was associated with a reduction in overall phytoplankton, potentially resulting from upwelling and/or decomposition.

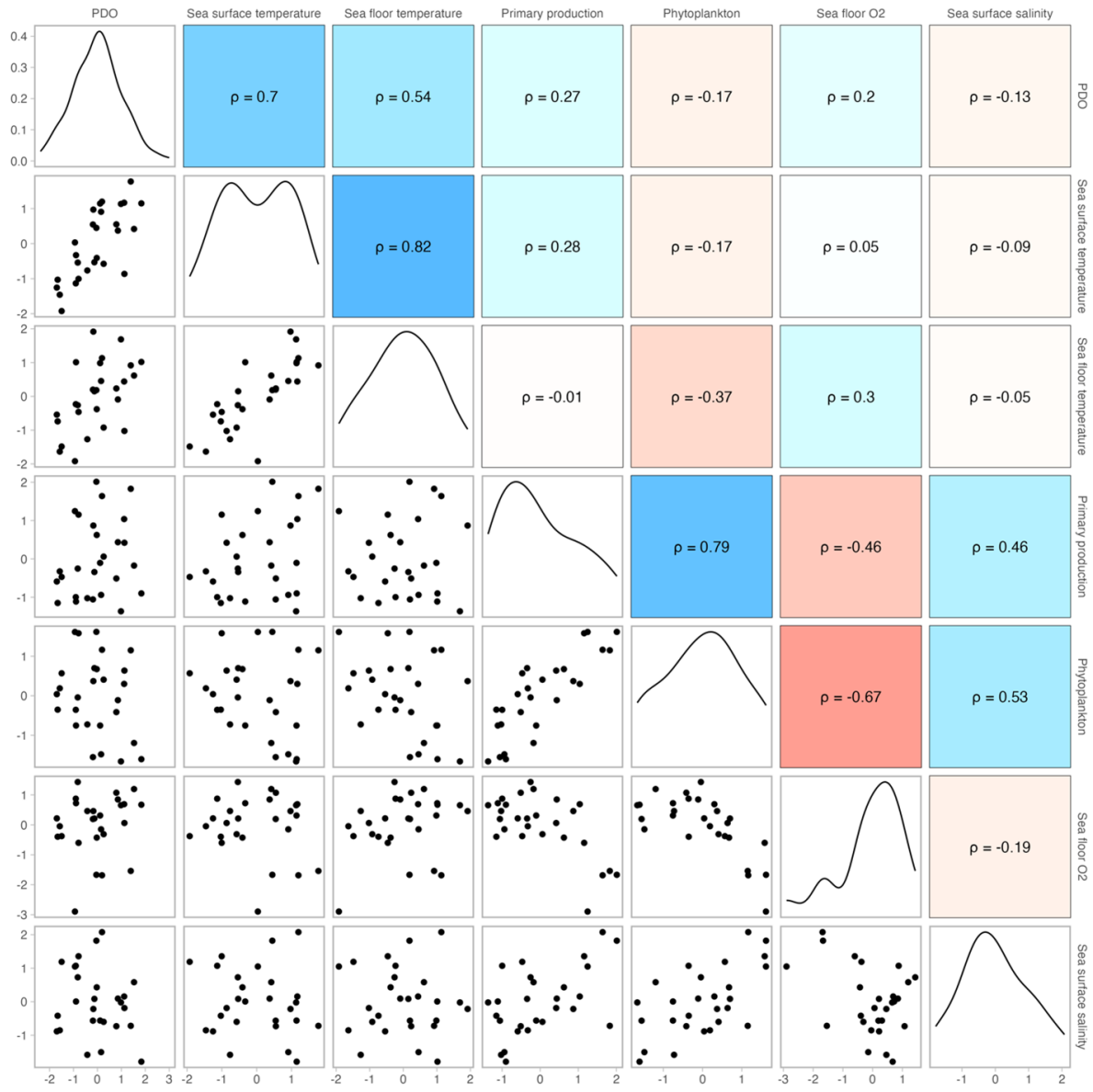


Figure I - 2. Spearman's rank correlations among an important climate index, PDO, and average BCCM physical-biogeochemical model variables aggregated as annual means across all cells containing any of the depths occupied by Petrale Sole. Different spatiotemporal aggregations and additional variables are considered in our analysis, but were not plotted for readability.

In order to examine potential influences of the above environmental variables on Petrale Sole in BC, we selected environmental variables for specific time periods that were hypothesized to impact recruitment or body condition based on known life history traits. Adult Petrale Sole

congregate at depth to spawn, so we calculated the mean sea floor oxygen concentration and temperature for all cells containing depths between 300 and 450 m (Love 2011) in each month and then took the average of these monthly values for months when spawning is most likely to occur (~January through March; Figure B - 5). Because the hypothesized mechanism for the importance of PDO for flatfish recruitment is related to wind direction moving larvae (Clark and Hare 2002, Stewart and Martell 2016), we also took an average of this index for the spawning months, when eggs and the smallest larvae are most subject to passive movement.

For the remaining pelagic period variables, we calculated the mean of all surface values from all cells containing depths occupied at any time of year (20–450 m; Love 2011). While Petrale Sole larvae have been found much further offshore, this depth range includes most areas inshore of the spawning depths and over any region of potential settlement habitats for juveniles so likely accounts for a high proportion of viable larval habitat (Pearcy et al. 1977). For surface temperature, we used the mean of the spawning period, a spring period (April through June) and a summer period (July through September) due to seasonal differences. Because PDO and temperature showed a relatively high correlation (Figure I - 2), we also included spring PDO to see which was explaining more variation. NPGO for the whole pelagic period was included as a possible indicator of upwelling conditions.

Of the two biotic variables in the BCCM, we chose phytoplankton because it is a surface variable, and may better represent accumulation in the surface layer rather than an underlying production rate (i.e., a measure of excess primary production). Phytoplankton was included as an average for the whole pelagic period. Finally, we also acquired indices of euphausiid abundance generated from summer surveys conducted in the same general areas as the WCVI and QCS synoptic surveys, as well as further offshore, from modelling work done by Evans et al. (2023). Given uncertainty in where Petrale Sole larvae are spending their pelagic period, we considered total euphausiid biomass anomalies for each of the above regions separately (WCVI, QCS, offshore) when assessing correlations with recruitment.

For BCCM variables with the potential to influence juvenile and adult body condition observed during our spring and summer surveys, we calculated the mean from all cells containing depths where 95% of this species' biomass was captured on these surveys (50–200 m). Of the available variables, we focused on sea floor temperature and oxygen, and depth-integrated primary production as those most specific to depths occupied by Petrale Sole. We used a mean of April through June values because our body condition indices are estimates generated for the summer solstice, which falls immediately after our period of most intense survey sample collection (mean June 14th; Figure I - 3). Because our body condition indices represent coastwide averages, regional inshore euphausiid indices were pooled. This allowed us to consider the biomass of the classically dominant species, *Euphausia pacifica*, as well as total euphausiid biomass. Both PDO and NPGO mean anomalies for April through June were also included as indicators of correlated oceanographic conditions that could suggest the importance of other variables not included in our analysis.

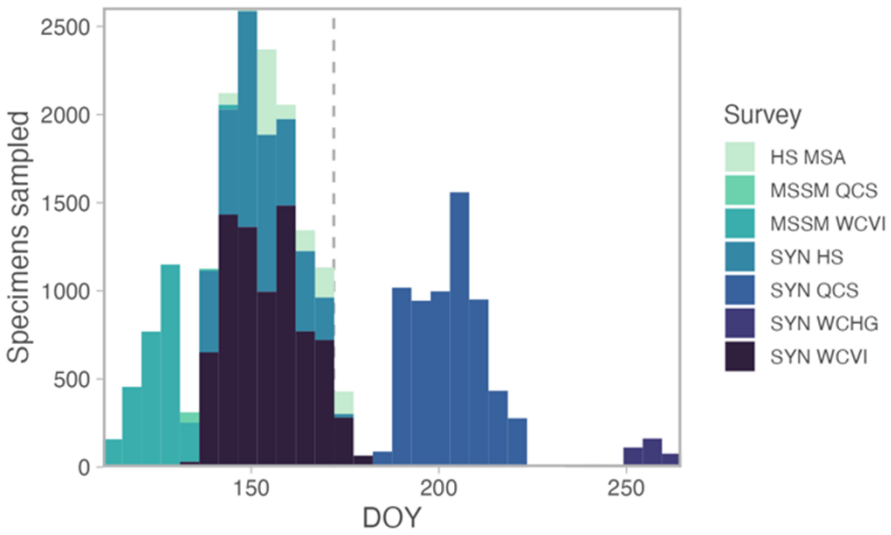


Figure I - 3. Distribution of sampling day of year (DOY) for specimens included in the body condition analyses. Dashed grey line indicates the summer solstice.

All environmental variables (except PDO, because it is already an anomaly) were centered by their mean and scaled by their SD before analysis.

I.2. BIOLOGICAL RESPONSE VARIABLES WITH UNCERTAINTY

To assess possible impacts of the above environmental variables, both recruitment and body condition were considered as biological responses. To propagate uncertainty in the estimation of the biological responses, 100 MCMC samples of the annual recruitment deviations were extracted from the base model (similar to an approach used in Haigh et al. 2019). However, we restricted analysis to the period from 1995 through 2018, the period for which the age data included in this assessment (2004 to 2019) had the potential to inform recruitment estimates. Likewise, we took 100 draws from the joint parameter precision matrix for each condition index (see Appendix J). Condition indices span 1998 through 2023, although spatial coverage was lower and therefore uncertainty higher before 2003 (Figure 62 and Figure J - 7).

Recruitment deviations already represent mean-centered multiplicative deviations from expected recruitment given each year's estimate of female spawning stock biomass, therefore we entered them into the models without transformation. Condition index values were centered on a Le Cren's score of 1 which represents the expected length-weight relationship and scaled within individual sample draws to represent 1 SD of change in body condition regardless of differences in estimated variability across different draws (Le Cren 1951).

I.3. TIME-SERIES REGRESSION

For each sampled time-series of our biological responses, we fit separate Bayesian hierarchical generalized linear mixed effects models (GLMMs) to assess the effect of each environmental variable, or the effect of the previous year's body condition on recruitment deviations. All predictor variables were fit as a second order orthogonal polynomial to allow for a curved predictor-response relationship and we accounted for temporal autocorrelation using a stationary autoregressive process with first-order (AR1) correlation.

$$
\begin{aligned}
y_t &= \beta_0 + \beta_1 D_{1t} + \beta_2 D_{2t} + \epsilon_t, \\
\epsilon_{t=1} &\sim \text{Normal}(0, \sigma^2), \\
\epsilon_{t>1} &\sim \text{Normal}(\rho_{\epsilon t-1}, \sigma^2),
\end{aligned}
$$

Eq. I - 1

where t is year, y is an annual recruitment or body condition deviation sample, β_1 and β_2 are coefficients, D_1 is the first orthogonal component of the polynomial (representing the linear slope portion), D_{2t} is the second orthogonal component of the polynomial (representing curvature), $\rho_{\epsilon t}$ is the correlation between subsequent time steps, and σ represents the observation error SD. The first time step is given a mean-zero prior with the same SD. We assigned weakly informative priors on all parameters: N(0,10) priors on all β parameters, N(0,1) on the ρ and a half-t(3, 0, 2) prior (i.e., degrees of freedom of 3 and scale of 2) on σ. Posteriors from 100 models representing the same biological response and environmental variable combination were then combined to provide estimates with uncertainty that incorporated both uncertainty in the biological values (derived from our stock assessment or the spatial body condition models) and in their relationship with each variable.

We fit these models in Stan (Carpenter et al., 2017) using the R package *brms* (Bürkner, 2017) and cmdstanr (Gabry et al., 2023). Stan implements the No-U-Turn Hamiltonian Markov chain Monte Carlo algorithm (Hoffman and Gelman 2014) to perform Bayesian statistical inference. For each sample draw we ran one chain with 500 iterations (250 warm-up); therefore our final inference was based on 250 × 100 = 25,000 iterations. We assessed model convergence on a model fit to the mean estimates for each biological variable with 3 chains each with 1,000 iterations (500 warmup). All models achieved Rhat (scale-reduction factors) of <1.01 and effective sample sizes of >600 (or 200 per chain).

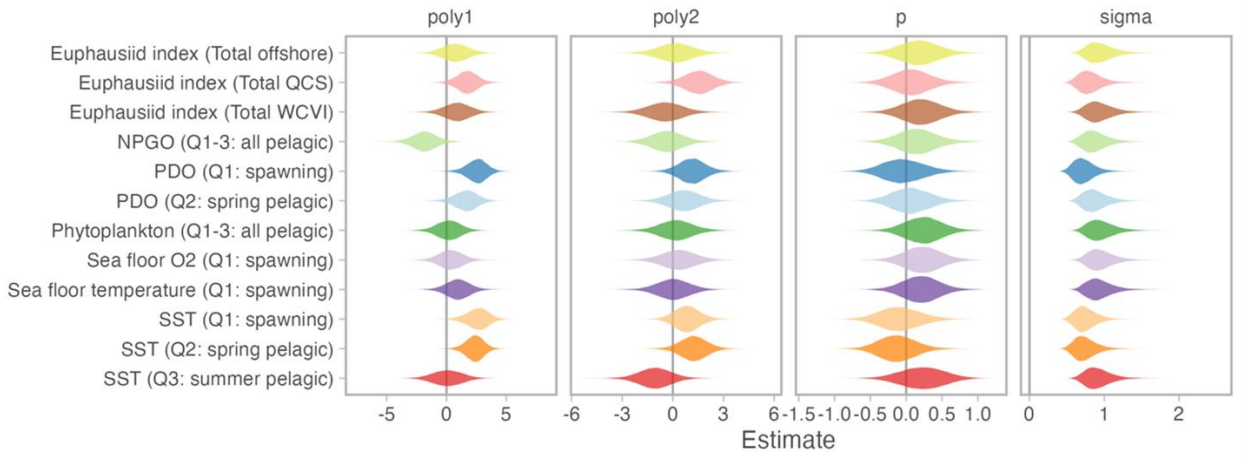


Figure I - 4. Density violin plots for all coefficient posteriors from time-series regressions on 100 MCMC samples of recruitment deviations from the base model (1995 and 2018). Each violin contains 25000 MCMC samples. Coefficients represent the first- (poly1: linear component) and second- (poly2: curvature component) order orthogonal polynomials, the correlation between subsequent time steps (p), and the observation error SD (sigma).

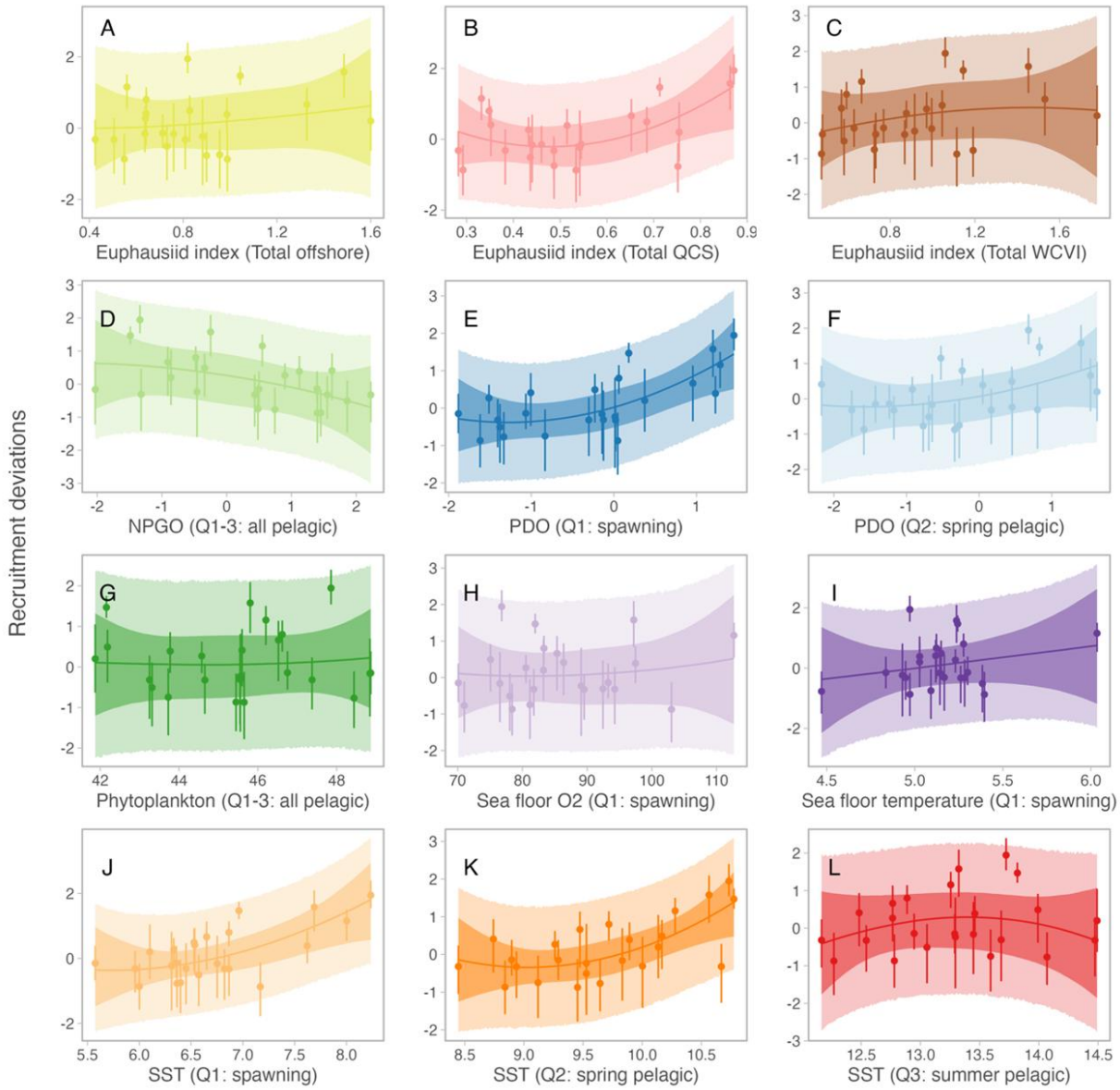


Figure I - 5. All predicted relationships between environmental conditions and recruitment deviations from the base model for 1995 through 2018. The darker shading represents the 95% CI in the predicted second-order orthogonal polynomial (i.e., quadratic) relationship based on the combined posteriors from 100 time-series regressions, one for each MCMC sample of recruitment deviations from the stock assessment model. Lighter shading indicates a 90% credible interval from the full posterior prediction (i.e., including uncertainty on new "observations" of recruitment deviations). Vertical dot-lines represent the median recruitment deviation and the 95% quantiles of observed values in the 100 MCMC samples.

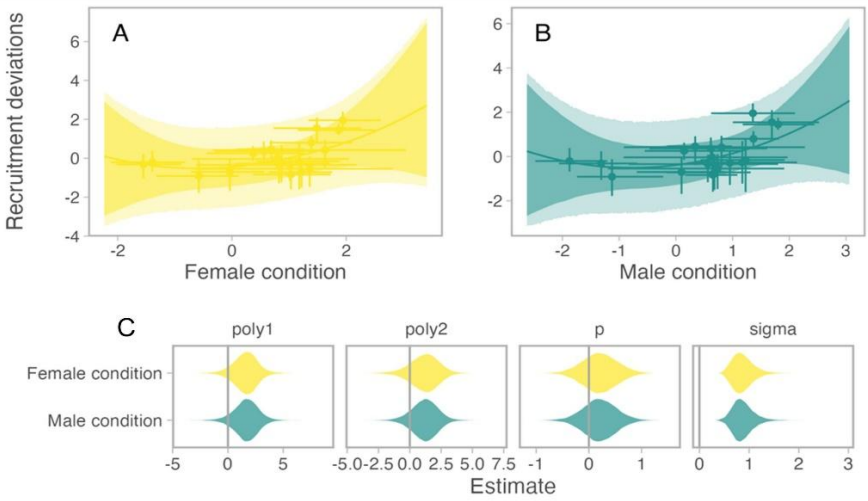


Figure I - 6. Predicted relationships between body condition in SDs from the mean of each time series for mature females (A, yellow) and mature males (B, turquois) and recruitment deviations from the model with an M of 0.154 from the ensemble base model for 1998 through 2018. The darker shading represents the uncertainty in the predicted second order orthogonal polynomial relationship based on the combined posteriors from 100 time-series regressions, one for each pair of recruitment and body condition samples. Lighter shading indicates a 95% credible interval from the full posterior prediction (i.e., including uncertainty on new "observations" of recruitment deviations). Vertical dot-lines represent the median recruitment deviation and the 95% quantiles of observed values in the 100 MCMC samples. Horizontal dot-lines represent the median and the 95% quantiles of scaled deviations in predicted annual body condition observed in 100 samples from the condition index. Density violin plots (C) are as described in Figure I - 4.

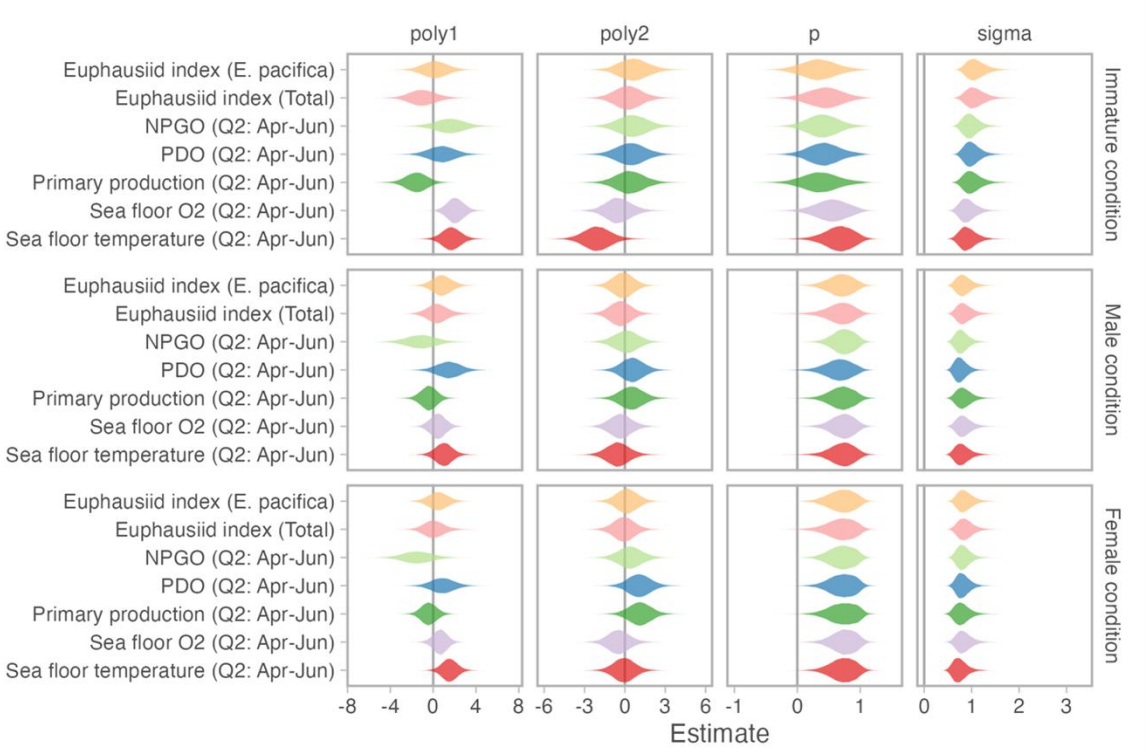


Figure I - 7. Density violin plots for all coefficient posteriors from time-series regressions on 100 samples from body condition indices between 1998 and 2023. PDO and NPGO use this whole timeseries, while all other environmental covariates were only available through 2019. Each violin contains 25000 samples of coefficients representing the first- (poly1: linear component) and second- (poly2: curvature component) order orthogonal polynomials, the correlation between subsequent time steps (p), and the observation error SD (sigma).

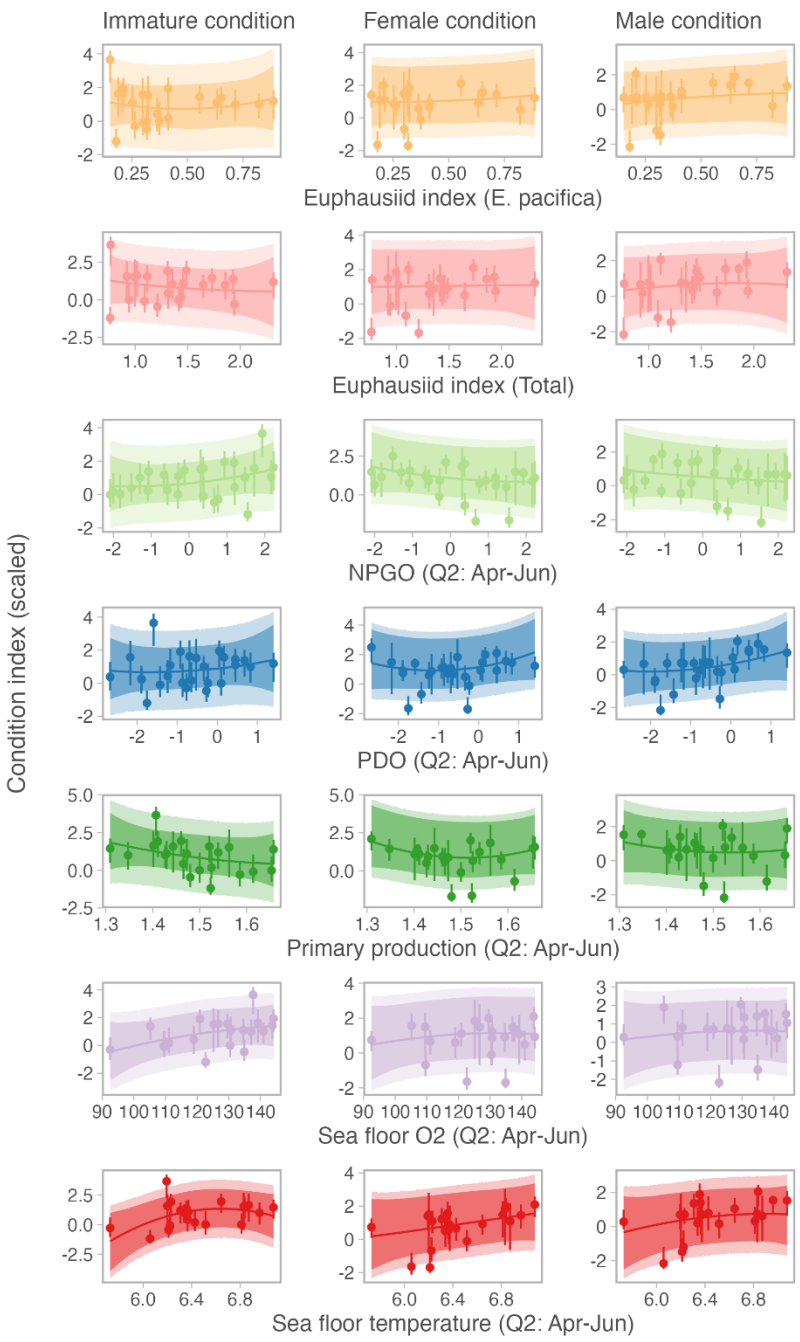


Figure I - 8. All predicted relationships between environmental conditions and body condition between 1998 and 2023 for immatures (left column), mature females (middle column), and mature males (right column). The darker shading represents the 95% CI in the predicted second order orthogonal polynomial relationship based on the combined posteriors from 100 time-series regressions, one for each MCMC sample. Lighter shading indicates a 95% credible interval from the full posterior prediction (i.e., including uncertainty on new "observations" of the condition index). Dot-lines represent the median and the 95% quantiles of scaled deviations in predicted annual body condition observed in 100 samples from the index. PDO and NPGO use this whole timeseries, while all other environmental covariates were only available through 2019.

LITERATURE CITED

Bürkner, P.C. 2017. brms: an R package for Bayesian multilevel models using Stan. Journal of Statistical Software. 80(1), 1–28.

Carpenter, B., Gelman, A., Hoffman, M. D., Lee, D., Goodrich, B., Betancourt, M., Brubaker, M., Guo, J., Li, P., and Riddell, A. 2017. Stan: a probabilistic programming language. Journal of Statistical Software, 76(1), 1–32.

Clark, W.G., and Hare, S.R. 2002. Effects of climate and stock size on recruitment and growth of Pacific Halibut. North American Journal of Fisheries Management. 22, 852-862.

Edwards A.M., Tai T.C., Watson J., Peña M.A., Hilborn A., Hannah C.G., Rooper C.N., Flynn K.L., and Oldford, G.L. 2024. pacea: An R package of Pacific ecosystem information to help facilitate an ecosystem approach to fisheries management.

Evans, R., English, P.A., Gauthier, S., and Robinson, C.L. 2023. Quantifying the effects of extreme events and oceanographic variability on the spatiotemporal biomass and distribution of two key euphausiid prey species. Frontiers in Marine Science, 10, 1031485.

Fuglstad, G.A., Simpson, D., Lindgren, F., and Rue, H. 2019. Constructing piors that penalize the complexity of Gaussian Random Fields. JASA, 114(525), 445–452.

Gabry, J., Češnovar, R., and Johnson, A. 2023. cmdstanr: R interface to 'CmdStan'.

Haigh, R., Starr, P.J., Edwards, A.M., King, J.R., and Lecomte, J.-B. 2019. Stock assessment for Pacific Ocean Perch (*Sebastes alutus*) in Queen Charlotte Sound, British Columbia in 2017. DFO Can. Sci. Advis. Sec. Res. Doc. 2018/038. v + 227 p.

Hoffman, M.D., and Gelman, A. 2014. The No-U-Turn sampler: adaptively setting path lengths in Hamiltonian Monte Carlo. Journal of Machine Learning Research, 15, 1593–1623.

Le Cren, E.D. 1951. The length-weight relationship and seasonal cycle in gonad weight and condition in the perch (*Perca fluviatilis*). Journal of Animal Ecology, 20, 201–219.

Love, M.S. 2011. Certainly more than you want to know about the fishes of the Pacific Coast: a postmodern experience. Really Big Press.

McCullagh, P., and Nelder, J.A. 1989. Generalized Linear Models. Chapman & Hall.

Pearcy, W.G., Hosie, M.J., and Richardson, S.L. 1977. Distribution and duration of pelagic life of larvae of Dover sole, *Microstomus pacificus*; rex sole, *Glyptocephalus zachirus*; and petrale sole, *Eopsetta jordani*, in waters off Oregon. Fisheries Bulletin, 75(1), 173-183

Peña, M.A., Fine, I., and Callendar, W. 2019. Interannual variability in primary production and shelf-offshore transport of nutrients along the northeast Pacific Ocean margin. Deep-Sea Research II, doi:10.1016/j.dsr2.2019.104637.

Stan Development Team. 2024. Stan modeling language user's guide and reference manual, Version 2.32.2.

Stewart, I.J., and Martell, S.J.D. 2016. Appendix: Development of the 2015 stock assessment Int. Pac. Halibut Comm. Report of Assessment and Research Activities 2015: (623) A1-A145.

APPENDIX J. SEX AND MATURITY SPECIFIC INDICES OF BODY CONDITION

Because the condition of mature male, mature female (B or SSB in this assessment), and immature individuals have different implications for population dynamics, observation error characteristics, and potentially even different ecological drivers, we first separated individuals and overall catches into immatures, mature males and mature females. We then estimated independent spatiotemporal biomass distributions, calculated individual Le Cren's relative body condition deviations, modelled spatiotemporal change in these deviations, and generated a density-weighted annual index of average condition for each component of the population.

J.1. SPLITTING SPECIMENS AND TOTAL CATCH BY SEX AND MATURITY

To maximize the sample size and spatiotemporal representation, we used morphological measurements collected from all fishery-independent surveys, and total catch weights from all surveys that had positive catches in at least three years and at least 1% positive catches overall between 1998 and 2023. These surveys were the Hecate Strait Multispecies Assemblage Survey (MSA), two Multispecies Small-mesh Bottom Trawl Surveys (MSSM), and four contemporary Synoptic bottom trawl surveys (SYN). The MSA was conducted mostly biennially between 1984 and 2003, but morphological measurements were only collected starting in 1998. This survey had a fixed-station design that was depth-stratified between 20 and 200 m. The MSSM surveys target shrimp and have been conducted off the west coast of Vancouver Island in most years since 1975 and in Queen Charlotte Sound between 1998 and 2016 (personal communications). This survey currently follows a fixed station design covering depths mostly between 50 and 200 m, but it has undergone some changes since its inception. We account for a gear change in 2006 by including different catchabilities before and after this change in our species distribution models. Protocols for collecting individual-level data varied between surveys and with the size of catches, but generally included sampling from the larger catches up to a maximum of 50 individuals per tow.

We assigned individual fish to maturity classes based on the average length at 50% maturity estimated with set ID as a random intercept:

$$\begin{aligned} M_i &\sim \text{Bernoulli}(p_i), \\ p_i &= \text{logit}^{-1}(\alpha + \alpha_j + \beta L_i), \\ \alpha_j &\sim \text{Normal}(0, \sigma_\alpha^2), \end{aligned}$$

Eq. J - 1

where M_i represents the mature (1) or immature (0) status of fish i, p_i represents the probability of maturity of fish i, α represents a global intercept, α_j represents a set-level deviation j that is allowed to vary with a variance of σ_α^2, β represents a coefficient, and L_i represents the length of fish i. The result was that males larger than 33.8 cm were deemed mature and females above 36.5 cm (Figure J - 1).

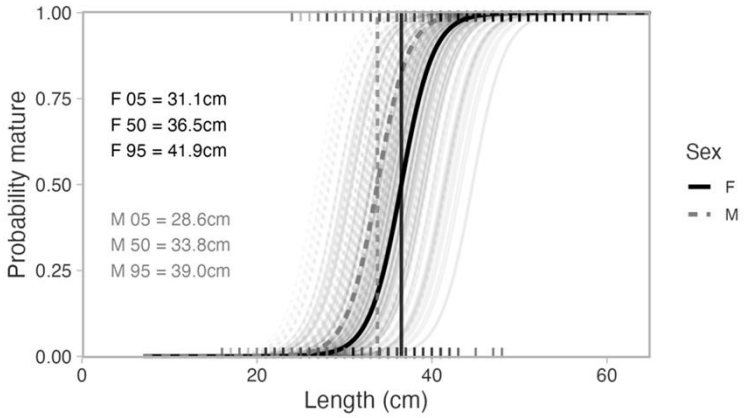


Figure J - 1. Length at maturity ogives and thresholds used to spilt individuals into immature vs. mature classes for females (solid lines) and males (dashed lines). Faint background ogives represent random effect estimates for each set ID.

When individual whole body weights were missing, but lengths were known, individuals were assigned estimated weights based on the overall average length-weight relationship (derived using Eq. B-3 but with the t distribution applied without the Gaussian mixture component and resulting in identical parameter estimates to at least 2 significant figures; Figure B - 3).

For each sampled tow, we then split the total catch of each species into immature, mature males, and mature females using the observed proportions by weight among the individually measured specimens. For unsampled tows in all survey-year combinations with at least six sampled tows, we applied the average proportion of each category from all sampled tows in that survey-year. For unsampled tows in any survey-year combinations with less than six tows (WCHG SYN in 2020 and 6 or 7 years for each MSSM surveys, mostly prior to 2003), we applied the average proportion of each category from all surveys in that year combined. When no samples were collected in 2020, the global average was used.

J.2. SPATIOTEMPORAL ESTIMATES OF BIOMASS DENSITY

In order to calculate a weighted-average body condition and account for possible density-dependence, we needed spatiotemporal estimates of biomass density for each maturity class. We fit separate spatiotemporal models for the estimated split catches representing relative catch weights of immatures, mature males, mature females, and all classes combined.

We used a delta (hurdle) approach (Aitchison 1955) with a Bernoulli distribution for presence-absence (technically detection-non-detection) and a lognormal distribution for the positive catches (both gamma and heavier-tailed distributions did not converge consistently). We modelled survey catch weights as representative of relative biomass density D for point in space s and time t as a product of two component models,

$$\mathrm{D_{s,t}} \sim \mathrm{Bernoulli}\left(\mu_{1,s,t}\right) \cdot \mathrm{lognormal}\left(\log\mu_{2,s,t} - \frac{\vartheta^2}{2}, \vartheta^2\right),$$

Eq. J - 2

where $\mu_{1,s,t}$ represents the expected probability of catching the species in a given tow and $\mu_{2,s,t}$ represents the expected biomass density conditional on a positive observation when ϑ is the standard deviation of positive observations in log-space. These two components were modelled as a function of a series of fixed and random effects:

$$\mu_{1,s,t} = \text{logit}^{-1}\left(\alpha_1 + \boldsymbol{X}_{1,s,t}\boldsymbol{\beta}_1 + \omega_{1,s} + \delta_{1,s,t}\right),$$
$$\mu_{2,s,t} = \exp\left(\alpha_2 + \boldsymbol{X}_{2,s,t}\boldsymbol{\beta}_2 + \omega_{2,s} + \delta_{2,s,t}\right),$$

Eq. J - 3

where α represents the intercept for synoptic trawl surveys, $\boldsymbol{X}_{s,t}$ represents a vector of predictors (factors for other survey types, and second order orthogonal polynomials of log depth and day-of-year relative to the summer solstice), and $\boldsymbol{\beta}$ represents a vector of corresponding parameters. The subscripts 1 and 2 denote the equivalent parameters from the first (Bernoulli) and second (lognormal) linear predictors.

We constrained the covariance via a Matérn covariance function with the range (distance at which correlation is effectively independent) being allowed to differ between the spatial and spatiotemporal fields. Each symbol $\boldsymbol{\omega}_s$ represents spatially correlated random effects (from a Gaussian Markov random field, GMRF) that are constant through time, which are assumed to follow a multivariate normal distribution with covariance matrix $\boldsymbol{\Sigma}_{\boldsymbol{\omega}}$:

$$\boldsymbol{\omega}_s \sim \text{MVNormal}(\boldsymbol{0}, \boldsymbol{\Sigma}_{\boldsymbol{\omega}}).$$

Eq. J - 4

Each $\delta_{s,t}$ term represents annual spatially correlated random effects where $\boldsymbol{\epsilon}_{s,t}$ were similarly constrained by a multivariate normal distribution with covariance matrix $\boldsymbol{\Sigma}_{\boldsymbol{\epsilon}}$, and where $\boldsymbol{\delta}_t$ are assumed to follow a random-walk process given by

$$\boldsymbol{\delta}_{t=1} \sim \text{MVNormal}(\boldsymbol{0}, \boldsymbol{\Sigma}_{\boldsymbol{\epsilon}}),$$
$$\boldsymbol{\delta}_{t>1} = \boldsymbol{\delta}_{t-1} + \boldsymbol{\epsilon}_{\boldsymbol{t-1}},\ \boldsymbol{\epsilon}_t \sim \text{MVNormal}(\boldsymbol{0}, \boldsymbol{\Sigma}_{\boldsymbol{\epsilon}}).$$

Eq. J – 5

We included all tows that sampled for a distance > 500 m. These values were combined with net opening to estimate the area swept (e.g., Williams et al. 2018, Anderson et al. 2019). When the tow-specific value was missing, we applied the mean net opening for that survey. These values were used to calculate log area swept in hectares for each tow. This was included as an offset term for the positive component of all species distribution models (p.~206, Mccullagh and Nelder 1989).

We fit all spatiotemporal models in R 4.3.2 with the package *sdmTMB* (Anderson et al. 2024) version 0.5.0.9005. Mesh vertices were constrained to be at least 20 km apart, with penalized complexity priors (Fuglstad et al., 2019) applied to the covariance parameters assuming a 95% probability that the range was >20 km and the marginal random field standard deviation was <2 in link space. Model fit was assessed using randomized quantile residuals (Dunn and Smyth 1996) with fixed effect at their maximum likelihood estimates and random effects taken from a single sample of their approximate distribution (Waagepetersen 2006; Thygesen et al. 2017). Convergence was determined by checking that the Hessian was positive definite, and that the maximum absolute log likelihood gradient with respect to fixed effects was <0.001.

From each of these models, we predicted relative biomass for each sampling location and for a 2 x 2 km grid covering the combined domains of the synoptic trawl surveys (Figure J - 2 to Figure J - 4)). We treated days since summer solstice and survey-catchability effects as catchability covariates (i.e. setting the covariates to reference values to control for them) and bottom depth as a density covariate (i.e., setting the covariate to relevant values for each grid cell). Grid values were first used to calculate area-weighted annual indices of relative biomass by summing the predicted biomass each year and applying a generic bias correction for the non-linear transformation of the random effects (Thorson et al. 2015, Thorson and Kristensen 2016). These indices represent expected relative biomass if the entire synoptic survey area was

sampled on the summer solstice with synoptic survey catchability. We summed the maturity-specific indices in each year to confirm that combined they resulted in the same pattern across years as the index of total biomass (Figure J - 5).These predictions also act as covariates and weighting for subsequent condition index generation.

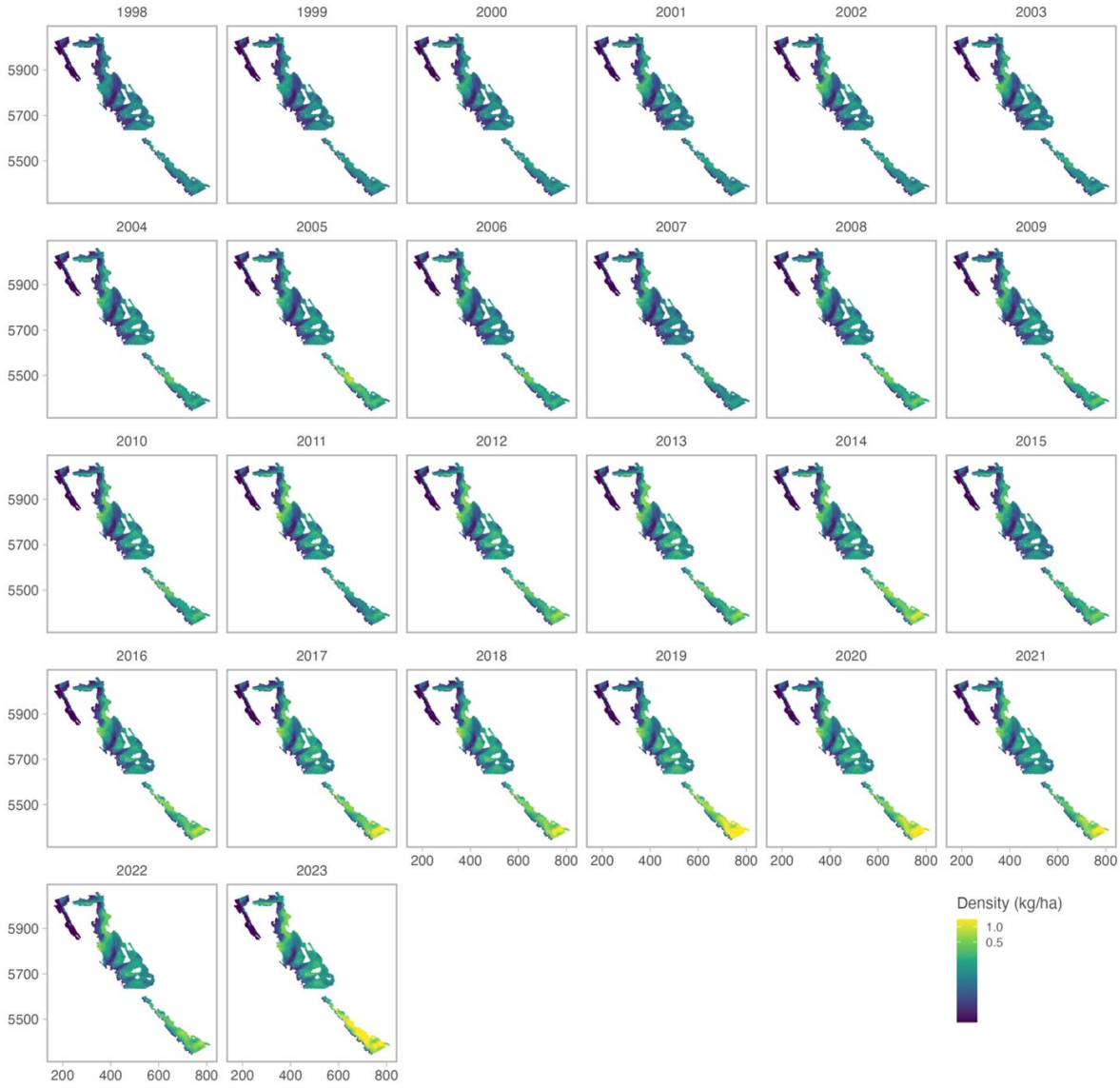


Figure J - 2. Predicted mature female biomass density distribution using catches from the multispecies assemblage (MSA; starting in 1998) and small-mesh surveys (starting in 2003), and all modern synoptic surveys).

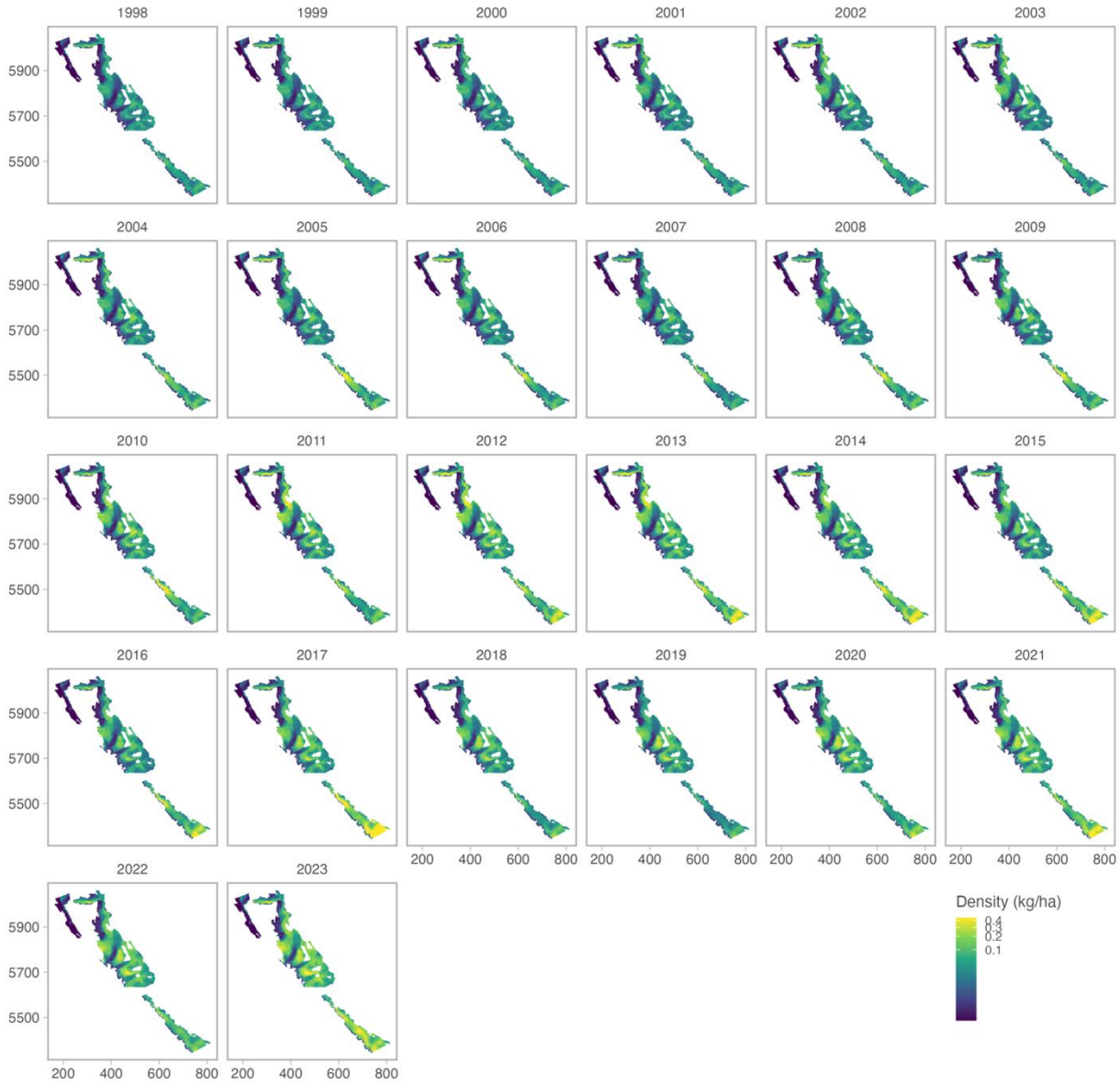


Figure J - 3. Predicted mature male biomass density distribution.

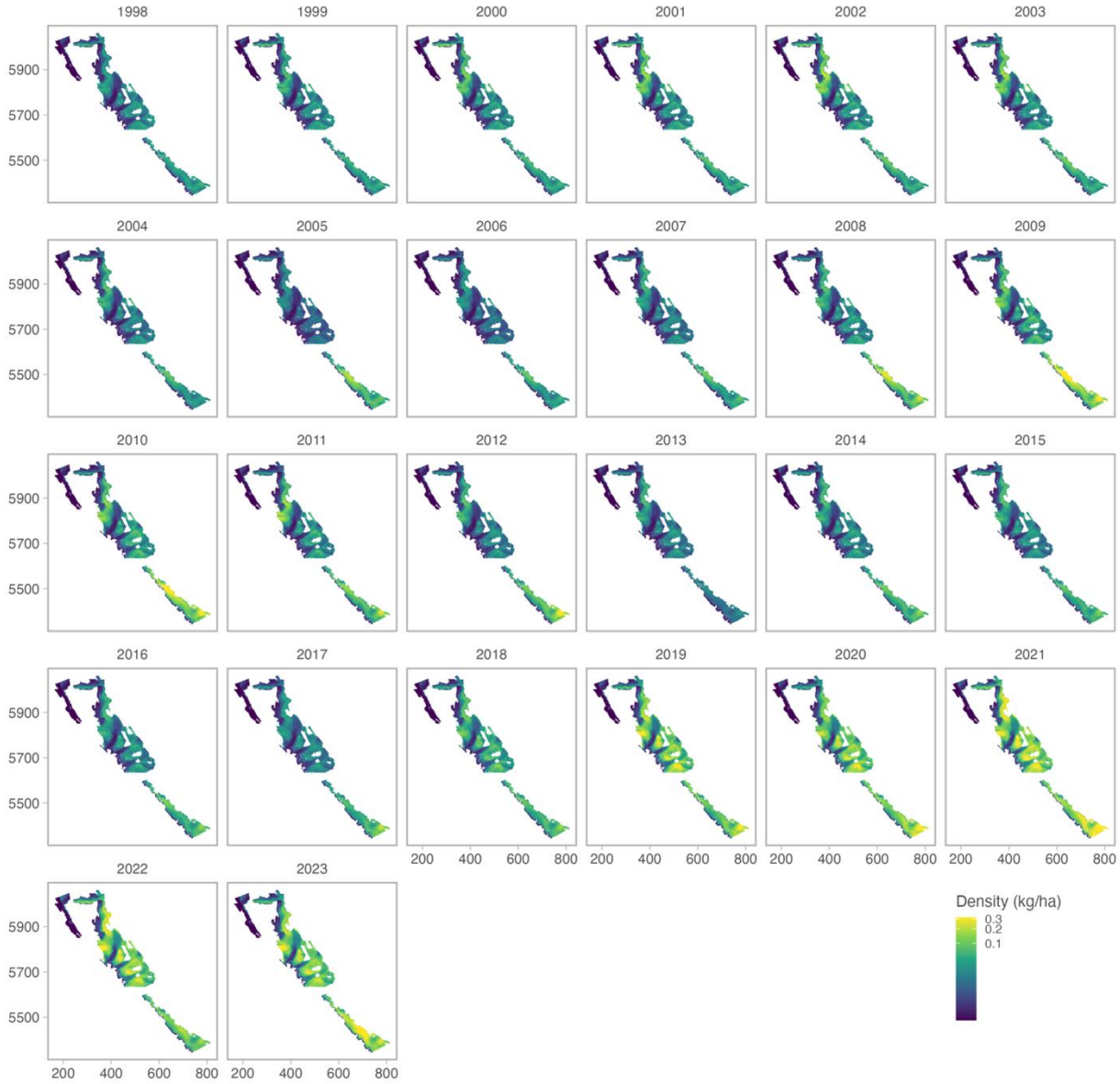


Figure J - 4. Predicted immature biomass density distribution.

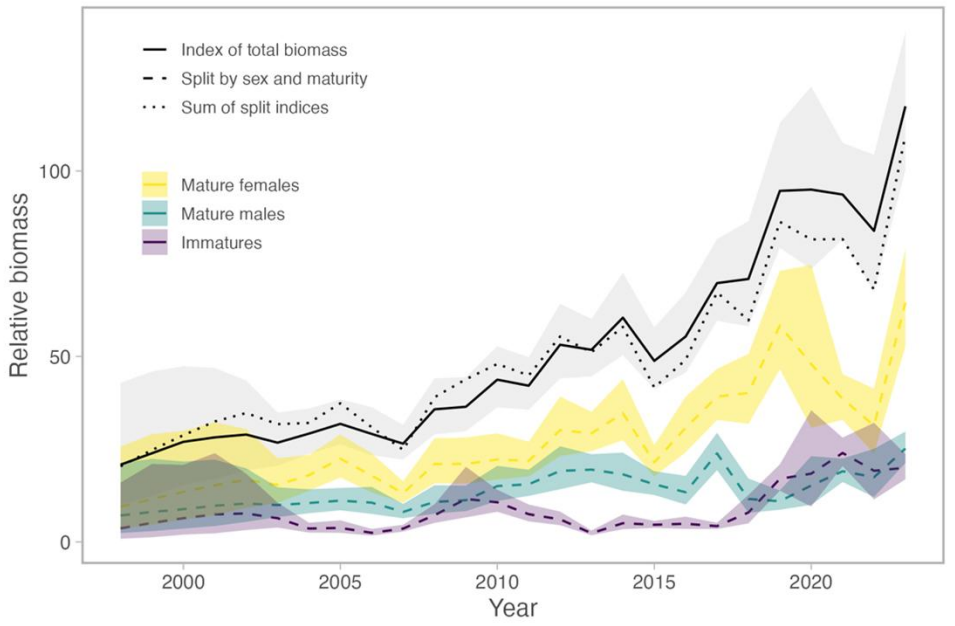


Figure J - 5. Spatiotemporal model-based biomass index means with 95% CIs for the full combined synoptic survey grid area based on total catches (solid black line and grey shading) and catches split into immature (purple dashed line and shading), mature males (turquoise dashed line and shading), and mature females (yellow dashed line and shading). The sum of the three split indices is indicated by the dotted line, which falls within the CI of the model based on all total catches.

J.3. POPULATION INDICES OF LE CREN'S BODY CONDITION

We calculated relative condition factors (K_{rel}; Le Cren 1951) as the ratio between the observed whole body weight of an individual fish and the predicted whole body weight. The predicted weight was derived from Eq. B-3 for average species-specific length-weight relationships across years and space, calculated separately for males and females. An individual with a K_{rel} = 1 is in average condition for that species. To avoid bias from extreme measurement errors, individuals whose length-weight residuals exceeded 2x the scale parameter for the observation error with a Student t distribution (*df* = 3) were excluded from further analyses (Figure J - 6).

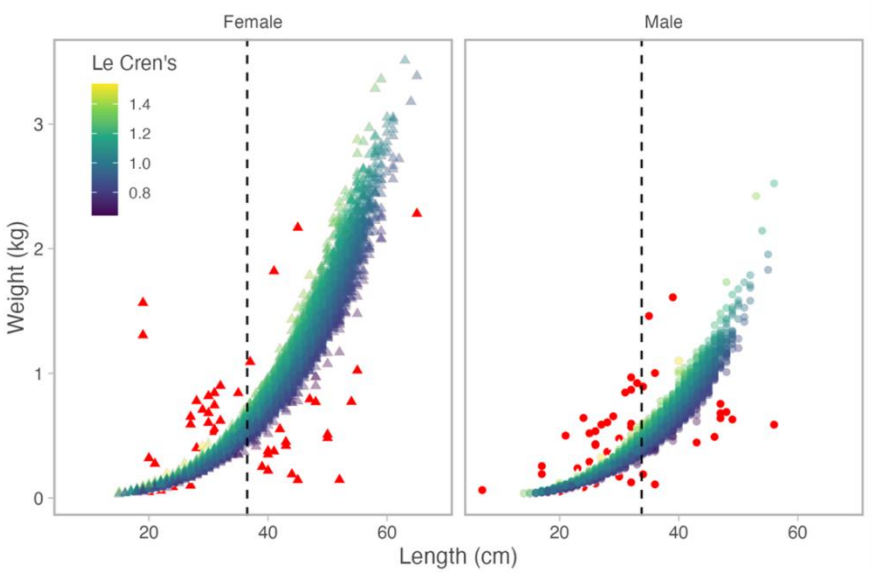


Figure J - 6. Le Cren's relative condition factors (colour scale) for females and males. Red indicates outliers that are assumed to have resulted from extreme measurement error (e.g., data entry errors) and therefore have been excluded from the spatiotemporal model. Dashed lines indicate the maturity thresholds such that samples to the left were included in the immature model and those to the right the mature models.

We then modelled spatiotemporal variability in relative body condition K_{rel} separately for each maturity class at each point in space s and time t assuming lognormal residuals

$$\begin{aligned} \mathrm{K_{rel}} &\sim \mathrm{lognormal}\left(\log\mu_{3,s,t} - \frac{\vartheta^2}{2}, \vartheta^2\right), \\ \mu_{3,s,t} &= \exp\left(\alpha_3 + X_{3,s,t}\beta_3 + \omega_{3,s} + \delta_{3,s,t}\right), \end{aligned}$$

Eq. J - 6

where ϑ is the standard deviation in log-space, α_3 represents the intercept for synoptic trawl surveys, $X_{3,s,t}$ represents a vector of predictors (other survey types, and second order polynomial for date relative to the summer solstice), and $\boldsymbol{\beta}_3$ represents a vector of corresponding parameters.

In these models, $\mu_{3,s,t}$ is defined by Eq. J - 6 with the only changes being that we no longer include a depth effect and we simplified the polynomial for date relative to solstice to a linear relationship when the range of dates sampled was <60.

Next, we tested for an effect of density-dependence by adding a predictor of estimated log biomass density (combined male and female mature biomass for mature classes, immature estimates otherwise). This variable was centered on the average estimated log density for the specimens included in the model. The slope of this density effect was not significantly negative, so we reverted to the density-agnostic model of relative body condition. When these models did not converge, model simplification involved allowing the spatial and spatiotemporal fields to share the same range parameter, or dropping the spatial field entirely when the marginal standard deviation of the spatial field when ϑ <0.001.

From the fitted density-agnostic models for each maturity class, we calculated average Le Cren's condition indices using the same general method as for the biomass indices. In this case, local condition estimates (Figure J - 7 to 10) were weighted by the proportion of each

year's predicted biomass that occurred in each cell (rather than the area of the cell). The resulting indices represent the predicted average body condition of an individual fish belonging each maturity class in each year (Figure 62). To propagate uncertainty through environmental analyses, we then took 100 samples of this overall condition index by constructing it from 100 samples of the joint parameter precision matrix.

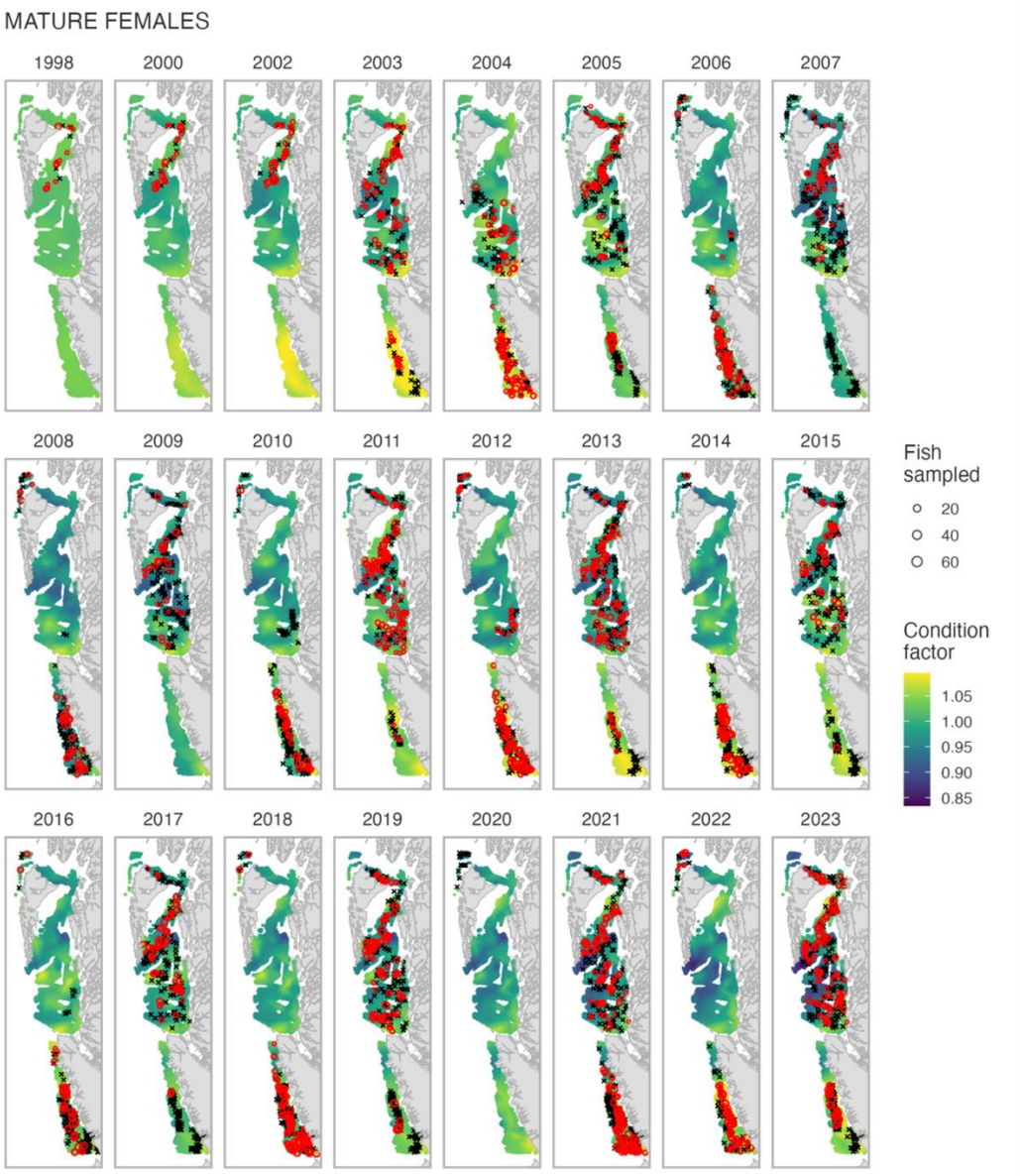


Figure J - 7. Annual predicted spatial distribution of average mature female body condition factors. Specimen locations are overlaid in red circles sized relative to the number of fish sampled. A black 'x' indicates a location where the species was caught, but no morphological data were collected.

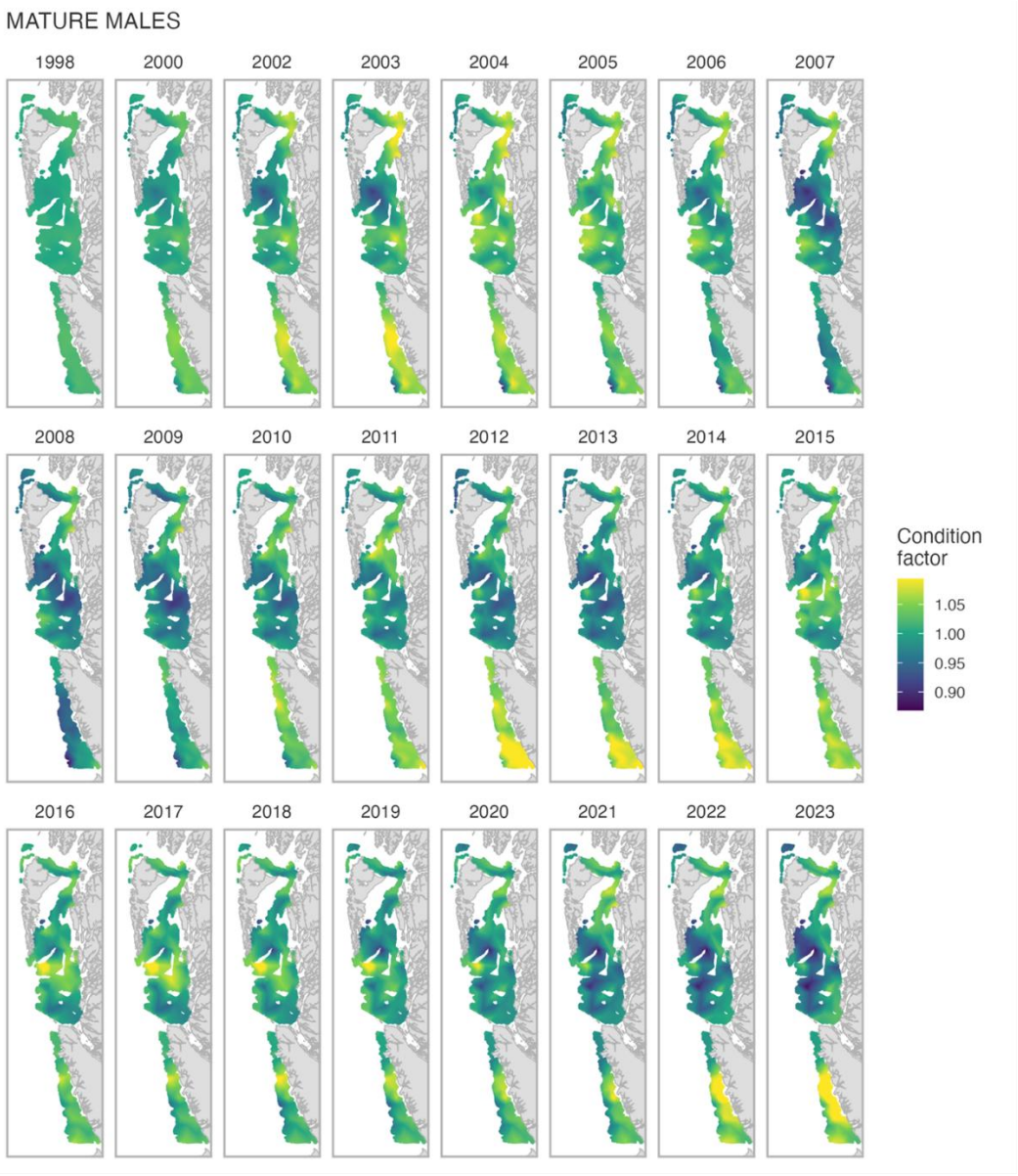


Figure J - 8. Annual predicted spatial distribution of average mature male body condition factors.

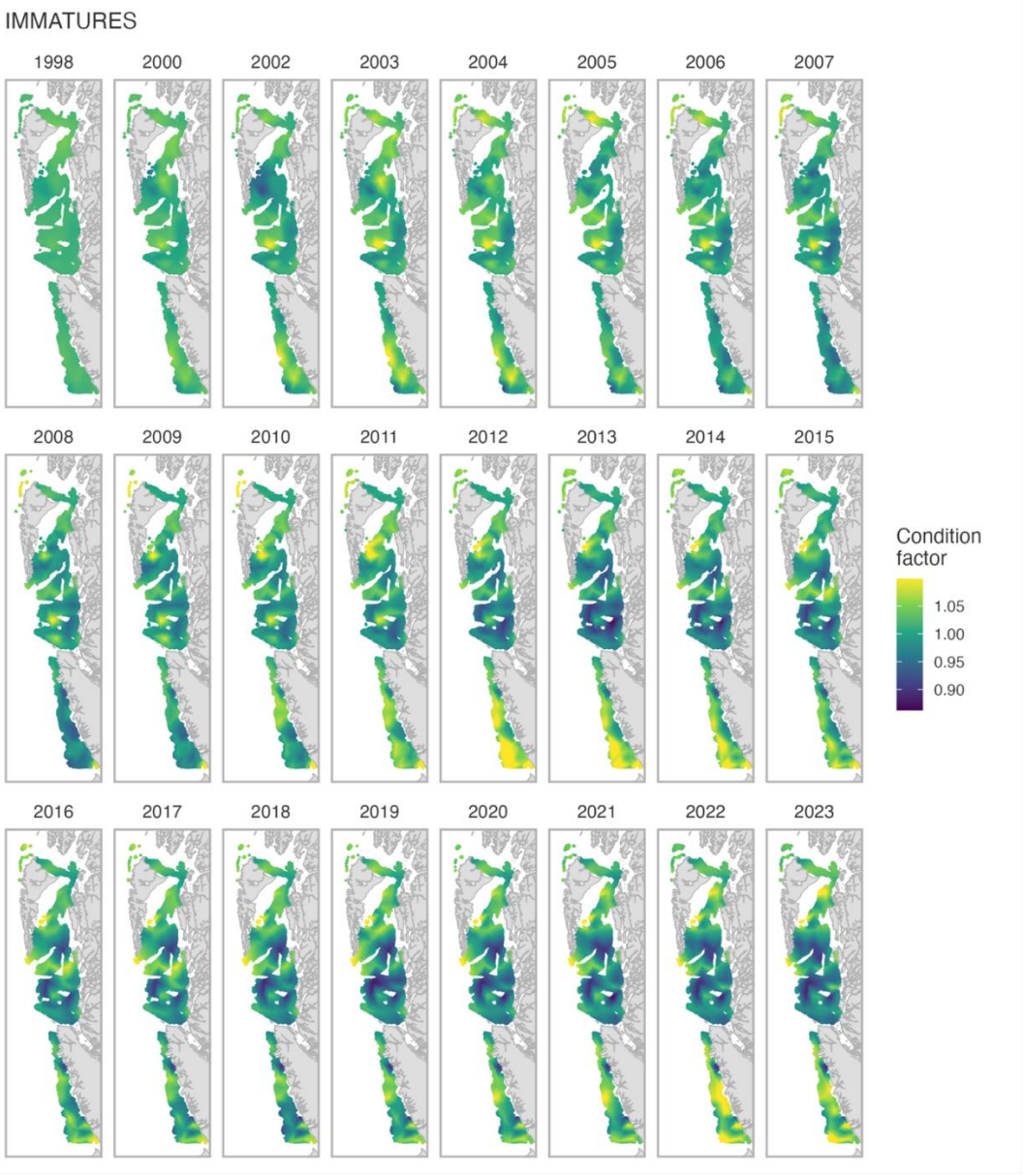


Figure J - 9. Annual predicted spatial distribution of average immature body condition factors.

LITERATURE CITED

Aitchison, J. 1955. On the distribution of a positive random variable having a discrete probability mass at the origin. Journal of the American Statistical Association 50, 901.

Anderson, S., Keppel, E.A., and Edwards, A.M. 2019. A reproducible data synopsis for over 100 species of British Columbia groundfish. DFO Can. Sci. Advis. Sec. Res. Doc. 2019/041. vii + 321 p.

Anderson, S.C., Ward, E.J., English, P.A., Barnett, L.A.K., and Thorson, J.T. 2024. sdmTMB: An R package for fast, flexible, and user-friendly generalized linear mixed effects models with spatial and spatiotemporal random fields. bioRxiv, 2022.03.24.485545.

Dunn, P.K., and Smyth, G.K. 1996. Randomized Quantile Residuals. Journal of Computational and Graphical Statistics, 5(3), 236–244.

Fuglstad, G.A., Simpson, D., Lindgren, F., and Rue, H. 2019. Constructing priors that penalize the complexity of Gaussian Random Fields. JASA, 114(525), 445–452.

Kristensen, K., Nielsen, A., Berg, C.W., Skaug, H. and Bell, B.M. 2016. TMB: automatic differentiation and Laplace approximation. Journal of Statistical Software, 70, 1–21.

Le Cren, E.D. 1951. The length-weight relationship and seasonal cycle in gonad weight and condition in the perch (*Perca fluviatilis*). Journal of Animal Ecology, 20, 201–219.

McCullagh, P., and Nelder, J.A. 1989. Generalized Linear Models. Chapman & Hall.

Thorson, J.T. and Kristensen, K. 2016. Implementing a generic method for bias correction in statistical models using random effects, with spatial and population dynamics examples. Fisheries Research, 175, 66–74.

Thorson, J.T., Shelton, A.O., Ward, E.J. and Skaug, H.J. 2015. Geostatistical delta-generalized linear mixed models improve precision for estimated abundance indices for West Coast groundfishes. ICES Journal of Marine Science, 72, 1297–1310.

Thygesen, U.H., Albertsen, C.M., Berg, C.W., Kristensen, K., and Nielsen, A. 2017. Validation of ecological state space models using the Laplace approximation. Environmental and Ecological Statistics, 24(2), 317–339.

Waagepetersen, R. 2006. A simulation-based goodness-of-fit test for random effects in Generalized Linear Mixed Models. Scandinavian Journal of Statistics, 33(4), 721–731.

Williams, D.C., Nottingham, M.K., Olsen, N. and Wyeth, M.R. 2018. Summary of the Queen Charlotte Sound synoptic bottom trawl survey, July 6 – August 8, 2015. DFO Can. Manuscr. Rep. Fish. Aquat. Sci. 3136, viii + 64 p.